

**NIST-GCR-98-750**

---

---

**ENHANCED BURNING OF DIFFICULT TO  
IGNITE/BURN FUELS INCLUDING HEAVY  
OILS**

---

---

Niel Wu and Jose L. Torero

Department of Fire Protection Engineering  
University of Maryland  
College Park, MD 20742-3031

**NIST**

United States Department of Commerce  
Technology Administration  
National Institute of Standards and Technology

**NIST-GCR-98-750**

---

---

**ENHANCED BURNING OF DIFFICULT TO  
IGNITE/BURN FUELS INCLUDING HEAVY  
OILS**

---

**Prepared for**  
**U.S. Department of Commerce**  
**National Institute of Standards and Technology**  
**Gaithersburg, MD 20899**

**By**  
**Niel Wu and Jose L. Torero**  
**Department of Fire Protection Engineering**  
**University of Maryland**  
**College Park, MD 20742-3031**

**April 1998**  
**Issued June 1998**



### Notice

This report was prepared for the Building and Fire Research Laboratory of the National Institute of Standards and Technology under grant number 60NANB6D0073. The statement and conclusions contained in this report are those of the authors and do not necessarily reflect the views of the National Institute of Standards and Technology or the Building and Fire Research Laboratory.

**ENHANCED BURNING OF DIFFICULT TO IGNITE/BURN  
FUELS INCLUDING HEAVY OILS**

**Niel Wu and Jose L. Torero**  
Department of Fire Protection Engineering  
University of Maryland  
College Park, MD20742-3031

**FINAL REPORT**

April 1998

Prepared for:

U.S. Department of Commerce  
National Institute of Standards and Technology  
Building and Fire Research Laboratory  
Gaithersburg, MD20899-0001

## Abstract

An experimental technique has been developed to systematically study the ignition, flame spread and mass burning characteristics of liquid fuels spilled on a water bed. The final objective of this work is to provide a tool that will serve to assess a fuel's ease to ignite, to spread and to sustain a flame, thus helping to better define the combustion parameters that affect in-situ burning of oil spills. A systematic study of the different parameters that affect ignition, flame spread and mass burning has been conducted in an attempt to develop a bench scale procedure to evaluate the burning efficiency of liquid fuels in conditions typical of oil spill scenarios. To study ignition and flame spread, the Lateral Ignition and Flame Spread (LIFT) standard test method (ASTM E-1321) has been modified to allow the use of liquid fuels and a water bed. Characteristic parameters such as the critical heat flux for ignition, ignition delay time and flame spread velocity as a function of the external heat flux have been obtained. A series of "fire properties" corresponding to the fuel can be extrapolated from these tests and used to assess the tendency of a fuel to ignite and to sustain flame spread. The ignition and flame spread data is complemented by means of the Flash Point Temperature as obtained from the ASTM D56 Tag Closed Cup Flash point tester. Mass burning has been studied by determining the burning efficiency of different fuels ( $\chi$ ) under conditions where a simple one-dimensional heat conduction model describes the surface regression rate. The methodology was validated using SAE 30W oil and different crude oils in their natural state and under different levels of weathering. The present results show that Flame spread velocity is controlled by the thermal properties of the heavier fractions of the fuel and the flash point temperature. Weathering has therefore no effect on the thermal properties but significantly affects the flame spread rate and the minimum external heat flux necessary to sustain spread. The thermal properties determining the ignition delay time are, again, determined by the heavier fractions but the critical heat flux necessary for ignition is a strong function of the weathering level. A relative evaluation of the efficiency of the mass burning process ( $\chi$ ) can be obtained experimentally under controlled bench scale conditions and used to evaluate the efficiency of the burning process under more realistic scenarios.

## ACKNOWLEDGEMENTS

This work was supported by NIST and the authors wish to thank Dr. Marino diMarzo who is the main person responsible for this work being done. Special thanks to all the people that in one way or another contributed in this work; M. Baker, S. Gandhi, G. Kolb, J. McElroy, T. Mosman, S. M. Olenick, A. Tafreshi. The experimental data used to validate the burning efficiency factor was obtained by Dr. J.-P. Garo and Dr. J.-P. Vantelon at the Laboratoire de Combustion et de Detonique, ENSMA-University of Poitiers, France.

**BLANK PAGE**

## TABLE OF CONTENTS

ABSTRACT	iv
ACKNOWLEDGMENTS	v
TABLE OF CONTENTS	vii
1. Pre Boil-over Burning of a Slick of Oil on Water	3
2. A Simplified Theory to Assess the Burning Characteristics of a of Oil on Water	23
3. Some Observations on the Pre-Boil-over Burning of a Slick of Oil on Water	33
4. Ignition and Flame Spread and Mass Burning Characteristics of Liquid Fuels on a Water Bed	53
4.1. Arctic and Marine Oil Spill Program - Paper	55
4.2. Spill Science and Technology - <i>Extended Abstract</i>	83
5. Piloted Ignition of a Slick of Oil on Water	91
6. Piloted Ignition of a Slick of Oil on a Water Sub-Layer: The Effect of Weathering	97
7. The Effect of Weathering on Piloted Ignition and Flash Point of a Slick of Oil	123
7.1. Arctic and Marine Oil Spill Program - Paper	125
7.2. Spill Science and Technology - <i>Extended Abstract</i>	143
8. Determination of Fire Properties of Liquid Fuels Characteristic of Oil-Spills Using ASTM E-1321	151

**BLANK PAGE**

**1. Pre-Boilover Burning of a Slick of Oil on Water**

J.-P. Garo, J.-P. Vantelon, S.Gandhi and J.L. Torero  
*Spill Science and Technology* (submitted)

**BLANK PAGE**

# PRE-BOILOVER BURNING OF A SLICK OF OIL ON WATER

**J. P. Garo, J. P. Vantelon**

Laboratoire de Combustion et de Detonique  
ENSMA-Universite de Poitiers  
86960 Futuroscope Cedex  
FRANCE

**S. Gandhi and J. L. Torero\***

Department of Fire Protection Engineering  
University of Maryland  
College Park, MD20742-3031  
USA

Word Count: 4,048 words (Microsoft Word 6.0 - Word Count)  
8 Figures: 1,600 words  
2 Tables: 400 words  
**Total 6,048 words**

**BLANK PAGE**

## ABSTRACT

The burning rate of a slick of oil on a water bed is calculated by a simple expression derived from a one-dimensional heat conduction equation. Heat feedback from the flame to the surface is assumed to be a constant fraction of the total energy released by the combustion reaction. The total heat release, as a function of the pool diameter, is obtained from existing correlations. It is assumed that radiative heat is absorbed close to the fuel surface, that conduction is the dominant mode of heat transfer in the liquid phase and that the fuel boiling temperature remains constant. By matching the characteristic thermal penetration length scale for the fuel/water system and an equivalent single layer system, a combined thermal diffusivity can be calculated and used to obtain an analytical solution for the burning rate. Theoretical expressions were correlated with crude oil and heating oil, for a number of pool diameters and initial fuel layer thickness. Experiments were also conducted with emulsified and weathered crude oil. The simple analytical expression describes well the effects of pool diameter and initial fuel layer thickness permitting a better observation of the effects of weathering, emulsification and net heat feedback to the fuel surface. Experiments showed that only a small fraction of the heat released by the flame is retained by the fuel layer and water bed (of the order of 1%), that the effect of weathering on the burning rate decreases with the weathering period and that emulsification results in a linear decrease of the burning rate with water content.

**Keywords:** Oil spill, burning rate, crude oil, weathering, emulsification, pool fire

**BLANK PAGE**

## INTRODUCTION

The burning of oil in water is of great interest as a result of off-shore exploration, production and transportation of petroleum. This combustion phenomenon may constitute a hazard, i.e. and accidental burning slick drifting towards a platform, but it may also serve as a measure to minimize the environmental damage of an oil spill [1,2].

The available information on this phenomena is quite limited. Although great effort has been devoted to the understanding of pool fires [3] and flame spread over liquid pools [4,5,6] the specific issues related to a fuel burning over a water bed have deserved little attention. Most of the work being related to fires in fuel tanks and the phenomena commonly referred as "boilover" [7,8]. Only a few studies have dealt with the burning of a thin layer of fuel on a water bed. A good summary of existing knowledge is provided by Evans et al. [2].

In an attempt to provide an adequate methodology for ignition of oil-spills a review of the ignition methods commonly used for oil spill clean-up was provided by Jason [9]. Ignition source temperatures and successful ignition conditions have also been a subject of interest [10,11]. A cone calorimeter was used by Putorti et al. [12] to quantify the heat flux necessary to accomplish ignition of different fuel. In this work emphasis was given to the effects of weathering and emulsification on ignition.

Assuming that the fuel layer is ignitable an important concern is thin layer boil-over. The term "boilover" has been usually applied to a fire scenario in which an open top tank containing burning crude oil, after a long period of quiescent burning, shows a sudden increase in fire intensity associated with the expulsion of burning oil from the tank [13]. The term boilover has also been applied to the burning of thin layers of fuel on the surface of water in order to limit the spread of oil after an accident [14,15]. This scenario is commonly referred as thin layer boil-over. Although somehow different in nature, both cases result from the onset of boiling nucleation at the fuel/water interface and therefore, the time from ignition to the onset of boilover correlates well with the time needed for the thermal wave to reach the water [16].

The problems linked to thin layer boilover are related to the uncontrolled nature of the combustion process and the total fraction of fuel consumed during the burning process. The total fraction of fuel burnt before boilover increases with the fuel layer thickness if the layer is thinner than 10 mm and remains constant for thicker layers [16]. The amount of fuel consumed after the onset of boilover dramatically decreases with the fuel thickness [15]. Thick fuel layers lead to a "hot zone" formation that results in explosive boilover and low fuel consumption, thinner layers follow a smoother transition between pool like burning and boilover which leads to high fuel consumption.

Geometrical considerations pertaining burning rate are of great importance when considering the use of burning for oil spill cleanup. If the oil spill is not contained, the fuel layer thickness decreases till self-sustained burning is no longer possible. Typical values of the order of 0.5 mm have been identified as a minimum thickness for self-sustain burning [8,16,17]. The effect of fuel thickness, pool diameter and fuel boiling point on the burning rate has also been studied by Garo et

al. [16,18] who observed that the burning rate does not depend on the initial fuel layer thickness for fuel layers thicker than 10 mm and decreases for thinner layers.

One of the first attempts to model this type of problem was made by Twardus and Brzustowski [1], who developed a simple one-dimensional model to describe the combustion of oil slicks on water. This model describes the burning process as that of a pool fire with a heat loss term from the fuel to the water underneath. Heat losses from the fuel towards the water will increase as the fuel layer thickness decreases, therefore, a minimum thickness for self-sustained burning can be established. In a later model Brzustowski and Twardus [19] incorporated the effects of radiative absorption in the fuel and the effect of tilting by the wind. A more realistic model that incorporates radiative feedback and the effects of turbulent buoyant motion was subsequently developed by Alramadhan et al. [17], emphasis was given to the regressing surface and the gas phase and no account for heat transfer towards the water bed was made. Although these simple theories obtain expressions for the burning rate and minimum thickness for self-sustained burning, they all fail to describe the evolution of the burning rate as the fuel thickness decreases below 10 mm.

In this work a simple heat conduction model is used to describe the pre-boil over burning rate of crude oil and heating oil. The results from the model are then compared with experimental results. The parameters varied are the pool diameter, the fuel layer thickness, the weathering level and the percentage of water emulsified in the fuel.

## FORMULATION

Heat release rate from a pool fire has been documented extensively [3,20,21] and it has been found that the expression

$$\dot{Q} = \rho_{\infty} C_p (T_{\infty} g (T_f - T_{\infty}))^{1/2} d^{5/2}$$

correlates well with values measured experimentally [17]. The total heat release from the combustion process is denoted by  $\dot{Q}$ ,  $C_p$  is the specific heat at constant pressure and ambient temperature for air,  $T_{\infty}$  is the ambient temperature,  $T_f$  is an average flame temperature (for this work  $T_f \approx 1100$  K [20]),  $g$  is the acceleration of gravity ( $g=9.81$  m/s<sup>2</sup>),  $d$  (diameter of the fuel pool) is the characteristic length scale,  $\rho$  is the density and the sub-index  $\infty$  stands for ambient conditions.

The net heat fed back to the fuel represents a small fraction of the total heat release, this fraction ( $\chi$ ) has been found to be independent of the pool diameter [3,21] and thus, the heat flux per unit area reaching the surface can be expressed as

$$\dot{q}_s'' = \chi \frac{4 \rho_{\infty} C_p (T_{\infty} g (T_f - T_{\infty}))^{1/2} d^{1/2}}{\pi} \quad (1)$$

If conduction is assumed to be the dominant heat transfer mechanism and if the thermal wave has not reached the fuel/water interface the fuel can be considered as semi-infinite and an expression for the temperature as a function of time and position can be obtained. This treatment can also be used when fuel and water have similar thermal diffusivities [8,16]. This case will be referred as the “One-Dimensional Single Layer Conduction Model”. If fuel and water have significantly different thermal diffusivities and the thermal wave has already reached the fuel/water interface, fuel and water layers need to be treated independently. The water can still be assumed as semi-infinite but the fuel layer needs to be treated as a layer of finite thickness. This case will be referred as the “One-Dimensional Two Layer Conduction Model”.

Radiation through the fuel layer can be of importance [17,19] but for the fuels of interest it has been demonstrated that most of the radiative heat flux is absorbed very close to the surface [22]. Natural convection inside the fuel and water layers can significantly enhance heat transfer close to the fuel surface but seems to affect only weakly steady burning for highly viscous fuels [5]. The importance of natural convection decreases with viscosity and its effects can be neglected for those fuels relevant to this study, this is not the case for less viscous fuels (i.e. octane, xylane, etc.) [18]. For simplicity, this analysis will assume conduction to be the dominant heat transfer mechanism.

### *General Statements*

A schematic of the problem to be studied is presented in Figure 1. Assuming no convective motion and that radiation is fully absorbed at the surface, the following energy balance can be made at  $y=y_s(t)$

$$\dot{q}_s'' = H_v \rho_F r(t) + \dot{q}_c'' \quad (2)$$

where  $\dot{q}_c'' = -\lambda_F \left. \frac{\partial T}{\partial y} \right|_{y=y_s(t)}$  is the heat conducted into the fuel layer,  $H_v$  is the latent heat of vaporization,  $t$  is a specific time,  $T$  is the temperature,  $\lambda$  is the thermal conductivity,  $r(t) = \frac{\partial}{\partial t} (y_s(t))$  is the regression rate,  $y_s(t)$  is the location of the fuel surface at a specified time, and the sub-index  $F$  stands for fuel. For the entire analysis, it is assumed that the ignition source brings the surface temperature to  $T_s$  (vaporization temperature of the fuel) instantaneously. The vaporization temperature is considered to remain constant throughout the entire burning time.

### *One-Dimensional Single Layer Conduction Model*

This analysis is an extension of the works of Arai et al. [8] and Garo et al. [16]. Details of the formulation will not be presented here and therefore, the reader is referred to these works for further information.

The heat conduction equation for a one-dimensional semi-infinite element is given by:

$$\frac{\partial^2 T}{\partial y^2} = \frac{1}{\alpha_F} \frac{\partial T}{\partial t} \quad (3)$$

with initial condition at

$$t=0, \quad T = T_\infty$$

and boundary conditions

$$\begin{aligned} y = y_s(t), \quad T &= T_s \\ y \rightarrow \infty, \quad T &= T_\infty \end{aligned}$$

if  $\alpha_F$  is the thermal diffusivity of the fuel and “r” is assumed to be constant then the following expression for the temperature distribution can be obtained

$$\frac{T - T_\infty}{T_s - T_\infty} = \exp\left(-\frac{r}{\alpha_F} (y - y_s(t))\right) \quad (4)$$

this expression will be accurate if the thermal diffusivity of the fuel is approximately equal to the thermal diffusivity of water ( $\alpha_F \approx \alpha_w$ ) or for a time period “t” earlier than the characteristic time for the thermal front to reach the fuel/water interface ( $t < t_C$ ). The characteristic time,  $t_C$ , can be derived by scaling equation (3)

$$t_C \approx \frac{y_{s,i}^2}{\alpha_F + y_{s,i} r}$$

where  $y_{s,i}$  is the initial thickness of the fuel layer. Knowing the temperature distribution it is possible to calculate  $\dot{q}_C''$  and by substituting in equation (2) an expression for the average regression rate can be calculated.

#### *One-Dimensional Two Layer Conduction Model*

The thermal diffusivity of water is significantly bigger than that of the fuels of interest (Table 1) and as soon as the thermal wave reaches the fuel/water interface, the water bed starts acting like a heat sink ( $t > t_C$ ). A full description of this scenario is given by the following set of differential equations and boundary conditions.

$$\frac{\partial^2 T}{\partial y^2} = \frac{1}{\alpha_F} \frac{\partial T}{\partial t} \quad (5)$$

$$\frac{\partial^2 T}{\partial y^2} = \frac{1}{\alpha_w} \frac{\partial T}{\partial t} \quad (6)$$

with initial condition at

$$t=0, \quad T = T_\infty$$

and boundary conditions

$$\begin{aligned} y = y_s(t), \quad T &= T_s \\ y = 0, \quad -\lambda_f \frac{\partial T}{\partial y} \Big|_{y=0^+} &= -\lambda_w \frac{\partial T}{\partial y} \Big|_{y=0^-} \\ y \rightarrow \infty, \quad T &= T_\infty \end{aligned}$$

The use of equation (2) and a numerical solution of the equations (5) and (6) is necessary to obtain the corresponding temperature distributions and regression rate. The data available in the literature generally provides only average regression rates, therefore, only an order of magnitude comparison will be possible. A simplified approach that incorporates the main physical characteristics is, thus, used to solve the above system of equations in place of a numerical solution.

The average regression rate has been reported of the order of  $10^{-5}$  m/s [16] and the thermal diffusivity for the liquids of interest is small (Table 1), therefore, at each stage of the regression process only the steady conduction equation needs to be solved. The resulting temperature profiles are linear and an equivalent thermal diffusivity can be obtained. The equivalent thermal diffusivity results from matching the thermal penetration distance through a two layer bed with thermal diffusivities  $\alpha_f$  and  $\alpha_w$  and the thermal penetration distance in one single layer of thermal diffusivity  $\alpha_{EQ}$ . The characteristic length for the fuel layer will be  $y_{s,i}$  and the average regression rate,  $r$ , is assumed to be constant. From equations (5) and (6):

$$\alpha_{EQ} = \frac{r y_{s,i}}{\alpha_f} (\sqrt{\alpha_w} + \sqrt{\alpha_f})^2$$

The use of an equivalent thermal diffusivity allows to formulate the problem with one differential equation. The single differential equation corresponds to equation (3), where  $\alpha_f$  has been substituted by  $\alpha_{EQ}$  and the following expression for the average regression rate ( $r$ ) is obtained:

$$r = \frac{1}{H_v \rho_f} \left[ \chi \left( \frac{4 \rho_\infty C_p (T_\infty g (T_f - T_\infty))^{1/2}}{\pi} \right) d^{1/2} - \frac{\alpha_f \lambda_f (T_s - T_\infty)}{y_{s,i} (\sqrt{\alpha_f} + \sqrt{\alpha_w})^2} \right] \quad (7)$$

Equation (7) although simple and approximate provides an engineering tool that could be of great practical use.

## EXPERIMENT

The experimental apparatus, measurement methods and experimental procedures are those described by Garo et al. [16,22] and therefore will only be described briefly here. Pool burning tests of a layer of liquid fuel floating on water were conducted in a large test cell vented by natural convection. Fuel and water were placed in stainless steel pans of 0.15 m, 0.23 m, 0.30 m and 0.50 m in diameter and 0.06 m deep. Some experiments were conducted with pans of different depths to verify that the results were independent of the pan depth. The pans were placed on a load cell to measure the fuel consumption rate. The load cell had a response time of 60 ms and an accuracy within  $\pm 0.5$  g.

The thickness of the initial fuel layer was varied from a maximum of 20 mm to a minimum thickness of 2 mm. Before each test water was first poured in the pan and next the fuel until it reached 1 mm below the pan lip. During the combustion process the location of the fuel/water interface remained constant, therefore, the freeboard length increases during the experiment. The freeboard length changes were found to have very little effect on the steady-state burning rate.

A typical experiment can be described as a short unsteady ignition period followed by a steady state burning period. During steady burning the surface temperature increased slightly as the experiment progressed (lighter volatiles tend to burn off first). The steady burning period was followed by thin layer boil-over characterized by an increase in the burning rate as well as intense splashing of water and fuel. It is important to note that steady burning was followed by boilover and not extinction, therefore, no sudden decrease of the mass burning rate was observed.

The fuels used were heating oil (a mixture of hydrocarbons ranging from  $C_{14}$  to  $C_{21}$ ) and crude oil (63% Kittiway, 33% Arabian Light and 4% Oural). Experiments were also conducted with weathered fuels as well as different fuel/water emulsions. Weathering refers to the evaporation of the light components of the fuel that results in significant changes of the fuel properties (density, viscosity, boiling temperature, etc.), in the laboratory it was accomplished by means of a mixer turning at 700 r.p.m. and covering 75% of the horizontal cross section of the container. Mixing was conducted for 3 different periods, 24, 48 and 72 hours. Fuel/water emulsions were obtained by adding fixed quantities of water to the mixer and allowed to emulsify for no more than an hour. Experiments were conducted with crude oil aged for 24 hours and water contents of 10, 20, 30 and 40% in volume.

## EXPERIMENTAL RESULTS

Details of the experimental observations can be obtained from Garo et al. [16,18] and Garo [23] and will not be presented here. The discussion of the results will be limited to what concerns the regression rate ( $r$ ). Figure 2 shows the regression rate as a function of the initial fuel thickness ( $y_{s,i}$ ) for crude oil. The values presented here are averages but can be assumed as representative since the regression rate remained almost constant throughout the pre-boilover period. It can be observed that for  $y_{s,i} > 8$  mm the regression rate is independent of the initial fuel layer thickness, instead, for  $y_{s,i} < 8$  mm the regression rate decreases till no self-sustained burning can be obtained for  $y_{s,i} < 2$  mm. Figure 2 also shows an increase in the regression rate with the pool diameter. It is important to note that the pool size does not seem to

alter the effect of fuel layer thickness, for all pan diameters the regression rate begins to decrease for layers thinner than 8 mm.

The use of heating oil, weathered or weathered and emulsified crude oil does not seem to affect the qualitative characteristics of the curves, being a change in magnitude the only observable difference. The regression rate for heating oil is significantly lower than that corresponding to crude oil burning under equivalent conditions. The average regression velocity of weathered crude oil is also significantly slower than those characteristic of fresh oil. Experiments conducted for different weathering periods (Figure 3) showed that as the weathering time increases the regression rate decreases, with the most dramatic change occurring for the initial weathering period and with no further change observable as the weathering time extends over 72 hours.

Adding water to the fuel seems to have a similar effect on the regression rate. Figure 4 shows the average regression rate for a 15 mm layer of crude oil weathered for a period of 24 hours to which water has been added from 0 to 40% in volume. It can be observed that the average regression rate decreases as the water content increases.

## DISCUSSION AND DATA CORRELATION

Equation (7) has been used to calculate the average regression rate ( $r_T$ ) for crude oil and the results are presented in figure 5. The average regression rate matches well qualitatively and quantitatively the experimental values ( $r_E$ ). Figure 5 shows, again, that the regression rate is almost constant for  $y_{S,i} > 8\text{mm}$  and decreases dramatically with the fuel layer thickness for  $y_{S,i} < 8\text{mm}$ . For all data points a constant value of  $\chi = 2.9 \times 10^{-3}$  was used. The value of  $\chi$  was selected to best fit  $r_T$  with the experimental data for the constant regression rate zone.

Experimentally obtained average regression rates for heating oil, fresh crude oil, 24 hour weathered crude oil and 24 hour weathered and emulsified crude oil (20% water content) were divided by the calculated regression rate ( $r_E/r_T$ ) to provide an indication of the error associated with the assumptions used to model the average regression rate, the results are presented in figure 6. The data was obtained for different pan diameters and is presented as a function of the initial fuel layer thickness ( $y_{S,i}$ ). The predicted values are in excellent agreement with the theory for initial fuel layer thickness greater than 5 mm, for thinner fuel layers the error increases reaching, in the worst of cases, values close to 50%. This error is justifiable due to the great uncertainty present when conducting experiments with very thin fuel layers and to the average nature of the regression rates presented. The value of  $\chi$  had to be adjusted to  $\chi = 3.9 \times 10^{-3}$  for heating oil, to  $\chi = 2.4 \times 10^{-3}$  for 24 hour weathered crude oil and to  $\chi = 1.8 \times 10^{-3}$  for 24 hour weathered and emulsified crude oil (20% water content).

The heat feedback from the flame behaves in a similar way to a pool flame with no water bed, at least in the pre-boilover period. The dependence on the diameter and initial fuel layer thickness is, thus, well described by the heat flux obtained from equation (1). The use of a net heat flux as a boundary condition at the fuel surface seems also to be appropriate. It is important to note that only approximately between 0.18 % and 0.39 % of the energy released by the flame is effectively fed back to the fuel surface. The above values of  $\chi$  seem comparable to

data presented by Arai et al. [8] but no data obtained under similar experimental conditions has been found to verify these magnitudes.

As previously pointed out by many authors [8, 16, 17, 18, 19] the water bed acts as a heat sink. The thermal diffusivity of water is significantly larger than that of the fuel (Table 1), thus, as the fuel layer becomes thinner, the overall thermal diffusivity increases. Heat conduction through the fuel and water increases ( $\dot{q}_C''$ ) and the overall fraction of the total heat flux ( $\dot{q}_S''$ ) vaporizing the fuel decreases leading to a decrease in the regression rate that can eventually result in extinction ( $y_{S,i} < 2$  mm).

The data for weathered and emulsified crude oil is also well described by the predicted regression rate (figure 6). The same reasoning presented above applies for these cases, being the only difference the regression rate magnitude. Weathering and emulsification alter the thermal properties of the fuel and, thus, the magnitude of the regression rate. By changing the efficiency constant ( $\chi$ ) to fit the experimental data, a practical way is found to incorporate the effect of weathering and emulsification on the fuel properties. The variation of the efficiency constant as a function of the weathering period and the water content is shown on figures 7 and 8, respectively.

Figure 7 shows that initially the efficiency constant ( $\chi$ ) decreases fast, followed by less significant changes till it reaches an almost constant value ( $\chi = 2 \times 10^{-3}$ ). It is well known that the highly volatile hydrocarbons will evaporate very fast, i.e. after less than 24 hours the mass loss of hydrocarbons with boiling points below 500 K ( $<C_{11}$ ) has reached 95% and only reaches total evaporation after 48 hours [23]. Heavier hydrocarbons ( $C_{11}-C_{25}$ ) tend to evaporate significantly slower reaching 100% mass loss only after more than 10 days. The initial fast change in fuel properties results in an abrupt decrease of  $\chi$ , followed by an almost negligible change rate.

For emulsified fuels water addition will result in an almost linear decrease of  $\chi$  (figure 8). The properties of the emulsified fuel change significantly with the water content and, as shown by equation 7, this will have a significant effect on the average regression rate. The way in which emulsification affects the fuel properties is not fully understood but it is well known that properties such as the density vary in an almost linear way with the water content ( $\rho(\text{emulsified fuel}) = (1 - \text{water fraction})\rho_F + (\text{water fraction})\rho_W$ ) and other properties, such as viscosity, increase in a non-linear way (Table 2).

Although the efficiency constant ( $\chi$ ) does not provide a real explanation to the effects of weathering and emulsification on the average regression rate it serves to quantify the flammability of the fuel independent of the pool size and fuel layer thickness. The relationship between the fuel properties and the efficiency factor goes beyond the heat transfer and evaporation mechanisms controlling the burning rate and a complete explanation will require a comprehensive study that will include the effects of weathering and emulsification on the flame chemistry and radiative feedback. In detail analysis of these relationships go beyond the scope of this work.

## CONCLUSIONS

A simple one dimensional heat conduction model has been used to describe the regression rate of a fuel layer on a water bed. Crude and heating oil have been used to test the validity of the phenomenological model for a wide range of

conditions. The model describes accurately the regression rate for fuel layers thicker than 2 mm. Deviations from the predicted values arise from the assumptions used in the model and from the uncertainties in the experimental results for  $y_{s,i} < 5$  mm. The model accurately describes for all conditions the dependency of the average regression rate on the pool diameter and initial fuel layer thickness.

A value for an efficiency constant  $0.001 < \chi < 0.004$  is obtained under all experimental conditions. The efficiency constant represents the fraction of the energy released at the flame that will be retained by the fuel/water. For the conditions studied the efficiency constant does not depend on the pool diameter or the initial fuel layer thickness being only affected by the fuel characteristics. Determination of the range of validity of this statement requires further experimentation.

Weathering and emulsification affect the fuel properties and, thus, the regression rate. An increase in the weathering period and in the water content results in a decrease in the regression rate. Although weathering and emulsification affect the fuel properties, a practical way of incorporating this effect is by introducing the dependency in the efficiency constant. It was found that after a sudden decrease, the efficiency constant is almost independent of the weathering period ( $t > 36$  hours). A linear decrease of the efficiency constant was found with the water content.

#### **ACKNOWLEDGMENTS**

The authors express their thanks to the Centre de Documentation de Recherches et d'Experimentations sur les Pollutions Accidentelles des Eaux, Brest, France, for its interest and help in this study and to Prof. A.C. Fernandez-Pello for the many insightful discussions. This work was conducted while JLT was on leave from CNRS, France.

## REFERENCES

1. Twardus, E.M. and Brzustowski, T.A., *Archivum Combustionis*, Polish Academy of Sciences, 1, 1-2,49-60, 1981.
2. Evans, D., Walton, W., Baum, H., Lawson, R., Rehm, R., Harris, R., Ghoniem, A. and Holland, J., *Proceedings of the Third Arctic And Marine Oil Spill Program Technical Seminar*, Ministry of Supply and Services Canada, Cat. No. En40-11/5-1990, pp. 1-38, 1990.
3. Drysdale, D.D., *An Introduction to Fire Dynamics*, John Wiley and Sons, 1985.
4. Williams, F.A., *Combustion Theory*, The Benjamin/Cummings Publishing Company Inc., 1985.
5. Ross, H.D. *Progress in Energy and Combustion Science*, 20, pp.17-63, 1994.
6. Glassman, I. and Dryer, F., *Fire Safety Journal*, 3, 132, 1981.
7. Ito, A., Inamura, T. and Saito, K., *ASME/JSME Thermal Engineering Proceedings*, 5: 277-282, 1991.
8. Arai, M., Saito, K. and Altenkirch, R.A., *Combustion Science and Technology*, 71, pp.25-40, 1990.
9. Jason, N.H. *Proceedings of the Alaska Arctic Offshore Oil Spill Response Technology Workshop*, NIST SP762, U.S. Government Printing Office, Washington D.C., pp. 47-95, 1989.
10. Bech, C., Sveum, P. and Buist, I., *Proceedings of the Third Arctic And Marine Oil Spill Program Technical Seminar*, Ministry of Supply and Services Canada, pp. 735-748, 1990.
11. Thompson, C. H., Dawson, G. W. and Goodier, J. L. *Combustion: An Oil Spill Mitigation Tool*, PNL-2929, National Technical Information Service, Springfield, VA22161, 1979.
12. Putorti, A. D., Evans, D. D. and Tennyson, E. J., *Proceedings of the Seventeenth Arctic and Marine Oil Spill Program Technical Seminar*, pp.657-667, 1994.
13. Henry, M. and Klem, T., *Fire Safety Today*, 11-13, 6, 1983.
14. Koseki, H. and Mulholland, G.W., *Fire Technology*, 27(1), 55-65, 1991.
15. Koseki, H. Kokkala, M. and Mulholland, G.W., *Fire Safety Science-Proceedings of the Third International Symposium*, 865-875, 1991.
16. Garo, J. P., Vantelon, J. P. and Fernandez-Pello, A.C., *Twenty-fifth Symposium (International) on Combustion*, The Combustion Institute, 1481-1488, 1994.
17. Alramadhan, M.A., Arpaci, V.S. and Selamet A., *Combustion Science and Technology*, 72, 233-253, 1990.
18. Garo, J. P., Vantelon, J. P. and Fernandez-Pello, A.C., *Twenty-sixth Symposium (International) on Combustion*, The Combustion Institute,(in press), 1996.
19. Brzustowski, T.A. and Twardus, E.M., *Nineteenth Symposium (International) on Combustion*, The Combustion Institute, 847-854, 1982.
20. Pipkin, O. A. and Sliepcevich, C. M., *Ind. & Eng. Chem. Fundamentals*, 3, 2, 147, 1964.
21. McCaffrey, B. J., NBSIR 79-1910, National Bureau of Standards, Washington D.C., 1979.
22. Cox, G., *Combustion Fundamentals of Fire*, Academic Press, London, 1995.

23. Garo, J.P., "*Combustion d'Hydrocarbures Repandus en Nappe sur un Support Aqueux. Analyse du Phenomen de Boilover*", Ph.D. Thesis, University of Poitiers, France, 1996.
24. Desmarquest, J.P. "Les Polluants Petroliers et leur Evolution en Mer", Report CEDRE, R.83727.E, 1983.

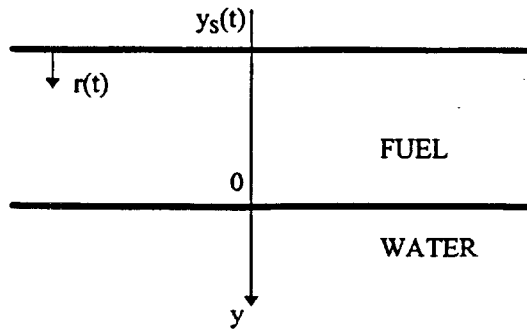


**Figure 1.** Schematic of the problem studied

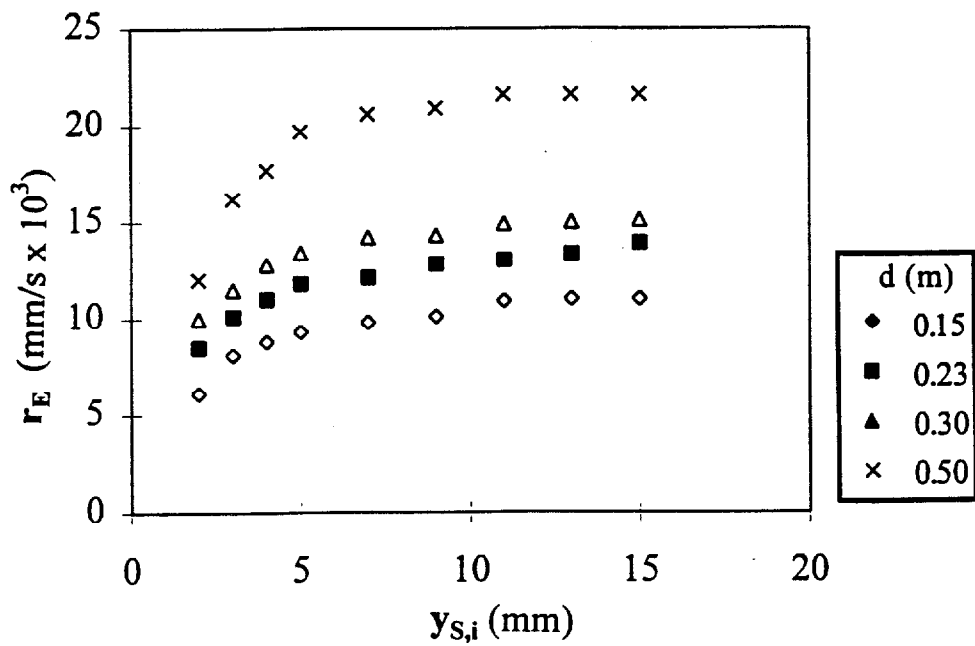


**Figure 2.** Regression rate as a function of initial fuel layer thickness for different pool diameters (experimental).

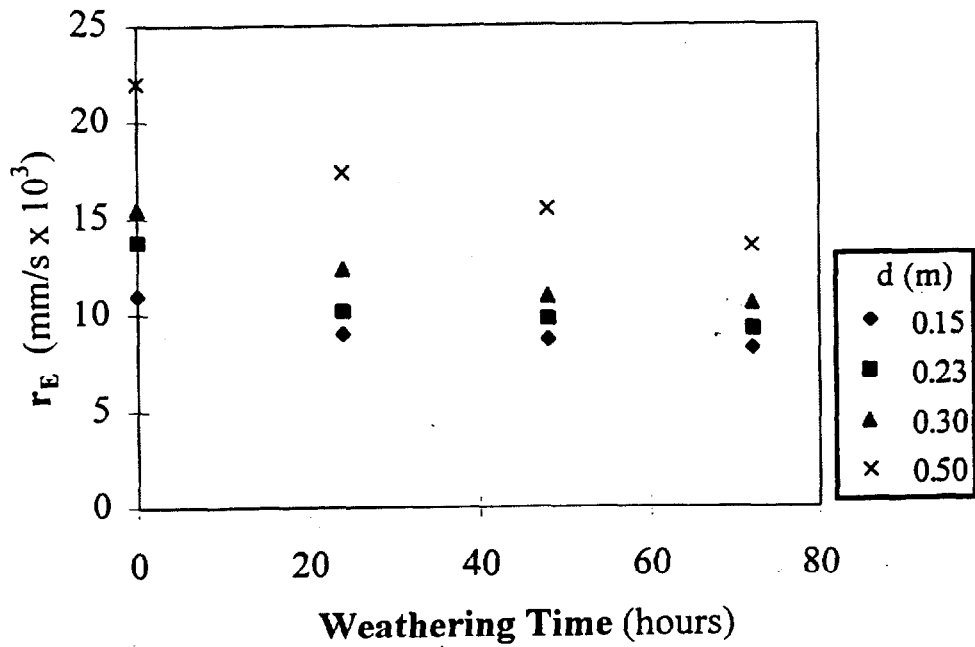


Figure 3. Regression rate as a function of the weathering period for different pool diameters.

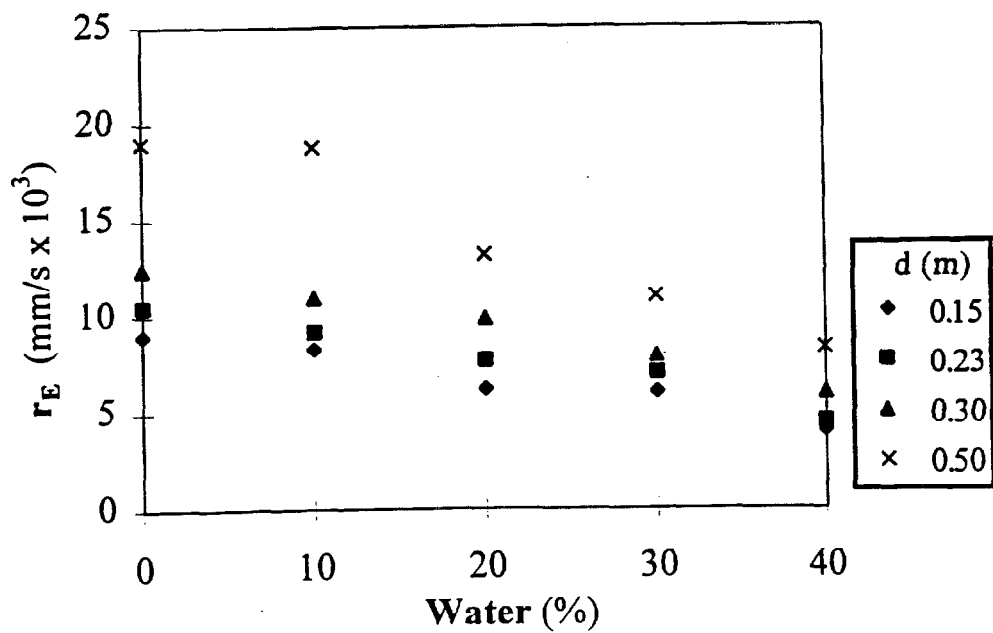
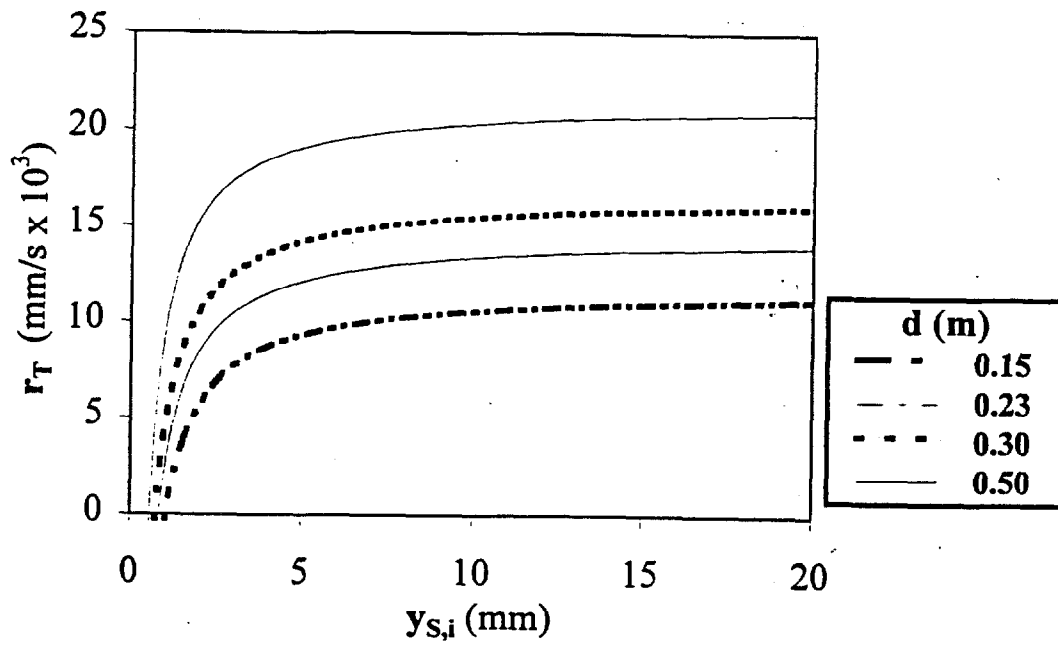
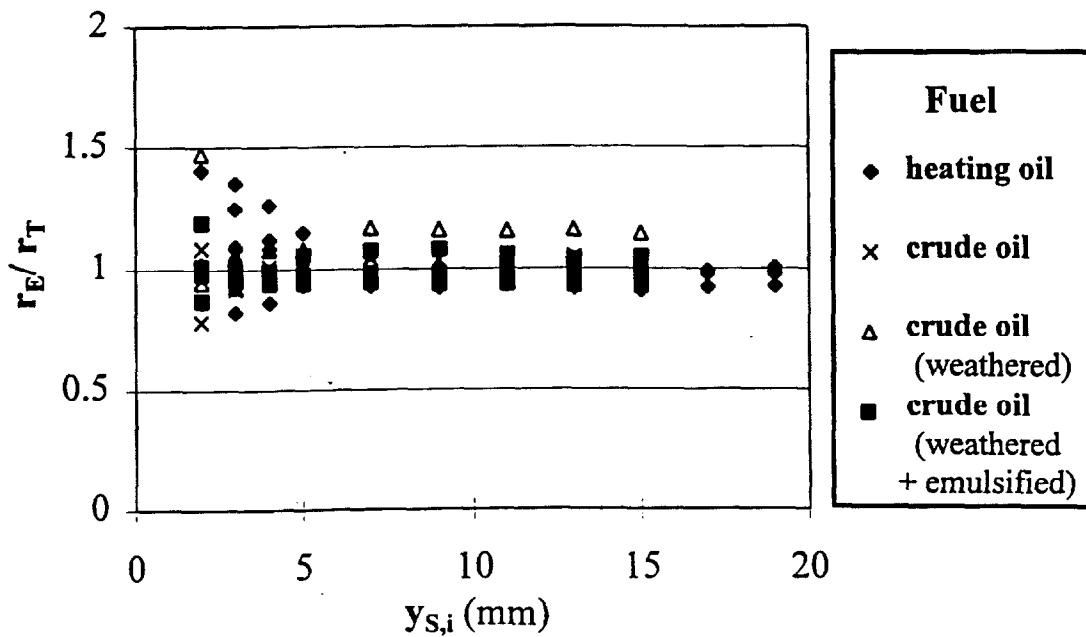


Figure 4. Regression rate as a function of the water content for different pool diameters.



**Figure 5.** Regression rate as a function of initial fuel layer thickness for different pool diameters (calculated).



**Figure 6.** Comparison between experimental ( $r_E$ ) and calculated ( $r_T$ ) regression rates

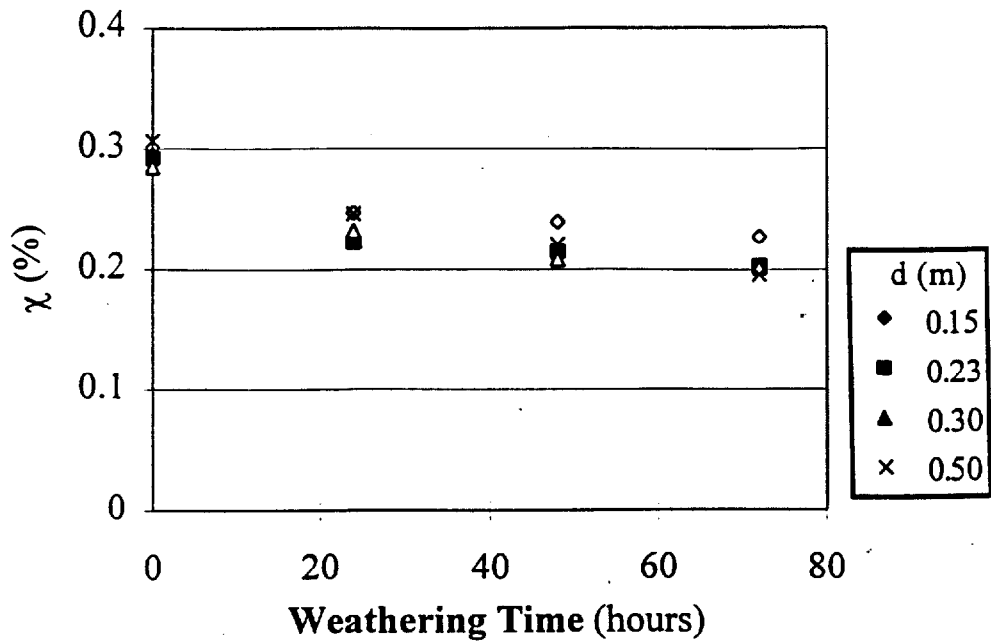


Figure 7. Efficiency constant as a function of the weathering period for crude oil

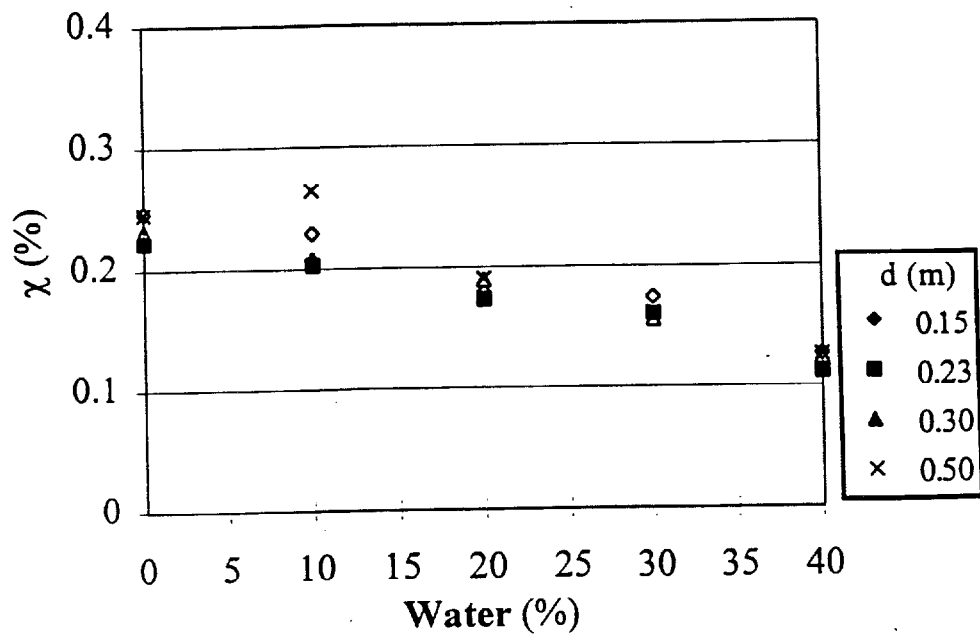


Figure 8. Efficiency constant as a function of the water content period for emulsified crude oil (weathered 24 hours)

	$T_s$	$\nu$ ( $\times 10^4$ ) (at 20°C) (m <sup>2</sup> /s)	$H_v$ (kJ/kg)	$\lambda$ (at 20°C) (W/m.K)	$\rho$ (at 20°C) (kg/m <sup>3</sup> )	$C_p$ (at 20°C) (kJ/kg.K)	$\alpha$ ( $\times 10^4$ ) (at 20°C) (m <sup>2</sup> /s)
Crude Oil	478	9.83	250	0.132	845	2.30	0.679
Heating Oil	538	5.31	377	0.137	844	1.90	0.854
Air	-	0.159	-	0.026	1.16	1.00	225.0
Water	373	1.00	2257	0.590	998	4.18	1.414

**Table 1 Properties**

Water Content	Density kg/m <sup>3</sup>	Viscosity m <sup>2</sup> /s ( $\times 10^6$ )
0 %	876	0.2454
10 %	887	0.4386
20 %	902	0.7561
30 %	921	1.6145
40 %	936	2.6987

**Table 2 Properties of crude oil weathered for 24 hours**

**2. A Simplified Theory to Assess the Burning Characteristics of a Slick of Oil on Water**

J.L. Torero

*XIV Congresso Brasileiro de Engenharia Mecânica, COBEM 97, Bauru, Sao Paulo, Brazil, December 1997*

**BLANK PAGE**

# A SIMPLIFIED THEORY TO ASSESS THE BURNING CHARACTERISTICS OF A SLICK OF OIL ON WATER

Jose L. Torero

*Department of Fire Protection Engineering  
University of Maryland, College Park, MD20742-3031  
USA-E-mail:jltorero@eng.umd.edu*

## **Abstract**

An experimental technique has been developed to systematically study the ignition, flame spread and mass burning characteristics of liquid fuels spilled on a water bed. The final objective of this work is to provide a tool that will serve to assess a fuels ease to ignite, to spread and to sustain a flame, thus helping to better define the combustion parameters that affect in-situ burning of oil spills.

## **Keywords**

In-situ burning, oil spills, mass burning, flame spread, ignition

## **1. INTRODUCTION**

A simple way to classify all studies relevant to in situ burning of an oil slick over a water bed is by dividing the combustion process in its three different stages, ignition, flame spread and self sustained burning (or mass burning). An external source of energy will lead to ignition, which will be followed by the spread of the flame across the fuel surface. Although flame spread might be an instantaneous process for many crude oils in their natural state, the loss of highly volatile compounds, due to weathering, and the presence of water in emulsions might lead to flame spread that needs to be assisted by external radiation. For thin fuel layers, heat losses to the water bed, might lead to a similar situation. For these particular cases a minimum size might be necessary to provide the necessary radiative heat feed back to self-sustain flame spread. Once the flame spread process is self sustained mass burning will follow.

Fuel properties vary significantly when subject to a strong heat insult, therefore, they need to be evaluated under fire conditions. Evaluation of the fuel "fire properties" that are independent of the length scale will permit the ranking of fuels and will reduce the number of large scale experiments necessary to determine in-situ burning protocols and procedures. By focusing on the fuel and introducing external radiation, large scale conditions can be simulated. It has to be noted that this is not a study of the burning

characteristics but of the fuel burning efficiency. Ignition and flame spread will be studied by using a modified Lateral Ignition and Flame Spread Test (ASTM E-1321) and mass burning by observing the regression rate under conditions where the characteristics of the flame can be predicted adequately.

This work attempts to identify an ideal configuration in which the ease by which a fuel can burn can be evaluated. The three aspects of the combustion process, ignition, flame spread and mass burning will be studied. The results should be independent of specific burning characteristics and geometrical constraints, and thus, extrapolation to a large scale should be possible.

## 2. IGNITION

The critical heat flux for ignition ( $\dot{q}_{0,ig}''$ ) is the minimum external heat flux that will lead to equilibrium at the pyrolysis temperature ( $T_p$ ), thus, is given by:

$$\dot{q}_{0,ig}'' = h(T_p - T_i) \quad (1)$$

where  $T_i$  is an ignition temperature and "h" is a global heat transfer coefficient. By assuming one-dimensional heat conduction in the fuel and  $t_{ig} \approx t_p$  ( $t_p$  is the time needed to reach  $T_p$ ) a characteristic ignition delay time ( $t_{ig}$ ) can be obtained:

$$t_{ig} = \frac{\pi}{4a} \left( \frac{h(T_p - T_i)}{\dot{q}_e''} \right)^2 \quad (2)$$

where ( $\dot{q}_e''$ ) is the external heat flux,  $k$  is the thermal conductivity and  $a = \alpha(h/k)^2$ . Mixing ( $t_M$ ), transport ( $t_T$ ) and chemical induction ( $t_{in}$ ) times are assumed neglectable when compared to  $t_p$ . This will be satisfied best as the external heat flux approaches the critical heat flux for ignition ( $\dot{q}_e'' \approx \dot{q}_{0,ig}''$ ) and  $t_p \rightarrow \infty$ . This is important because it implies that the error incurred in the experimental determination of  $t_{ig}$ , (due to the unknown nature of the flow) will decrease as  $\dot{q}_e''$  approaches  $\dot{q}_{0,ig}''$ . Therefore,  $\dot{q}_{0,ig}''$  is a property of the fuel that can be extrapolated, independent of the flow. More details on the derivation of the above expressions and on the characteristics of the hardware are provided by Quintiere (1981).

To validate this approach, SAE 30 W oil was used to conduct ignition tests. This fuel was used to make possible comparison with previously reported results on ignition delay time by Putorti et al (1990) and also because of its high flash point (approximately 250°C). A high flash point results in a longer ignition delay time providing a longer period to observe the different flow structures formed inside the liquid fuel and on the gas phase. The pilot size and location, the geometry of the fuel container and the flow around the sample have a significant effect on the ignition delay time ( $t_{ig}$ ) but for brevity only the study concerning the flow will be presented.

To study air entrainment into above the fuel sample, a 2W red diode laser (SDL-820) was used to create a light sheet for visualization of the smoke emerging from the fuel surface. Figures 2 and 3 are two typical images. In the absence of a flush floor eddies could be observed at the edges of the tray (figure 1), these eddies grow to cover

the entire surface of the fuel tray. When a floor surrounded the tray the eddies disappeared and a random flow of gases was observed (figure 2). The absence of eddies deters the mixing of fuel and oxidizer at the surface and as a consequence the ignition delay time increased by approximately 20%. By introducing a 0.1 m/s flow parallel to the surface a boundary layer is formed and all eddies were eliminated. By introducing the forced flow  $t_M$  and  $t_T$  are reduced significantly and  $t_{ig}$  approaches  $t_p$ . The choice of a small velocity (0.1 m/s) is not arbitrary, as the velocity increases the convective component of "h" increases and will have an effect on the value of the critical heat flux for ignition.



Figure 1- Smoke visualization for a tray with no flush floor.

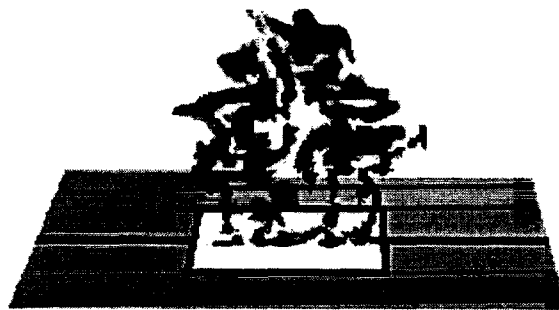


Figure 2- Smoke visualization for a tray with a flush floor.

The results from these experiments are presented in Figure 3 together with data obtained for the same fuel by Putorti et al. (1990) in a Cone Calorimeter. The ignition delay time is presented as  $t^{-1/2}$ , following equation (2). Although the ignition delay time differs from the values found by Putorti et al. all data converges to a unique critical heat flux for ignition. Since these experiments were conducted using different ignition procedures and under different environmental conditions,  $t_M$  and  $t_T$  are expected to be different, thus, affecting the ignition delay time. On the contrary,  $t_p$  should not be affected if convective losses are similar in magnitude or can be neglected. As  $\dot{q}_c''$  approaches  $\dot{q}_{0,ig}''$ ,  $t_M$  and  $t_T$  become neglectable compared to  $t_p$  and all data converges to a unique point ( $\dot{q}_{0,ig}'' \approx 6 \text{ kW/m}^2$ ).

### 3. FLAME SPREAD

Flame spread velocities ( $V_f$ ) can be obtained for external heat fluxes of magnitude smaller than  $\dot{q}_{0,ig}''$ . The following expressions were derived by Quintiere et al (1981).

$$V_f = \frac{\phi}{[\dot{q}_{0,ig}'' - \dot{q}_e'']^2} \quad \text{where} \quad \phi = \frac{4a\delta_f(\dot{q}_f'')^2}{\pi} \quad (3)$$

where  $\phi$  is a global material property determined from the experiments and  $\dot{q}_{0,ig}''$  can be obtained by increasing the external heat flux till  $V_f \rightarrow \infty$  and  $\delta_f$  is a characteristic thermal length scale. Reducing the external heat flux will eventually lead to no spread, thus a minimum velocity ( $V_{f,min}$ ) and external heat flux ( $\dot{q}_{0,s}''$ ) for flame spread can be recorded. This information, obtained under known experimental conditions, will serve as a useful way to assess and rank the fire performance of fuels and to identify the parameters that dominate their fire characteristics.

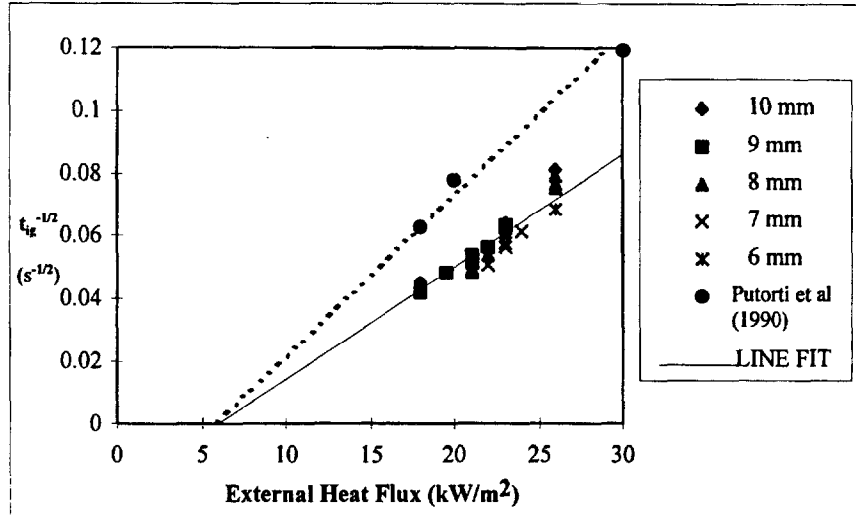


Figure 3-Ignition delay time for different external heat fluxes (SAE 30W oil). The delay times from Putorti et al (1990) were extracted as an average of the values obtained for 43 mm, 15 mm and 10 mm fuel layers.

Preliminary results showed that flame propagation transitions from a continuous flame spread mode, for the higher heat fluxes, to a pulsating mode as the external heat flux decreased. For  $\dot{q}_e'' < 6 \text{ kW/m}^2$  propagation ceased. Figure 4 shows a series of characteristic results for SAE 30W oil for different fuel layer thickness. It can be noted that flame spread regime significantly exceeds  $\dot{q}_{0,ig}''$ , specially for thinner fuel layer thickness. The flame spread velocity corresponding to a specific external heat flux increases with the fuel layer thickness. Further testing is still required to fully clarify this phenomena.

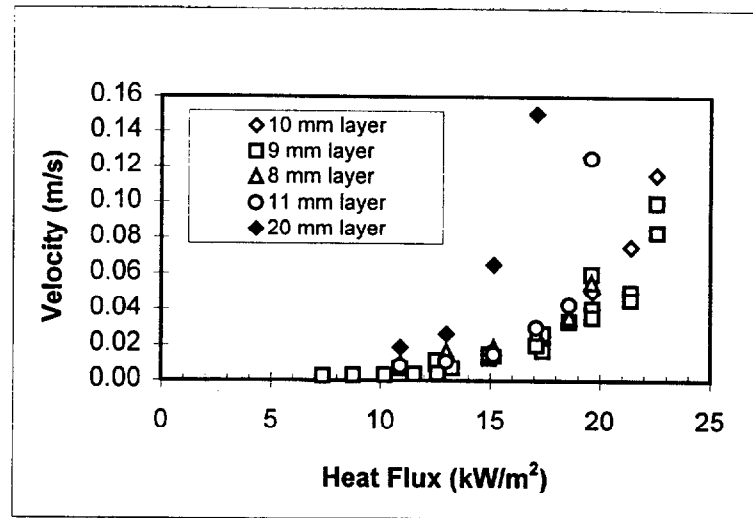


Figure 4 - Flame spread velocity for different external heat fluxes (SAE 30W).

#### 4. MASS BURNING

A simple way to assess the relative potential of a fuel to sustain mass burning is by using a burning efficiency ( $\chi$ ) extracted from a simple one-dimensional heat conduction model under conditions where the flame characteristics are known. The model relies on the concept that a fraction ( $\chi$ ) of the energy released by the flame is effectively used to support burning of the fuel. The higher the value of  $\chi$  the more effective the combustion process. The value of  $\chi$  is independent of the geometry (size, fuel layer thickness, etc.) and is only a function of the fuel. This value represents the mass burning efficiency of the fuel and is independent of the ignition and flame spread parameters. The experimental apparatus, measurement methods and experimental procedures used to validate this approach are described by Garo et al. (1996) who obtained  $\chi = 3.9 \times 10^{-3}$  for heating oil (a mixture of hydrocarbons ranging from  $C_{14}$  to  $C_{21}$ ) and  $\chi = 2.9 \times 10^{-3}$  for crude oil (63% Kittiway, 33% Arabian Light and 4% Oural). Experiments were also conducted with weathered fuels as well as different fuel/water emulsions.

Experimentally obtained average regression rates for heating oil, fresh crude oil, 24 hour weathered crude oil and 24 hour weathered and emulsified crude oil (20% water content) were divided by the calculated regression rate ( $r_E/r_T$ ) to provide an indication of the error associated with the assumptions used to model the average regression rate. The data was obtained for different pan diameters and is a function of the initial fuel layer thickness ( $y_{s,i}$ ) and is presented in figure 5. The regression rate was calculated using the above mentioned values of  $\chi$ . The predicted values are in excellent agreement with the theory for initial fuel layer thickness greater than 5 mm, for thinner fuel layers the error increases reaching, in the worst of cases, values close to 50%. This error is justifiable due to the great uncertainty present when conducting experiments with very thin fuel layers and to the average nature of the regression rates presented. The value of  $\chi$  had to be adjusted to  $\chi = 3.9 \times 10^{-3}$  for heating oil, to  $\chi = 2.4 \times 10^{-3}$  for 24 hour weathered crude oil and to  $\chi = 1.8 \times 10^{-3}$  for 24 hour weathered and emulsified crude oil (20% water content).

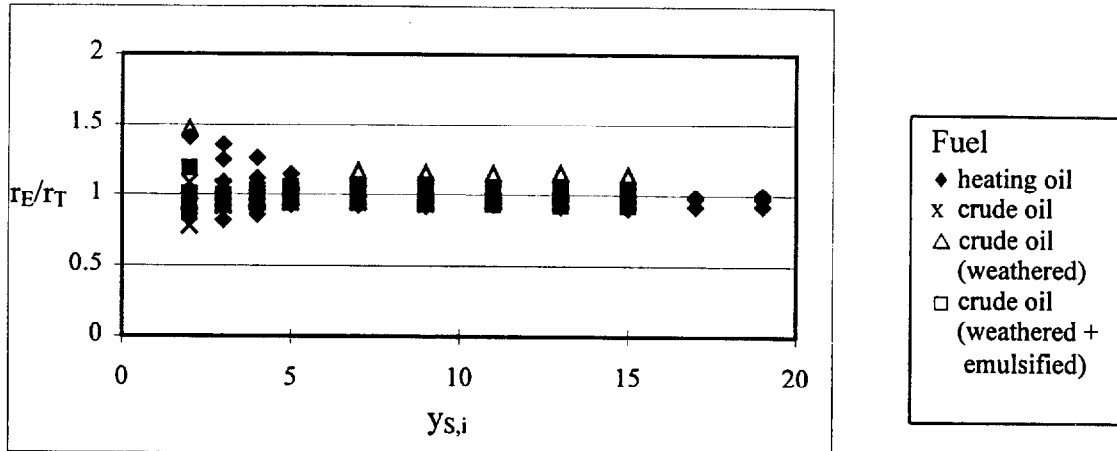


Figure 5-Experimental to Theoretical Regression Rate Ratio for Different Fuels and Pan Diameters

The heat released by the flame behaves in a similar way to a pool flame with no water bed, at least in the pre-boilover period and, therefore, a simple dependence on the diameter commonly used for pool fires successfully describes the heat release. The initial fuel layer thickness and the effect of the water bed are incorporated through an equivalent thermal diffusivity and the heat feed back from the flame to the fuel surface is well described as a fraction,  $\chi$ , of the total heat flux obtained from the flame. The net heat flux is used as a boundary condition at the fuel surface. It is important to note that only approximately between 0.18 % and 0.39 % of the energy released by the flame is effectively fed back to the fuel surface. The above values of  $\chi$  seem comparable to data presented by Arai *et al.* (1990) but no data obtained under similar experimental conditions has been found to verify these magnitudes.

The data for weathered and emulsified crude oil is also well described by the predicted regression rate. The same reasoning presented above applies for these cases, being the only difference the regression rate magnitude. Weathering and emulsification alter the thermal properties of the fuel and, thus, the magnitude of the regression rate. By changing the efficiency constant ( $\chi$ ) to fit the experimental data, a practical way is found to incorporate the effect of weathering and emulsification on the fuel properties. The variation of the efficiency constant as a function of the weathering period and the water content is shown on figures 6 and 7, respectively.

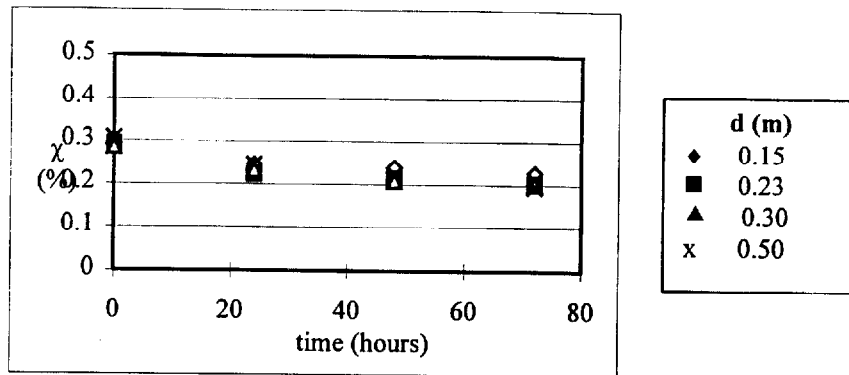


Figure 6. Efficiency Factor as a Function of Weathering Time

Figure 6 shows that initially the efficiency constant ( $\chi$ ) decreases fast, followed by less significant changes till it reaches an almost constant value ( $\chi = 2 \times 10^{-3}$ ). It is well known that the highly volatile hydrocarbons will evaporate very fast, i.e. after less than 24 hours the mass loss of hydrocarbons with boiling points below 500 K ( $<C_{11}$ ) has reached 95% and only reaches total evaporation after 48 hours (Demarquest, 1983). Heavier hydrocarbons ( $C_{11}-C_{25}$ ) tend to evaporate significantly slower reaching 100% mass loss only after more than 10 days. The initial fast change in fuel properties results in an abrupt decrease of  $\chi$ , followed by an almost negligible change rate.

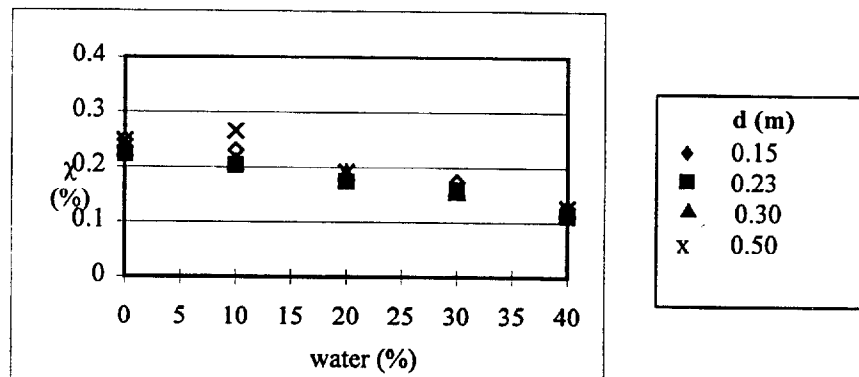


Figure 7. Efficiency Factor as a Function of the Water Content (emulsification)

For emulsified fuels water addition will result in an almost linear decrease of  $\chi$  (figure 7). The properties of the emulsified fuel change significantly with the water content and this will have a significant effect on the average regression rate. The way in which emulsification affects the fuel properties is not fully understood but it is well known that properties such as the density vary in an almost linear way with the water content ( $\rho(\text{emulsified fuel}) = (1 - \text{water fraction})\rho_F + (\text{water fraction})\rho_W$ ) and other properties, such as viscosity, increase in a non-linear way.

Although the efficiency constant ( $\chi$ ) does not provide a real explanation to the effects of weathering and emulsification on the average regression rate it serves to quantify the flammability of the fuel independent of the pool size and fuel layer thickness. The relationship between the fuel properties and the efficiency factor goes beyond the heat transfer and evaporation mechanisms controlling the burning rate and a complete explanation will require a comprehensive study that will include the effects of

weathering and emulsification on the flame chemistry and radiative feedback. In detail analysis of these relationships go beyond the scope of this work.

## 5. CONCLUSIONS

The methodology to assess the burning characteristics of a liquid fuel on a water bed has been presented and verified. Three different and complementary tests are deemed necessary to characterize the three different regimes of the burning process: ignition, flame spread and mass burning. For ignition; the critical heat flux for ignition as identified in ASTM E-1321 was found to be the parameter that better describes the capability of a fuel to ignite. For flame spread; the minimum external heat flux that will sustain propagation together with the parameter  $\phi$  (function of the fuel properties) will serve to describe the flame spread characteristics. The complexity of flame spread over liquid fuels makes necessary further validation of this experimental approach. For mass burning; the efficiency factor,  $\chi$ , serves as unique parameter to characterize the regression rate during the mass burning process.  $\chi$  is a property of the fuel that can be extrapolated to different scales and environmental conditions but should be evaluated under conditions where is independent of the flame diameter and the fuel layer thickness.

## 6. ACKNOWLEDGMENTS

This work was conducted under the financial support of the National Institute of Standards and Technology.

## 7. REFERENCES

- Arai, M., Saito, K. and Altenkirch, R.A., " A Study of Boilover in Liquid Pool Fires Supported on Water Part I: Effect of a Water Sublayer on Pool Fires", *Combustion Science and Technology*, 71, pp.25-40, 1990.
- Desmarquest, J.P. "Les Polluants Petroliers et leur Evolution en Mer", Report CEDRE, R.83727.E, 1983.
- Garo, J.P., Vantelon, J.P., Gandhi, S. and Torero, J.L. (1996) "Some Observations on the Pre-Boilover Burning of a Slick of Oil on Water," *Proceedings of the Nineteenth Arctic and Marine Oil Spill Program Technical Seminar*, pp.1611-1626.
- Putorti, A. D., Evans, D. D. and Tennyson, E. J. (1994) "Ignition of Weathered and Emulsified oils," *Proceedings of the Seventeenth Arctic and Marine Oil Spill Program Technical Seminar*, pp.657-667.
- Quintere, J. (1981) "A Simplified Theory for Generalizing Results from a Radiant panel Rate of Flame Spread Apparatus," *Fire and Materials*, 5, 2, pp. 52-60.

**3. Some Observations on the Pre-Boil-over Burning of a Slick of Oil on Water**

J.-P. Garo, J.-P. Vantelon, S. Gandhi and J.L. Torero

*19<sup>th</sup> Arctic and marine Oilspill Program (AMOP) Technical Seminar,  
Calgary, Canada, June 1996.*

**BLANK PAGE**

## **SOME OBSERVATIONS ON THE PRE-BOILOVER BURNING OF A SLICK OF OIL ON WATER**

**J. P. Garo, J. P. Vantelon**

Laboratoire de Combustion et de Detonique  
ENSMA-Universite de Poitiers  
86960 Futuroscope Cedex  
FRANCE

**S. Gandhi and J. L. Torero\***

Department of Fire Protection Engineering  
University of Maryland  
College Park, MD20742-3031  
USA

### **ABSTRACT**

The burning rate of a slick of oil on a water bed is calculated by a simple expression derived from a one-dimensional heat conduction equation. By treating the fuel layer as semi-infinite a well known analytical solution for the burning rate can be obtained. The heat feedback from the flame to the surface as, a function of the pool diameter, is obtained from an existing correlation and is incorporated into the analytical solution. It is assumed that radiative heat is absorbed close to the fuel surface and that the fuel boiling temperature remains constant before boilovert. The calculations agree well with experiments conducted with crude oil and heating oil, for a number of pool diameters and for initial fuel layers greater than 10 mm thick. The thermal diffusivity of water is significantly larger than that of the fuels used, therefore, for fuel layers thinner than 10 mm heat conduction from the fuel to the water layer has to be accounted when determining the burning rate. Theoretical expressions were also correlated with emulsified and weathered crude oil, again good agreement was obtained.

---

\* Corresponding Author

**BLANK PAGE**

## INTRODUCTION

The burning of oil in water is of great interest as a result of off-shore exploration, production and transportation of petroleum. This combustion phenomenon may constitute a hazard, i.e. and accidental burning slick drifting towards a platform, but it may also serve as a measure to minimize the environmental damage of an oil spill. For example, the burning of crude oil slicks during the spring break-up of Arctic ice has been proposed as the principal means of protecting the fragile marine and shoreline environment in the Arctic from the worst effects of sub-sea blow-out of an oil well during the winter months (Twardus and Brzustowski (1981), Evans et al., (1990)).

The available information on this phenomena is quite limited. Even though great effort has been devoted to the understanding of pool fires (Drysdale, 1985), flame spread over liquid pools (Williams (1985), Ross (1994), Glassman and Dryer (1981)) the specific issues related to a fuel burning over a liquid bed have deserved little attention. Most of the work being related fires in fuel tanks and the phenomena commonly referred as "boilover" (Ito et al. (1991), Arai et al. (1990)). Only a few studies have dealt with the burning of a thin layer of fuel on a water bed. A good summary of existing knowledge is provided by Evans et al. (1990), other more recent studies will be mentioned throughout this work.

One of the issues that has been widely addressed is that of ignition. In an attempt to provide an adequate methodology for ignition of oil-spills a review of the ignition methods commonly used for oil spill clean-up was provided by Jason (1989). Ignition source temperatures and successful ignition conditions have also been a subject of interest (Bech et al (1993), Thompson et al. (1979)). A cone calorimeter was used by Putorti et al. (1994) to quantify the heat flux necessary to accomplish ignition of different fuels, in this work emphasis was given to the effects of weathering and emulsification.

Assuming that the fuel layer is ignitable, one important issue of concern is that of thin layer boil-over. The term "boilover" has been usually applied to a fire scenario in which an open top tank containing burning crude oil, after a long period of quiescent burning, shows a sudden increase in fire intensity associated with the expulsion of burning oil from the tank (Henry and Klem, 1983). Recently, the term boilover has also been applied to the burning of thin layers of fuel on the surface of water in order to limit the spread of oil after leakage from a tanker or other spill accident (Koseki and Mulholland (1991), Koseki et al., 1991). This scenario is commonly referred as thin layer boil-over.

The problems linked to thin layer boilover are not only those related to the uncontrolled nature of the combustion process. One of the main issues related to thin layer boilover is the total fraction of fuel consumed during the burning process. After flame extinction a residue of significantly different characteristics to the original oil is left behind. It has been found that the fraction of fuel burnt before boil over starts increases with the fuel layer thickness until it reaches a constant value for a thickness greater than 10 mm (Garo et al, 1994). On the other hand the amount of fuel consumed after the onset of boil over dramatically decreases with the fuel thickness (Koseki et al., 1991). This phenomenon seems to be associated with the intensity of

boilover, thick fuel layers lead to a "hot zone" formation that results in explosive boilover and low fuel consumption, thinner layers follow a smoother transition between pool like burning and boilover which leads to higher fuel consumption. The issues related of thin layer boilover are of extreme importance when determining the adequacy of burning as an oil spill clean-up mechanism, nevertheless, the fundamental knowledge in this area is very limited.

Geometrical considerations pertaining burning rate are of great importance when considering the use of burning for oil spill cleanup. If the oil spill is not contained, the fuel layer thickness decreases till self-sustained burning is no longer possible. Typical values of the order of 0.5 mm have been identified as minimum thickness that will self-sustain burning (Alramadhan et al. (1990), Arai et al. (1990) and Garo et al. (1994)). The effect of fuel thickness, pool diameter and fuel boiling point on the burning rate has also been studied by Garo et al. (1994, 1996). Garo et al. (1994) showed that the burning rate remains constant for fuel layers thicker than 10 mm and decreases, with the fuel thickness, for layers thinner than 10 mm.

One of the first attempts to model this type of problem was made by Twardus and Brzustowski (1981), who developed a simple one-dimensional model to describe the combustion of oil slicks on water. This model treats the burning process in a similar way as that of a pool fire only incorporating a heat loss term from the fuel to the water underneath. Heat losses from the fuel to the surface will increase as the fuel layer thickness decreases, therefore a minimum burning thickness can be established. A minimum thickness of the order of 0.5 mm was found to be necessary for self-sustained burning of crude oil. In a later model Brzustowski and Twardus (1982) incorporated the effects of radiative absorption in the fuel and the effect of tilting by the wind. In this model the fuel layer is considered infinite in length and therefore the problem remains one-dimensional. The effect of the wind was only incorporated in what concerns tilting of the flame, where a simple empirical correlation is used to modify the radiative heat back from the flame (Pipkin and Sliepcevich, 1964). The heat flux from the flame was taken as a given parameter of the problem and therefore no empirical verification of the quantitative results was provided in these works. A more realistic model for radiative feedback and the effects of turbulent buoyant motion were subsequently incorporated in the model by Alramadhan et al. (1990) but emphasis was given to the regressing surface and the gas phase and no account for heat transfer towards the water bed is made.

In this paper a simple heat conduction model is used to describe the pre-boil over burning rate of a crude oil and heating oil. The results from the model are then compared with experimental results. The parameters varied are the pool diameter, the fuel layer thickness, the weathering level and the percentage of water emulsified in the fuel.

## FORMULATION

Heat release rates from a pool fire has been documented extensively (Mc Caffrey, 1979) and it has been found that the expression

$$\dot{Q} = \rho_{\infty} C_p (T_{\infty} g (T_f - T_{\infty}))^{1/2} d^{5/2}$$

obtained from simple scaling analysis correlates well with values measured experimentally. This expression has been previously used by Alramadhan et al. (1990) to describe the effects of radiation on a liquid fuel burning on water. The total heat release from the combustion process is denoted by  $\dot{Q}$ ,  $C_p$  is the specific heat at constant pressure and ambient temperature for air,  $T_{\infty}$  is the ambient temperature,  $T_f$  is an average flame temperature (for this work  $T_f \approx 1100$  K will be used (McCaffrey, 1979)),  $g$  is the acceleration of gravity ( $g=9.81$  m/s<sup>2</sup>),  $d$  (diameter of the fuel pool) is the characteristic length scale  $\rho$  is the density and the sub-index  $\infty$  stands for ambient conditions.

It has been observed that a constant fraction of the energy released by the flame is feedback to the fuel surface by radiation. The magnitude of the radiant fraction is independent of the pool size and total heat release. It has also been observed that a constant fraction of the total heat released is radiated towards the outside environment (Cox, 1995). It is therefore, only natural to assume that the total heat feedback from the flame to the fuel surface would be a constant fraction of the total heat released by the flame. This constant fraction will be denoted as  $\chi$ . Therefore the heat flux per unit area reaching the surface is given by

$$\dot{q}_s'' = \frac{\chi \rho_{\infty} C_p (T_{\infty} g (T_f - T_{\infty}))^{1/2} d^{1/2}}{\pi} \quad (1)$$

Heat transfer through the fuel and water bed will be assumed to be one-dimensional, semi-infinite and controlled by conduction. These assumptions require that fuel and water have similar thermal diffusivities (Arai et al (1990), Garo et al (1994)). As it can be observed on Table 1, fuel and water have significantly different thermal diffusivities and the thermal wave generally reaches the fuel/water interface long before the flame extinguishes or boilover is attained. This assumption originates a significant error, as it will be shown on the following sections, and a more accurate result will only be obtained if fuel and water layers are treated independently. The water can still be assumed as semi-infinite but the fuel layer needs to be treated as a layer of finite thickness that is a function of time. This case will be referred to as the "One-Dimensional Two Layer Conduction Model".

Radiation through the fuel layer can be of importance (Alramadhan et al. (1990), Brzustowski and Twardus (1982)) but for the fuels of interest it has been demonstrated that most of the radiative heat flux is absorbed very close to the surface (Garo, 1996). Natural convection inside the fuel and water layers can also represent a significant heat transfer mechanism close to the fuel surface and significantly affect processes such as flame spread but seem to play a minor role for steady burning (Ross, 1994). For simplicity, this analysis will assume conduction to be the dominant heat transfer mechanism.

### General Statements

A schematic of the problem to be studied that applies to both cases is presented in Figure 1. Assuming no convective motion and that radiation is all absorbed at the surface, the following energy balance can be made at  $y=y_s(t)$

$$\dot{q}_s'' = H_v \rho_F r(t) + \dot{q}_c'' \quad (2)$$

where  $\dot{q}_c'' = -\lambda_F \frac{\partial T}{\partial y} \Big|_{y=y_s(t)}$  is the heat conducted into the fuel layer,  $H_v$  is the latent heat of vaporization,  $t$  is a specific time,  $T$  is the temperature,  $\lambda$  is the thermal conductivity,  $r(t) = \frac{\partial}{\partial t} (y_s(t))$  is the regression rate,  $y_s(t)$  is location of the fuel surface at a specified time, and the sub-index  $F$  stands for fuel. For the entire analysis it is assumed that the ignition source is strong enough that the surface temperature is brought to  $T_s$  (vaporization temperature of the fuel) instantaneously. The vaporization temperature is considered to remain constant throughout the entire burning time.

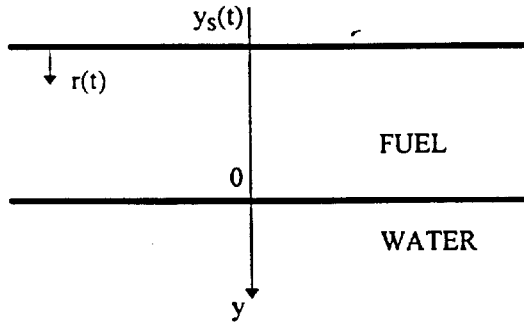


Figure 1. Schematic of the problem studied

### One-Dimensional Single Layer Conduction Model

This analysis is an extension of the works of Arai et al. (1990) and Garo et al. (1994). Details of the formulation will not be presented here and therefore, the reader is referred to these works for further information.

The heat conduction equation for a one-dimensional semi-infinite element is given by:

$$\frac{\partial^2 T}{\partial y^2} = \frac{1}{\alpha_F} \frac{\partial T}{\partial t} \quad (3)$$

with initial condition at

$$t=0, \quad T = T_{\infty}$$

and boundary conditions

$$y = y_s(t), \quad T = T_s$$

$$y \rightarrow \infty, \quad T = T_{\infty}$$

if  $\alpha_F$  is the thermal diffusivity of the fuel and "r" is assumed to be constant then the following expression for the temperature distribution can be obtained

$$\frac{T - T_{\infty}}{T_s - T_{\infty}} = \exp\left(-\frac{r}{\alpha_F}(y - y_s(t))\right) \quad (4)$$

this expression will be valid if the thermal diffusivity of the fuel is approximately equal to the thermal diffusivity of water ( $\alpha_F \approx \alpha_w$ ) or for a time period "t" earlier than the characteristic time for the thermal front to reach the fuel/water interface ( $t < t_c$ ). Where  $t_c$  can be derived by scaling equation (3)

$$t_c \approx \frac{y_{s,i}^2}{\alpha_F + y_{s,i}r}$$

where  $y_{s,i}$  is the initial thickness of the fuel layer. Knowing the temperature distribution it is possible to calculate  $\dot{q}_c''$  and by substituting in equation (1) an expression for the regression rate can be calculated

$$r = \frac{\alpha_F \chi \rho_{\infty} C_p (T_{\infty} g(T_F - T_{\infty}))^{1/2}}{\pi(H_v \rho_F \alpha_F + \lambda_F (T_s - T_{\infty}))} d^{1/2} \quad (5)$$

### *One-Dimensional Two Layer Conduction Model*

The thermal diffusivity of water is in general significantly bigger than that of the fuels of interest (Table 1), therefore, as soon as the thermal wave reaches the fuel/water interface the water bed starts acting like a heat sink ( $t > t_c$ ). A full description of this scenario is given by the following set of differential equations and boundary conditions.

$$\frac{\partial^2 T}{\partial y^2} = \frac{1}{\alpha_F} \frac{\partial T}{\partial t} \quad (6)$$

$$\frac{\partial^2 T}{\partial y^2} = \frac{1}{\alpha_w} \frac{\partial T}{\partial t} \quad (7)$$

with initial condition at

$$t=0, \quad T = T_\infty$$

and boundary conditions

$$\begin{aligned} y = y_s(t), \quad T = T_s \\ y = 0, \quad -\lambda_F \left. \frac{\partial T}{\partial y} \right|_{y=0^+} = -\lambda_w \left. \frac{\partial T}{\partial y} \right|_{y=0^-}, \quad T(0^+) = T(0^-) \\ y \rightarrow \infty, \quad T = T_\infty \end{aligned}$$

The use of equation (2) and a numerical solution of the differential equations is necessary to obtain the corresponding temperature distributions and regression rate. The data available in the literature, in general, provides only average regression rates, therefore, only an order of magnitude comparison will be possible. In this work, these problem statement will be used only to describe the discrepancies between the one-dimensional single layer conduction model and the experiments.

	$T_s$	$\nu$ ( $\times 10^4$ ) (at 20°C) ( $m^2/s$ )	$H_v$ (kJ/Kg)	$\lambda$ (at 20°C) (W/m.K)	$\rho$ (at 20°C) ( $kg/m^3$ )	$C_p$ (at 20°C) (kJ/kg.K)	$\alpha$ ( $\times 10^7$ ) (at 20°C) ( $m^2/s$ )
Crude Oil	478	9.83	250	0.132	845	2.30	0.679
Heating Oil	538	5.31	377	0.137	844	1.90	0.854
Air	-	0.159	-	0.026	1.16	1.00	225.0
Water	373	1.00	2257	0.590	998	4.18	1.414

Table 1 Properties

## EXPERIMENT

The experimental apparatus, measurement methods and experimental procedures are similar to those described by Garo et al. (1994, 1996) and therefore will only be described briefly here. Pool burning tests of a layer of liquid fuel floating on water were conducted in a large test cell vented by natural convection, using stainless steel pans of 0.15 m, 0.23 m, 0.30 m and 0.50 m in diameter and 0.06 m deep. Experiments were conducted with pans of different depths to verify that the results were independent of the pan depth. The pans were placed on a load cell to measure the fuel consumption rate. The load cell had a response time of 60 ms and an accuracy within +/- 0.5 g.

The thickness of the initial fuel layer was varied from a maximum of 15 mm to a minimum thickness of 2 mm. Before each test water was first poured in the pan and next the fuel until it reached 1 mm below the pan lip, such that the location of the

initial fuel surface was always constant. During the combustion process the location of the fuel/water interface remained constant, therefore, the freeboard length increases during the experiment. The freeboard length changes were found to have very little effect on the steady-state burning rate.

A typical experiment can be described as a short unsteady ignition period followed by a steady state burning period. During steady burning the surface temperature increased slightly as the experiment progressed (lighter volatiles tend to burn off first). The steady burning period was followed by thin layer boil-over characterized by an increase in the burning rate as well as intense splashing of water and fuel.

The fuels used were heating oil (a mixture of hydrocarbons ranging from  $C_{14}$  to  $C_{21}$ ) and crude oil (63% Kittiway, 33% Arabian Light and 4% Oural). Experiments were also conducted with aged fuels as well as different fuel/water emulsions. Aging refers to the evaporation of the light components of the fuel that results in significant changes of the fuel properties (density, viscosity, etc.), in the laboratory it was accomplished by means of a mixer turning at 700 r.p.m. and covering 75% of the horizontal cross section of the container. Mixing was conducted for 4 different periods, 24, 48 and 72 hours. Fuel/water emulsion were obtained by adding fixed quantities of water to the mixer and allowed to emulsify for no more than an hour. Experiments were conducted with crude oil aged for 24 hours and water contents of 10, 20, 30 and 40% in volume.

## EXPERIMENTAL RESULTS

Details of the experimental observations can be obtained from Garo et al. (1994, 1996) and Garo (1996) and will not be presented here. The discussion of the results will be limited to what concerns the regression rate ( $r$ ). Figures 2 and 3 show the regression rate as a function of the initial fuel thickness ( $y_{s,i}$ ). It has to be noted that the values presented are averages but can be assumed as representative since experimental conditions were set to achieve boilover before the regression rate started to decrease with time. Figure 2 shows the regression rate for crude oil and Figure 3 for heating oil. It can be observed that for a fuel thickness greater than 8 mm the regression rate reaches a constant value. For a fuel thickness below 8 mm the regression rate decreases till no self-sustained burning can be obtained for less than 2 mm. The pool diameter has a significant effect on the regression rate which increases with the pool size. The pool size does not seem to alter the effect of fuel layer thickness, for all pool diameters the regression rate decreases for layers thinner than 8 mm.

The regression rate as a function of fuel layer thickness is presented in Figure 4 for crude oil weathered for 24 hours. The basic characteristics of the curves do not seem to vary with the exemption of the magnitude. The regression rate of weathered crude oil is significantly slower than that of fresh oil, but weathering does not seem to affect the shape of the curves. Experiments were also conducted for different weathering periods and the results are presented in Figure 5. It can be observed that as the weathering period increases the regression rate decreases, the most dramatic

change occurring for the initial weathering period and reaching an almost constant value as the weathering period extends over 72 hours.

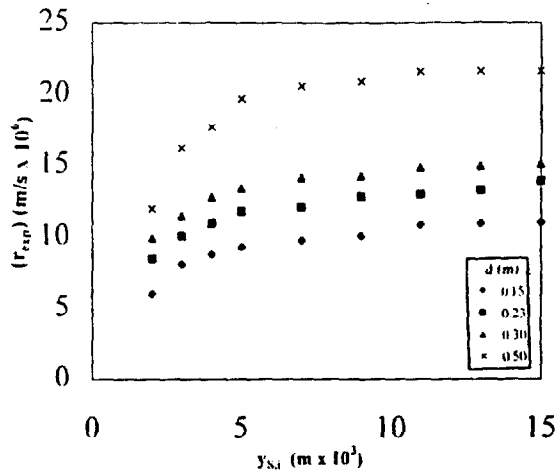


Figure 2 Regression rate for crude oil

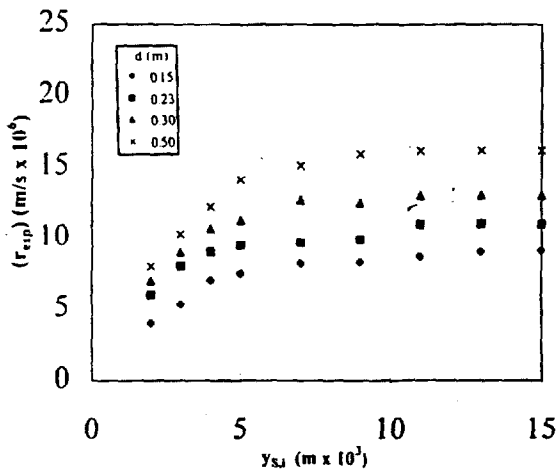


Figure 3 Regression rate for heating oil

Adding water to the fuel seems to have a similar effect on the regression rate. As shown by Figure 6 addition of water slows the regression rate. Figure 6 shows the regression rate as a function of the fuel layer thickness and the pool diameter for a crude oil with 20% water content that has been weathered 24 hours. It can be noted, from comparison with figure 4, that the regression rate further decreases when water has been added to the fuel. Again, the shape of the curves does not change with respect to Figures 2 and 4. The effect of water emulsification is more obvious on Figure 7 where it can be observed that the maximum regression rate decreases as the water content increases. The greatest effect occurs with the largest pool diameters.

## DISCUSSION AND DATA CORRELATION

The data from Figures 2, 3, 4 and 6 was divided by the calculated regression rate and is presented in Figures 8, 9, 10, and 11. For all data points a constant value of  $\chi=0.03$  was used. This value was selected to best fit the correlation for the

constant regression rate zone for both fresh crude and heating oils. It is clear that the assumptions implicit in the simplified model previously presented are adequate for fuel layer thickness greater than 8 mm, where the predicted values are in excellent agreement with the theory. The heat feedback from the flame behaves in a similar way to a pool flame with no water bed, at least in the pre-boilover period. The diameter dependence is, thus, eliminated by using the heat flux given by equation (2) as boundary condition at the fuel surface. It is important to note that only approximately 3% of the energy released by the flame is effectively fed back to the fuel surface. It has been pointed out by many authors that the radiative feedback from the flame to the fuel surface is of the order of 30% (Cox, 1995), therefore, heat losses from the surface by conduction, convection and re-radiation have to account for the discrepancy.

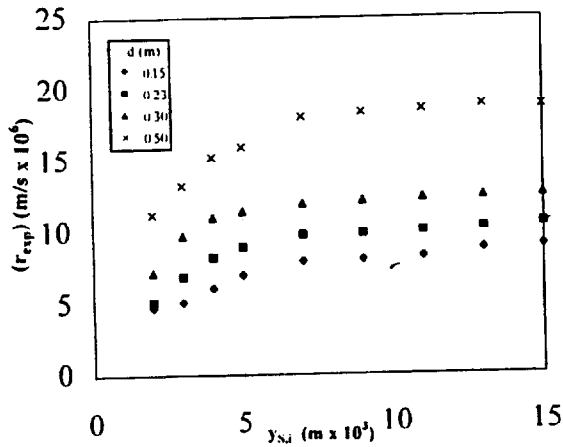


Figure 4 Regression rate for 24 hour weathered crude oil

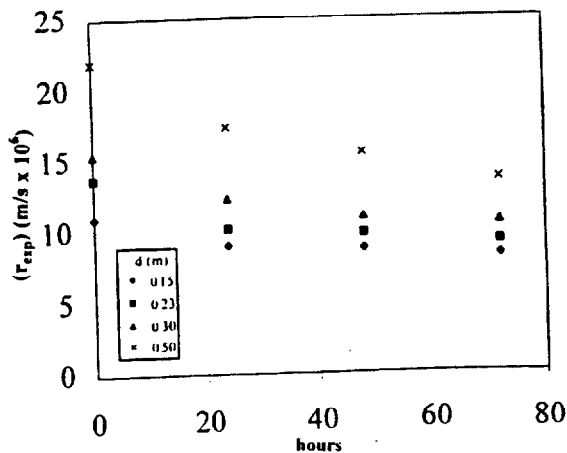


Figure 5 Regression rate for crude oil as a function of weathering period

Although the diameter dependency is eliminated, equation (5) fails to describe the regression rate for initial fuel thickness smaller than 8 mm. It has been pointed out by many authors (Brzustowski, and Twardus (1981), Alramadhan (1990), Arai et al. (1990), Garo et al. (1994, 1996)) that the water bed acts as a heat sink. Since the thermal diffusivity of the water is significantly greater than that of the fuel (Table 1), as the fuel layer becomes thinner the overall thermal diffusivity increases. Heat conduction through the fuel and water increases ( $\dot{q}_C''$ ) and the overall fraction of the total heat flux ( $\dot{q}_S''$ ) used to vaporize the fuel decreases. The resulting decrease in the regression rate can eventually lead to extinction.

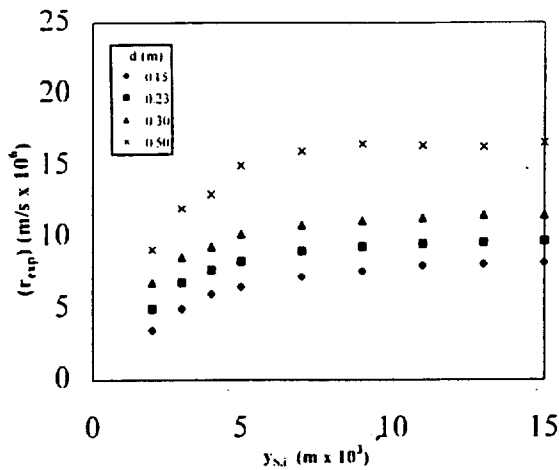


Figure 6 Regression rate for 20% water emulsified, 24 hour weathered crude oil

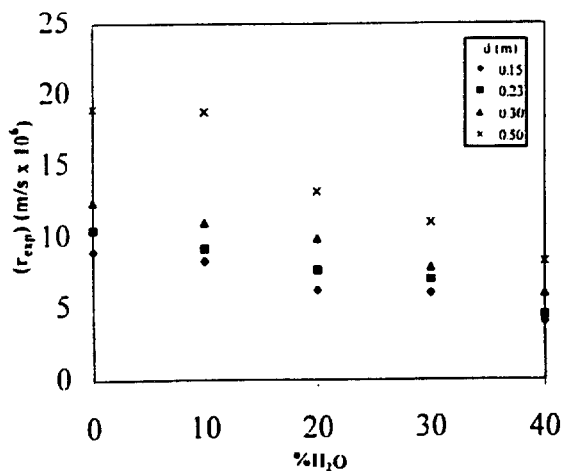


Figure 7 Regression rate change with water content (24 hour weathered crude oil)

It is also of great importance to point out that the data for weathered and emulsified crude oil also falls into one single curve when scaled by the predicted regression rate (Figures 10 and 11). The same reasoning presented above applies for these cases being the only difference the regression rate magnitude. Weathering and

emulsification alter the thermal properties of the fuel and , thus, the magnitude of the regression rate. By changing the efficiency constant ( $\chi$ ) to fit the experimental data, a practical way is found to incorporate the effect of weathering and emulsification on the fuel properties. The variation of the efficiency constant as a function of the weathering period and the water content is shown in Figures 12 and 13, respectively. Figure 11 shows fast decrease of the efficiency constant ( $\chi$ ) is observed initially that later develops into a slow almost linear decrease. It is well known that the highly volatile hydrocarbons will evaporate very fast, i.e. after less than 24 hrs the mass loss of hydrocarbons with boiling points below 500 K ( $<C_{11}$ ) has reached 95% and only reaches total evaporation after 48 hours (Desmarquest, 1983). Heavier hydrocarbons ( $C_{11}-C_{25}$ ) tend to evaporate significantly slower reaching 100% mass loss only after more than 10 days. The initial fast change in fuel properties results in an abrupt decrease of  $\chi$ , followed by a less dramatic change that can be approximated by a linear decrease. For emulsified fuels water addition will result in a linear decrease of  $\chi$  (Figure 13). The properties of the emulsified fuel can be obtained by averaging the fuel and water properties and, thus, is expected to change linearly. Addition of water increases the latent heat of vaporization ( $H_V$ ) and the thermal conductivity ( $\lambda_F$ ), the former one almost by an order of magnitude and the latter almost five fold, the thermal diffusivity ( $\alpha_F$ ) is also doubled (Table 1). From observing equation (5) it can be concluded that the regression rate should decrease linearly while the flame can supply enough heat to support fuel and water evaporation. Eventually the linear dependency of  $\chi$  with the water content will break and extinction will follow.

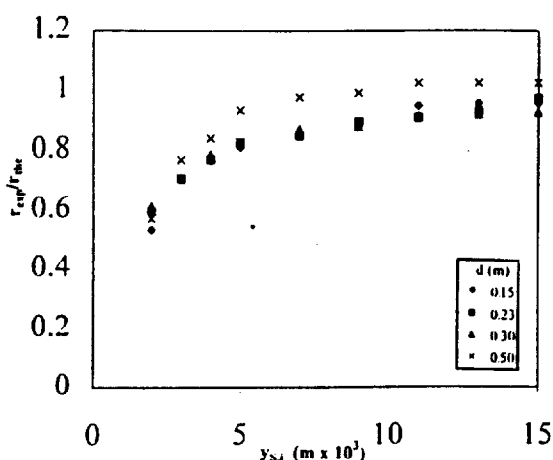


Figure 8 Non-dimensional regression rate (crude oil)

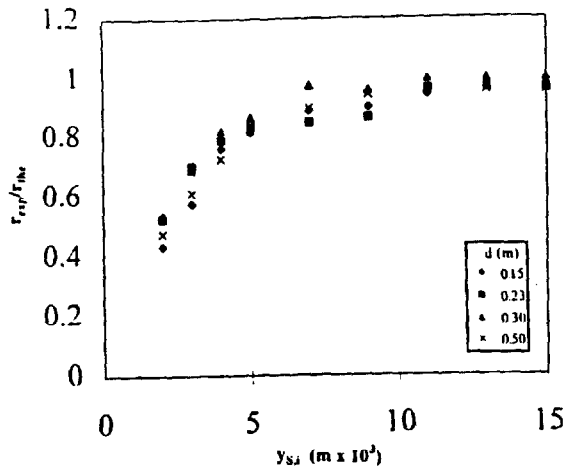


Figure 9 Non-dimensional regression rate (heating oil)

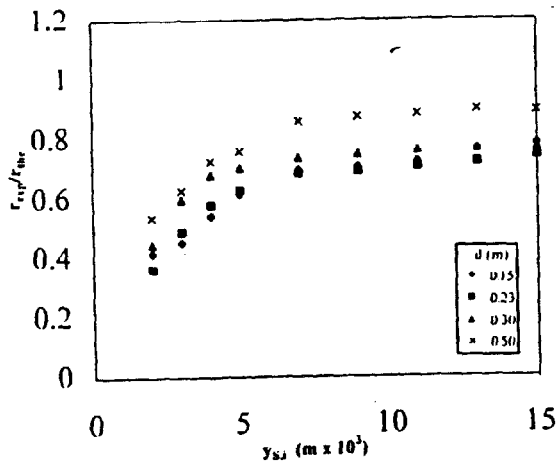


Figure 10 Non-dimensional regression rate (24 hour weathered crude oil)

## CONCLUSIONS

A simple one dimensional heat conduction model has been used to describe the regression rate of a fuel layer on a water bed. Crude and heating oil have been used to test the validity of the model for a wide range of conditions. The model describes accurately the regression rate for fuel layers thicker than 8 mm. Deviations from the predicted values arise from the assumption that fuel and water have similar thermal properties. For fuel layer thinner than 8 mm the higher thermal diffusivity of water reduces the regression rate. The model accurately describes for all conditions the pool diameter effect.

A value for an efficiency constant,  $\chi$ , of 0.03 is obtained for both fuels under all experimental conditions. The efficiency constant represents the fraction of the energy released at the flame that will be retained by the fuel/water. The efficiency constant seems to be fuel independent but this statement requires verification with other fuels.

Weathering and emulsification affect the fuel properties and, thus, the regression rate. An increase in the weathering period and in the water content results in a decrease in the regression rate. Although weathering and emulsification affect the fuel properties, a practical way of incorporating this effect is by introducing this dependency in the efficiency constant. It was found that after a sudden decrease, the efficiency constant decreases linearly with the weathering period. A linear decrease was also found with the water content.

## ACKNOWLEDGMENTS

The authors express their thanks to the Centre de Documentation de Recherches et d'Experimentations sur les Pollutions Accidentelles des Eaux, Brest, France, for its interest and help in this study.

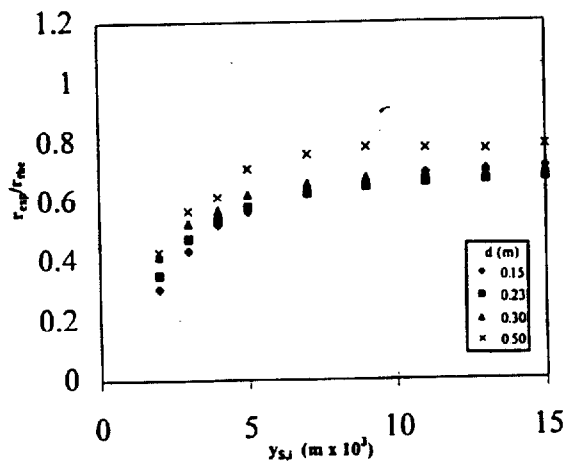


Figure 11 Non-dimensional regression rate (24 hour weathered, 20% water crude oil)

## REFERENCES

Alramadhan, M.A., Arpaci, V.S. and Selamet A., *Combustion Science and Technology*, 72, 233-253, 1990.

Arai, M., Saito, K. and Altenkirch, R.A., *Combustion Science and Technology*, 71, pp.25-40, 1990.

Bech, C., Sveum, P. and Buist, I., *Proceedings of the Third Arctic And Marine Oil Spill Program Technical Seminar*, Ministry of Supply and Services Canada, pp. 735-748, 1990.

Brzustowski, T.A. and Twardus, E.M., *Nineteenth Symposium (International) on Combustion*, The Combustion Institute, 847-854, 1982.

Cox, G., *Combustion Fundamentals of Fire*, Academic Press, London, 1995.

Desmarquest, J.P. "Les Polluants Petroliers et leur Evolution en Mer", Report CEDRE, R.83727.E, 1983.

Drysdale, D.D., *An Introduction to Fire Dynamics*, John Wiley and Sons, 1985.

Williams, F.A., *Combustion Theory*, The Benjamin/Cummings Publishing Company Inc., 1985.

Evans, D., Walton, W., Baum, H., Lawson, R., Rehm, R., Harris, R., Ghoniem, A. and Holland, J., *Proceedings of the Third Arctic And Marine Oil Spill Program Technical Seminar*, Ministry of Supply and Services Canada, Cat. No. En40-11/5-1990, pp. 1-38, 1990.

Garo, J. P., Vantelon, J. P. and Fernandez-Pello, A.C., *Twenty-fifth Symposium (International) on Combustion*, The Combustion Institute, 1481-1488, 1994.

Garo, J. P., Vantelon, J. P. and Fernandez-Pello, A.C., *Twenty-fifth Symposium (International) on Combustion*, The Combustion Institute, (in press), 1996.

Garo, J.P., "Combustion d'Hydrocarbures Repandus en Nappe sur un Support Aqueux. Analyse du Phenomen de Boilover", Ph.D. Thesis, University of Poitiers, France, 1996.

Henry, M. and Klem, T., *Fire Safety Today*, 11-13, 6, 1983.

Ito, A., Inamura, T. and Saito, K., *ASME/JSME Thermal Engineering Proceedings*, 5: 277-282, 1991.

Jason, N.H. *Proceedings of the Alaska Arctic Offshore Oil Spill Response Technology Workshop*, NIST SP762, U.S. Government Printing Office, Washington D.C., pp. 47-95, 1989.

Koseki, H. and Mulholland, G.W., *Fire Technology*, 27(1), 55-65, 1991.

Koseki, H. Kokkala, M. and Mulholland, G.W., *Fire Safety Science-Proceedings of the Third International Symposium*, 865-875, 1991.

McCaffrey, B. J., NBSIR 79-1910, National Bureau of Standards, Washington D.C., 1979.

Pipkin, O. A. and Sliepcevich, C. M., *Ind. & Eng. Chem. Fundamentals*, 3, 2, 147, 1964.

Putorti, A. D., Evans, D. D. and Tennyson, E. J., *Proceedings of the Seventeenth Arctic and Marine Oil Spill Program Technical Seminar*, pp.657-667, 1994.

Ross, H.D. *Progress in Energy and Combustion Science*, 20, pp.17-63, 1994.  
 Glassman, I. and Dryer, F., *Fire Safety Journal*, 3, 132, 1981.

Thompson, C. H., Dawson, G. W. and Goodier, J. L. *Combustion: An Oil Spill Mitigation Tool*, PNL-2929, National Technical Information Service, Springfield, VA22161, 1979.

Twardus, E.M. and Brzustowski, T.A., *Archivum Combustionis*, Polish Academy of Sciences, 1, 1-2,49-60, 1981.

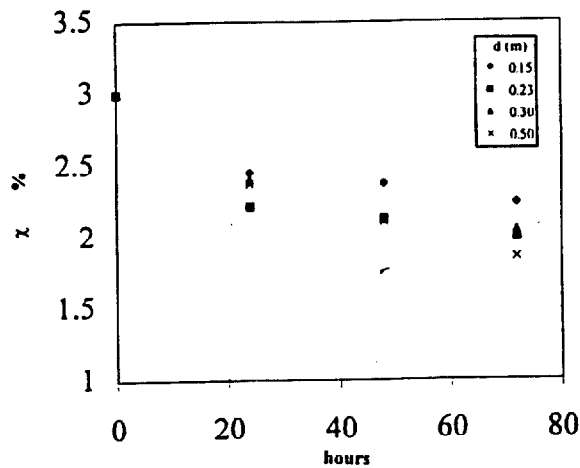


Figure 12 Efficiency constant (weathered crude oil)

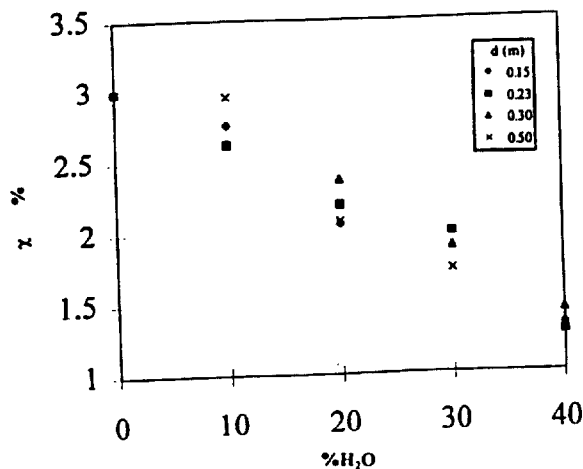


Figure 13 Efficiency constant (24 hour weathered, emulsified crude oil)

**BLANK PAGE**

#### **4. Ignition and Flame Spread and Mass Burning Characteristics of Liquid Fuels on a Water Bed**

**BLANK PAGE**

**4.1. Ignition and Flame Spread and Mass Burning Characteristics of Liquid Fuels on a Water Bed**

N. Wu, M. Baker, G.Kolb and J.L. Torero

*20<sup>th</sup> Arctic and marine Oilspill Program (AMOP) Technical Seminar,  
Vancouver, Canada, June 1997.*

**BLANK PAGE**

# Ignition, Flame Spread and Mass Burning Characteristics of Liquid Fuels on a Water Bed

Neil Wu, Michael Baker, Gilles Kolb and Jose L. Torero\*  
Department of Fire Protection Engineering  
University of Maryland, College Park, MD20742-3031  
USA

## Abstract

An experimental technique has been developed to systematically study the ignition, flame spread and mass burning characteristics of liquid fuels spilled on a water bed. The final objective of this work is to provide a tool that will serve to assess a fuel's ease to ignite, to spread and to sustain a flame, thus helping to better define the combustion parameters that affect in-situ burning of oil spills. A systematic study of the different parameters that affect ignition, flame spread and mass burning has been conducted in an attempt to develop a bench scale procedure to evaluate the burning efficiency of liquid fuels in conditions typical of oil spill scenarios. To study ignition and flame spread, the Lateral Ignition and Flame Spread (LIFT) standard test method (ASTM E-1321) has been modified to allow the use of liquid fuels and a water bed. Characteristic parameters such as the critical heat flux for ignition, ignition delay time and flame spread velocity as a function of the external heat flux have been obtained. A series of "fire properties" corresponding to the fuel can be extrapolated from these tests and used to assess the tendency of a fuel to ignite and to sustain flame spread. Mass burning has been studied by determining the burning efficiency of different fuels ( $\chi$ ) under conditions where a simple one-dimensional heat conduction model describes the surface regression rate.

## 1.0 Introduction

The burning of oil in water is of great interest as a result of off-shore exploration, production and transportation of petroleum. This combustion phenomenon may constitute a hazard, i.e. and accidental burning slick drifting towards a platform, but it may also serve as a measure to minimize the environmental damage of an oil spill (Twardus *et al.*, 1981, Evans *et al.*, 1990, Walavalkar *et al.*, 1996).

The available information on this phenomena is quite limited. Although great effort has been devoted to the understanding of pool fires (Drysdale, 1985) and flame spread over liquid pools (Williams, 1985, Ross, 1994, Glassman *et al.*, 1981) the specific issues related to a fuel burning over a water bed have deserved little attention. Most of the work being related to fires in fuel tanks and the phenomena commonly referred as "boilover" (Ito *et al.*, 1991, Arai *et al.*, 1990). Only a few studies have dealt with the burning of a thin layer of fuel on a water bed. A good summaries of the existing knowledge are provided by Evans *et al.* (1990) and Walavalkar and Kulkarni (1996).

In an attempt to provide an adequate methodology for ignition of oil-spills a review of the ignition methods commonly used for oil spill clean-up was provided by Jason (1989). Ignition source temperatures and successful ignition conditions have also

---

\* Corresponding author

been a subject of interest (Bech *et al.*, 1990, Thompson *et al.*, 1979). A cone calorimeter was used by Putorti *et al.* (1994) to quantify the heat flux necessary to accomplish ignition of different fuel. In this work emphasis was given to the effects of weathering and emulsification on the ignition delay time.

Assuming that the fuel layer is ignitable an important concern is thin layer boil-over. The term "boilover" has been usually applied to a fire scenario in which an open top tank containing burning crude oil, after a long period of quiescent burning, shows a sudden increase in fire intensity associated with the expulsion of burning oil from the tank (Henry *et al.*, 1983). The term boilover has also been applied to the burning of thin layers of fuel on the surface of water in order to limit the spread of oil after an accident (Koseki *et al.*, 1991a, 1991b). This scenario is commonly referred as thin layer boil-over. Although somehow different in nature, both cases result from the onset of boiling nucleation at the fuel/water interface and therefore, the time from ignition to the onset of boilover correlates well with the time needed for the thermal wave to reach the water (Garo *et al.*, 1994).

Geometrical considerations pertaining to burning rate are of great importance when considering the use of burning for oil spill cleanup. If the oil spill is not contained, the fuel layer thickness decreases till self-sustained burning is no longer possible. Typical values on the order of 0.5 mm have been identified as a minimum thickness for self-sustain burning (Arai *et al.*, 1990, Garo *et al.*, 1994, Alramadhan *et al.*, 1990). The effect of fuel thickness, pool diameter and fuel boiling point on the burning rate has also been studied by Garo *et al.* (1994, 1996) who observed that the burning rate does not depend on the initial fuel layer thickness for fuel layers thicker than 10 mm and decreases for thinner layers.

One of the first attempts to model this type of problem was made by Twardus and Brzustowski (1981), who developed a simple one-dimensional model to describe the combustion of oil slicks on water. This model describes the burning process as that of a pool fire with a heat loss term from the fuel to the water underneath. Heat losses from the fuel towards the water will increase as the fuel layer thickness decreases, therefore, a minimum thickness for self-sustained burning can be established. In a later model Brzustowski and Twardus (1982) incorporated the effects of radiative absorption in the fuel and the effect of tilting by the wind. A more realistic model that incorporates radiative feedback and the effects of turbulent buoyant motion was subsequently developed by Alramadhan *et al.* (1990), emphasis was given to the regressing surface and the gas phase and no account for heat transfer towards the water bed was made. Although these simple theories obtain expressions for the burning rate and minimum thickness for self-sustained burning, they all fail to describe the evolution of the burning rate as the fuel thickness decreases below 10 mm.

A simple way to classify all studies relevant to in situ burning of an oil slick over a water bed is by dividing the combustion process in its three different stages, ignition, flame spread and self sustained burning (or mass burning). An external source of energy will lead to ignition, which will be followed by the spread of the flame across the fuel surface. Although flame spread might be an instantaneous process for many crude oils in their natural state, the loss of highly volatile compounds, due to weathering, and the presence of water in emulsions might lead to flame spread that needs to be assisted by external radiation. For thin fuel layers, heat losses to the water bed, might lead to a

similar situation. For these particular cases a minimum size might be necessary to provide the necessary radiative heat feed back to self-sustain flame spread. Once the flame spread process is self sustained mass burning will follow. For all three distinctive processes boiling of the water bed underneath the fuel might occur and its effect on the characteristics of the combustion process needs to be considered.

This work attempts to identify an ideal configuration in which the ease by which a fuel can burn can be evaluated. The three aspects of the combustion process, ignition, flame spread and mass burning will be studied in an attempt to obtain results that depend only on the fuel. The results should be independent of specific burning characteristics and geometrical constraints, and thus, extrapolation to a large scale should be possible.

## 2.0 Methodology

Fuel properties vary significantly when subject to a strong heat insult, therefore, they need to be evaluated under fire conditions. Evaluation of the fuel “fire properties” that are independent of the length scale will permit the ranking of fuels in their natural state, weathered, emulsified and with additives and will allow the reduction of the number of large scale experiments necessary to determine in-situ burning protocols and procedures. By focusing on the fuel and introducing external radiation, large scale conditions can be simulated (radiation feedback from the flame to the fuel increases with length scale). It has to be noted that this is not a study of the burning characteristics but of the fuel burning efficiency. Ignition and flame spread will be studied by using the Lateral Ignition and Flame Spread Test (ASTM E-1321) and mass burning by observing the regression rate under conditions where the characteristics of the flame can be predicted adequately.

### 2.1 The Lateral Ignition and Flame Spread Test (ASTM E-1321)

The Lateral Ignition and Flame Spread Test (LIFT) provides characteristic “fire properties” for ignition and flame spread. Results are normally presented on “Flammability Diagrams” that provide ignition delay times and flame spread velocities as a function of the external heat flux (or characteristic length scale of the fire). The LIFT has the advantage that it allows for ignition and flame spread to be studied together which provides a more realistic scenario than other test methods, such as the cone calorimeter. The theoretical background behind this test method is extensive and more clear than for other tests therefore it provides an adequate framework for the study of complex fuels such as composite materials or crude oils.

#### 2.1.1 Theoretical Background

The basis of the theoretical model behind this test method can be described as ignition and flame spread as a result of inert heating of a thermally thick homogeneous solid to an ignition temperature. The flame configuration applies to a flame spreading into an opposed ambient flow which corresponds well to flame spread occurring in in-situ burning. The fuel is considered thermally thick and its initial temperature and that of the ambient is constant at  $T_i$ . An inert fuel layer is assumed with negligible pyrolysis before ignition, and an ignition temperature ( $T_{ig}$ ) is employed as criterion for flame spread. The position of the flame or pyrolysis front is identified by  $x_f$  as where the surface temperature has reached  $T_{ig}$ . Heat is transferred to the solid ahead from the pyrolysis

front from the external source ( $\dot{q}_e''(x, t)$ ) and from the flame ( $\dot{q}_f''$ ). Flame heat transfer ahead of the pyrolysis front is considered to occur over a region  $\delta_f$  with a uniform heat flux of  $\dot{q}_f''$  unaffected by  $\dot{q}_e''(x, t)$ . Although the flame heat flux is represented as a surface heat flux, more general heat transfer effects could be considered without changing the form of the final results.

The problem is analyzed by considering the heat transfer history, due to flame and external fluxes, at the flame front  $x_f(t)$ . This constitutes a conduction problem with an arbitrary time varying heat flux  $\dot{q}_e''(x, t)$  which depends on the position of the flame front,  $x=x_f(t)$ , as well. The solution to this problem is readily derivable from results given by Carslaw and Jaeger (1963) or by standard analytical techniques. An elaboration of additional assumptions and the derivation of the solution are given by Quintiere (1981). There it is shown that the transient solution for the flame spread velocity can be derived from the following expression

$$T_{ig} - T_i = \frac{\dot{q}_f''}{h} \frac{2}{\sqrt{\pi}} \sqrt{\frac{a\delta_f}{V_f}} \left( 1 - \frac{\sqrt{\pi}}{2} \sqrt{\frac{a\delta_f}{V_f}} \right) + \frac{\sqrt{a}}{h\sqrt{\pi}} \int_b^t \frac{\dot{q}_e''(x_f, s)}{\sqrt{t-s}} ds - \frac{a}{h} \int_b^t \dot{q}_e''(x_f, s) \exp(a(t-s)) \operatorname{erfc}(\sqrt{a(t-s)}) ds \quad (1)$$

where

$$V_f = \frac{dx_f}{dt} \quad (2)$$

The characteristic time to reach thermal equilibrium can be expressed as  $1/a$  where  $a = \alpha (h/k)^2$ . Typically,  $a$  is of  $O(10^{-3})$  to  $O(10^{-2})$   $s^{-1}$ , and  $a\delta_f/V_f$  is of similar order of magnitude.

The definition of "h" deserves special attention. The parameter "h" represents the summation of the convective heat losses and the fraction of the external heat flux not absorbed by the surface. Both heat loss terms can be expressed by  $h(T_{ig}-T_i)$  as a result of a linear approximation to convective and radiative heat losses (Mikkola *et al.*, 1989).

Equation (1) is then an integro-differential equation for the flame front position  $x_f$ . The left-hand side represents the temperature rise required to sustain flame spread and the right-hand side represents the sum of the temperature increases due to the flame heat transfer,  $\dot{q}_f''$ , and the heating imposed by the flux field,  $\dot{q}_e''(x, t)$ . Making the imposed flux field independent of time will result in significant simplification of equation (1) and of the experimental procedure, therefore,  $\dot{q}_e''$  will be considered only a function of  $x$  and thus, equation (1) can be written as:

$$h(T_{ig} - T_i) - \dot{q}_e''(x_f)[1 - \exp(at)\operatorname{erfc}(\sqrt{at})] = \frac{2}{\sqrt{\pi}} \dot{q}_f'' \sqrt{\frac{a\delta_f}{V_f}} \left( 1 - \frac{\sqrt{\pi}}{2} \sqrt{\frac{a\delta_f}{V_f}} \right) \quad (3)$$

### 2.1.2 The Ignition Mechanisms

The gas phase ignition of a solid combustible is generally the combined result of an externally imposed heat flux (radiation and convection) that causes the gasification of the solid, and the presence of conditions (in the gas or external to it) that will lead to the onset of a sustained combustion reaction. If the reaction is initiated by an ignition source

(open flame, electrical spark, flying ember, etc.), ignition is normally referred to as piloted ignition. If ignition occurs without a pilot, the process is normally referred as spontaneous, or auto, ignition. For both cases, when the solid combustible is suddenly exposed to a sufficiently strong external heat flux ignition occurs after a certain time, this time is commonly referred in the literature as ignition delay time. The ignition delay time has been defined by Fernandez-Pello (1995) as:

$$t_{ig} = t_p + t_{in} \quad (4)$$

where  $t_p$  is a characteristic time for fuel gasification and  $t_{in}$  is a characteristic time for gas phase ignition. The mechanisms leading to gas phase ignition under these circumstances are complicated and difficult to predict. In a phenomenological way the process is as follows: after fuel pyrolysis, the vapor (pyrolysate) leaves the surface, and is diffused and convected outwards, mixing with the ambient oxidizer and creating a flammable mixture near the solid surface. This period corresponds to the pyrolysis time and depends uniquely on the material and the heating conditions. If the mixture temperature is increased, either by heat transfer from the hot ambient gas, a pilot or any other mechanism, the combustion reaction between the fuel vapor and the oxidizer gas may become strong enough to overcome the heat losses to the solid and ambient, and become self-sustained at which point flaming ignition will occur. This period corresponds to the induction time and is derived from a complex combination of fuel properties and flow characteristics. Under ideal conditions, introducing a pilot reduces the induction time making it negligible when compared to the pyrolysis time. Thus, the fuel and oxidizer mixture becomes flammable almost immediately after solid pyrolysis starts and therefore, pyrolysis temperatures and times are commonly referred as ignition temperature and ignition time (Quintiere, 1981, Quintiere *et al.*, 1983, 1984).

$$\text{if } t_{in} \ll t_p \Rightarrow t_{ig} = t_p \text{ and } T_{ig} = T_p \quad (5)$$

Although such a definition is not physically correct (Alvares *et al.*, 1971) it can be very useful in some practical applications since it not only yields fairly accurate results but also provides a reference parameter that could serve to characterize the ignitability of a solid material. For most practical situations, the flow over the fuel surface will control the mixing of fuel and oxidizer ( $t_M$ ) as well as the transport ( $t_T$ ) of this mixture towards the pilot, therefore, can have a significant effect on  $t_{in}$  and on the validity of equation (5). The relative effect of the flow on  $t_{ig}$  will decrease as the characteristic velocity of the system increases (characteristic time for mixing and transport decrease) and as  $\dot{q}_e''$  decreases ( $t_p$  increases).

Before ignition, no heat is being supplied by the flame,  $\dot{q}_f'' = 0$ , therefore, equation (3) can be reduced to

$$h(T_{ig} - T_i) = \dot{q}_e''(x_f)[1 - \exp(-at)\text{erfc}(at)] \quad (6)$$

for values of  $\dot{q}_e''$  lower than a critical value  $\dot{q}_{0,ig}''$ , the system reaches thermal equilibrium ( $T_{EQ}$ ) before the surface temperature arrives to the ignition temperature therefore no ignition occurs and for  $t \rightarrow \infty$  equation (6) becomes:

$$T_{EQ} = T_i + \frac{\dot{q}_c''}{h}$$

if  $T_{EQ} \geq T_p$ , ignition is expected to occur and a critical heat flux for ignition can be derived from equation (6) if  $T_{EQ}=T_p$ , and is given by:

$$\dot{q}_{0,ig}'' = h(T_p - T_i) \quad (7)$$

The practical implications of equations (6) and (7) are many. A characteristic ignition delay time ( $t_{ig}$ ) results from equation (6). By assuming that

$[1 - \exp(-at)\text{erfc}(\sqrt{at})] \approx \frac{2}{\sqrt{\pi}} (at)^{1/2}$  (for  $\dot{q}_c'' > \dot{q}_{0,ig}''$ ) then:

$$t_{ig} = \frac{\pi}{4a} \left( \frac{h(T_p - T_i)}{\dot{q}_c''} \right)^2 \quad (8)$$

and used to attempt the prediction of  $t_p$  (Putorti *et al.*, 1994). It needs to be noted that for this expression to be valid, both mixing ( $t_M$ ) and transport ( $t_T$ ) times have to be neglectable when compared to  $t_p$  ( $t_M \approx t_T \ll t_p$ ). This will be satisfied best as the external heat flux approaches the critical heat flux for ignition ( $\dot{q}_c'' \approx \dot{q}_{0,ig}''$ ) and  $t_p \rightarrow \infty$ . This is important because it implies that the error incurred in the experimental determination of  $t_{ig}$ , (due to the unknown nature of the flow) will decrease as  $\dot{q}_c''$  approaches  $\dot{q}_{0,ig}''$ . Therefore,  $\dot{q}_{0,ig}''$  is a property of the fuel that can be extrapolated, independent of the flow. Instead, equation (8) could be extrapolated only if the experimental conditions at which “a” and “h” were obtained satisfy the assumption that  $t_M \approx t_T \ll t_p$ .

From equation (7) a value of “h” can be extracted from the experimental results and is given by:

$$h = \frac{\dot{q}_{0,ig}''}{(T_p - T_i)} \quad (9)$$

As mentioned before,  $h(T_p - T_i)$  accounts for the total convective and radiative heat losses. The relative importance of convective and radiative heat losses is extremely difficult to determine, although, if the fuel requires a high external heat flux to ignite or the flow velocity over the fuel surface is very low, it can be assumed that external radiation will be the dominant element and heat losses could be effectively represented as a fraction of the external heat flux that only depends on the fuel and is independent of the flow. For this particular case, h, will become a property of the fuel that characterizes the fraction of the incident heat flux that is absorbed by the fuel. Beyond a critical value, changes in the flow velocity will affect the value of “h” and will serve to quantify the effect that a wind might have on the ignition characteristics of a fuel.

### 2.1.3 Flame Spread

Once the flame is ignited and propagation starts all terms in equation (3) have to be used to describe the temperature evolution of the solid. For most fuels of interest the

term  $\sqrt{a\delta_f}/V_f \ll 1$  and if the pilot is not started till the solid has been preheated to thermal equilibrium, the time dependency is eliminated from equation (3) and the following expression describes the flame spreading process

$$V_f^{-1/2} = \left[ \frac{\sqrt{\pi}}{2\sqrt{a\delta_f}\dot{q}_f''} \right] [h(T_{ig} - T_i) - \dot{q}_e''(x_f)] \quad (10)$$

It has to be noted, from equation (3), that  $V_f \rightarrow \infty$  when  $\dot{q}_e'' = \dot{q}_{0,ig}''$ , meaning that for an external heat flux of  $\dot{q}_{0,ig}''$  the heat from the flame is not needed any more for the reaction to propagate through the solid fuel. Under these conditions, the flame will instantaneously establish over the entire heated surface.

#### 2.1.4 Flame Extinction Mechanisms

The process leading to non-spreading and subsequent extinction of the diffusion flame is the result of a complex combination of the flow field characteristics and fuel properties with a finite chemical reaction. Solutions to the extinction problem have been previously reported, and it has been demonstrated that an appropriate description demands an elliptic resolution of the complete Navier-Stokes equations (Kodama *et al.*, 1987, Chen *et al.*, 1986). Non-spreading or extinction of a flame occurs when the heat generated by a finite chemical reaction (Frey *et al.*, 1979) added to the heat flux from an external source can not balance the heat necessary to increase the temperature of the fuel and oxidizer flow to that of the flame plus heat losses. Among the heat losses are those to the geometrical boundaries, flame radiation to the environment and surface radiation (McCaffrey, 1979).

The solution to equation (1) has a lower limit,  $V_f = \pi a \delta_f$ , that, under the condition of thermal equilibrium, yields a minimum external heat flux,  $\dot{q}_{0,s}''$ , necessary for the flame to spread.

$$\dot{q}_{0,s}'' \equiv \dot{q}_e'' = h(T_{ig} - T_i) - \frac{\dot{q}_f''}{\pi} \quad (11)$$

#### 2.1.5 Summary

The above exposed theory represents the basis of an experimental procedure to give a relative assessment of the "flammability" of a fuel (Quintiere, 1981, Quintiere *et al.*, 1983, 1984). Materials can be ranked based on three different principles, readiness to pilot ignition, susceptibility to flame spread and extinction characteristics. The experimentally obtained parameters should be environment independent so as to be considered properties of the material.

By heating the combustible material with a constant heat flux till piloted ignition occurs, a diagram of the characteristic ignition time can be obtained. From these experiments the minimum heat flux for ignition ( $\dot{q}_{0,ig}''$ ) can be extracted and, by using equation (7), incorporated in equation (6) leading to

$$\frac{\dot{q}_e''}{\dot{q}_{0,ig}''} = \frac{1}{[1 - \exp(at)\text{erfc}(\sqrt{at})]} \quad (12)$$

For simplicity, the approximate expression given by equation 8 can be used for  $\dot{q}'' > \dot{q}_{e,ig}''$ .

Verification of the minimum external heat flux for ignition can be obtained by conducting experiments with variable external heat fluxes of magnitude smaller than  $\dot{q}_{0,ig}''$ . By substituting equation (7) in equation (10) the following expression is obtained

$$V_f = \frac{\phi}{[\dot{q}_{0,ig}'' - \dot{q}_e'']^2} \quad \text{where} \quad \phi = \frac{4a\delta_f (\dot{q}_f'')^2}{\pi} \quad (13)$$

where  $\phi$  is a material property determined from the experiments and  $\dot{q}_{0,ig}''$  can be obtained by increasing the external heat flux till  $V_f \rightarrow \infty$ , thus, by conducting ignition and flame spread experiments the value for minimum heat flux for ignition can be verified. Reducing the external heat flux will eventually lead to extinction, thus a minimum velocity ( $V_{f,min}$ ) and external heat flux ( $\dot{q}_{0,s}''$ ) for flame spread can be recorded. As mentioned before  $\dot{q}_{0,s}''$  does not necessarily coincide with the minimum external heat flux for flame spread predicted by equation (11).

Using the values of  $\dot{q}_{0,ig}''$  and  $\dot{q}_{0,s}''$ , obtained experimentally and equations (12) and (13) a "flammability diagram" (Quintiere *et al.*, 1983, 1984) can be obtained for each material of interest. These diagrams, under known experimental conditions, will serve as a useful way to assess and rank the fire performance of fuels and to identify the parameters that dominate their fire characteristics.

## 2.2 Experimental Apparatus

### 2.2.1 The L.I.F.T.

The experimental configuration used as starting point for the design of these experiments is the Lateral Ignition and Flame Spread Test (L.I.F.T.) which is an ASTM standard for the determination of material ignition and flame spread properties (ASTM-E-1321, 1993). Details on the dimensions and geometrical characteristics of this apparatus can be found in the above referred standard.

The procedure and theory behind this test was established by Quintiere *et al.* (1981, 1983, 1984) and consists of two independent tests, a pilot ignition test and a lateral flame spread test. For both tests the fuel sample is placed in front of a radiant panel (483 mm x 280 mm) forming an angle of 15° with the fuel surface with a minimal distance between fuel and panel of 125 mm. The radiant panel provides a heat flux distribution to the fuel surface which is almost constant where sample and specimen are closer and decays as the distance between the panel and the sample increases. Characteristic heat flux distributions can be found in references (Quintiere, 1981, Quintiere *et al.*, 1983, 1984, and ASTM Standards, 1993). The ignition specimen (155 mm x 155 mm) is placed in the region of nearly uniform heat flux and the full sample (155 mm x 806 mm) is used to study the effect of external radiation on lateral flame spread. Recent tests with PMMA have shown that the fuel sample size can be significantly reduced without any significant changes (Cordova *et al.*, 1997) in the "fire properties" this observation has motivated the reduction of the sample size for the experiments to be conducted with liquid fuels.

### 2.2.2 The H.I.F.T.

The experimental apparatus described above has been used to study the ignition and flame spread characteristics of liquid fuels on a water bed. The L.I.F.T. hardware had to be significantly modified for this purpose. Figure 1 shows a schematic of the modified hardware. Since both the panel and fuel tray are, in this case, horizontal, the modified hardware is commonly referred as H.I.F.T. (Horizontal Ignition and Flame Spread Test). This geometrical configuration has been previously used to study materials from which the vertical configuration was not convenient (Motevalli *et al.*, 1992).

When the fuel sample is placed parallel to the gravity vector natural convection serves to transport the fuel towards the pilot flame. By placing the sample horizontally the dominant direction for the flow is lost. This change in geometry imposes significant disadvantages to the study of ignition. Natural convection over a horizontal hot surface is much more complex than a vertical natural boundary layer and makes ignition more susceptible to environmental changes and to geometry. For the L.I.F.T. the pilot flame can be placed away from the sample, since buoyancy will carry the pyrolysis products towards the pilot. In the absence of a forced flow (for the H.I.F.T.) it is necessary to place the pilot directly above the fuel surface. Many studies have shown that although pilot flames are the most consistent mechanism for ignition they tend to enhance local evaporation (Ross, 1994, Glassman *et al.*, 1981) therefore spark ignition is generally preferred (Putorti *et al.*, 1994). A number of different pilot locations have been tested to try to show this effect and the results will be presented in following sections. A detailed study that involved changes in pilot location, flow structure and tray geometry lead to the configuration shown in figure 1.

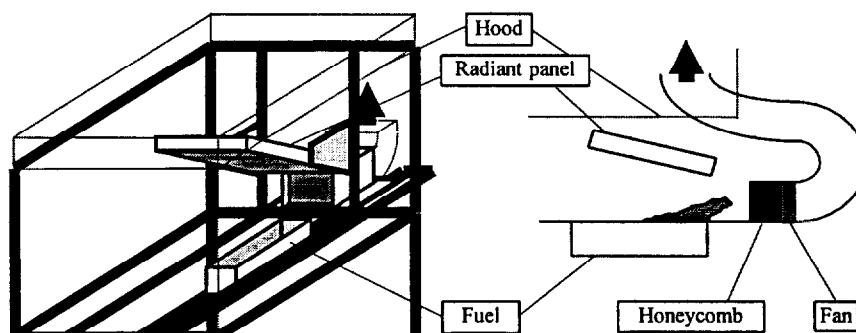
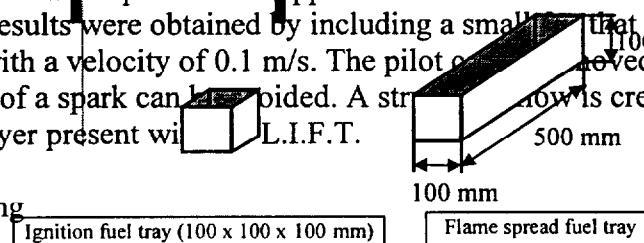


Figure 1. Schematic of the Experimental Apparatus

Consistent results were obtained by including a small fan that induces, by aspiration, a flow with a velocity of 0.1 m/s. The pilot flame is placed above the fuel surface and the use of a spark can be provided. A stratified flow is created simulating the natural boundary layer present with the L.I.F.T.

### 2.3 Mass Burning



A simple way to assess the relative potential of a fuel to sustain mass burning is by using a burning efficiency ( $\chi$ ) extracted from a simple one-dimensional heat conduction model under conditions where the flame characteristics are known. The model relies on the concept that a fraction ( $\chi$ ) of the energy released by the flame is effectively used to support burning of the fuel. The higher the value of  $\chi$  the more effective the combustion process. The value of  $\chi$  is independent of the geometry (size, fuel layer thickness, etc.) and is only a function of the fuel. This value represents the mass burning efficiency of the fuel, is independent of the ignition and flame spread parameters and serves as a complement to the H.I.F.T. data.

### 2.3.1 Formulation

Heat release rate from a pool fire has been documented extensively (Drysdale, 1985, Cox, 1995, Garo, 1996) and it has been found that the expression

$$\dot{Q} = \rho_{\infty} C_p (T_{\infty} g (T_f - T_{\infty}))^{1/2} d^{5/2}$$

correlates well with values measured experimentally (Alramadhan *et al.*, 1990). The total heat release from the combustion process is denoted by  $\dot{Q}$ ,  $C_p$  is the specific heat at constant pressure and ambient temperature for air,  $T_{\infty}$  is the ambient temperature,  $T_f$  is an average flame temperature (for this work  $T_f \approx 1100$  K, Cox, 1995),  $g$  is the acceleration of gravity ( $g=9.81$  m/s<sup>2</sup>),  $d$  (diameter of the fuel pool) is the characteristic length scale,  $\rho$  is the density and the sub-index  $\infty$  stands for ambient conditions.

The net heat fed back to the fuel represents a small fraction of the total heat release, this fraction ( $\chi$ ) has been found to be independent of the pool diameter (Drysdale, 1985, Cox, 1995) and thus, the heat flux per unit area reaching the surface can be expressed as

$$\dot{q}_s'' = \chi \frac{4 \rho_{\infty} C_p (T_{\infty} g (T_f - T_{\infty}))^{1/2} d^{1/2}}{\pi} \quad (14)$$

If conduction is assumed to be the dominant heat transfer mechanism and if the thermal wave has not reached the fuel/water interface the fuel can be considered as semi-infinite and an expression for the temperature as a function of time and position can be obtained. This treatment can also be used when fuel and water have similar thermal diffusivities (Arai *et al.*, 1990, Garo *et al.*, 1994). This case will be referred as the “One-Dimensional Single Layer Conduction Model”. If fuel and water have significantly different thermal diffusivities and the thermal wave has already reached the fuel/water interface, fuel and water layers need to be treated independently. The water can still be assumed as semi-infinite but the fuel layer needs to be treated as a layer of finite thickness. This case will be referred as the “One-Dimensional Two Layer Conduction Model”.

Radiation through the fuel layer can be of importance (Alramadhan *et al.*, 1990) but for the fuels of interest it has been demonstrated that most of the radiative heat flux is absorbed very close to the surface (Garo, 1996). Natural convection inside the fuel and water layers can significantly enhance heat transfer close to the fuel surface but seems to affect only weakly steady burning for highly viscous fuels (Ross, 1994). The importance

of natural convection decreases with viscosity and its effects can be neglected for those fuels relevant to this study, this is not the case for less viscous fuels (i.e. octane, xylene, etc.) (Garo *et al.*, 1996). For simplicity, this analysis will assume conduction to be the dominant heat transfer mechanism.

Assuming no convective motion and that radiation is fully absorbed at the surface, the following energy balance can be made at  $y=y_s(t)$

$$\dot{q}_s'' = H_v \rho_F r(t) + \dot{q}_c'' \quad (15)$$

where  $\dot{q}_c'' = -\lambda_F \left. \frac{\partial T}{\partial y} \right|_{y=y_s(t)}$  is the heat conducted into the fuel layer,  $H_v$  is the latent heat of vaporization,  $t$  is a specific time,  $T$  is the temperature,  $\lambda$  is the thermal conductivity,  $r(t) = \frac{\partial}{\partial t} (y_s(t))$  is the regression rate,  $y_s(t)$  is the location of the fuel surface at a specified time, and the sub-index F stands for fuel. For the entire analysis, it is assumed that the ignition source brings the surface temperature to  $T_s$  (vaporization temperature of the fuel) instantaneously. The vaporization temperature is considered to remain constant throughout the entire burning time.

### 2.3.2 One-Dimensional Single Layer Conduction Model

This analysis is an extension of the works of Arai *et al.* (1990) and Garo *et al.* (1994). Details of the formulation will not be presented here and therefore, the reader is referred to these works for further information.

The heat conduction equation for a one-dimensional semi-infinite element is given by:

$$\frac{\partial^2 T}{\partial y^2} = \frac{1}{\alpha_F} \frac{\partial T}{\partial t} \quad (16)$$

with initial condition at

$$t=0, \quad T = T_\infty$$

and boundary conditions

$$y = y_s(t), \quad T = T_s$$

$$y \rightarrow \infty, \quad T = T_\infty$$

if  $\alpha_F$  is the thermal diffusivity of the fuel and “r” is assumed to be constant then the following expression for the temperature distribution can be obtained

$$\frac{T - T_\infty}{T_s - T_\infty} = \exp\left(-\frac{r}{\alpha_F} (y - y_s(t))\right) \quad (17)$$

this expression will be accurate if the thermal diffusivity of the fuel is approximately equal to the thermal diffusivity of water ( $\alpha_F \approx \alpha_w$ ) or for a time period “t” earlier than

the characteristic time for the thermal front to reach the fuel/water interface ( $t < t_c$ ). The characteristic time,  $t_c$ , can be derived by scaling equation (14)

$$t_c \approx \frac{y_{s,i}^2}{\alpha_F + y_{s,i}r}$$

where  $y_{s,i}$  is the initial thickness of the fuel layer. Knowing the temperature distribution it is possible to calculate  $\dot{q}_c''$  and by substituting in equation (15) an expression for the average regression rate can be calculated.

### 2.3.3 One-Dimensional Two Layer Conduction Model

The thermal diffusivity of water is significantly bigger than that of the fuels of interest and as soon as the thermal wave reaches the fuel/water interface, the water bed starts acting like a heat sink ( $t > t_c$ ). A full description of this scenario is given by the following set of differential equations and boundary conditions.

$$\frac{\partial^2 T}{\partial y^2} = \frac{1}{\alpha_F} \frac{\partial T}{\partial t} \quad (18)$$

$$\frac{\partial^2 T}{\partial y^2} = \frac{1}{\alpha_w} \frac{\partial T}{\partial t} \quad (19)$$

with initial condition at

$$t=0, T = T_\infty$$

and boundary conditions

$$\begin{aligned} y = y_s(t), T &= T_s \\ y = 0, -\lambda_F \frac{\partial T}{\partial y} \Big|_{y=0^+} &= -\lambda_w \frac{\partial T}{\partial y} \Big|_{y=0^-} \\ y \rightarrow \infty, T &= T_\infty \end{aligned}$$

The use of equation (15) and a complex solution of the equations (18) and (19) is necessary to obtain the corresponding temperature distributions and regression rate. The data available in the literature generally provides only average regression rates, therefore, only an order of magnitude comparison will be possible. A simplified approach that incorporates the main physical characteristics is, thus, used to solve the above system of equations in place of a numerical solution.

The average regression rate has been reported of the order of  $10^{-5}$  m/s (Garo *et al.*, 1994) and the thermal diffusivity for the liquids of interest is small, therefore, at each stage of the regression process only the steady conduction equation needs to be solved. The resulting temperature profiles are linear and an equivalent thermal diffusivity can be obtained. The equivalent thermal diffusivity results from matching the thermal penetration distance through a two layer bed with thermal diffusivities  $\alpha_F$  and  $\alpha_w$  and the thermal penetration distance in one single layer of thermal diffusivity  $\alpha_{EQ}$ . The characteristic length for the fuel layer will be  $y_{s,i}$  and the average regression rate,  $r$ , is assumed to be constant. From equations (18) and (19):

$$\alpha_{EQ} = \frac{r y_{S,i}}{\alpha_F} (\sqrt{\alpha_W} + \sqrt{\alpha_F})^2$$

The use of an equivalent thermal diffusivity enables formulation of the problem with one differential equation. The single differential equation corresponds to equation (16), where  $\alpha_F$  has been substituted by  $\alpha_{EQ}$  and the following expression for the average regression rate ( $r$ ) is obtained:

$$r = \frac{1}{H_V \rho_F} \left[ \chi \left( \frac{4 \rho_\infty C_p (T_\infty g (T_F - T_\infty))^{1/2}}{\pi} \right) d^{1/2} - \frac{\alpha_F \lambda_F (T_S - T_\infty)}{y_{S,i} (\sqrt{\alpha_F} + \sqrt{\alpha_W})^2} \right] \quad (20)$$

Equation (20) although simple and approximate provides an engineering tool that could be of great practical use.

### 2.3.5 Experimental Apparatus

The experimental apparatus, measurement methods and experimental procedures are those described by Garo *et al.* (1994, 1996) and therefore will only be described briefly here. Pool burning tests of a layer of liquid fuel floating on water were conducted in a large test cell vented by natural convection. Fuel and water were placed in stainless steel pans of 0.15 m, 0.23 m, 0.30 m and 0.50 m in diameter and 0.06 m deep. Some experiments were conducted with pans of different depths to verify that the results were independent of the pan depth. The pans were placed on a load cell to measure the fuel consumption rate. The load cell had a response time of 60 ms and an accuracy within +/- 0.5 g.

## 3.0 Experimental Results and Discussion

### 3.1 Ignition

To calibrate the H.I.F.T., SAE 30 W oil was used for ignition and flame spread tests. This fuel was used to make possible comparison with previously reported results on ignition delay time (Putorti *et al.*, 1994) and also because of its high flash point (approximately 250°C). A higher flash point results in a longer ignition delay time providing a longer period to observe the different flow structures formed inside the liquid fuel and on the gas phase. Radiation absorption is also lower with SAE 30 oil favoring boiling of the water bed. Although the viscosity of SAE 30 oil is generally higher than that of crude oils, it is very sensitive to temperature (approximately  $1 \times 10^{-2}$  at 0°C and  $1 \times 10^{-5}$  at 100°C) reaching comparable values after only a small temperature increase.

To assess the effect of the geometry on the ignition delay time different configurations were tested. Two different trays were used, a first tray with a 5mm lip surrounding the entire upper edge of the tray and a second tray where the lip was eliminated. Both trays were tested with and without a flush floor.

The main assumption regarding the theoretical models presented above is that the fuel will behave as a semi-infinite solid. The same methodology could still be applied if that was not the case but the solution will acquire unnecessary complications. It has been previously observed that the container has significant effects on the formation of recirculation currents inside the liquid. These recirculation currents enhance heat transfer

inside the liquid resulting in a more homogeneous temperature distribution (Venkatesh *et al.*, 1996) and in longer ignition delay times. Eight chromel-alumel thermocouples (0.5 mm in diameter) were placed in the liquid with the tip at the center of the tray to verify the effects of heat transfer from the tray towards the fuel. The thermocouples were placed at different depths and spaced to provide a finer grid close to the surface and to cover the entire depth of the tray.

Radiative heat flux from the panel increases the temperature of the fuel but also of the container. The inclusion of a 5 mm lip surrounding the upper edge of the tray increased the solid surface receiving radiation from the panel. The temperature of the upper part of the lip tray was observed to be significantly higher than that observed for the no-lip tray. Thermocouple measurements in the liquid showed that fuel surface temperature was consistently higher for the no-lip tray, while the temperatures recorded deeper in the fluid were higher for the lip tray.

Ignition was consistently observed when the surface temperature attained 254°C. Experiments using the no-lip tray will attain this surface temperature faster than those using the lip tray. Therefore, ignition delay times for experiments using the 5mm interior lip tray were 30% slower than those corresponding to similar tests with the tray that had no-lip. Despite identical fuel layer thickness and external heat flux, boiling occurred only in the lip tray.

Conduction into the metal walls of the container was suspect of the dramatic ignition delay time differential. A fine metallic powder was used to coat the surface of the sample in both trays. Observations of the flow in the lip tray indicated increased eddy activity of the fuel layer. By selecting the no-lip configuration, effect of conduction through the boundaries was minimized.

It has been shown by Kolb *et al.* (1997) that the flow surrounding the flame has a significant effect on the structure of the entrained air, this might lead to significant differences in the ignition delay time as well as on the flame height, once the flame is established. The importance of the mixing ( $t_M$ ) and transport times ( $t_T$ ) with respect to the pyrolysis time ( $t_p$ ) was assessed above. When the hot surface is placed horizontal, characteristic flow velocities are very low, therefore,  $t_M$  and  $t_T$  can be expected to have a significant effect on the ignition delay time therefore, there is a need to observe the flow characteristics.

To study the air entrainment into above the fuel sample, a 2W red diode laser (SDL-820) was used to create a light sheet for visualization of the smoke emerging from the fuel surface. The images have been processed using an EPIX video card. A threshold value was established below which all pixels were assigned a 0 value, to obtain a more clear image of the flow structure, as evidenced by the smoke. The threshold value is arbitrary and is chosen with the single purpose of eliminating all background images. Figures 2 and 3 are two typical images.

In the absence of a flush floor both trays displayed identical air entrainment and gaseous fuel evolution patterns. Clear eddies could be observed at the edges of the tray (figure 2), as observed these eddies grow to cover the entire surface of the fuel tray. When a floor surrounded the tray the eddies disappeared and a random flow of gases was observed (figure 3). The absence of eddies (for the flush floor case) deters the mixing of fuel and oxidizer at the surface and as a consequence the ignition delay time increased by approximately 20% over experiments conducted with no floor. By introducing a 0.1 m/s

flow parallel to the surface a boundary layer is formed and the all eddies were eliminated. By introducing the forced flow  $t_M$  and  $t_T$  are reduced significantly and  $t_{ig}$  approaches  $t_p$ . The choice of a small velocity (0.1 m/s) is not arbitrary, as the velocity increases the convective component of “h” increases and will have an effect on the value of the critical heat flux for ignition. This issue will be discussed below.



Figure 2. Smoke Visualization for a Tray with No-Lip and No Flush Floor.

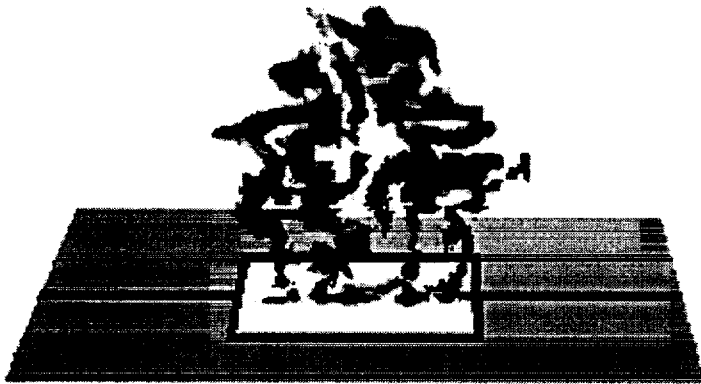


Figure 3. Smoke Visualization for a Tray with No-Lip and Flush Floor.

Premature ignition can be caused by a pilot flame and if the pilot needs to be placed over the fuel surface, it can only be reduced by decreasing the unaccountable radiation from the pilot to the surface. A small propane diffusion flame established on a 4 mm diameter stainless-steel nozzle was used as a pilot. The pilot size was change and its effect on the ignition delay time recorded, it was observed that for a specific location on the fuel surface, no change in the ignition delay time could be observed for pilots smaller than 10 mm, instead extinction of the pilot was commonly seen when fuel ignition occurred. The distance from the fuel surface was observed not to affect the ignition delay time between 10 and 20 mm, decreasing if the pilot is placed closer and increasing as the distance goes beyond 20 mm. It was therefore concluded that the heat contributed by a 10 mm pilot flame at a distance of 10 mm from the surface can be considered negligible. This size and distance from the surface was used to vary the pilot location. The pilot was placed at the center of the tray, at the edges, corners and 10 mm outside the tray. Significant differences among ignition delay times were observed for different pilot

locations. Changing the pilot location has no effect on  $t_p$ , for pilot flames smaller than 10 mm and more than 10 mm away from the fuel surface, but directly affects the delay for the fuel and oxidizer to reach the pilot, having therefore relating directly to  $t_M$  and  $t_T$ .

A set of characteristic values is presented in Table 1 to show typical ignition delay times for fixed heat flux ( $14 \text{ kW/m}^2$ ) and fuel bed characteristics (SAE 30, layer thickness: 10 mm). All values presented are averages of no less than 5 tests. It can be noted that the ignition delay time is a strong function of all the parameters shown in Table 1. It was concluded that a stable laminar flow is necessary, both to eliminate the need to keep the pilot flame over the fuel surface and to create a robust flow structure that can be considered independent of the environment. A series of experiments were conducted in this configuration, for different heat fluxes, pilot sizes and pilot location and in all cases the ignition delay time remained inside a 7% deviation from the mean.

Pilot Location	Time (sec)			
	No-Lip Tray (with no floor)	Lip Tray (with no floor)	No-Lip Tray (with floor)	Lip Tray (with floor)
0 mm	342	777	1075	1470
50 mm	455	820	415	727
100 mm	510	830		

Table 1. SAE 30 Weight Oil Ignition Tests at  $14 \text{ kW/m}^2$

The results from these experiments are presented in Figure 4 together with data obtained for the same fuel by Putorti *et al.* (1994). The ignition delay time is presented as  $t^{-1/2}$ , following equation (8). It can be observed that, although the ignition delay time significantly differs from the values found by Putorti *et al.* all data converges to a unique critical heat flux for ignition. Since these experiments were conducted using different ignition procedures and under significantly different environmental conditions,  $t_M$  and  $t_T$  are expected to be different, thus, affecting the ignition delay time. On the contrary,  $t_p$  should not be affected if convective losses are similar in magnitude or can be neglected. As the external heat flux approaches  $\dot{q}_{0,ig}''$ ,  $t_M$  and  $t_T$  become neglectable compared to  $t_p$  and all data converges to a unique point ( $\dot{q}_{0,ig}'' \approx 6 \text{ kW/m}^2$ ), as observed in Figure 4. This observation implies that convective losses are either similar or neglectable for both cases, increasing the value of the forced flow will enhance the convective heat losses and will result in a shift of  $\dot{q}_{0,ig}''$ . Due to the low velocities characteristic of this particular configuration, convective heat losses are expected to be negligible, but verification by systematic variation of the velocity still needs to be done.

For the particular case of an oil-slick on a water bed, the water underneath the fuel might attain boiling before ignition occurs. Heating of the bed can be treated as a semi-infinite solid and temperature distributions can be predicted quite accurately (Garo *et al.*, 1994). The analytical prediction of a characteristic time to boiling goes beyond the scope of this work, but the determination of a minimum heat flux that will lead to boiling ( $\dot{q}_{0,B}''$ ) before ignition can occur is of great practical importance therefore needs to be included as a complement to the critical heat flux for ignition.

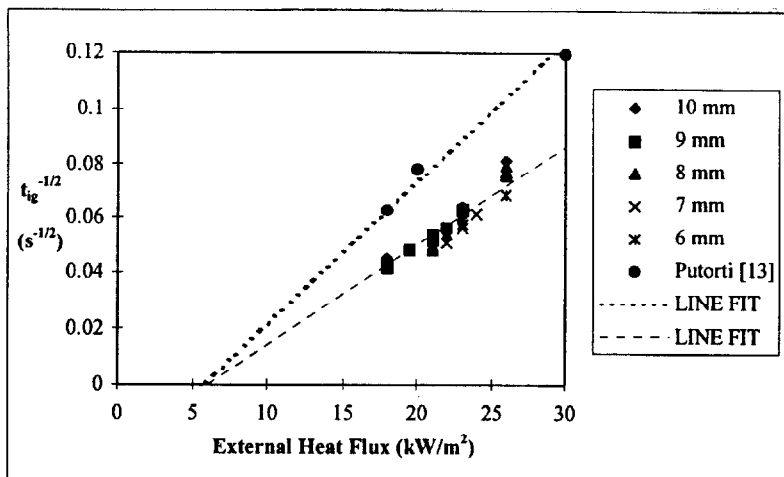


Figure 4. Ignition Delay Time for Different External Heat Fluxes (SAE 30W oil) (The delay times from reference (Putorti *et al.*, 1994) were extracted as an average of the values obtained for 43 mm, 15 mm and 10 mm fuel layers).

As the external heat flux decreases the temperature gradient at the surface decreases and thermal penetration increases before the surface attains  $T_p$ . If the thermal wave can increase the water temperature at the fuel/water interface to the boiling point before the surface reaches  $T_p$ , boiling will prevent ignition from occurring. The minimum heat flux that will allow the surface temperature to reach  $T_p$  before boiling is given by  $\dot{q}''_{0,B}$  and presented in figure 5. Under the assumption that convective heat losses are negligible,  $\dot{q}''_{0,B}$  can be considered independent of the environmental conditions and only a property of the fuel and the fuel layer thickness. Figure 5 shows the progression of  $\dot{q}''_{0,B}$  as a function of the fuel layer thickness. As the fuel layer decreases in thickness, the heat wave will reach the water faster allowing for a shorter available time for the surface to reach  $T_p$  and consequently requiring a higher temperature gradient at the surface (higher  $\dot{q}''_{0,B}$ ).

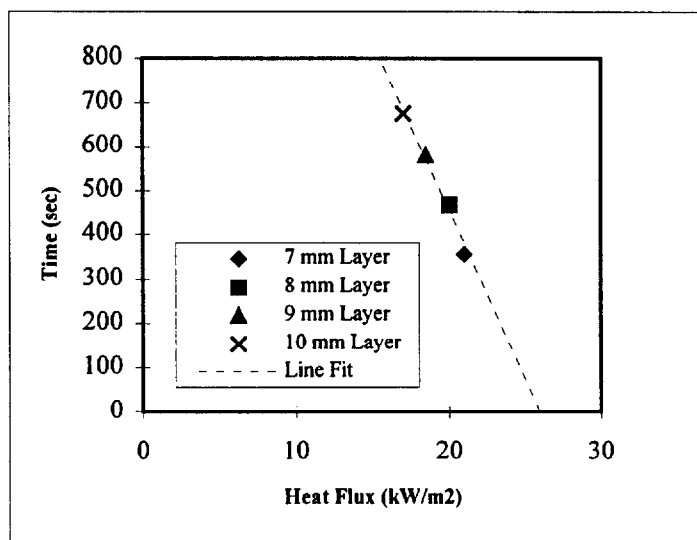


Figure 5. Critical Heat Flux and Time for Boiling (SAE 30W oil)

To further demonstrate the validity of this experimental methodology a series of tests were conducted with Cook Inlet crude oil. Figure 6 shows these results and other obtained for ANS crude oil by Putorti *et al.* (1994). The data presented for the Cook Inlet crude oil is an average of at least five experiments conducted under identical conditions. It was observed that Cook Inlet crude oil in its natural state ignited at ambient temperature, therefore no external heat flux was necessary, when evaporated to a 10% mass loss  $\dot{q}''_{0,ig}$  increased to approximately  $6.5 \text{ kW/m}^2$  showing a significant increase in the difficulty to ignite. The critical heat flux for ignition extrapolated from Putorti *et al.* (1994) for ANS crude oil (evaporated to a 30% mass loss) was approximately  $2.5 \text{ kW/m}^2$  indicating greater ease of ignition than Cook Inlet crude oil (10% evaporated) and being more difficult to ignite than the same oil in its natural state.

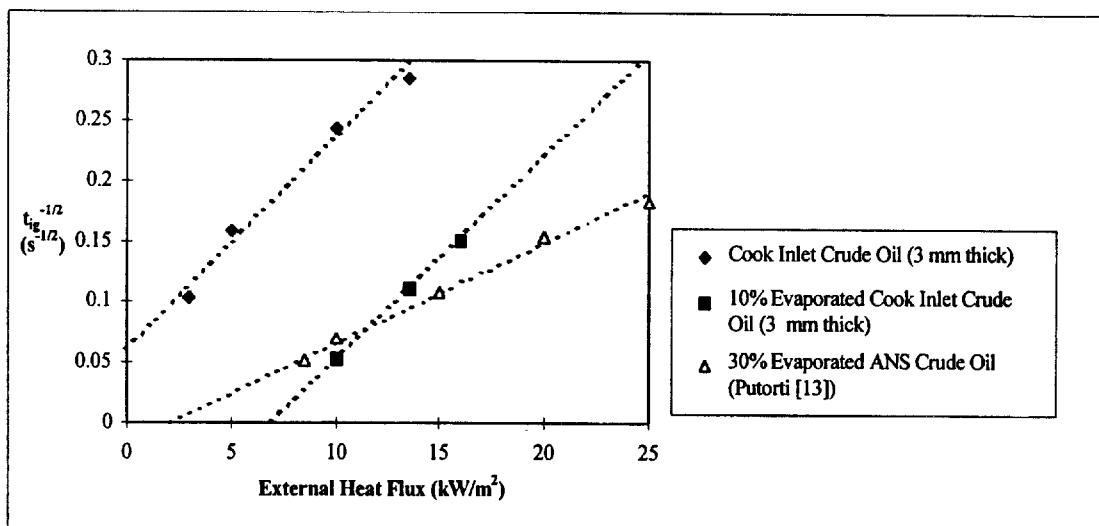


Figure 6. Ignition Delay Time for Different External Heat Fluxes.

### 3.2 Flame Spread

Several flame spread tests were conducted with SAE 30 W oil to validate the use of the H.I.F.T. It was observed that flame propagation transitions from a continuous flame spread mode, for the higher heat fluxes, to a pulsating mode as the external heat flux decreased. For  $\dot{q}''_c < 6 \text{ kW/m}^2$  propagation ceased. Figure 7 shows a series of characteristic results for SAE 30W oil for different fuel layer thicknesses. It can be noted that flame spread regime significantly exceeds  $\dot{q}''_{0,ig}$ , specially for thinner fuel layer thickness. The flame spread velocity corresponding to a specific external heat flux increases with the fuel layer thickness showing that the fuel layer thickness has a significant effect on the propagation velocity. Further testing is still required to fully clarify this phenomena. Flame spread over liquid is a complex phenomena that is significantly affected by surface tension and buoyancy driven flows (Ross, 1994, Glassman *et al.*, 1981), the basic criteria presented in equation (13) has been demonstrated to be a viable way to determine the propensity of a fuel to sustain flame spread.

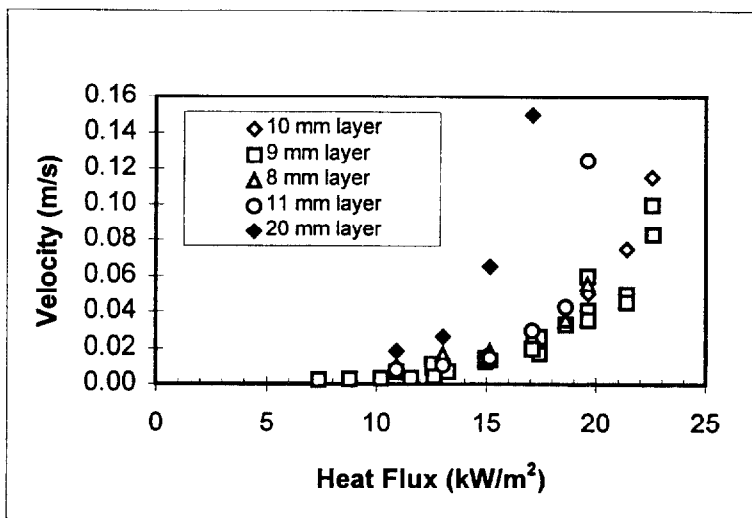


Figure 7. Flame Spread Velocity for Different External Heat Fluxes (SAE 30W).

### 3.3 Mass Burning

The thickness of the initial fuel layer was varied from a maximum of 20 mm to a minimum thickness of 2 mm. Before each test water was first poured in the pan and next the fuel until it reached 1 mm below the pan lip. During the combustion process the location of the fuel/water interface remained constant, therefore, the freeboard length increases during the experiment. The freeboard length changes were found to have very little effect on the steady-state burning rate.

A typical experiment can be described as a short unsteady ignition period followed by a steady state burning period. During steady burning the surface temperature increased slightly as the experiment progressed (lighter volatile tend to burn off first). The steady burning period was followed by thin layer boil-over characterized by an increase in the burning rate as well as intense splashing of water and fuel. It is important to note that steady burning was followed by boilover and not extinction, therefore, no sudden decrease of the mass burning rate was observed.

The fuels used were heating oil (a mixture of hydrocarbons ranging from  $C_{14}$  to  $C_{21}$ ) and crude oil (63% Kittiway, 33% Arabian Light and 4% Oural). Experiments were also conducted with weathered fuels as well as different fuel/water emulsions. Weathering refers to the evaporation of the light components of the fuel that results in significant changes of the fuel properties (density, viscosity, boiling temperature, etc.), in the laboratory it was accomplished by means of a mixer turning at 700 r.p.m. and covering 75% of the horizontal cross section of the container. Mixing was conducted for 3 different periods, 24, 48 and 72 hours. Fuel/water emulsions were obtained by adding fixed quantities of water to the mixer and allowed to emulsify for no more than an hour. Experiments were conducted with crude oil aged for 24 hours and water contents of 10, 20, 30 and 40% in volume.

Equation (20) has been used to calculate the average regression rate ( $r_T$ ) for crude oil. The average regression rate matches well qualitatively and quantitatively the experimental values ( $r_E$ ). The regression rate is almost constant for  $y_{s,i} > 8\text{mm}$  and decreases dramatically with the fuel layer thickness for  $y_{s,i} < 8\text{mm}$ . For all data points a

constant value of  $\chi = 2.9 \times 10^{-3}$  was used. The value of  $\chi$  was selected to best fit  $r_T$  with the experimental data for the constant regression rate zone.

Experimentally obtained average regression rates for heating oil, fresh crude oil, 24 hour weathered crude oil and 24 hour weathered and emulsified crude oil (20% water content) were divided by the calculated regression rate ( $r_E/r_T$ ) to provide an indication of the error associated with the assumptions used to model the average regression rate. The data was obtained for different pan diameters and is a function of the initial fuel layer thickness ( $y_{s,i}$ ) and is presented in figure 8. The predicted values are in excellent agreement with the theory for initial fuel layer thickness greater than 5 mm, for thinner fuel layers the error increases reaching, in the worst of cases, values close to 50%. This error is justifiable due to the great uncertainty present when conducting experiments with very thin fuel layers and to the average nature of the regression rates presented. The value of  $\chi$  had to be adjusted to  $\chi = 3.9 \times 10^{-3}$  for heating oil, to  $\chi = 2.4 \times 10^{-3}$  for 24 hour weathered crude oil and to  $\chi = 1.8 \times 10^{-3}$  for 24 hour weathered and emulsified crude oil (20% water content).

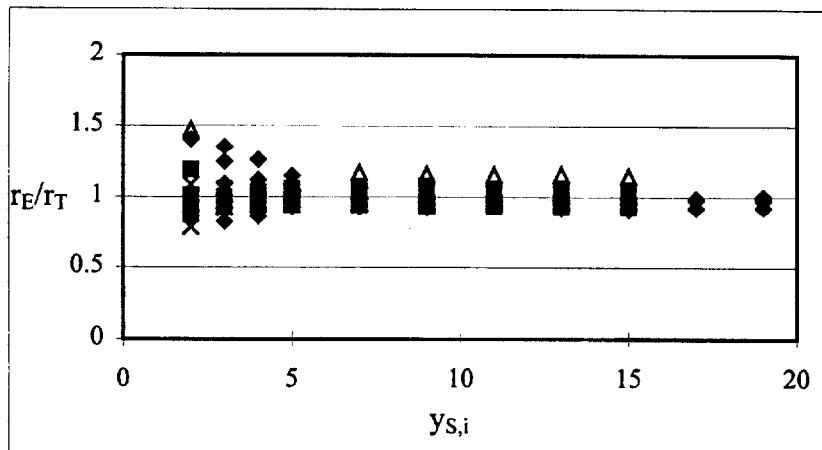


Figure 8. Experimental to Theoretical Regression Rate Ratio for Different Fuels and Pan Diameters

The heat feedback from the flame behaves in a similar way to a pool flame with no water bed, at least in the pre-boilover period. The dependence on the diameter and initial fuel layer thickness is, thus, well described by the heat flux obtained from equation (14). The use of a net heat flux as a boundary condition at the fuel surface seems also to be appropriate. It is important to note that only approximately between 0.18 % and 0.39 % of the energy released by the flame is effectively fed back to the fuel surface. The above values of  $\chi$  seem comparable to data presented by Arai *et al.* (1990) but no data obtained under similar experimental conditions has been found to verify these magnitudes.

As previously pointed out by many authors (Arai *et al.*, 1990, Garo *et al.*, 1994, 1996, Alramadhan *et al.*, 1990) the water bed acts as a heat sink. The thermal diffusivity of water is significantly larger than that of the fuel thus, as the fuel layer becomes thinner, the overall thermal diffusivity increases. Heat conduction through the fuel and water increases ( $\dot{q}''_C$ ) and the overall fraction of the total heat flux ( $\dot{q}''_S$ ) vaporizing the fuel

decreases leading to a decrease in the regression rate that can eventually result in extinction ( $y_{s,i} < 2$  mm).

The data for weathered and emulsified crude oil is also well described by the predicted regression rate. The same reasoning presented above applies for these cases, being the only difference the regression rate magnitude. Weathering and emulsification alter the thermal properties of the fuel and, thus, the magnitude of the regression rate. By changing the efficiency constant ( $\chi$ ) to fit the experimental data, a practical way is found to incorporate the effect of weathering and emulsification on the fuel properties. The variation of the efficiency constant as a function of the weathering period and the water content is shown on figures 9 and 10, respectively.

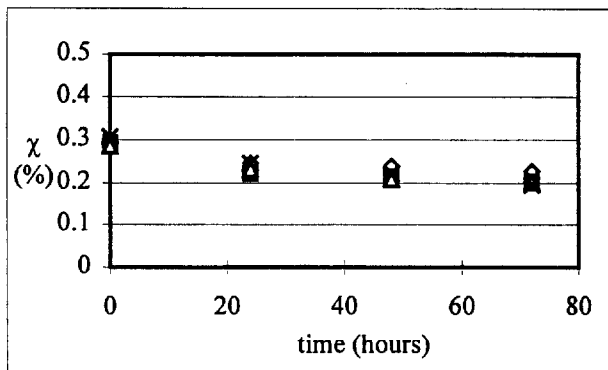


Figure 9. Efficiency Factor as a Function of Weathering Time

Figure 9 shows that initially the efficiency constant ( $\chi$ ) decreases fast, followed by less significant changes till it reaches an almost constant value ( $\chi = 2 \times 10^{-3}$ ). It is well known that the highly volatile hydrocarbons will evaporate very fast, i.e. after less than 24 hours the mass loss of hydrocarbons with boiling points below 500 K ( $<C_{11}$ ) has reached 95% and only reaches total evaporation after 48 hours (Demarquest, 1983). Heavier hydrocarbons ( $C_{11}-C_{25}$ ) tend to evaporate significantly slower reaching 100% mass loss only after more than 10 days. The initial fast change in fuel properties results in an abrupt decrease of  $\chi$ , followed by an almost negligible change rate.

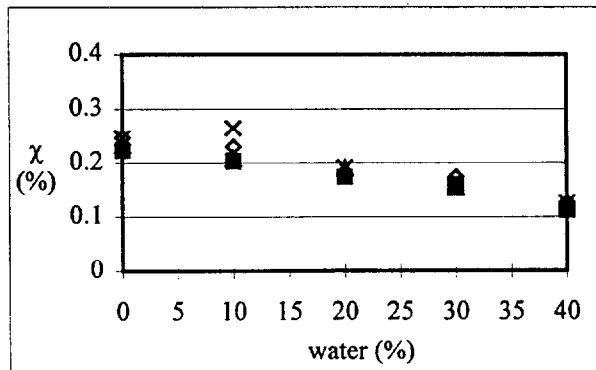


Figure 10. Efficiency Factor as a Function of the Water Content (emulsification)

For emulsified fuels water addition will result in an almost linear decrease of  $\chi$  (figure 10). The properties of the emulsified fuel change significantly with the water content and, as shown by equation (20), this will have a significant effect on the average regression rate. The way in which emulsification affects the fuel properties is not fully understood but it is well known that properties such as the density vary in an almost linear way with the water content ( $\rho(\text{emulsified fuel})=(1-\text{water fraction})\rho_F+(\text{water fraction})\rho_W$ ) and other properties, such as viscosity, increase in a non-linear way.

Although the efficiency constant ( $\chi$ ) does not provide a real explanation to the effects of weathering and emulsification on the average regression rate it serves to quantify the flammability of the fuel independent of the pool size and fuel layer thickness. The relationship between the fuel properties and the efficiency factor goes beyond the heat transfer and evaporation mechanisms controlling the burning rate and a complete explanation will require a comprehensive study that will include the effects of weathering and emulsification on the flame chemistry and radiative feedback. In detail analysis of these relationships go beyond the scope of this work.

#### **4.0 Conclusions**

The methodology to assess the burning characteristics of a liquid fuel on a water bed has been presented and verified with different fuels, weathering conditions and water content. Three different and complementary tests are deemed necessary to characterize the three different regimes of the burning process: ignition, flame spread and mass burning.

For ignition; the critical heat flux for ignition as identified in ASTM E-1321 was found to be the parameter that better describes the capability of a fuel to ignite. The critical heat flux for ignition was found to be independent of the geometry and flow conditions and a parameter that could be extrapolated to attempt the characterization of the ignition for more realistic length scales. The minimum heat flux for ignition needs to be accompanied by a minimum heat flux that will lead to boiling of the water bed. The ignition delay time, although a relevant parameter of the ignition process, was found to be dependent of the experimental conditions, and thus, difficult to extrapolate to a different scale.

For flame spread; the minimum external heat flux that will sustain propagation together with the parameter  $\phi$  (function of the fuel properties) will serve to describe the flame spread characteristics. The complexity of flame spread over liquid fuels makes necessary further validation of this experimental approach.

For mass burning; the efficiency factor,  $\chi$ , serves as unique parameter to characterize the regression rate during the mass burning process.  $\chi$  is a property of the fuel that can be extrapolated to different scales and environmental conditions but should be evaluated under conditions where is independent of the flame diameter and the fuel layer thickness. The validity of this approach is constrained to the pre-boilover regime and the assessment of its relevance to the time for the onset of boilover requires further experimentation.

#### **5.0 Acknowledgments**

This work was conducted under the financial support of the National Institute of Standards and Technology and the authors express their thanks to Dr. D. Evans, Mr. D.

Madrzykowski and Mr. J. McElroy for their multiple suggestions and their help in the development of the experimental hardware. The mass burning experiments used to validate the burning efficiency factor were conducted by Drs. J.-P. Garo and J.-P. Vantelon at the Laboratoire de Combustion et de Detonique, University of Poitiers, France.

## 6.0 References

- Alramadhan, M.A., Arpaci, V.S. and Selamet A., "Radiation Affected liquid Fuel Burning on Water", *Combustion Science and Technology*, 72, pp. 233-253, 1990.
- Alvares, N. J. and Martin, S. B., "Mechanisms of Ignition of Thermally Irradiated Cellulose", *Thirteenth Symposium (International) on Combustion, The Combustion Institute*, pp. 905-914, 1971.
- Annual Book of ASTM Standards, vol. 04-07,1055-1077, 1993.
- Arai, M., Saito, K. and Altenkirch, R.A., "A Study of Boilover in Liquid Pool Fires Supported on Water Part I: Effect of a Water Sublayer on Pool Fires", *Combustion Science and Technology*, 71, pp.25-40, 1990.
- Bech, C., Sveum, P. and Buist, I., "The Effect of Wind, Ice, and Waves on The In Situ Burning of Emulsions and Aged Oils", *Proceedings of the Thirteenth Arctic And Marine Oil Spill Program Technical Seminar*, Ministry of Supply and Services Canada, pp. 735-748, 1990.
- Brzustowski, T.A. and Twardus, E.M., "A Study of the Burning of a Slick of Crude Oil on Water", *Nineteenth Symposium (International) on Combustion*, The Combustion Institute, 847-854, 1982.
- Carslaw, H.S. and Jaeger, J.C., "Conduction of Heat in Solids," *Oxford University Press*, 2nd Edition, pp. 70-76, 1963.
- Chen, C.H. and T'ien, J.S., "Diffusion Flame Stabilization at the Leading Edge of a Fuel Plate", *Combustion Science and Technology*, 50, pp. 283-306, 1986.
- Cordova, J.L., Ceamanos, J., Fernandez-Pello, A.C, Long, R.T., Torero, J.L. and Quintiere, J.G., "Flow Effect on the Flammability Diagrams of Solid Fuels", *4th International Micro-Gravity Combustion Workshop*, Cleveland, Ohio, May, 1997.
- Cox, G., *Combustion Fundamentals of Fire*, Academic Press, London, 1995.
- Desmarquest, J.P. "Les Polluants Petroliers et leur Evolution en Mer", Report CEDRE, R.83727.E, 1983.
- Drysdale, D.D., *An Introduction to Fire Dynamics*, John Wiley and Sons, 1985.
- Evans, D., Walton, W., Baum, H., Lawson, R., Rehm, R., Harris, R., Ghoniem, A. and Holland, J., "Measurement of Large Scale Oil Spill Burns", *Proceedings of the Thirteenth Arctic And Marine Oil Spill Program Technical Seminar*, Ministry of Supply and Services Canada, Cat. No. En40-11/5-1990, pp. 1-38, 1990.
- Fernandez-Pello, A.C., "Combustion Fundamentals on Fire: The Solid Phase," *Academic Press*, pp. 31-100, 1995.

- Frey, A.E. and T'ien, J.S., "A Theory of Flame Spread Over a Solid Fuel Including Finite Rate Chemical Kinetics", *Combustion and Flame*, 36, pp.263-289, 1979.
- Garo, J. P., Vantelon, J. P. and Fernandez-Pello, A.C., "Experimental Study of the Burning of a Liquid Fuel Spilled on Water", *Twenty-fifth Symposium (International) on Combustion*, The Combustion Institute, pp. 1481-1488, 1994.
- Garo, J. P., Vantelon, J. P. and Fernandez-Pello, A.C., "Effect of the Fuel Boiling Point on the Boilover Burning of Liquid Fuel Spilled on Water", *Twenty-sixth Symposium (International) on Combustion*, The Combustion Institute, (in press), 1996.
- Garo, J.P., "Combustion d'Hydrocarbures Répandus en Nappe sur un Support Aqueux. Analyse du Phénomène de Boilover", *Ph.D. Thesis*, University of Poitiers, France, 1996.
- Glassman, I. and Dryer, F., "Flame Spreading Across Liquid Fuels", *Fire Safety Journal*, 3, pp. 132, 1981.
- Henry, M. and Klem, T., "Scores Die in Tank Fire Boilover", *Fire Safety Today*, 6, pp. 11-13, 1983.
- Ito, A., Saito, K. and Inamura, T., "Holographic Interferometry Temperature Measurements in Liquids for Pool Fires Supported on Water", *Transactions of the ASME*, 114, pp.944, 1992.
- Jason, N.H. *Alaska Arctic Offshore Oil Spill Response Technolog Workshop Proceedings*, NIST SP762, U.S. Government Printing Office, Washington D.C., pp. 47-95, 1989.
- Kodama, H., Miyasaka, K. and Fernandez-Pello, A.C., "Extinction and Stabilization of a Diffusion Flame on a Flat Combustible Surface with Emphasis on Thermal Controlling Mechanisms", *Combustion Science and Technology*, 54, pp.37-50, 1987.
- Kolb, G., Audouin, L., Most, J.-M. and Torero, J.L., "Confinement Effect on the Mean Flame Height of Buoyant Diffusion Flame", *Spring Meeting, Central States Section*, The Combustion Institute, Point Clear, Alabama, pp. 113-118, 1997.
- Koseki, H. and Mulholland, G.W., "The Effect of Diameter on the Burning of Crude Oil Fires", *Fire Technology*, 27:1, pp. 54-65, 1991a.
- Koseki, H. Kokkala, M. and Mulholland, G.W., "Experimental Study of Boilover in Crude Oil Fires", *Fire Safety Science-Proceedings of the Third International Symposium*, pp. 865-875, 1991b.
- McCaffrey, B. J., "Purely Buoyant Diffusion Flames: Some Experimental Results", NBSIR 79-1910, National Bureau of Standards, Washington D.C., 1979.
- Mikkola, E. and Wichman, I.S., "On the Thermal Ignition of Combustible Materials", *Fire and Materials*, 14, 87-96, 1989.
- Motevalli, V., Chen, Y., Gallagher, G., Sheppard, D., "Measurement of Horizontal Flame Spread on Charring and Non-charring Material using the LIFT Apparatus", *Fire and Materials*, Interscience Communications Limited, pp. 23-32, 1992.
- Putorti, A. D., Evans, D. D. and Tennyson, E. J., "Ignition of Weathered and Emulsified Oils", *Proceedings of the Seventeenth Arctic and Marine Oil Spill Program Technical Seminar*, pp.657-667, 1994.

- Quintere, J., "A Simplified Theory for Generalizing Results from Radiant Panel Rate of Flame Spread Apparatus", *Fire and Materials*, 5, 2, pp. 52-60, 1981.
- Quintere, J., Harkleroad, M. and Walton, D., "Measurement of Material Flame Spread Properties", *Combustion Science and Technology*, 32, pp. 67-89, 1983.
- Quintiere, J. and Harkleroad, M., "New Concepts for Measuring Flame Spread Properties," U.S. Department of Commerce, NBSIR 84-2943, 1984.
- Ross, H.D., "Ignition of and Flame Spread Over Laboratory-Scale Pools of Pure Liquid Fuels", *Progress in Energy and Combustion Science*, 20, pp.17-63, 1994.
- Thompson, C. H., Dawson, G. W. and Goodier, J. L., "Combustion: An Oil Spill Mitigation Tool", PNL-2929, *National Technical Information Service, Springfield, VA22161*, 1979.
- Twardus, E.M. and Brzustowski, T.A., "The Burning of Crude Oil Spilled on Water", *Archivum Combustionis*, Polish Academy of Sciences, 1, 1-2, pp. 49-60, 1981.
- Venkatesh, S., Ito, A., Saito, K. and Wichman, I.S., "Flame Base Structure of Small Scale Pool Fires," NIST-GCR-96-704, 1996.
- Walavalkar, A.Y. and Kulkarni, A.K., " A Comprehensive Review of Oil Spill Combustion Studies", *Proceedings of the Nineteenth Arctic And Marine Oil Spill Program Technical Seminar*, pp.1081-1103, 1996.
- Williams, F.A., *Combustion Theory*, The Benjamin/Cummings Publishing Company Inc., 1985.

**BLANK PAGE**

**4.2. Ignition and Flame Spread and Mass Burning Characteristics of Liquid Fuels on a Water Bed**

N. Wu, M. Baker, G.Kolb and J.L. Torero  
*Spill Science and Technology (in press), 1998.*

**BLANK PAGE**

# **Ignition, Flame Spread and Mass Burning Characteristics of Liquid Fuels on a Water Bed**

Neil Wu, Michael Baker, Gilles Kolb and Jose L. Torero\*  
Department of Fire Protection Engineering  
University of Maryland, College Park, MD20742-3031  
USA

## **Abstract**

An experimental technique has been developed to systematically study the ignition, flame spread and mass burning characteristics of liquid fuels spilled on a water bed. The final objective of this work is to provide a tool that will serve to assess a fuels ease to ignite, to spread and to sustain a flame, thus helping to better define the combustion parameters that affect in-situ burning of oil spills.

## **Introduction**

A simple way to classify all studies relevant to in situ burning of an oil slick over a water bed is by dividing the combustion process in its three different stages, ignition, flame spread and self sustained burning (or mass burning). An external source of energy will lead to ignition, which will be followed by the spread of the flame across the fuel surface. Although flame spread might be an instantaneous process for many crude oils in their natural state, the loss of highly volatile compounds, due to weathering, and the presence of water in emulsions might lead to flame spread that needs to be assisted by external radiation. For thin fuel layers, heat losses to the water bed, might lead to a similar situation. For these particular cases a minimum size might be necessary to provide the necessary radiative heat feed back to self-sustain flame spread. Once the flame spread process is self sustained mass burning will follow.

Fuel properties vary significantly when subject to a strong heat insult, therefore, they need to be evaluated under fire conditions. Evaluation of the fuel "fire properties" that are independent of the length scale will permit the ranking of fuels and will reduce the number of large scale experiments necessary to determine in-situ burning protocols and procedures. By focusing on the fuel and introducing external radiation, large scale conditions can be simulated. It has to be noted that this is not a study of the burning characteristics but of the fuel burning efficiency. Ignition and flame spread will be studied by using a modified Lateral Ignition and Flame Spread Test (ASTM E-1321) and mass burning by observing the regression rate under conditions where the characteristics of the flame can be predicted adequately.

This work attempts to identify an ideal configuration in which the ease by which a fuel can burn can be evaluated. The three aspects of the combustion process, ignition, flame spread and mass burning will be studied. The results should be independent of specific burning characteristics and geometrical constraints, and thus, extrapolation to a large scale should be possible.

## **Ignition**

---

\* Corresponding author

The critical heat flux for ignition ( $\dot{q}_{0,ig}''$ ) is the minimum external heat flux that will lead to equilibrium at the pyrolysis temperature ( $T_p$ ), thus, is given by:

$$\dot{q}_{0,ig}'' = h(T_p - T_i) \quad (1)$$

where  $T_i$  is an ignition temperature and “h” is a global heat transfer coefficient. By assuming one-dimensional heat conduction in the fuel and  $t_{ig} \approx t_p$  ( $t_p$  is the time needed to reach  $T_p$ ) a characteristic ignition delay time ( $t_{ig}$ ) can be obtained:

$$t_{ig} = \frac{\pi}{4a} \left( \frac{h(T_p - T_i)}{\dot{q}_e''} \right)^2 \quad (2)$$

where ( $\dot{q}_e''$ ) is the external heat flux,  $k$  is the thermal conductivity and  $a = \alpha(h/k)^2$ . Mixing ( $t_M$ ), transport ( $t_T$ ) and chemical induction ( $t_{in}$ ) times are assumed neglectable when compared to  $t_p$ . This will be satisfied best as the external heat flux approaches the critical heat flux for ignition ( $\dot{q}_e'' \approx \dot{q}_{0,ig}''$ ) and  $t_p \rightarrow \infty$ . This is important because it implies that the error incurred in the experimental determination of  $t_{ig}$ , (due to the unknown nature of the flow) will decrease as  $\dot{q}_e''$  approaches  $\dot{q}_{0,ig}''$ . Therefore,  $\dot{q}_{0,ig}''$  is a property of the fuel that can be extrapolated, independent of the flow. More details on the derivation of the above expressions and on the characteristics of the hardware are provided by Quintiere (1981).

To validate this approach, SAE 30 W oil was used to conduct ignition tests. This fuel was used to make possible comparison with previously reported results on ignition delay time by Putorti et al (1990) and also because of its high flash point (approximately 250°C). A high flash point results in a longer ignition delay time providing a longer period to observe the different flow structures formed inside the liquid fuel and on the gas phase. The pilot size and location, the geometry of the fuel container and the flow around the sample have a significant effect on the ignition delay time ( $t_{ig}$ ) but for brevity only the study concerning the flow will be presented.

To study air entrainment into above the fuel sample, a 2W red diode laser (SDL-820) was used to create a light sheet for visualization of the smoke emerging from the fuel surface. Figures 2 and 3 are two typical images. In the absence of a flush floor eddies could be observed at the edges of the tray (figure 1), these eddies grow to cover the entire surface of the fuel tray. When a floor surrounded the tray the eddies disappeared and a random flow of gases was observed (figure 2). The absence of eddies deters the mixing of fuel and oxidizer at the surface and as a consequence the ignition delay time increased by approximately 20%. By introducing a 0.1 m/s flow parallel to the surface a boundary layer is formed and all eddies were eliminated. By introducing the forced flow  $t_M$  and  $t_T$  are reduced significantly and  $t_{ig}$  approaches  $t_p$ . The choice of a small velocity (0.1 m/s) is not arbitrary, as the velocity increases the convective component of “h” increases and will have an effect on the value of the critical heat flux for ignition.



Figure 1. Smoke visualization for a tray with no flush floor.

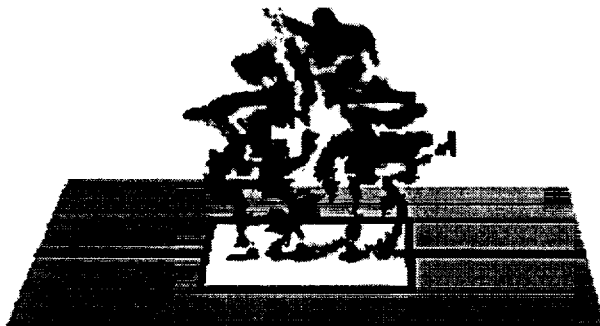


Figure 2. Smoke visualization for a tray with a flush floor.

The results from these experiments are presented in Figure 3 together with data obtained for the same fuel by Putorti et al. (1990) in a Cone Calorimeter. The ignition delay time is presented as  $t^{-1/2}$ , following equation (2). Although the ignition delay time differs from the values found by Putorti et al. all data converges to a unique critical heat flux for ignition. Since these experiments were conducted using different ignition procedures and under different environmental conditions,  $t_M$  and  $t_T$  are expected to be different, thus, affecting the ignition delay time. On the contrary,  $t_p$  should not be affected if convective losses are similar in magnitude or can be neglected. As  $\dot{q}_e''$  approaches  $\dot{q}_{0,ig}''$ ,  $t_M$  and  $t_T$  become neglectable compared to  $t_p$  and all data converges to a unique point ( $\dot{q}_{0,ig}'' \approx 6 \text{ kW/m}^2$ ).

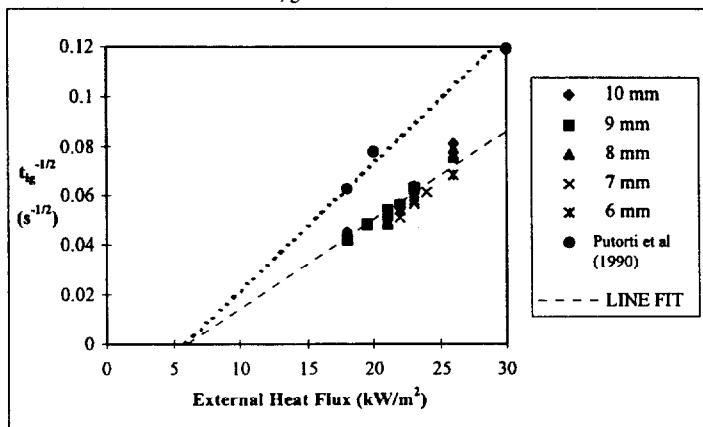


Figure 3. Ignition delay time for different external heat fluxes (SAE 30W oil). The delay times from Putorti et al (1990) were extracted as an average of the values obtained for 43 mm, 15 mm and 10 mm fuel layers.

### Flame Spread

Flame spread velocities ( $V_f$ ) can be obtained for external heat fluxes of magnitude smaller than  $\dot{q}_{0,ig}''$ . The following expressions were derived by Quintiere et al (1981)

$$V_f = \frac{\phi}{[\dot{q}_{0,ig}'' - \dot{q}_e'']^2} \quad \text{where} \quad \phi = \frac{4a\delta_f(\dot{q}_f'')^2}{\pi} \quad (3)$$

where  $\phi$  is a global material property determined from the experiments and  $\dot{q}_{0,ig}''$  can be obtained by increasing the external heat flux till  $V_f \rightarrow \infty$  and  $\delta_f$  is a characteristic thermal length scale. Reducing the external heat flux will eventually lead to no spread, thus a minimum velocity ( $V_{f,min}$ ) and external heat flux ( $\dot{q}_{0,s}''$ ) for flame spread can be recorded. This information, obtained under known experimental conditions, will serve as a useful way to assess and rank the fire performance of fuels and to identify the parameters that dominate their fire characteristics.

Preliminary results showed that flame propagation transitions from a continuous flame spread mode, for the higher heat fluxes, to a pulsating mode as the external heat flux decreased. For  $\dot{q}_e'' < 6 \text{ kW/m}^2$  propagation ceased. Figure 4 shows a series of characteristic results for SAE 30W oil for different fuel layer thickness. It can be noted that flame spread regime significantly exceeds  $\dot{q}_{0,ig}''$ , specially for thinner fuel layer thickness. The flame spread velocity corresponding to a specific external heat flux increases with the fuel layer thickness. Further testing is still required to fully clarify this phenomena.

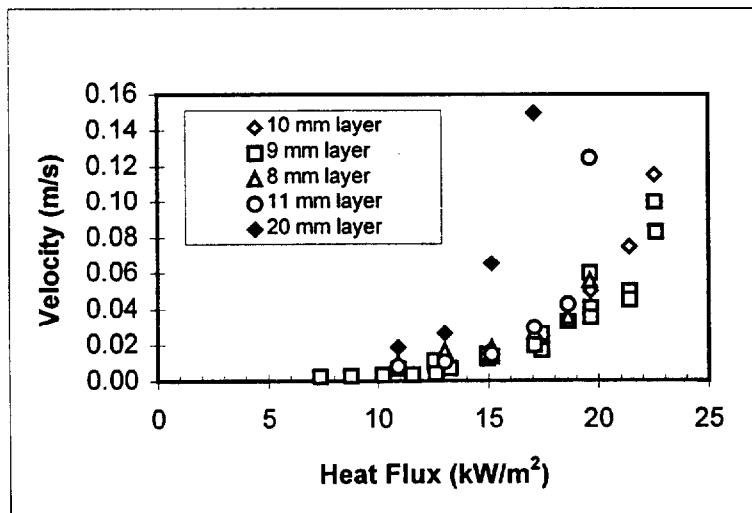


Figure 4. Flame spread velocity for different external heat fluxes (SAE 30W).

### Mass Burning

A simple way to assess the relative potential of a fuel to sustain mass burning is by using a burning efficiency ( $\chi$ ) extracted from a simple one-dimensional heat conduction model under conditions where the flame characteristics are known. The

model relies on the concept that a fraction ( $\chi$ ) of the energy released by the flame is effectively used to support burning of the fuel. The higher the value of  $\chi$  the more effective the combustion process. The value of  $\chi$  is independent of the geometry (size, fuel layer thickness, etc.) and is only a function of the fuel. This value represents the mass burning efficiency of the fuel and is independent of the ignition and flame spread parameters. The experimental apparatus, measurement methods and experimental procedures used to validate this approach are described by Garo et al. (1996) who obtained  $\chi = 3.9 \times 10^{-3}$  for heating oil (a mixture of hydrocarbons ranging from C<sub>14</sub> to C<sub>21</sub>) and  $\chi = 2.9 \times 10^{-3}$  for crude oil (63% Kittiway, 33% Arabian Light and 4% Oural). Experiments were also conducted with weathered fuels as well as different fuel/water emulsions.

### Conclusions

The methodology to assess the burning characteristics of a liquid fuel on a water bed has been presented and verified. Three different and complementary tests are deemed necessary to characterize the three different regimes of the burning process: ignition, flame spread and mass burning. For ignition; the critical heat flux for ignition as identified in ASTM E-1321 was found to be the parameter that better describes the capability of a fuel to ignite. For flame spread; the minimum external heat flux that will sustain propagation together with the parameter  $\phi$  (function of the fuel properties) will serve to describe the flame spread characteristics. The complexity of flame spread over liquid fuels makes necessary further validation of this experimental approach. For mass burning; the efficiency factor,  $\chi$ , serves as unique parameter to characterize the regression rate during the mass burning process.  $\chi$  is a property of the fuel that can be extrapolated to different scales and environmental conditions but should be evaluated under conditions where is independent of the flame diameter and the fuel layer thickness.

### Acknowledgments

This work was conducted under the financial support of the National Institute of Standards and Technology and the authors express their thanks to Dr. D. Evans, Mr. D. Madrzykowski and Mr. J. McElroy for their multiple suggestions and their help in the development of the experimental hardware.

### References

- Garo, J.P., Vantelon, J.P., Gandhi, S. and Torero, J.L. (1996) "Some Observations on the Pre-Boilover Burning of a Slick of Oil on Water," *Proceedings of the Nineteenth Arctic and Marine Oil Spill Program Technical Seminar*, pp.1611-1626.
- Putorti, A. D., Evans, D. D. and Tennyson, E. J. (1994) "Ignition of Weathered and Emulsified oils," *Proceedings of the Seventeenth Arctic and Marine Oil Spill Program Technical Seminar*, pp.657-667.
- Quintere, J. (1981) "A Simplified Theory for Generalizing Results from a Radiant panel Rate of Flame Spread Apparatus," *Fire and Materials*, 5, 2, pp. 52-60.

**BLANK PAGE**

**5. Piloted Ignition of a Slick of Oil on Water**

N. Wu and J.L. Torero

*Eastern States Section of the Combustion Institute, Fall technical Meeting,  
pp. 245-248, October 1997.*

**BLANK PAGE**

# PILOTED IGNITION OF A SLICK OF OIL ON WATER

Neil Wu and Jose L. Torero  
Department of Fire Protection Engineering  
University of Maryland, College Park, MD 20742-3031  
USA  
e-mail: jltorero@glue.umd.edu

## ABSTRACT

An experimental technique has been developed to systematically study the ignition characteristics of liquid fuels spilled on a water bed. The final objective of this work is to provide a tool that will serve to assess a fuels ease to ignite, thus helping to better define the combustion parameters that affect in-situ burning of oil spills. A systematic study of the different parameters that affect ignition has been conducted in an attempt to develop a bench scale procedure to evaluate the burning efficiency of liquid fuels in conditions typical of oil spill scenarios. To study ignition, the Lateral Ignition and Flame Spread (LIFT) standard test method, ASTM E1321, has been modified to allow for the use of liquid fuels on a water bed. Characteristic parameters such as critical heat flux for ignition and ignition delay time have been obtained as functions of the external heat flux. A series of "fire properties" corresponding to the fuel can be extrapolated from this test and used to assess the tendency of a fuel to ignite.

Fuel properties vary significantly when subject to a strong heat insult, therefore, they need to be evaluated under fire conditions. Evaluation of the fuel "fire properties" that are independent of the length scale, will permit the ranking of fuels and will reduce the number of large scale experiments necessary to determine in-situ burning protocols and procedures. By focusing on the fuel and introducing external radiation, large scale conditions can be simulated. It must be noted that this is not a study of the burning characteristics but of the fuel burning efficiency.

Ignition will be studied by using a modified Lateral Ignition and Flame Spread Test (ASTM E-1321). Figure 1 shows a schematic of the modified LIFT apparatus.

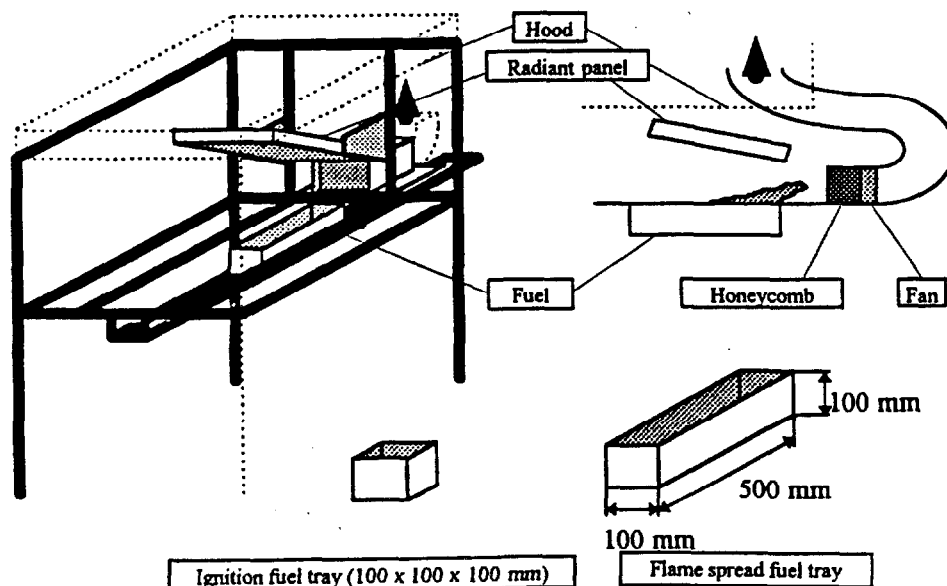


Figure 1-Schematic of the experimental apparatus.

This work attempts to identify an ideal configuration in which the ease by which a fuel can burn can be evaluated. The results should be independent of specific burning characteristics and geometrical constraints, and thus, extrapolation to a large scale should be possible. The critical heat flux for ignition ( $\dot{q}_{0,ig}''$ ) is the minimum external heat flux that will lead to equilibrium at the pyrolysis temperature ( $T_p$ ), thus, is given by:

$$\dot{q}_{0,ig}'' = h(T_p - T_i) \quad (1)$$

where  $T_i$  is an ignition temperature and "h" is a global heat transfer coefficient. By assuming one-dimensional heat conduction in the fuel and  $t_{ig} \approx t_p$  ( $t_p$  is the time needed to reach  $T_p$ ) a characteristic ignition delay time ( $t_{ig}$ ) can be obtained:

$$t_{ig} = \frac{\pi}{4a} \left( \frac{h(T_p - T_i)}{\dot{q}_c''} \right)^2 \quad (2)$$

where ( $\dot{q}_c''$ ) is the external heat flux,  $k$  is the thermal conductivity and  $a = \alpha(h/k)^2$ .

Mixing ( $t_M$ ), transport ( $t_T$ ) and chemical induction ( $t_{in}$ ) times are assumed negligible when compared to  $t_p$ . This will be satisfied best as the external heat flux approaches the critical heat flux for ignition ( $\dot{q}_c'' \approx \dot{q}_{0,ig}''$ ) and  $t_p \rightarrow \infty$ . This is important because it implies that the error incurred in the experimental determination of  $t_{ig}$ , (due to the unknown nature of the flow) will decrease as  $\dot{q}_c''$  approaches  $\dot{q}_{0,ig}''$ . Therefore,  $\dot{q}_{0,ig}''$  is a property of the fuel that can be extrapolated, independent of the flow. More details on the derivation of the above expressions and on the characteristics of the hardware are provided by Quintiere (1981).

To validate this approach, SAE 30W oil was used to conduct ignition tests. This fuel was used for comparison with previously reported results on ignition delay time by Putorti et al.(1994) and also because of its high flash point (approximately 250°C). A high flash point results in a longer ignition delay time providing a longer period to observe the different flow structures formed inside the liquid fuel and on the gas phase. The pilot size and location, the geometry of the fuel container and the flow around the sample have a significant effect on the ignition delay time ( $t_{ig}$ ) but for brevity only the study concerning the flow will be presented.

To study air entrainment into above the fuel sample, a 2W red diode laser (SDL-820) was used to create a light sheet for visualization of the smoke emerging from the fuel surface. Figures 2 and 3 are two typical images. In the absence of a flush floor, eddies could be observed at the edges of the tray (Figure 2). These eddies grow to cover the entire surface of the fuel tray. When a floor surrounded the tray the eddies disappeared and a random flow of gases was observed (Figure 3). The absence of eddies deters the mixing of fuel and oxidizer at the surface and as a consequence the ignition delay time increased by approximately 20%.

By introducing a 0.1 m/s flow parallel to the surface a boundary layer is formed and all eddies were eliminated. By introducing the forced flow  $t_M$  and  $t_T$  are reduced significantly and  $t_{ig}$  approaches  $t_p$ . The choice of a small velocity (0.1 m/s) is not arbitrary, as the velocity increases the convective component of "h" increases and will have an effect on the value of the critical heat flux for ignition.



Figure 2- Smoke visualization for a tray with no flush floor.



Figure 3- Smoke visualization for a tray with a flush floor.

The results from these experiments are presented in Figure 4 together with data obtained for the same fuel by Putorti et al. (1994) in a Cone Calorimeter. The ignition delay time is presented as  $t_{ig}^{-1/2}$ , following equation (2). Although the ignition delay time differs from the values found by Putorti et al. all data converges to a unique critical heat flux for ignition. Since these experiments were conducted using different ignition procedures and under different environmental conditions,  $t_M$  and  $t_T$  are expected to be different, thus, affecting the ignition delay time. On the contrary,  $t_p$  should not be affected if convective losses are similar in magnitude or can be neglected. As  $\dot{q}_e''$  approaches  $\dot{q}_{0,ig}''$ ,  $t_M$  and  $t_T$  become negligible compared to  $t_p$  and all data converges to a unique point ( $\dot{q}_{0,ig}'' \approx 6 \text{ kW/m}^2$ ).

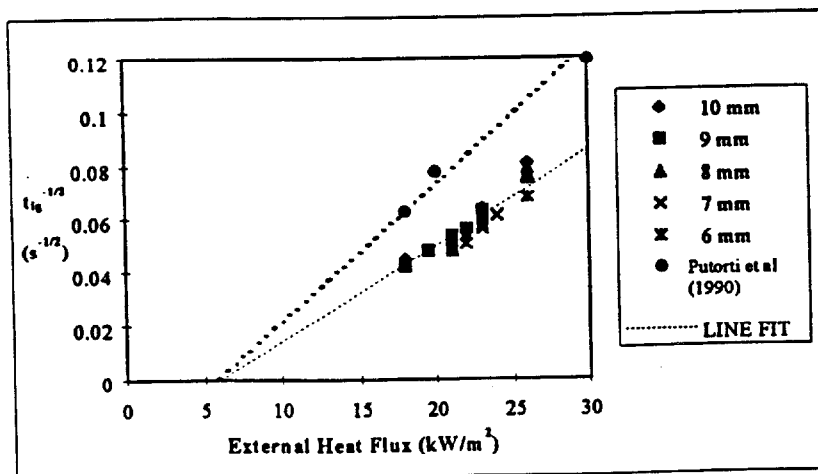


Figure 4-Ignition delay time for different external heat fluxes (SAE 30W oil). The delay times from Putorti et al (1994) were extracted as an average of the values obtained for 43 mm, 15 mm and 10 mm fuel layers

To further demonstrate the validity of this experimental methodology a series of tests were conducted with Cook Inlet and Alaskan North Slope (ANS) crude oils. Figure 5 shows these results and other obtained for ANS crude oil by Putorti *et al.* (1994). The data presented for the crude oils is an average of at least five experiments conducted under identical conditions. It was observed that Cook Inlet and ANS crude oils in their natural state ignited at ambient temperature, therefore no external heat flux was necessary. However, when Cook Inlet was evaporated to a 25% mass loss  $\dot{q}_{0,ig}''$  increased to approximately 3 kW/m<sup>2</sup> showing a significant increase in the difficulty to ignite. Similar phenomena occurred when the ANS crude was ignited in its evaporated state. The critical heat flux for ignition extrapolated from Putorti *et al.* (1994) for ANS crude oil (evaporated to a 30% mass loss) was approximately 4.5 kW/m<sup>2</sup> indicating greater difficulty of ignition than Cook Inlet crude oil (25% evaporated) and igniting more readily than the Cook Inlet Crude oil in its natural state.

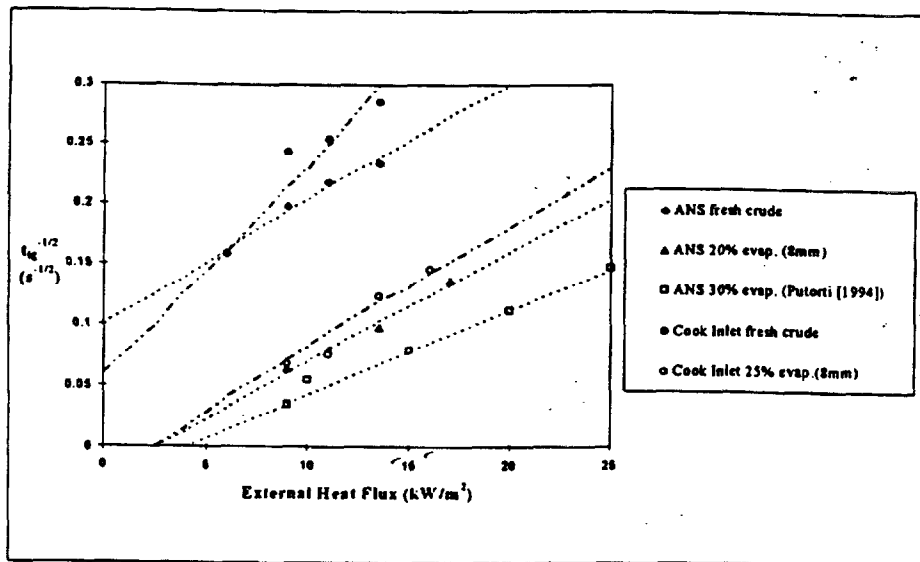


Figure 5. Ignition Delay Time for Different External Heat Fluxes.

The methodology to assess the ignition characteristics of a liquid fuel on a water bed has been presented and verified. For ignition, the critical heat flux for ignition as identified in ASTM E-1321 was found to be the parameter that better describes the capability of a fuel to ignite. To study ignition, the Lateral Ignition and Flame Spread (LIFT) standard test method apparatus has been modified to allow for the use of liquid fuels on a water bed.

## REFERENCES

- Putorti, A. D., Evans, D. D. and Tennyson, E. J. (1994) "Ignition of Weathered and Emulsified oils," *Proceedings of the Seventeenth Arctic and Marine Oil Spill Program Technical Seminar*, pp.657-667.
- Quintere, J. (1981) "A Simplified Theory for Generalizing Results from a Radiant panel Rate of Flame Spread Apparatus," *Fire and Materials*, 5, 2, pp. 52-60.

**6. Piloted Ignition of a Slick of Oil on a Water Sub-layer: The Effect of Weathering**

N. Wu, G. Kolb and J.L. Torero

*27<sup>th</sup> Combustion Symposium (International) on Combustion, The Combustion Institute, (in press) 1998.*

**BLANK PAGE**

**PILOTED IGNITION OF A SLICK OF OIL ON A WATER SUBLAYER:  
THE EFFECT OF WEATHERING**

Neil Wu, Gilles Kolb and Jose L. Torero\*  
Department of Fire Protection Engineering  
University of Maryland  
College Park, MD 20742-3031  
USA

**\* Corresponding Author:**

*1.*

**Jose L. Torero**  
Department of Fire Protection Engineering  
University of Maryland, College Park, MD20742, USA  
*Telephone: 1-301-405-0043, FAX: 1-301-405-9383, e-mail: jltorero@eng.umd.edu*

**Word Count**

Text	3,991 words (Word 6.0 word count)
Equations	105 words
<u>7 Figures</u>	<u>1,400 words</u>
<b>TOTAL</b>	<b>5,496 words</b>

**BLANK PAGE**

## **PILOTED IGNITION OF A SLICK OF OIL ON A WATER SUBLAYER: THE EFFECT OF WEATHERING**

Neil Wu, Gilles Kolb and Jose L. Torero\*  
Department of Fire Protection Engineering  
University of Maryland  
College Park, MD 20742-3031  
USA

### **Abstract**

Piloted ignition of a slick of oil on a water sub-layer has been experimentally studied. The objective of this work is to provide a tool that will serve to assess a fuels ease to ignite under conditions that are representative of oil spills. The fuel is exposed suddenly to external radiation to increase the its temperature until ignition occurs. The strength and geometrical placement of the pilot were chosen to minimize gas phase induction time and heat feedback from the pilot to the fuel surface. Temperature measurements, flow visualization and ignition delay time are used to characterize piloted ignition and an existing one-dimensional heat transfer model is used correlate the experimental results. Two different crude oils and SAE 30W oil were used for these experiments. Crude oils were tested in their natural state and at different levels of weathering. It was observed that the ignition delay time is a strong function of the flow structures formed both in the liquid and gas above the pool. Piloted ignition is inhibited by premature boiling of the water sub-layer and weathering significantly increases the ignition delay time. It was determined that a critical heat flux for ignition could be obtained and better serve as a parameter to characterize the fuel propensity to ignite in the presence of a strong pilot. The minimum heat flux that will permit ignition before boiling of the water sub layer occurs also needs to be considered.

---

\* Corresponding Author

**BLANK PAGE**

## **Introduction**

Burning of an oil spill is of interest as a result of offshore exploration, production, and transportation of petroleum [1]. In the case of an accidental spill at sea, in-situ burning can provide an effective means for the removal of an oil slick reducing negative environmental impact. The efficiency of the ignition and burning process is crucial for the successful elimination of the crude oil.

Information available on burning of a thin fuel layer on a water sub-layer is quite limited. Thin layer boil-over [1, 2, 3] has been found generally to enhance burning rate although Koseki et al. [1] noted that boiling at the fuel-water interface can limit flame spread. The effect of minimum fuel layer thickness necessary for sustained combustion has been studied extensively [2, 3]. Several models have been developed to describe the heat losses from a pool fire to the supporting water layer [4] and to attempt description of in-depth absorption of radiation by the fuel layer [5]. Flame spread across the liquid fuel surface has also been emphasized and excellent review papers have been published by Glassman [6] and Ross [7]. Glassman, summarizes the extensive literature on ignition, however, it is clear that little attention has been drawn to characterize the ignition process of liquid fuels on a water sub-layer.

Ignition behavior of petroleum fractions has not been studied beyond flash and fire points under quiescent conditions [6, 8, 9]. Weathering and oil/water emulsions on the flash and fire points have yet to be studied. Flash or fire point tests do not incorporate the effects that high heat insult has on the nature of the fuel, i.e. emulsions break down when subject to a high heat flux, thus are of reduced application for an oil spill scenario. Furthermore, heat transfer towards the water sub-layer is entirely dependent on the fuel properties and can preclude ignition, therefore needs to be incorporated when characterizing the ignition process. To the knowledge of the authors, the only study that addresses the effect of weathering and formation of emulsions on ignition under conditions pertinent to the oil-spill scenario is due to Putorti et al. [10]. This study quantified the necessary heat flux for ignition of various liquid fuels and emphasis was placed on the ignition delay time of weathered and emulsified samples.

Most accidental and deliberate burns of spilled oil at sea suffer from the effects of wind and waves. Volatiles tend to evaporate rapidly with time (weathering) and mixing

tend to form oil/water emulsions making the oil difficult to ignite. Consequently, alteration of the physical or chemical properties of the oil can require additional energy for ignition. Several studies reported have attempted to characterize weathering and emulsions typical of oil-spill scenarios [11].

In-situ burning of an oil spill requires the fuel to ignite and that ignition to be followed by spread and eventually leading to mass burning. Many studies have shown that ignition is not always followed by spread [12] therefore, is not sufficient to guarantee efficient removal of the oil slick. The need to understand the three stages necessary for the efficient removal of crude oil have resulted in the choice to use a modified version L.I.F.T. (ASTM-E-1321) [13] apparatus to characterize the burning process.

The overall objective of this study is to characterize the entire burning process but in the present work emphasis will be given to piloted ignition. This choice does not provide optimal conditions for the study of each individual element but it is justified in the general context of this problem. This study will use two different crude oils, as representative of those commonly transported by oil-tankers, and SAE 30W oil as a reference of a better characterized fuel. Crude oils will be studied in their natural state and subject to different levels of weathering. The formation of emulsions and its effect on ignition will be a subject of future study but goes beyond the objectives of the present work.

## **Background**

Fuel properties vary when subject to a strong heat insult, therefore, need to be evaluated under “fire conditions” [14]. The concept of minimum heat flux for ignition has been commonly applied to solid fuels and ignition behavior can be predicted or measured using small, bench-scale experiments. In a similar fashion, ignition behavior of liquid fuels can be studied and evaluation of the “fire properties” allows ranking of fuels in various states; natural, weathered, and emulsified. The scale dependency will always be a matter of controversy, thus, large scale tests remain a necessity for validation.

The mechanisms leading to gas phase ignition can be described as follows. The liquid bed is considered initially at ambient temperature,  $T_i$ . After suddenly imposing an external heat flux ( $\dot{q}_c''$ ) the temperature of the bed rises until the surface reaches the

pyrolysis or evaporation temperature ( $T_p$ ). The time required for the fuel surface to attain  $T_p$  will be referred as the pyrolysis time,  $t_p$ . After attaining  $T_p$ , the vapor (pyrolysate) leaves the surface, is diffused and convected outwards, mixes with the ambient oxidizer, and creates a flammable mixture near the solid surface. This period will be referred here as the mixing time,  $t_m$ . If the mixture temperature is increased the combustion reaction between the fuel vapor and the oxidizer gas may become strong enough to overcome the heat losses to the solid and ambient. Thus becoming self-sustained and at which point flaming ignition will occur. This period corresponds to the induction time,  $t_i$ .

Extending the analysis proposed by Fernandez-Pello [15], the ignition time ( $t_{ig}$ ) will be given then by

$$t_{ig} = t_p + t_m + t_i \quad (1)$$

Introducing a pilot reduces the induction time making it negligible when compared to  $t_p$  and  $t_m$ . Furthermore, mixing has been commonly considered as a fast process compared to heating of the fuel, therefore, the fuel and oxidizer mixture becomes flammable almost immediately after pyrolysis starts. Pyrolysis temperatures and times are, thus, commonly referred as ignition temperature and ignition time [14] and equation (1) simplifies to

$$t_{ig} = t_p \quad (2)$$

and  $T_{ig}$  can be defined as  $T_p$ . Although such a definition is not physically correct [16] it can be very useful in some practical applications since provides a reference parameter that could serve to characterize ignition.

The flow over the fuel surface will control mixing of fuel and oxidizer as well as the transport of this mixture towards the pilot ( $t_m$ ), therefore, can have a significant effect on  $t_{ig}$  and on the validity of equation (2). Equation (2) could be extrapolated only if the experimental conditions at which the ignition delay time is obtained satisfy the assumption that  $t_m \approx t_i \ll t_p$ . Slight changes in the flow structure, especially for a horizontal configuration, can strongly affect  $t_m$  without changing  $t_p$  significantly. This effect is least significant as the external heat flux approaches the critical heat flux for pyrolysis ( $\dot{q}_e'' \approx \dot{q}_{0,p}''$ ) and  $t_p \rightarrow \infty$ . This is important because it implies that the error

incurred in the experimental determination of  $t_{ig}$ , (due to the unknown nature of the flow) will decrease as  $\dot{q}_e''$  approaches  $\dot{q}_{0,p}''$ .

To obtain  $t_p$  the fuel and water bed are assumed as one thermally thick material with properties corresponding to an unknown combination of both liquids. The bed is assumed a semi-infinite slab, thus all convective and thermo-capillary motion in the bed is neglected. This assumption is not necessarily correct [7], and will be addressed later, but will be accepted as a possible source of error. Throughout the heating process the fuel layer is assumed inert with negligible pyrolysis before ignition. The solution to the one-dimensional transient heating of a semi-infinite slab is given by Carslaw and Jaeger [17] and an elaboration of all additional assumptions and the derivation pertaining to the present study are given by Quintiere [14].

The boundary condition for this solution is imposed by heat balance at the surface which needs to incorporate convective heat losses, re-radiation, in-depth absorption and the fraction of the external heat flux not absorbed [18]. Losses result in a minimum external heat flux necessary,  $\dot{q}_{0,p}''$ , to attain  $T_p$ . For  $\dot{q}_e'' < \dot{q}_{0,p}''$  the surface will attain thermal equilibrium at  $T_{EQ} < T_p$ . A linearized heat transfer coefficient,  $h$ , is commonly used to describe heat transfer at the surface and all heat loss terms can be reduced to  $h(T_p - T_i)$ . Values for “ $h$ ” have been shown to vary with orientation and environmental effects. Examples of typical values found in the literature are:  $8.0 \text{ Wm}^2\text{K}^{-1}$  for natural turbulent convection and a vertical sample [14],  $13.5 \text{ Wm}^2\text{K}^{-1}$  for a horizontal orientation [18], and up to  $15.0 \text{ Wm}^2\text{K}^{-1}$  obtained by Mikkola and Wichman [19] while conducting experiments on a vertical orientation with wood.

These assumptions lead to the following solution for the attainment of the pyrolysis temperature as a function of time

$$h(T_p - T_i) = \dot{q}_e'' [1 - \exp(-at_p) \text{erfc}(at_p)] \quad (3)$$

where  $t_p$  is the time necessary to attain  $T_p$  at the surface,  $a = \alpha(h/k)^2$ , “ $\alpha$ ” the thermal diffusivity and “ $k$ ” the thermal conductivity. It needs to be noted that “ $k$ ” and “ $\alpha$ ” are not the fuel or water properties but an equivalent set of properties that includes the contribution of both liquids. If  $\dot{q}_e'' = \dot{q}_{0,p}''$ ,  $T_p$  is expected to be reached when  $t \rightarrow \infty$  and

the critical heat flux that would lead to pyrolysis can be derived from equation (3) and is given by

$$\dot{q}_{0,p}'' = h(T_p - T_i) \quad (4)$$

For  $\dot{q}_e'' \gg \dot{q}_{0,p}''$  it can be assumed that  $[1 - \exp(-at_p) \operatorname{erfc}(\sqrt{at_p})] \approx \frac{2}{\sqrt{\pi}} (at_p)^{1/2}$  which leads to the approximate expression valid for short times ( $t_p$ )

$$t_p = \frac{\pi}{4a} \left( \frac{\dot{q}_{0,p}''}{\dot{q}_e''} \right)^2 \quad (5)$$

Equation (5) is of great practical importance since shows that a plot of  $t_p^{-1/2}$  as a function of the corresponding  $\dot{q}_e''$  will be linear for  $\dot{q}_e'' > \dot{q}_{0,p}''$  and from the slope of this line the value of “a” can be determined. The fire literature generally refers to “a” as a global thermal property of the material.

In the present study, the magnitudes of  $t_m$  and  $t_i$  will be addressed but the geometry will be chosen to make them minimal, thus  $\dot{q}_{0,p}'' \approx \dot{q}_{0,ig}''$  and, from equation (2),

$$t_p \approx t_{ig}$$

## Methodology

The LIFT requires the sample to be positioned vertically, and a uniform radiant flux is suddenly applied. For this study the LIFT had to be rotated 90° to a horizontal position (Fig.1). A fan, capable of inducing an air flow velocity of 0.1 m/s, was placed at the trailing edge of the sample. A homogeneous flow is guaranteed by means of a duct placed in front of the fan. The duct is filled with steel wool sandwiched between two honeycomb plates.

A radiation shield (marinite board) is placed in front of the panel before the sample is introduced to its test position (Fig. 1). Once the sample has been placed, the radiation shield is removed and time recording starts. It was observed that increasing the pilot size reduced the ignition delay time and increasing the distance from the fuel surface had an opposite result. Thus, choice for size and location of the pilot resulted from a systematic study that minimized the effect of heat feed back from the pilot to the fuel surface and to guaranteed best repeatability of the results. Premature ignition by a pilot flame has been

addressed by several authors who showed similar observations [6]. This systematic study lead to a small propane diffusion flame (20 mm in height) established on a 4 mm stainless-steel nozzle to be used as an ignition pilot. The nozzle was placed 10 mm above the fuel surface plane in the centerline and 10 mm downstream of the trailing edge of the ignition tray (Fig.1).

The fuel tray was placed under a 200 mm square plate with a 100 mm square hole in the middle where the fuel was located. Details on this plate and its use will be provided in later sections.

The fuel was placed in 100 mm cubical stainless steel trays with one open side. Two different ignition trays were used for the tests. The first tray contained an interior lip measuring 5 mm surrounding the edge of the open end. The second tray, of similar construction, had no interior lip. Previous studies on ignition using the cone-calorimeter [10] will be used throughout this work as reference data. In these experiments Putorti et al. used a tray of square section of similar dimensions to the ones used in the present study and with a 5 mm interior lip.

The radiant panel forms an angle of  $15^\circ$  with the sample, with the objective of producing a heat flux distribution as the one shown in Fig.2. Despite the inclination the incident heat flux for the region up to 150 mm is relatively uniform (Fig.2(a)) providing a constant heat flux boundary condition for the fuel/air interface. Thermocouples measurements have been used to characterize the temperature evolution of the fuel and have shown neglectable differences at several locations along the fuel surface (Fig.2(b)). Detailed hardware characteristics, typical heat flux distributions and experimental procedures involving the LIFT have been well documented [14] and will not be repeated here.

## **Experimental Results and Discussion**

### ***2. The Effect of Temperature Gradients Between the Fuel and the Container***

The container has significant effects on the formation of recirculation currents inside the liquid. Temperature gradients in the fuel surface induce thermo-capillary motion combined with natural convection [7] enhancing heat transfer inside the liquid

and resulting in a more homogeneous temperature distribution and, thus, in longer ignition delay times. Eight chromel-alumel thermocouples (0.5 mm in diameter) were placed in the liquid bed with the tip at the axis of symmetry. The thermocouples were spaced to provide a finer grid close to the surface and to cover the entire depth of the tray (distance from the thermocouple to the surface: 0 mm, 3mm, 6 mm, 10 mm, 18 mm, 43 mm, 68 mm and 93 mm).

Heat from the radiant panel increases the temperature of the fuel but also of the container. The inclusion of a 5 mm lip increased the solid surface receiving radiation from the panel. Temperatures of the upper part of the tray were observed to be significantly higher than those observed for the no-lip tray. In contrast the fuel surface temperature was found to be consistently higher for the no-lip tray, while the temperatures recorded by the thermocouples deeper in the fluid were higher for the lip tray. Recirculation inside the liquid bed resulted in a 30% increase in the ignition delay time when the tray with a lip was used. For identical fuel layer thickness and external heat flux, boiling occurred faster in the tray with an interior lip.

A fine metallic powder was used to coat the surface of the fuel with both trays. Observations of the flow in the lip tray indicated increasing eddy activity of the fuel layer as the temperature difference between the container and the fuel increased. These flow patterns were found to be restricted to approximately 10 mm from the tray in the absence of an interior lip. Motion of the powder was observed to be almost negligible in a circle approximately 80 mm in diameter. This issue is worth an independent study but escapes the objectives of the present work. By selecting the no-lip configuration, effect of heat transfer from the tray was considered minimized.

### ***3. Flow Structures Above the Fuel Surface***

To study the flow characteristics over the fuel sample, a 0.5W red diode laser (SDL-820) was used to create a light sheet for visualization of the smoke emerging from the fuel surface. The images have been processed using an EPIX video card. To obtain a clear image of the flow structure, as evidenced by the smoke, a threshold was established

below which all pixels were assigned a 0 value. Figure 3 shows a set of three typical images.

In the absence of a flush floor surrounding the fuel tray, clear eddies could be observed at the edges of the tray (Fig. 3(a)). It was observed that these eddies could grow and cover the entire surface of the fuel tray. When a floor surrounded the fuel tray (as shown in Fig. 1) the eddies disappeared and a random upward flow of gases was observed (Fig. 3(b)). As a consequence of the decreased mixing of fuel and air, the ignition delay time increased by approximately 20% over the no-floor case. By introducing a flush floor and 0.1 m/s flow parallel to the surface a boundary layer is formed and the all eddies were eliminated (Fig. 3(c)). Although the ignition delay time remained dependent on the magnitude of the flow, this configuration allowed for greatest repeatability.

#### *Ignition Delay Time*

To calibrate the apparatus, SAE 30 W oil was first used for the ignition tests. This fuel was used to make possible comparison with previously reported results on ignition delay time [10] and also because of the high flash point (approximately 250°C). The higher flash point results in a longer ignition delay time providing a longer period to observe the different processes affecting ignition. Radiation absorption is also lower with SAE 30 oil favoring boiling of the water bed. Although the viscosity of SAE 30 oil is generally higher than that of crude oils, it is very sensitive to temperature (approximately  $1 \times 10^{-2}$  at 0°C and  $1 \times 10^{-5}$  at 100°C) reaching comparable values after only a small temperature increase.

The results from these experiments are presented in Figure 4 together with data obtained for the same fuel by Putorti et al. [10]. Following equation (5) the ignition delay time is presented as  $t^{-1/2}$ . It can be observed that, although the ignition delay time significantly differs from the values found by Putorti et al. al. data converges to a unique critical heat flux for ignition. Since these experiments where conducted using different ignition procedures and under different environmental conditions,  $t_m$  is expected to be different, thus, affecting the ignition delay time. On the contrary,  $t_p$  should not be affected if convective losses are similar in magnitude. As the external heat flux

approaches  $\dot{q}''_{0,ig}$ ,  $t_m$  becomes neglectable compared to  $t_p$  and all data converges to a unique point ( $\dot{q}''_{0,ig} \approx 5 \text{ kW/m}^2$ ), as observed in Figure 4. This linear dependency corresponds well with data reported in the literature for solid fuels [14, 19] and serves to validate the above mentioned assumptions.

For the particular case of an oil-slick on a water bed, the water underneath the fuel might attain boiling before ignition occurs. It was observed that once boiling started ignition of the fuel was precluded. Heating of the bed can be treated as a semi-infinite solid and temperature distributions can be predicted quite accurately [4]. The analytical prediction of a characteristic time to boiling goes beyond the scope of this work. But, the determination of a minimum heat flux that will lead to boiling ( $\dot{q}''_{0,B}$ ) before ignition can occur is of great practical importance therefore needs to be included as a complement to the critical heat flux for ignition.

As the external heat flux decreases the temperature gradient at the surface decreases and thermal penetration increases before the surface attains  $T_p$ . If the thermal wave can increase the water temperature at the fuel/water interface to the boiling point before the surface reaches  $T_p$ , boiling will prevent ignition from occurring. The minimum heat flux that will allow the surface temperature to reach  $T_p$  before boiling is given by  $\dot{q}''_{0,B}$  and presented in Fig. 5. As the fuel layer decreases in thickness, the heat wave will reach the water faster allowing for a shorter available time for the surface to reach  $T_p$  and consequently requiring a higher temperature gradient at the surface (higher  $\dot{q}''_{0,B}$ ).

#### ***4. Crude Oils and the Effect of Weathering***

A series of tests were conducted with two crude oils. Figure 6 shows ignition delay times for different external heat fluxes obtained for ANS crude oil and data reported by Putorti et al. [10]. The data presented is an average of at least five experiments conducted under identical conditions. It was observed that ANS crude oil in its natural state ignited at ambient temperature, therefore no external heat flux was necessary. Flash points for this type of fuel have been reported as low as 19°C [8] showing agreement with the above observation. When weathered, the ignition delay time

decreases as the heat flux increases and a linear dependency between the external heat flux and  $t_{ig}^{-1/2}$  is obtained. The intercept with the horizontal axis will provide the critical heat flux for ignition. Figure 6 shows that the critical heat flux for ignition will increase with weathering. The experimental data from Putorti [10] fits well with the data collected in the present work.

The critical heat flux for ignition ( $\dot{q}_{O,ig}''$ ) as obtained from figures such as Fig. 6 is presented in Fig. 7. Results are presented for Cook Inlet and ANS crude oils for different fuel layer thickness. Figure 7 shows a discrepancy between the critical heat flux for ignition for 3 mm as opposed to almost identical values obtained for 8 and 15 mm layers. For layers thicker than 8 mm the effect of fuel layer thickness was mostly manifested on the curves being truncated by boiling before attaining  $\dot{q}_{O,ig}''$ . The increasing value of  $\dot{q}_{O,ig}''$  with mass loss shows that weathering makes ignition more difficult, the increasing slope of the curve points towards the possibility of an asymptotic value at which the crude oil will not ignite. Based on the values for  $\dot{q}_{O,ig}''$  ANS crude oil was observed to be more prompt to ignition than Cook Inlet crude oil. Cook inlet ignited without an external heat flux for a mass loss rate smaller than 10 % and ANS crude oil for a mass loss smaller than 7%. The results presented are representative of all other cases studied.

## Conclusion

To study piloted ignition of a slick of oil on a water sub layer, a modified LIFT apparatus is used. Ignition delay times and a critical heat flux for ignition can be extracted using this testing methodology. The ignition delay time is a strong function of the flow structures formed both in the liquid and gas above the pool. Piloted ignition is inhibited by premature boiling of the water sub-layer. The minimum heat flux that will permit ignition before boiling of the water sub-layer needs to be considered. The critical heat flux for ignition will serve as an appropriate parameter to characterize the fuel propensity to ignite. Cook Inlet, ANS crude oils and SAE 30W oils were used for these experiments and crude oils were tested in their natural state and at different levels of weathering. Weathering of the crude oils significantly increases the ignition delay time.

The data extracted can be used as a tool to rank fuels in various states; natural and weathered.

## 5. Acknowledgements

Funding for this work was provided by NIST. The technical comments, encouragement and support of Dr. Marino di Marzo are greatly acknowledged.

## References

1. Koseki, H., Kokkala, M., and Mulholland, G.W., *Fire Safety Science-Proceedings of the Third International Symposium*, 865-875, 1991.
2. Garo, J.P., Vantelon, J.P., and Fernandez-Pello, A.C., *Twenty-fifth Symposium (International) on Combustion*, The Combustion Institute, Pittsburgh, PA, 1481-1488, 1994.
3. Arai, M., Saito, K., and Altenkirch, R.A., *Combustion Science and Technology*, 71, 25-40 1990.
4. Brzustowski, T.A., and Twardus, E.M., *Nineteenth Symposium (International) on Combustion*, The Combustion Institute, Pittsburgh, PA, 847-854, 1982.
5. Twardus, E.M. and Brzustowski, T.A., *Archivum Combustionis*, Polish Academy of Sciences, 1, 1-2, 49-60, 1981.
6. Glassman, I., and Dryer, F., *Fire Safety Journal*, 3, 123-138, 1980.
7. Ross, H., *Progress in Energy and Combustion Science*, 20, 17-63, 1994.
8. *SFPE Handbook*, 2<sup>nd</sup> Edition, Society of Fire Protection Engineers, Quincy, MA, 2.161-2.170, 1994.
9. Hillstrom, W., *Eastern States Section: Combustion Institute Fall Technical Meeting*, The Combustion Institute, 1975.
10. Putorti, A., Evans, D., and Tennyson, E., *Proceedings from the Seventeenth Arctic and Marine Oil Spill Program Technical Seminar*, 657-667, 1994.

11. Bobra, M., "A Study of the Evaporation of Petroleum Oils," Publication EE-135, Environmental Canada, Ottawa, Ontario, K1A OH3, 1992.
12. Kasiwagi, T., Mell, W.E., McGrattan, K.B. and Baum, H.R., *Fourth International Micro-gravity Combustion Workshop*, NASA Lewis Research Center, 411-416, 1997.
13. Annual Book of ASTM Standards, *ASTM E-1321 Standard Test Method for Material Ignition and Flammability*, Vol. 04.07, 1055-1077, 1994.
14. Quintiere, J., *Fire and Materials*, 5, 2, 52-60, 1981.
15. Fernandez-Pello, A.C., "Combustion Fundamentals on Fire: The Solid Phase," *Academic Press*, 31-100, 1995.
16. Alvares, N. and Martin, S.B., *Thirteenth Symposium (International) on Combustion*, The Combustion Institute, 905-914, 1971.
17. Carslaw, H.S. and Jaeger, J.C., *Conduction of Heat in Solids*, 2<sup>nd</sup> Edition, Oxford University Press, Oxford, 70-76, 1963.
18. Janssens, M., *Fire Safety Science-Proceedings of the Third International Symposium*, 167-176, 1991.
19. Mikkola, E. and Wichman, I., *Fire and Materials* 14, 1989.

## List of Figures

**Figure 1.** Schematic of the experimental apparatus.

**Figure 2.** (a) Incident radiant flux distribution for the HIFT apparatus (b) Ignition sample thermocouple temperatures for SAE 30W oil. Upper temperature curves correspond to surface temperatures in the corner, side and center of the tray. Lower temperature curves correspond to temperature 5 mm blow fuel surface in the corner, side and center of the tray.

**Figure 3.** Smoke visualization of sample tray (a) in the absence of flush floor, (b) surrounded by a flush floor, and (c) surrounded by a flush floor with a weak draft.

**Figure 4.** Ignition delay times of SAE 30W oil for various external fluxes.

**Figure 5** Critical heat flux and time for boiling using SAE30W oil.

**Figure 6.** Ignition delay times for various external heat fluxes for crude oils.

**Figure 7.** Critical heat flux for ignition ( $\dot{q}''_{O,ig}$ ) for ANS and Cook Inlet crude oils weathered at various different levels (% mass loss).

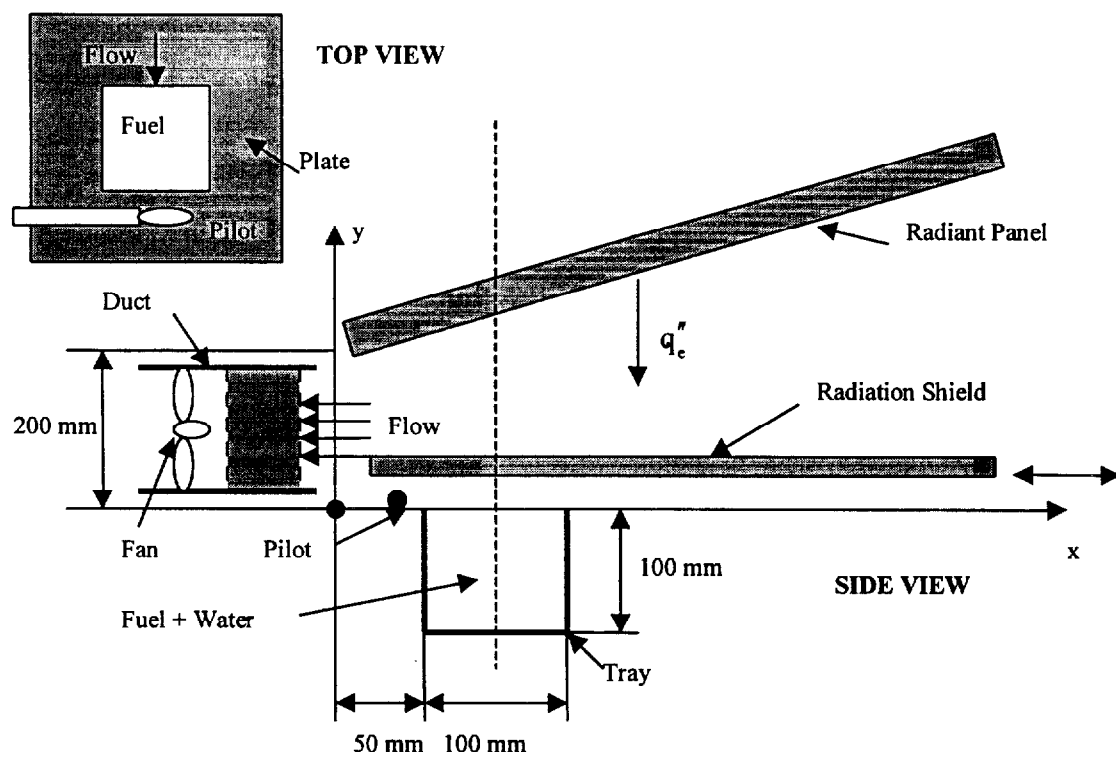


**Figure 1**

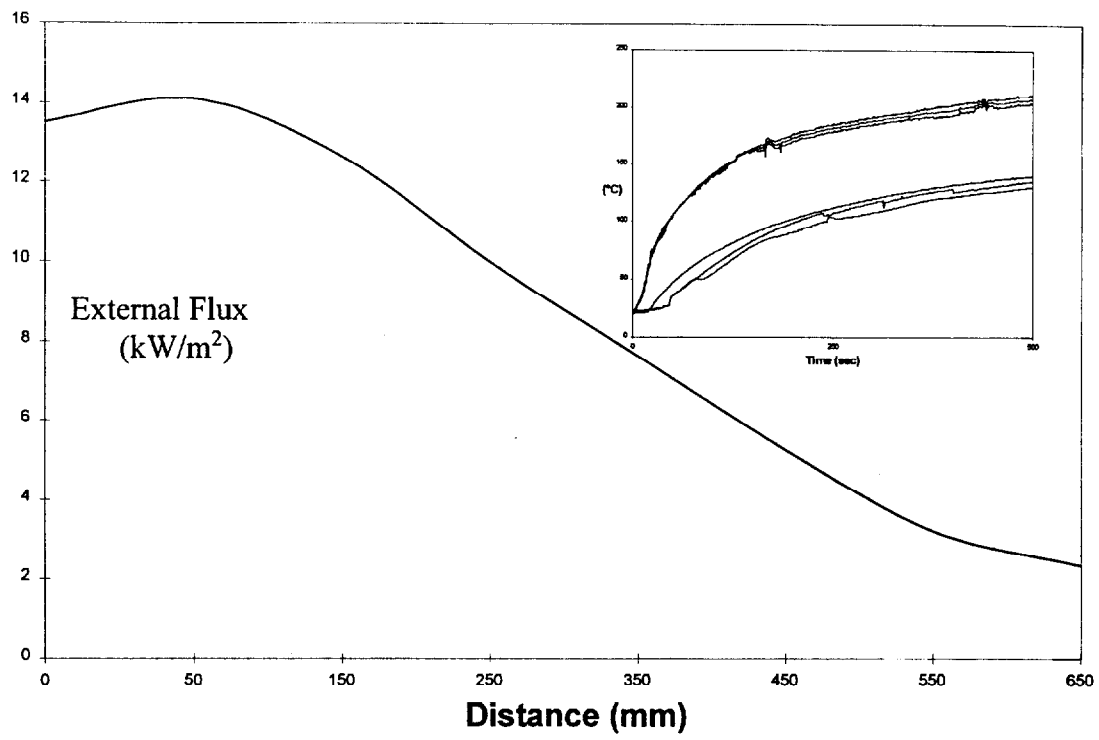
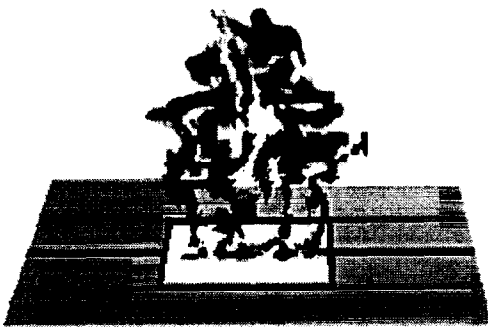


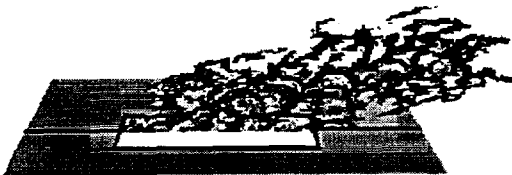
Figure 2



(a)



(b)



(c)

**Figure 3**

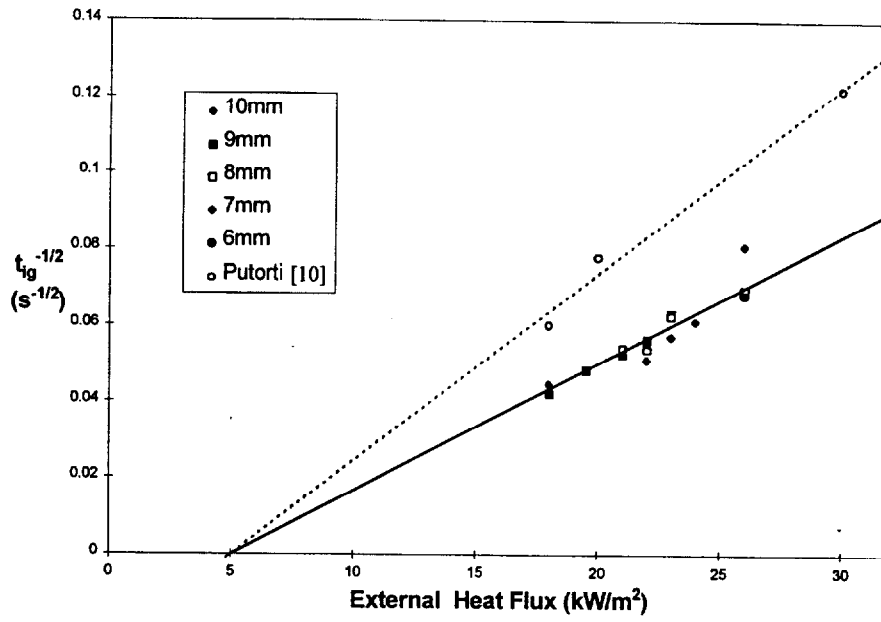
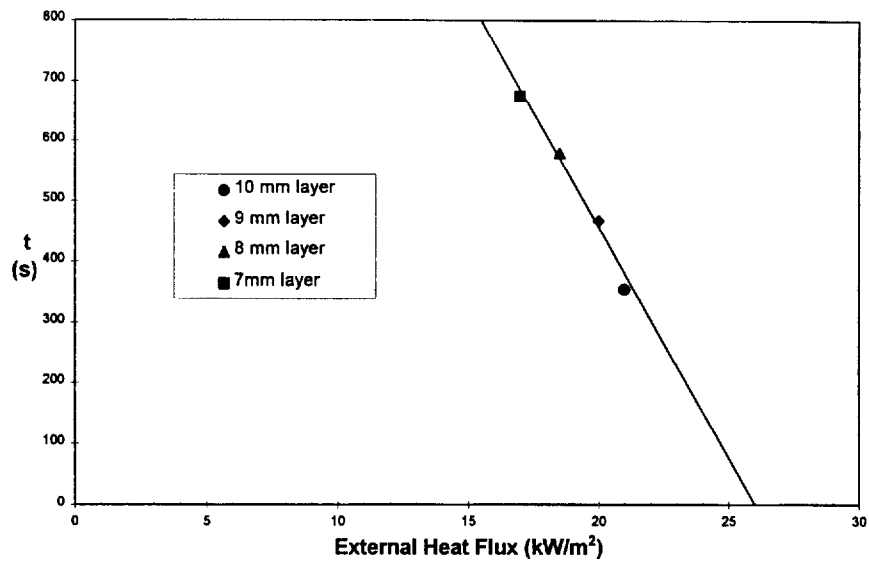


Figure 4



**Figure 5**

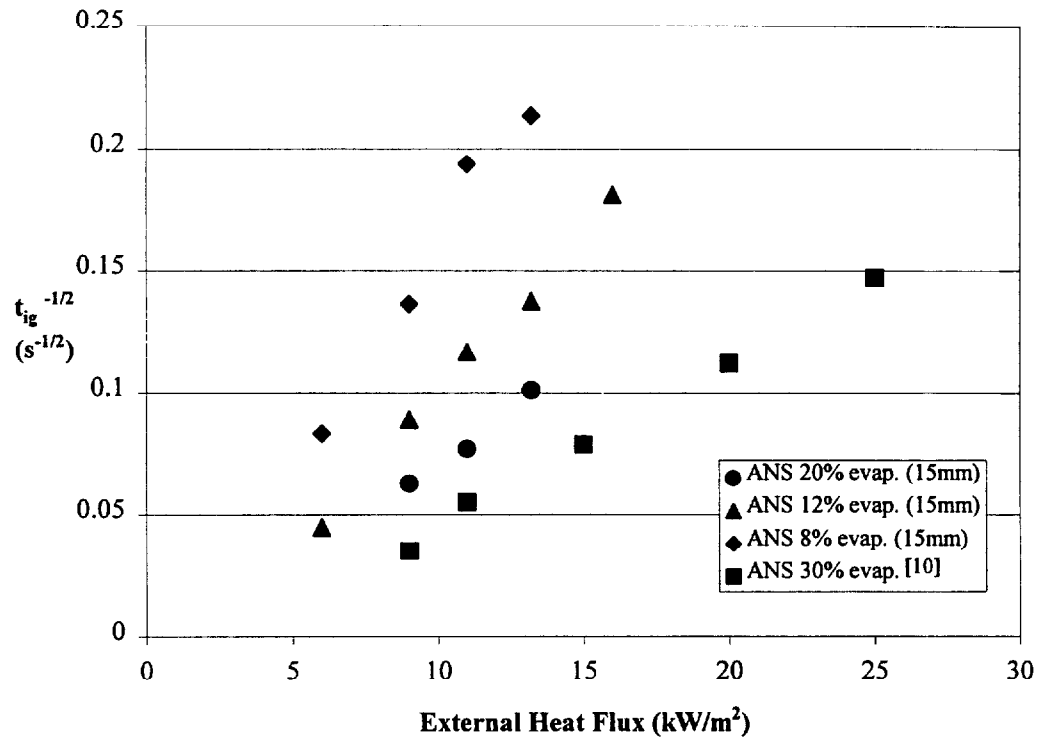
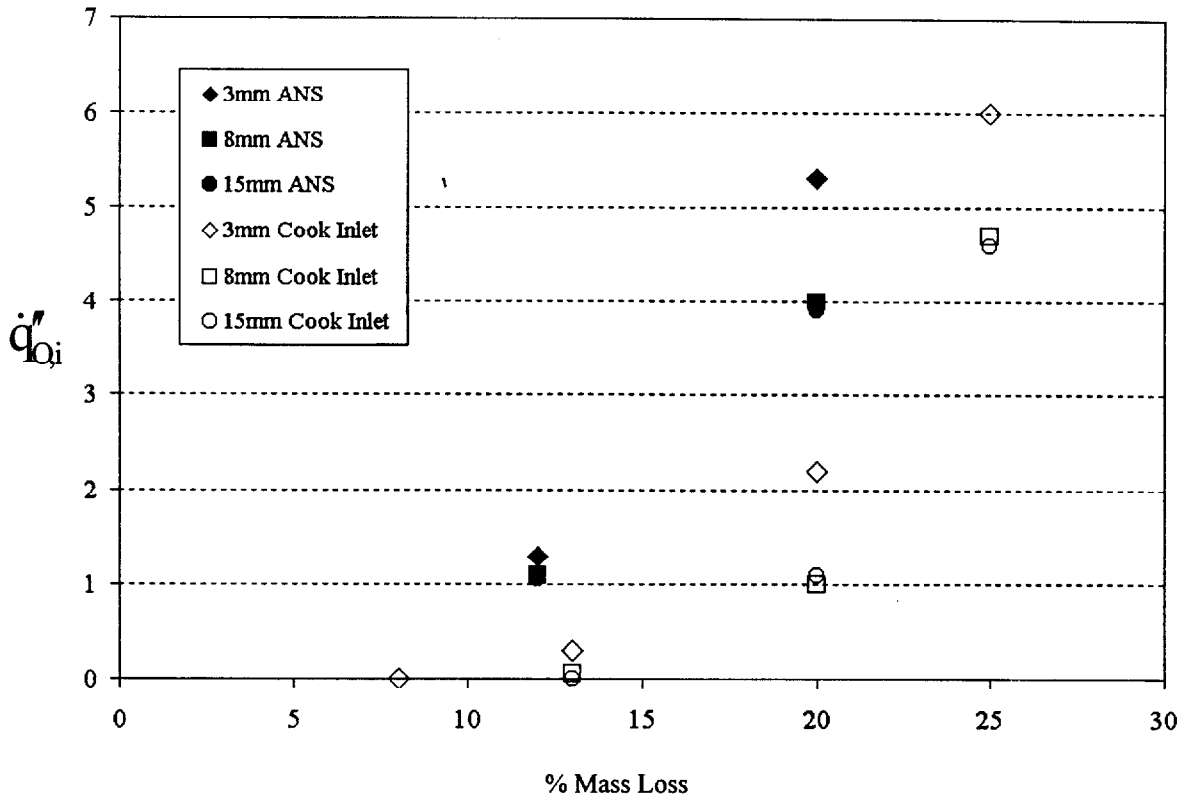


Figure 6



**Figure 7**

## **7. The Effect of Weathering on Piloted Ignition and Flash Point Of a Slick of Oil**

**BLANK PAGE**

**7.1. The Effect of Weathering on Piloted Ignition and Flash Point Of a Slick of Oil**

N. Wu, T. Mosman, S. M. Olenick

*21<sup>st</sup> Arctic and Marine Oilspill Program (AMOP) Technical Seminar,  
Edmonton, Canada, June 1998.*

**BLANK PAGE**

## **The Effect of Weathering on Piloted Ignition and Flash Point of a Slick of Oil**

N. Wu, T. Mosman, S. M. Olenick and J. L. Torero  
Department of Fire Protection Engineering  
University of Maryland  
College Park, MD 20742-3031, USA  
E-mail: jltorero@eng.umd.edu , Telephone: 1-301-405-0043

### **Abstract**

Ignition of a slick of oil on a water sub-layer has been experimentally studied. The objective of this work is to provide a tool that will serve to assess a fuel's ease to ignite under conditions that are representative of oil spills. Two different techniques are used and the results compared, piloted ignition when the fuel is exposed to a radiant heat flux and flash point as measured by the ASTM D56 Tag Closed Cup Test. For the piloted ignition tests the fuel is exposed suddenly to external radiation to increase its temperature until ignition occurs. Temperature measurements and ignition delay time are used to characterize piloted ignition and an existing one-dimensional heat transfer model is used to correlate the experimental results. For the flash point test, the bulk temperature of the fuel is increased until thermal equilibrium is attained and then a pilot is introduced. The temperature at which the first flashes are observed is called the flash point. Two different crude oils were used for these experiments, ANS and Cook Inlet. Crude oils were tested in their natural state and at different levels of weathering. Piloted ignition and flash point are strong functions of the weathering level. Premature boiling of the water sub-layer inhibits ignition. The flash point temperature can be used as a characteristic pyrolysis temperature and the weathering level has a negligible effect on the thermal properties of the fuel. It was determined that a critical heat flux for ignition could be obtained and better serve as a parameter to characterize the fuel propensity to ignite in the presence of a strong pilot. The minimum heat flux that will permit ignition before boiling of the water sub-layer occurs also needs to be considered.

### **1.0 Introduction**

Burning of an oil spill is of interest as a result of offshore exploration, production, and transportation of petroleum (Koseki et al., 1991). In the case of an accidental spill at sea, in-situ burning can provide an effective means for the removal of an oil slick reducing negative environmental impact. The efficiency of the ignition and burning process is crucial for the successful elimination of the crude oil.

Information available on burning of a thin fuel layer on a water sub-layer is quite limited. Thin layer boil-over (Koseki et al., 1991, Garo et al., 1994, Arai et al, 1990) has been found generally to enhance burning rate although Koseki et al. (1991) noted that boiling at the fuel-water interface can limit flame spread. The effect of minimum fuel layer thickness necessary for sustained combustion has been studied extensively (Garo et al., 1994, Arai et al, 1990). Several models have been developed to describe the heat losses from a pool fire to the supporting water layer (Brzustowski and Twardus, 1982) and to attempt description of in-depth absorption of radiation by the fuel layer (Twardus and Brzustowski, 1981). Flame spread across the liquid fuel surface has also been emphasized and excellent review papers have been published by Glassman and Dryer

(1980) and Ross (1994). Glassman and Dryer (1980) summarize the extensive literature on ignition, however, it is clear that little attention has been drawn to characterize the ignition process of liquid fuels on a water sub-layer.

Ignition behavior of petroleum fractions has not been studied beyond flash and fire points under quiescent conditions (Glassman and Dryer, 1980, SFPE Handbook, 1994, Hillstrom, 1975). The influence of weathering and the formation of oil/water emulsions on the flash and fire points have yet to be studied. Flash or fire point tests do not incorporate the effects that high heat insult has on the nature of the fuel, i.e. emulsions break down when subject to a high heat flux, thus are not sufficient to describe ignition in an oil spill scenario. Furthermore, heat transfer towards the water sub-layer is entirely dependent on the fuel properties and can preclude ignition, therefore needs to be incorporated when characterizing the ignition process. To the knowledge of the authors, the only study that addresses the effect of weathering and formation of emulsions on ignition under conditions pertinent to the oil-spill scenario is due to Putorti et al. (1994). This study was conducted in a cone calorimeter and quantified the necessary heat flux for ignition of various liquid fuels. In this work, emphasis was placed on the ignition delay time of weathered and emulsified samples.

Most accidental and deliberate burns of spilled oil at sea suffer from the effects of wind and waves. Volatiles tend to evaporate rapidly with time (weathering) and mixing tend to form oil/water emulsions making the oil difficult to ignite. Consequently, alteration of the physical or chemical properties of the oil can require additional energy for ignition. Several studies reported have attempted to characterize weathering and emulsions typical of oil-spill scenarios (Bobra, 1992).

In-situ burning of an oil spill requires the fuel to ignite and that ignition to be followed by spread and eventually leading to mass burning. Many studies have shown that ignition is not always followed by spread (Kashiwagi et al, 1997) therefore, is not sufficient to guarantee efficient removal of the oil slick. The need to understand the three stages necessary for the efficient removal of crude oil have resulted in the choice to use a modified version L.I.F.T., ASTM-E-1321 (ASTM Standards, 1994) apparatus to characterize the burning process.

Although the overall objective of this study is to characterize the entire burning process, the task is formidable. In the present work emphasis will be given to ignition. This choice does not provide optimal conditions for the study of each individual element but it is justified in the general context of this problem. This study will use two different crude oils (Cook Inlet and ANS) as representative of those commonly transported by oil-tankers. Crude oils will be studied in their natural state and subject to different levels of weathering. The formation of emulsions and its effect on ignition will be a subject of future study but goes beyond the objectives of the present work.

## **2.0 Background**

### **2.1 Closed Cup Flash Point Test**

The ASTM D56 Tag Closed Cup flash point tester was used to characterize the thermal properties under a controlled environment. The standard should be referenced for details of the apparatus (ASTM-Fire Test Standards, 1990). Flash point is defined as the lowest temperature corrected to as pressure of 760 mm Hg at which application of a

test flame causes the vapors of a portion of the sample to ignite under specified conditions. The flash point measures the tendency of a fuel to form a combustible mixture with air under a controlled laboratory condition. It is only one of a number of properties that must be considered in assessing the overall thermal characteristics of a liquid fuel.

For the test for flash point, a liquid fuel is placed in the cup of the tester. With the lid closed, the sample is heated up at a slow constant rate. A small flame of specified size is directed into the cup at regular intervals. The lowest temperature at which application of the flame ignites the vapors above the sample specifies the flash point. The flash point temperature gives an indication of the pyrolysis temperature of the fuel but not of the thermal properties that will lead to the attainment of this temperature. Therefore, the flash point temperature is of importance but not sufficient to describe the ignition process.

## 2.2 Piloted Ignition

Ignition of a combustible material can be accomplished in two ways. The first is by heating the material until ignition of the fumes occurs, this mechanism is commonly referred as spontaneous ignition. If the combustible material is only heated until the mixture between the fuel vapor and the ambient air reaches the lean flammability limit and ignition is achieved by means of a hot spot, this mechanism is called piloted ignition. For the specific application of in-situ burning piloted ignition will be the appropriate mechanism to consider.

Fuel properties vary significantly when subject to a strong heat insult, therefore, they need to be evaluated under "fire conditions." These properties are generally referred as "fire properties" (Quintiere, 1981). The concept of minimum heat flux for ignition has been commonly applied to solid fuels and ignition behavior can be predicted or measured using small, bench-scale experiments. In a similar fashion, ignition behavior of liquid fuels can be studied and evaluation of the "fire properties" allows ranking of fuels in various states; natural, weathered, and emulsified. The scale dependency will always be a matter of controversy, thus, large scale tests remain a necessity for validation. Yet, the number of tests needed to determine feasibility, protocols, and procedures for in-situ burning could be greatly reduced.

The mechanisms leading to gas phase ignition can be described as follows. The liquid bed is considered initially at ambient temperature,  $T_i$ . After suddenly imposing an external heat flux ( $\dot{q}_c''$ ) the temperature of the bed rises till the surface reaches the pyrolysis or evaporation temperature ( $T_p$ ). The time required for the fuel surface to attain  $T_p$  will be referred the pyrolysis time,  $t_p$ . After attaining  $T_p$ , the vapor (pyrolysate) leaves the surface, is diffused and convected outwards, mixes with the ambient oxidizer, and creates a flammable mixture near the solid surface. This period will be referred here as the mixing time,  $t_m$ . The flow and geometrical characteristics determine the mixing time. If the mixture temperature is increased the combustion reaction between the fuel vapor and the oxidizer gas may become strong enough to overcome the heat losses to the solid and ambient. Thus becoming self-sustained and at which point flaming ignition will occur. This period corresponds to the induction time,  $t_i$ , and is derived from a complex combination of fuel properties and flow characteristics.

Extending the analysis proposed by Fernandez-Pello (1995), the ignition time ( $t_{ig}$ ) will be given then by

$$t_{ig}=t_p+t_m+t_i \quad (1)$$

Under ideal conditions, introducing a pilot reduces the induction time making it negligible when compared to  $t_p$  and  $t_m$ . Furthermore, mixing has been commonly considered as a fast process compared to heating of the fuel, therefore, the fuel and oxidizer mixture becomes flammable almost immediately after pyrolysis starts. Pyrolysis temperatures and times are, thus, commonly referred as ignition temperature and ignition time (Quintiere, 1981) and equation (1) simplifies to

$$t_{ig}=t_p \quad (2)$$

and  $T_{ig}$  can be defined as  $T_p$ . Although such a definition is not physically correct (Alvares and Martin, 1971) it can be very useful in some practical applications since provides a reference parameter that could serve to characterize ignition. In the present study the geometry will be chosen to make  $t_m$  and  $t_i$  minimal, thus  $\dot{q}_{o,p}'' \approx \dot{q}_{o,ig}''$  and, from equation (2),  $t_p \approx t_{ig}$ .

The flow over the fuel surface will control mixing of fuel and oxidizer as well as the transport of this mixture towards the pilot ( $t_m$ ), therefore, can have a significant effect on  $t_{ig}$  and on the validity of equation (2). The relative effect of  $t_m$  on  $t_{ig}$  will decrease as the characteristic velocity of the system increases, characteristic time for mixing and transport decrease. Equation (2) could be extrapolated only if the experimental conditions at which the ignition delay time is obtained satisfy the assumption that  $t_m \approx t_i \ll t_p$ . Slight changes in the flow structure, especially for a horizontal configuration, can strongly affect  $t_m$  without changing  $t_p$  significantly. This effect will be least significant as the external heat flux approaches the critical heat flux for pyrolysis ( $\dot{q}_c'' \approx \dot{q}_{o,p}''$ ) and  $t_p \rightarrow \infty$ . This is important because it implies that the error incurred in the experimental determination of  $t_{ig}$ , (due to the unknown nature of the flow) will decrease as  $\dot{q}_c''$  approaches  $\dot{q}_{o,p}''$ .

To obtain  $t_p$  the fuel and water bed are assumed as one thermally thick material with properties corresponding to an unknown combination of both liquids. The bed is assumed a semi-infinite slab, thus all convective and thermo-capillary motion in the bed is neglected. This assumption is not necessarily correct (Ross, 1994, Wu et al. 1997) but will be accepted as a possible source of error. Throughout the heating process the fuel layer is assumed inert with negligible pyrolysis before ignition. The solution to the one-dimensional transient heating of a semi-infinite slab is given by Carslaw and Jaeger (1963) and an elaboration of all additional assumptions and the derivation pertaining to the present study are given by Quintiere (1981).

The boundary condition for this solution is imposed by heat balance at the surface which needs to incorporate convective heat losses, re-radiation, in-depth absorption and the fraction of the external heat flux not absorbed. Losses result in a minimum external

heat flux necessary,  $\dot{q}_{0,p}''$ , to attain  $T_p$ . For  $\dot{q}_c'' < \dot{q}_{0,p}''$  the surface will attain thermal equilibrium at  $T_{EQ} < T_p$ .

A linearized heat transfer coefficient,  $h$ , is commonly used to describe heat transfer at the surface and all heat loss terms can be reduced to

$$\varepsilon\sigma(T^4 - T_\infty^4) + h_c(T - T_\infty) \approx h(T - T_\infty) \quad (3)$$

where  $h_c$  is the convective heat transfer coefficient,  $\varepsilon$  the emissivity of the fuel,  $\sigma$  the Stefan-Boltzmann constant ( $\sigma=5.67 \times 10^{-8} \text{ W/m}^2 \cdot \text{K}^4$ ) and  $T_\infty$  the ambient temperature. The value of “ $h$ ” incorporates the convective heat losses, which depend on the present configuration, and the re-radiation from the surface of the fuel, which is only linked to the emissivity of the fuel, thus is a property of the fuel and needs to be evaluated under fire conditions. As expected, values for “ $h$ ” have been shown to vary with orientation, fuel and environmental effects. Examples of typical values found in the literature are:  $8.0 \text{ Wm}^2\text{K}^{-1}$  for natural turbulent convection and a vertical sample (Quintiere, 1981),  $13.5 \text{ Wm}^2\text{K}^{-1}$  for a horizontal orientation (Janssens, 1991), and up to  $15.0 \text{ Wm}^2\text{K}^{-1}$  obtained by Mikkola and Wichman (1989) while conducting experiments on a vertical orientation with wood.

These assumptions lead to the following solution for the attainment of the pyrolysis temperature as a function of time

$$h(T_p - T_i) = \dot{q}_c'' [1 - \exp(-at_p) \text{erfc}(at_p)] \quad (4)$$

where  $t_p$  is the time necessary to attain  $T_p$  at the surface,  $a = \alpha(h/k)^2$ , “ $\alpha$ ” the thermal diffusivity and “ $k$ ” the thermal conductivity. It needs to be noted that “ $k$ ” and “ $\alpha$ ” are not the fuel or water properties but an equivalent set of properties that includes the contribution of both liquids. If  $\dot{q}_c'' = \dot{q}_{0,p}''$ ,  $T_p$  is expected to be reached when  $t \rightarrow \infty$  and the critical heat flux that would lead to pyrolysis can be derived from equation (4) and is given by

$$\dot{q}_{0,p}'' = h(T_p - T_i) \quad (5)$$

It has to be noted that equation (5) predicts a linear dependency between the pyrolysis temperature and the critical heat flux for ignition. The flash point temperature could be used as an approximate value for the pyrolysis temperature, therefore correlation between the critical heat flux for ignition and the flash point temperature will serve as validation for this approach.

For  $\dot{q}_c'' \gg \dot{q}_{0,p}''$  it can be assumed that  $[1 - \exp(-at_p) \text{erfc}(\sqrt{at_p})] \approx \frac{2}{\sqrt{\pi}} (at_p)^{1/2}$  which leads to the approximate expression valid for short times ( $t_p$ )

$$t_p = \frac{\pi}{4a} \left( \frac{\dot{q}_{0,p}''}{\dot{q}_c''} \right)^2 \quad (6)$$



and Dryer, 1980). This systematic study led to small propane diffusion flame (20 mm in height) established on a 4 mm stainless-steel nozzle to be used as an ignition pilot. The nozzle was placed 10 mm above the fuel surface plane in the centerline and 10 mm downstream of the leading edge of the ignition tray (figure 1).

The fuel tray was placed under a 200 mm square plate with a 100 mm square hole in the middle where the fuel was located. Details on this plate and its use will be provided by Wu et al. (1997).

The radiant panel forms an angle of  $15^\circ$  with the sample, with the objective of producing a heat flux distribution as the one shown by Quintiere (1981). Despite the inclination the incident heat flux for the region up to 150 mm is relatively uniform providing a constant heat flux boundary condition for the fuel/air interface. Thermocouples measurements have been used to characterize the temperature evolution of the fuel and have shown neglectable differences at several locations along the fuel surface. Detailed hardware characteristics, typical heat flux distributions and experimental procedures involving the LIFT have been well documented (Quintiere, 1981, Wu et al. 1997) and will not be repeated here.

## 4.0 Experimental Results and Discussion

### 4.1 Ignition Delay Time

To calibrate the apparatus, SAE 30 W oil was first used for the ignition tests. This fuel was used to make possible comparison with previously reported results on ignition delay time (Putorti et al. 1994) and also because of the high flash point (approximately  $250^\circ\text{C}$ ). The higher flash point results in a longer ignition delay time providing a longer period to observe the different processes affecting ignition. Radiation absorption is also lower with SAE 30 oil favoring boiling of the water bed. Although the viscosity of SAE 30 oil is generally higher than that of crude oils, it is very sensitive to temperature (approximately  $1 \times 10^{-2}$  at  $0^\circ\text{C}$  and  $1 \times 10^{-5}$  at  $100^\circ\text{C}$ ) reaching comparable values after only a small temperature increase.

The results from these experiments are presented in Figure 2 together with data obtained for the same fuel by Putorti et al. (1994). Following equation (6) the ignition delay time is presented as  $t^{-1/2}$ . It can be observed that, although the ignition delay time significantly differs from the values found by Putorti et al. (1994) data converges to a unique critical heat flux for ignition. Since these experiments were conducted using different ignition procedures and under different environmental conditions,  $t_m$  is expected to be different, thus, affecting the ignition delay time. On the contrary,  $t_p$  should not be affected if convective losses are similar in magnitude or can be neglected. As the external heat flux approaches  $\dot{q}_{0,ig}''$ ,  $t_m$  becomes neglectable compared to  $t_p$  and all data converges to a unique point ( $\dot{q}_{0,ig}'' \approx 5 \text{ kW/m}^2$ ), as observed in Figure 2. This linear dependency corresponds well with data reported in the literature for solid fuels (Quintiere, 1981, Mikkola and Wichman, 1989) and serves to validate the above mentioned assumptions.

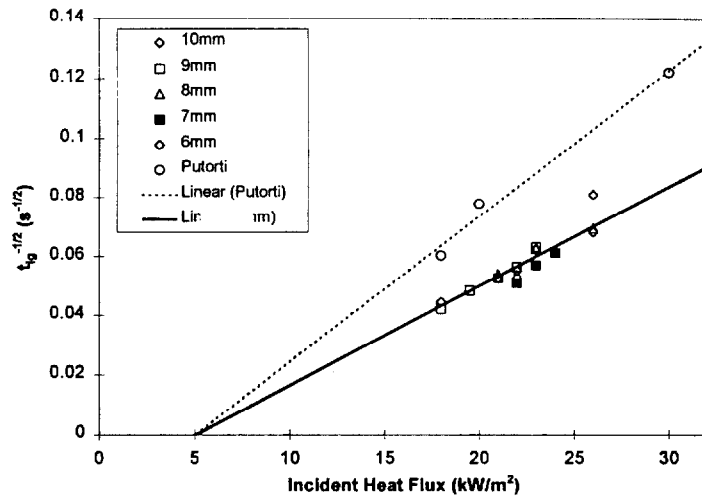


Figure 2 Ignition Delay Times for SAE 30W Oil Using the HIFT Apparatus and Cone Calorimeter.

For the particular case of an oil-slick on a water bed, the water underneath the fuel might attain boiling before ignition occurs. It was observed that once boiling started ignition of the fuel was precluded. Heating of the bed can be treated as a semi-infinite solid and temperature distributions can be predicted quite accurately (Brzustowski and Twardus, 1982). The analytical prediction of a characteristic time to boiling goes beyond the scope of this work. But, the determination of a minimum heat flux that will lead to boiling ( $\dot{q}_{0,B}''$ ) before ignition can occur is of great practical importance therefore needs to be included as a complement to the critical heat flux for ignition.

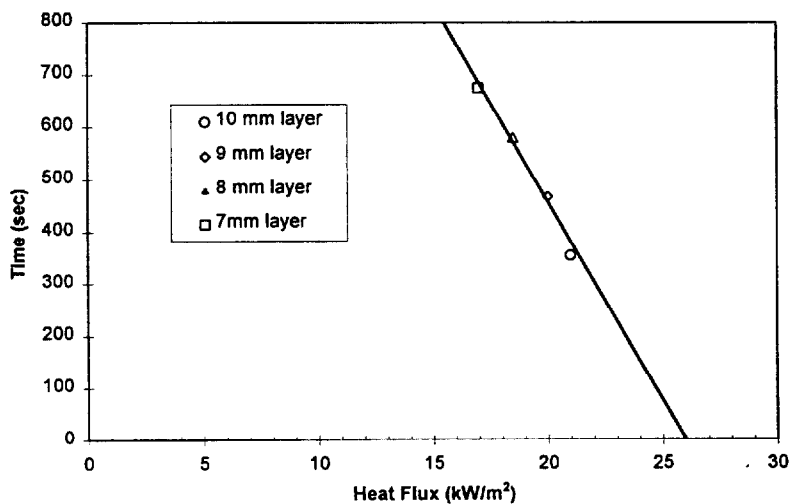


Figure 3. Critical Heat Flux to Boil ( $\dot{q}_{0,B}''$ ) for SAE 30W Oil Using the HIFT Apparatus.

As the external heat flux decreases the temperature gradient at the surface decreases and thermal penetration increases before the surface attains  $T_p$ . If the thermal wave can increase the water temperature at the fuel/water interface to the boiling point before the surface reaches  $T_p$ , boiling will prevent ignition from occurring. The minimum heat flux

that will allow the surface temperature to reach  $T_p$  before boiling is given by  $\dot{q}''_{0,B}$  and presented in figure 3. As the fuel layer decreases in thickness, the heat wave will reach the water faster allowing for a shorter available time for the surface to reach  $T_p$  and consequently requiring a higher temperature gradient at the surface (higher  $\dot{q}''_{0,B}$ ).

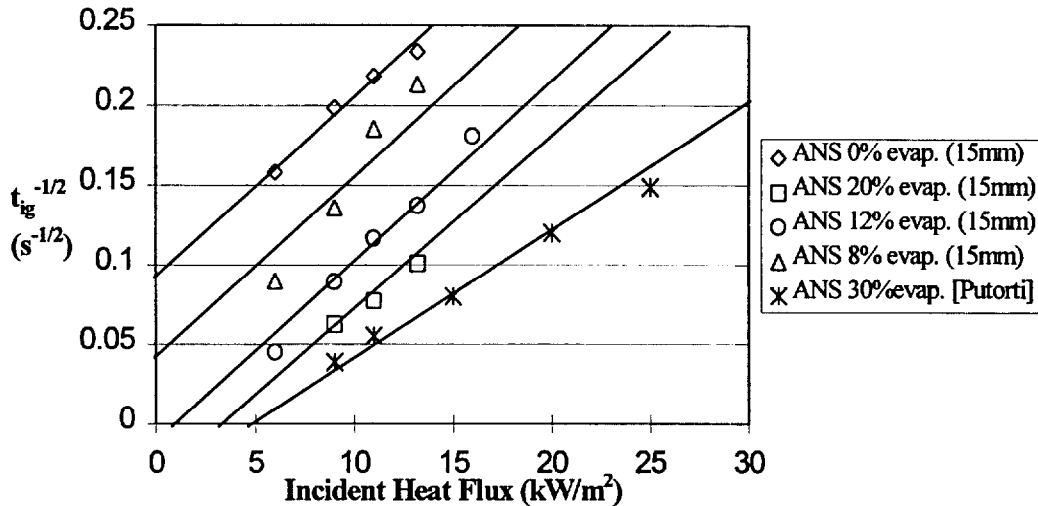


Figure 4. ANS Crude Oil Ignition Delay Time for Various Levels of Evaporation.

#### 4.2 Crude Oils and the Effect of Weathering

A series of tests were conducted with two crude oils. Figures 4 and 5 show ignition delay times for different external heat fluxes obtained for ANS crude oil, data reported by Putorti et al. (1994) and Cook Inlet crude oil. The data presented is an average of at least five experiments conducted under identical conditions. It was observed that ANS crude oil in its natural state ignited at ambient temperature, therefore no external heat flux was necessary. Flash points for this type of fuel have been reported as low as 19°C (SFPE Handbook, 1994) showing agreement with the above observation. When weathered, the ignition delay time decreases as the heat flux increases and a linear dependency between the external heat flux and  $t_{ig}^{-1/2}$  is obtained. The intercept with the horizontal axis will provide the critical heat flux for ignition with negative values implying that the fuel will ignite at ambient temperature. Figure 4 shows that the critical heat flux for ignition will increase with weathering. When a line fit is made through the data corresponding to a specific mass loss it can be observed that these slopes remain invariant with the weathering level. The critical heat flux corresponding to the experimental data reported by Putorti et al (1994) fits well with the data collected in the present work. As previously mentioned the different experimental conditions account for the difference in slope.

Tests were conducted for different levels of evaporation and fuel layer thickness. Figure 5 corresponds to an example of the complete set of data for Cook Inlet crude oil. It is important to observe that for a fuel layer thicker than 8 mm the results are independent of this thickness. Systematic determination of the critical heat flux for ignition should be done using layers thicker than 8 mm. In contrast, it will be necessary to determine  $\dot{q}''_{0,B}$  for all fuel layers.

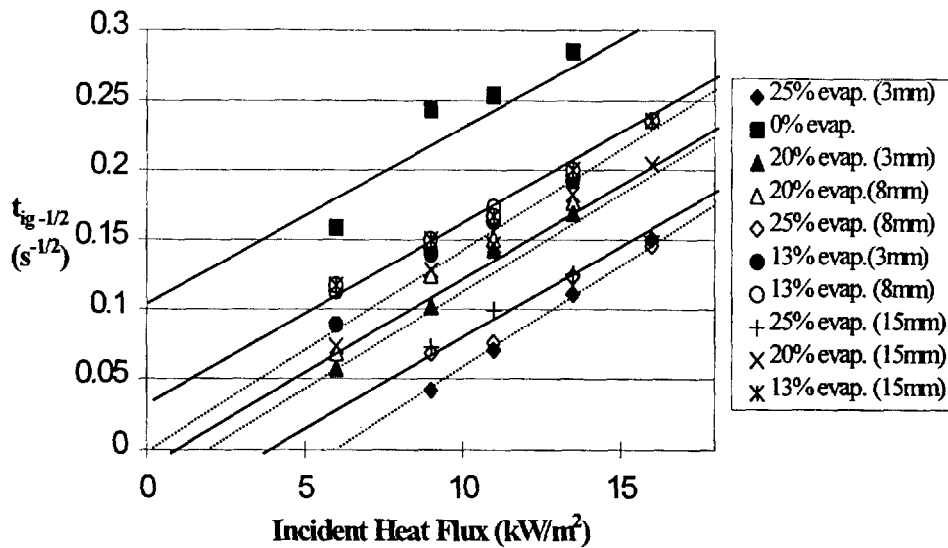


Figure 5. Cook Inlet Ignition Delay Time for Various Levels of Evaporation.

As demonstrated by equation (6) the slope of the line fit to the data from presented in figures 4 and 5 provides the thermal property, “a”, of the fuel. Figures 4 and 5 show that the slope remains invariant with the mass loss due to weathering. This is important since it proves that although the ignition event is controlled by the most volatile fractions of the crude oil, this is affected by weathering, the heating process and the properties that characterize it are determined by the heavier fractions, thus invariant with weathering. In opposition figure 5 shows that the water bed has a significant influence on both the global thermal properties and the critical heat flux for ignition.

The critical heat flux for ignition ( $\dot{q}_{O,ig}''$ ) as obtained from figures such as figure 4 and 5 is presented in figure 6. Results are presented for Cook Inlet and ANS crude oils for different fuel layer thickness. Figure 6 shows a discrepancy between the critical heat flux for ignition for 3 mm as opposed to almost identical values obtained for 8 and 15 mm layers. Thus, it can be verified that the fuel layer thickness affects the critical heat flux for ignition up to a thickness of 8 mm, with thicker layers resulting in almost identical results. The effect of fuel layer thickness was mostly manifested on the curves being truncated by boiling before attaining  $\dot{q}_{O,ig}''$ . The increasing value of  $\dot{q}_{O,ig}''$  with mass loss shows that weathering makes ignition more difficult, the increasing slope of the curve points towards the possibility of an asymptotic value at which the crude oil will not ignite. Based on the values for  $\dot{q}_{O,ig}''$  ANS crude oil was observed to be more prompt to ignition than Cook Inlet crude oil. Cook inlet ignited without an external heat flux for a mass loss rate smaller than 10 % and ANS crude oil for a mass loss smaller than 7%. The results presented are representative of all other cases studied.

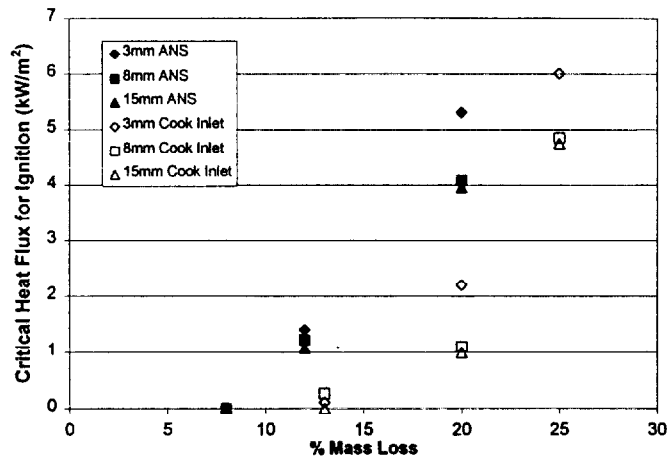


Figure 6.  $\dot{q}_{o,ig}''$  for ANS and Cook Inlet Crude Oils at Various Fuel Layer Thickness.

### 4.3 Flash Point Temperature

Results from flash point test for the crude oils as a function of the mass loss due to weathering are presented in figure 7. Each point in the figure represents the average of 10 tests conducted in accordance with ASTM D56 standard. As seen from the figure, flash points extracted using the ASTM D56 closed cup tester have a linear dependence on the level of evaporation for both crude oils. More importantly, the flash points for ANS crude oils are significantly higher than the Cook Inlet crude. Note that data is only presented for flash point temperatures above ambient ( $>20^{\circ}\text{C}$ ), since no ignition tests were conducted for temperatures lower than ambient. A mass loss greater than 20% has been demonstrated to need weeks of weathering under natural conditions (Ostazeski, 1996), therefore 20% will be used as an upper limit to the mass loss.

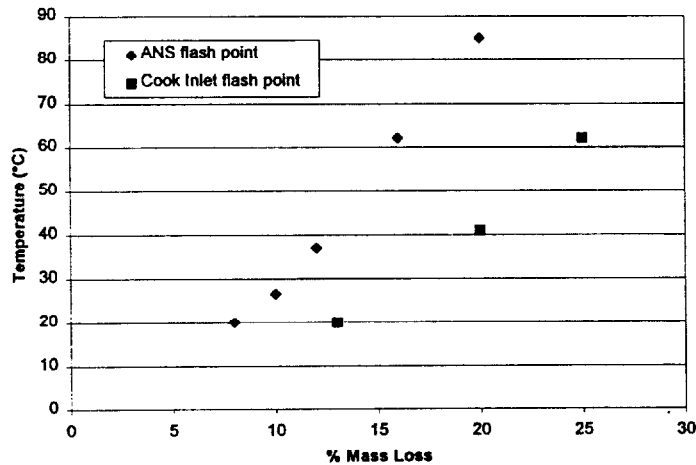


Figure 7. ASTM D56 Closed Cup Flash Point Tests for ANS and Cook Inlet Crude Oils.

Evaporation is the dominant weathering process that affects the crude oils in the marine environment. Depending on the conditions, the physical, chemical, and toxicological properties of a crude oil can be altered significantly by evaporation. Few references are available that provide sound results relating accelerated laboratory evaporation of crude oils to actual field conditions. Hydrocarbons constitute the most

important fraction in any crude oil. Although the proportions of each fraction varies significantly, (e.g. from 30-40% to 100% in gas condensates), they account for up to 70% in all petroleum on the average (Petrov, 1987). The light boiling fractions of standard crude oil can contain up to 150 different hydrocarbons. The complexity of petroleum hydrocarbon makes identification of individual elements difficult. However, in the early 1960's an elaborate analytical method was developed called gas chromatography-mass spectrometry. This allowed classification of fractions individual groups according to molecular structure: (1) Alkenes ( $C_5$ - $C_{40}$ ); (2) Napthenes or Cycloalkenes; and (3) Aromatic Hydrocarbons (Arenes).

The least complicated are the Alkenes, which are divided into three fractions. Fraction I is of primary interest since the  $C_5$ - $C_{11}$  hydrocarbons are distilled from the crude oil at a temperature range of 30-200 °C. McAuliffe (1989) characterizes evaporation as a function of time to liberate the  $C_9$  and lower hydrocarbons. The selection of this criteria is not arbitrary as the lighter fractions were not only the most likely to evaporate, but also the most biologically hazardous. This is the referencing standard to compare accelerated laboratory weathering to field conditions. Therefore, an analysis of only simple unsaturated hydrocarbons ( $<C_{11}$ ) is made between individual petroleum fractions and weathered Cook Inlet and ANS crude oils. Complicated components such as saturated cyclic hydrocarbons (naphthenes) and aromatic hydrocarbons have been omitted because of the complex nature of these fractions. Weathering under very similar conditions as those presented here was conducted by Garo (1996) with a mixture of crude oils (63% Kittiway, 33% Arabian Light and 4% Oural) showing a variation of the flash point consistent with the above presented data. By means of gas chromatography Garo (1996) determined that hydrocarbons smaller than  $C_8$  will be almost entirely evaporated before a mass loss of 10% is achieved. All these hydrocarbons have a flash point below 20°C, therefore the flash point of the weathered oil remained below this temperature. If 15% mass loss is attained hydrocarbons smaller than  $C_{10}$  are almost entirely evaporated. Flash point temperatures below 50°C characterize hydrocarbons in the range  $C_8$  to  $C_{10}$ , thus the flash point of the weathered crude oil remains in this range. Further evaporation to approximately 20% leads to almost complete evaporation of hydrocarbons smaller than  $C_{16}$  resulting in an increase of the flash point to a value characteristic of these fractions ( $<80^\circ\text{C}$ ).

A comparison of the flash point temperature and critical heat flux for ignition as obtained by the HIFT ignition tests is presented in figure 8. The data points correspond to different levels of weathering. It can be noticed that the flash point temperature has a linear dependency with the critical heat flux for ignition ( $\dot{q}_{o,ig}''$ ), as predicted by equation (5). The line fit, for ANS and Cook Inlet oils, converge to ambient temperature (20°C) for  $\dot{q}_{o,ig}'' = 0$ . This observation is of great importance since it shows that the flash point temperature can be used as characteristic ignition temperature. Furthermore, by means of equation (5) the global heat transfer coefficient can be evaluated and corresponds to the slope of the line fit.

This information can be used in two ways. As shown by equation (3) the global heat transfer coefficient consists of radiative and convective components. The convective component is independent of the fuel, thus the slope of the data presented in figure 8 provides an indirect measure of the emissivity of the fuel. More important, if the global heat transfer coefficient ( $h$ ) is known, and "a" is extracted from the ignition delay time, a

“fire property,” the product of the thermal conductivity, the density and the specific heat capacity ( $k\rho C$ ) can be obtained.

$$(k\rho C) = \frac{h^2}{a} \quad (7)$$

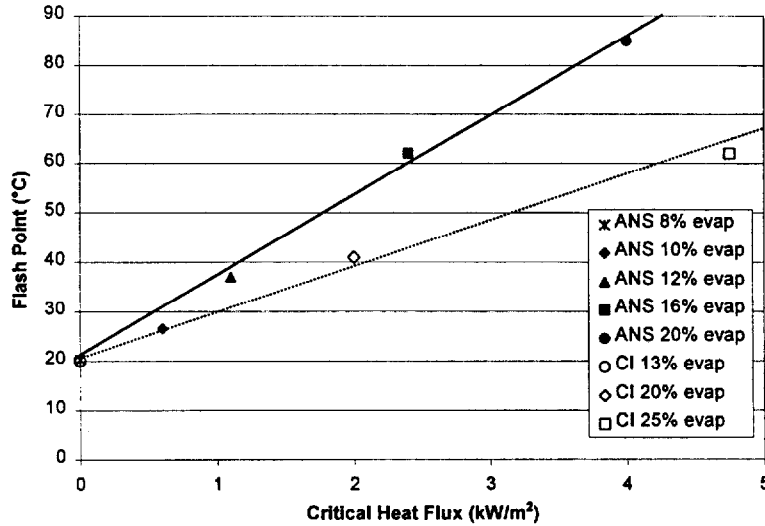


Figure 8. Flash Points of ANS and Cook Inlet Crude Oils at Various Levels of Weathering.

## 5.0 Conclusion

To study piloted ignition of a slick of oil on a water sub layer, a modified LIFT apparatus is used. As for solid fuels, ignition delay times and a critical heat flux for ignition of a liquid fuel supported by water can be extracted using this testing methodology. Open cup flash point temperature measurements are presented to complement the piloted ignition tests. The propensity of a crude oil to ignite can be characterized by three different parameters:

1. The critical heat flux for ignition ( $\dot{q}_{o,ig}'' \approx \dot{q}_{o,p}''$ ), it is independent of the environmental and experimental conditions and provides a measure of the minimum heat insult necessary to guarantee attainment of a pyrolysis temperature, thus production of enough gaseous fuel for ignition. The critical heat flux for ignition is obtain by extrapolation to  $t_{ig} \rightarrow \infty$  of the ignition delay time data.
2. The critical heat flux for boiling ( $\dot{q}_{o,B}''$ ), which provides a measure of the minimum heat flux necessary to attain ignition before boiling of the sub layer occurs.
3. The thermal “fire property” of the fuel ( $k\rho C$ ) can be extracted from the ignition delay time in combination with the critical heat flux and provides a measure of the heating process. It is a function of the fuel and is independent of the experimental and environmental conditions.

The experimental methodology and its theoretical underpinnings were validated with SAE30W oil, ANS and Cook Inlet crude oils in its natural state and under different levels of weathering. The results show consistency and correlate well with other data present in the literature.

For a comprehensive evaluation of the ignition potential of a crude oil in an oil spill scenario the conclusions pertaining ignition should be accompanied by similar information on the characteristics of the flame spread and mass burning processes.

## 6.0 Acknowledgements

Funding for this work was provided by NIST. The technical comments, encouragement and support of Dr. Marino di Marzo are greatly appreciated. The corresponding author is J.L. Torero.

## 7.0 References

Alvares, N. and Martin, S.B., "Mechanisms of Ignition of Thermally Irradiated Cellulose," *Thirteenth Symposium (International) on Combustion*, The Combustion Institute, 905-914, 1971.

Annual Book of ASTM Standards, *ASTM E-1321 Standard Test Method for Material Ignition and Flammability*, vol. 04.07, 1055-1077, 1994.

Arai, M., Saito, K., and Altenkirch, R.A., "A Study of Boilover in Liquid Pool Fires Supported on Water, part I: Effect of a Water Sublayer on Pool Fires," *Combustion Science and Technology*, 71, 25-40 1990.

ASTM E1321-90, "Standard for "Determining Material Ignition and Flame Spread Properties", American Society for Testing and Materials, 1990.

Bobra, M., "A Study of the Evaporation of Petroleum Oils," Publication EE-135, Environmental Canada, Ottawa, Ontario, K1A OH3, 1992.

Brzustowski, T.A., and Twardus, E.M., "A Study of the Burning of a Slick of Crude Oil on Water," *Nineteenth Symposium (International) on Combustion*, The Combustion Institute, Pittsburgh, PA, 847-854, 1982.

Carslaw, H.S. and Jaeger, J.C., "Conduction of Heat in Solids," 2<sup>nd</sup> Edition, Oxford University Press, Oxford, 70-76, 1963.

Fernandez-Pello, A.C., "Combustion Fundamentals on Fire: The Solid Phase," *Academic Press*, 31-100, 1995.

Garo, J.P., Vantelon, J.P., and Fernandez-Pello, A.C., "Experimental Study of the Burning of a Liquid Fuel Spilled on Water," *Twenty-fifth Symposium (International) on Combustion*, The Combustion Institute, Pittsburgh, PA, 1481-1488, 1994.

Garo, J.P. "Combustion d'Hydrocarbures Repandus en Nappe sur un Support Aqueux: Analyse du Phenomene de Boilover," *Ph.D. Thesis*, University of Poitiers, France, 1996.

Glassman, I., and Dryer, F., "Flame Spreading Across Liquid Fuels," *Fire Safety Journal*, 3, 123-138, 1980.

Hillstrom, W.W., "Temperature Effects of Flame Spreading Over Liquid Fuels", *Proceedings of the Eastern States Section/Combustion Institute*, Fall Technical Meeting, 1975.

Janssens, M., "A Thermal Model for Piloted Ignition of Wood Including Variable Thermophysical Properties," *Fire Safety Science-Proceedings of the Third International Symposium*, 167-176, 1991.

Kashiwagi, T., Mell, W.E., McGrattan, K.B. and Baum, H.R., *Fourth International Micro-gravity Combustion Workshop*, NASA Lewis Research Center, 411-416, 1997.

Koseki, H., Kokkala, M., and Mulholland, G.W., "Experimental Study of Boilover in Crude Oil Fires," *Fire Safety Science-Proceedings of the Third International Symposium*, 865-875, 1991.

McAuliffe, "The Weathering of Volatile Hydrocarbons from Crude Oil Slicks on Water", *Proceedings Form the 1989 Oil Spill Conference*, Feb 1989, San Antonio, Texas, pp. 357-363

Mikkola, E. and Wichman, I., "On the Thermal Ignition of Combustible Materials," *Fire and Materials* 14, 1989.

Ostazeski, S.A., Daling, P.S., Macomber, S.C., Fredricksson, D.W., Durell, G.S., Uhler, A.D., Jones, M., and Bitting, K., "Weathering Properties and the Prediction Behavior at Sea of a Lapio Oil (weathered No. 6 Fuel Oil)", *Proceedings of the 19<sup>th</sup> AMOP Technical Seminar*, Alberta, Canada, 1996, pp137-162.

Petrov, A.A., *Petroleum Hydrocarbons*. Springer-Verlag, 1987.

Putorti, A., Evans, D., and Tennyson, E., "Ignition of Weathered and Emulsified Oils," *Proceedings from the Seventeenth Arctic and Marine Oil Spill Program Technical Seminar*, 657-667, 1994.

Quintiere, J., "A Simplified Theory for Generalizing Results from Radiant Panel Rate of Flame Spread Apparatus," *Fire and Materials*, 5, 2, 52-60, 1981.

Ross, H., "Ignition and Flame Spread Over Laboratory-Scale Pools of Pure Liquid Fuels," *Progress in Energy and Combustion Science*, 20, 17-63, 1994.

*SFPE Handbook*, 2<sup>nd</sup> Edition, Society of Fire Protection Engineers, Quincy, MA, 2.161-2.170, 1994.

Twardus, E.M. and Brzustowski, T.A., "The Burning of Crude Oil Spilled on Water,"  
*Archivum Combustionis*, Polish Academy of Sciences, 1, 1-2, 49-60, 1981.

**7.2. The Effect of Weathering on Piloted Ignition and Flash Point Of a Slick of Oil**

N. Wu, T. Mosman, S. M. Olenick

*Spill Science and Technology (submitted), 1998.*

**BLANK PAGE**

# The Effect of Weathering on Piloted Ignition and Flash Point of a Slick of Oil

N. Wu, T. Mosman, S. M. Olenick and J. L. Torero

Department of Fire Protection Engineering

University of Maryland

College Park, MD 20742-3031, USA

E-mail: jltorero@eng.umd.edu , Telephone: 1-301-405-0043

## Abstract

Ignition of a slick of oil on a water bed has been studied to provide a tool that will serve to assess a fuels ease to ignite under conditions that are representative of oil spills. Two different techniques are used, piloted ignition when the fuel is exposed to a radiant heat flux and flash point as measured by the ASTM D56 Tag Closed Cup Test. Two different crude oils were used for these experiments, ANS and Cook Inlet. Crude oils were tested in their natural state and at different levels of weathering, showing that piloted ignition and flash point are strong functions of weathering level.

## 1.0 Introduction

Burning of an oil spill is of interest as a result of offshore exploration, production, and transportation of petroleum. In-situ burning can provide an effective means for the removal of an oil slick reducing negative environmental impact. The efficiency of the ignition and burning process is crucial for the successful elimination of the crude oil. Burns of spilled oil at sea suffer from the effects of wind and waves. Volatiles tend to evaporate with time (weathering) and mixing forms oil/water emulsions. Consequently, alteration of the physical or chemical properties of the oil can require additional energy for ignition. In-situ burning of an oil spill requires the fuel to ignite and that ignition to be followed by spread and leading to mass burning. In the present work emphasis will be given to ignition. This study will use two different crude oils (Cook Inlet and ANS) in their natural state and subject to different levels of weathering.

## 2.0 Background

The ASTM D56 Tag Closed Cup flash point tester was used to characterize the thermal properties under a controlled environment. The standard should be referenced for details of the apparatus and procedures (ASTM, 1990). Flash point is defined as the lowest temperature, at a pressure of 760 mm Hg, at which application of a test flame causes the vapors to ignite. The flash point measures the tendency of a fuel to form a combustible mixture with air under a controlled laboratory condition.

Ignition of a combustible material can be accomplished in two ways, by heating the material until ignition of the fumes occurs, spontaneous ignition, or by heating the combustible material until the mixture between the fuel and air reaches the lean flammability limit. Ignition is achieved by means of a hot spot, piloted ignition. For in-situ burning piloted ignition will be the appropriate mechanism to consider.

The mechanisms leading to gas phase ignition can be described as follows. The liquid bed is considered initially at ambient temperature,  $T_i$ . After imposing an external heat flux ( $\dot{q}_c''$ ) the temperature of the bed rises until the surface reaches the pyrolysis temperature ( $T_p$ ). The time required for the fuel surface to attain  $T_p$  is the pyrolysis time,

$t_p$ . After attaining  $T_p$ , the vapor leaves the surface mixes with the ambient oxidizer, and creates a flammable mixture near the solid surface. This period is the mixing time,  $t_m$ . If the temperature is increased until the reaction becomes self-sustained flaming ignition will occur. This is the induction time,  $t_i$ . Extending the analysis by Fernandez-Pello (1995), the ignition time ( $t_{ig}$ ) will be given then by

$$t_{ig}=t_p+t_m+t_i \quad (1)$$

Introducing a pilot reduces the induction time making it negligible when compared to  $t_p$  and  $t_m$ . Furthermore, mixing can be considered as a fast process compared to heating of the fuel, therefore, pyrolysis temperatures and times are, thus, commonly referred as ignition temperature and ignition time (Quintiere, 1981) and

$$t_{ig}=t_p \quad (2)$$

and  $T_{ig}$  can be defined as  $T_p$ . In the present study the geometry will be chosen to make  $t_m$  and  $t_i$  minimal, thus  $\dot{q}_{o,p}'' \approx \dot{q}_{o,ig}''$  and, from equation (2),  $t_p \approx t_{ig}$ .

To obtain  $t_p$  the fuel and water bed are assumed as one thermally thick material. Carslaw and Jaeger (1963) give the solution to the one-dimensional transient heating of a semi-infinite slab and Quintiere (1981) elaborates on all additional assumptions. A linearized heat transfer coefficient,  $h$ , is used to describe heat transfer at the surface and all heat loss terms can be reduced to

$$\varepsilon\sigma(T^4 - T_\infty^4) + h_c(T - T_\infty) \approx h(T - T_\infty) \quad (3)$$

where  $h_c$  is the convective heat transfer coefficient,  $\varepsilon$  the emissivity of the fuel,  $\sigma$  the Stefan-Boltzmann constant ( $\sigma=5.67 \times 10^{-8} \text{ W/m}^2 \cdot \text{K}^4$ ) and  $T_\infty$  the ambient temperature.

These assumptions lead to the following solution for the attainment of the pyrolysis temperature as a function of time

$$h(T_p - T_i) = \dot{q}_e'' [1 - \exp(-at_p) \text{erfc}(at_p)] \quad (4)$$

where  $a = \alpha(h/k)^2$ , " $\alpha$ " the thermal diffusivity, " $k$ " the thermal conductivity and both are equivalent set of properties that include the contribution of both liquids. If  $\dot{q}_e'' = \dot{q}_{o,ig}''$ ,  $T_p$  will be reached when  $t \rightarrow \infty$  and a critical heat flux would be

$$\dot{q}_{o,ig}'' = h(T_p - T_i) \quad (5)$$

Equation (5) predicts a linear dependency between  $T_p$  and  $\dot{q}_{o,ig}''$ . The flash point temperature can be used as a value for  $T_p$  but validation is necessary. For  $\dot{q}_e'' \gg \dot{q}_{o,ig}''$  it

can be assumed that  $[1 - \exp(-at_p) \text{erfc}(\sqrt{at_p})] \approx \frac{2}{\sqrt{\pi}} (at_p)^{1/2}$  which leads to

$$t_p = \frac{\pi}{4a} \left( \frac{\dot{q}_{0,p}''}{\dot{q}_e''} \right)^2 \quad (6)$$

Equation (6) is of importance since shows that  $\dot{q}_e''$  has a linear dependency on  $t_p^{-1/2}$  for  $\dot{q}_e'' > \dot{q}_{0,p}''$ , from the slope of this line the value of “a” can be determined. The experimental methodology was described by Quintiere (1981) and more recently, in the present application, by Wu et al. (1997), therefore will not be repeated here.

### 3.0 Experimental Results and Discussion

Wu et al. (1997) showed that, although the ignition delay time varies with the geometry, data converges to a unique critical heat flux for ignition. For the particular case of an oil-slick on a water bed, the water underneath might attain boiling before ignition occurs. Once boiling starts ignition of the fuel was precluded, thus, a complete description ignition can only be achieved by determination of  $\dot{q}_{0,B}''$  and  $\dot{q}_{0,ig}''$ .

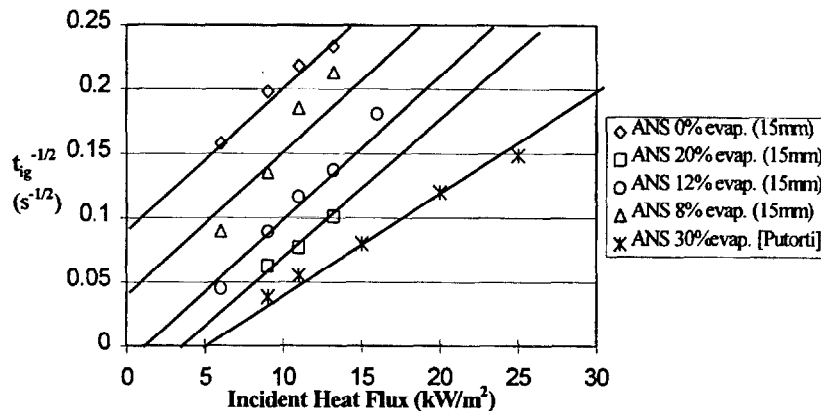


Figure 1. ANS Crude Oil Ignition Delay Time for Various Levels of Evaporation.

A series of tests were conducted with the two crude oils. Figure 1 shows ignition delay times for different external heat fluxes obtained for ANS crude oil, data reported by Putorti et al. (1994). It was observed that ANS crude oil in its natural state ignited at ambient temperature. When weathered,  $t_{ig}$  decreases as the heat flux increases and a linear dependency between the incident heat flux and  $t_{ig}^{-1/2}$  is obtained. The intercept with the horizontal axis will provide  $\dot{q}_{0,ig}''$  showing that  $\dot{q}_{0,ig}''$  increases with weathering. It can be observed that the slopes remain invariant with the weathering level. The  $\dot{q}_{0,ig}''$  value corresponding to the data reported by Putorti et al (1994) fits well with the present work. As previously mentioned the different experimental conditions account for the difference in slope.

As demonstrated by equation (6) the slope of the line fit to the data presented in figures 1 provides the thermal property, “a”, of the fuel. Figure 1 shows that the slope remains invariant with the mass loss due to weathering. This proves that although the ignition event is controlled by the most volatile fractions of the crude oil, thus is affected

by weathering, the heating process is determined by the heavier fractions, thus invariant with weathering. The critical heat flux for ignition ( $\dot{q}_{o,ig}''$ ) as obtained from figure 1 is presented in figure 2. Results are presented for Cook Inlet and ANS crude oils. Figure 2 shows a discrepancy between the critical heat flux for ignition for 3 mm as opposed to almost identical values obtained for 8 and 15 mm layers. The effect of fuel layer thickness was mostly manifested on the curves being truncated by boiling before attaining  $\dot{q}_{o,ig}''$ . Based on the values for  $\dot{q}_{o,ig}''$  ANS crude oil was observed to be more prompt to ignition than Cook Inlet crude oil. Cook inlet ignited without an external heat flux for a mass loss rate smaller than 10 % and ANS crude oil for a mass loss smaller than 7%. The results presented are representative of all other cases studied.

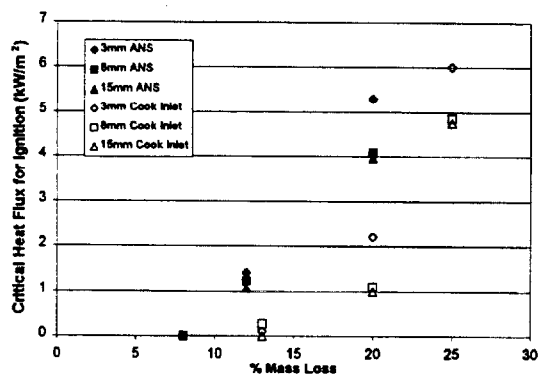


Figure 2.  $\dot{q}_{o,ig}''$  for ANS and Cook Inlet Crude Oils at Various Fuel Layer Thickness.

The flash point for the crude oils as a function of the mass loss are presented in figure 3. Each point in the figure represents the average of 10 tests conducted in accordance with ASTM D56 standard. Flash points show a linear dependence on the level of evaporation for both crude oils. More importantly, the flash points for ANS crude oils are significantly higher than the Cook Inlet crude.

Figure 4 shows that the flash point temperature has a linear dependency with the critical heat flux for ignition ( $\dot{q}_{o,ig}''$ ), as predicted by equation (5). The line fits converge to the ambient temperature (20°C) for  $\dot{q}_{o,ig}'' = 0$ . This shows that the flash point temperature can be used as characteristic ignition temperature. Furthermore, by means of equation (5) the global heat transfer coefficient can be evaluated and corresponds to the slope of the line fit.

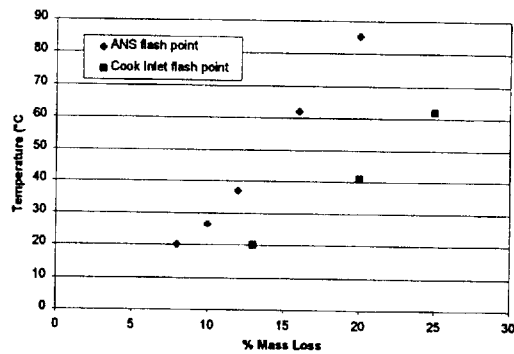


Figure 3. ASTM D56 Closed Cup Flash Point Tests for ANS and Cook Inlet.

If the global heat transfer coefficient ( $h$ ) is known, and “ $a$ ” is extracted from the ignition delay time, a “fire property,” the product of the thermal conductivity, the density and the specific heat capacity ( $k\rho C$ ) can be obtained ( $(k\rho C)=h^2/a$ ).

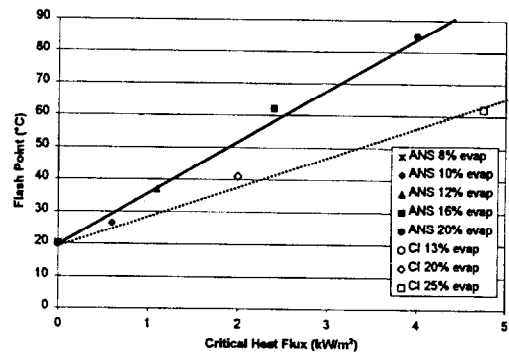


Figure 4. Flash Points at Various Levels of Weathering.

#### 4.0 Conclusion

The propensity of a crude oil to ignite can be characterized by three different parameters:

4. The critical heat flux for ignition ( $\dot{q}_{o,ig}'' \approx \dot{q}_{o,P}''$ ).
5. The critical heat flux for boiling ( $\dot{q}_{o,B}''$ )
6. The thermal “fire property” of the fuel ( $k\rho C$ ).

For a comprehensive evaluation of the ignition potential of a crude oil in an oil spill scenario the conclusions pertaining ignition should be accompanied by similar information on the characteristics of the flame spread and mass burning processes.

#### 5.0 Acknowledgements

Funding for this work was provided by NIST, the support of Dr. Marino di Marzo is greatly appreciated. The corresponding author is J.L. Torero.

#### 6.0 References

Annual Book of ASTM Standards, *ASTM E-1321 Standard Test Method for Material Ignition and Flammability*, vol. 04.07, 1055-1077, 1994.

Carslaw, H.S. and Jaeger, J.C., "Conduction of Heat in Solids," 2<sup>nd</sup> Edition, Oxford University Press, Oxford, 70-76, 1963.

Fernandez-Pello, A.C., "Combustion Fundamentals on Fire: The Solid Phase," *Academic Press*, 31-100, 1995.

Koseki, H., Kokkala, M., and Mulholland, G.W., "Experimental Study of Boilover in Crude Oil Fires," *Fire Safety Science-Proceedings of the Third International Symposium*, 865-875, 1991.

Putorti, A., Evans, D., and Tennyson, E., "Ignition of Weathered and Emulsified Oils," *Proceedings from the Seventeenth Arctic and Marine Oil Spill Program Technical Seminar*, 657-667, 1994.

Quintiere, J., "A Simplified Theory for Generalizing Results from Radiant Panel Rate of Flame Spread Apparatus," *Fire and Materials*, 5, 2, 52-60, 1981.

**8. Determination of Fire Properties of Liquid Fuels Characteristic of Oil-Spills  
Using ASTM E-1321**

N. Wu

*Master of Science, Department of Fire Protection Engineering, University  
of Maryland, College Park, MD20742-3031, April 23<sup>rd</sup>, 1998.*

**BLANK PAGE**

DETERMINATION OF FIRE PROPERTIES OF LIQUID FUELS  
CHARACTERISITIC OF OIL SPILLS USING ASTM E-1321

by

Neil P. Wu

Thesis submitted to the Faculty of the Graduate School of the  
University of Maryland at College Park in partial fulfillment  
of the requirements for the degree of  
Master of Science  
1998

Advisory Committee:

Professor Jose Torero, Chairman/Advisor  
Professor Marino diMarzo  
Professor James Quintiere

**BLANK PAGE**

## ABSTRACT

Title of Thesis: DETERMINATION OF FIRE PROPERTIES OF LIQUID FUELS CHARACTERISITIC OF OIL SPILLS USING ASTM E-1321

Degree Candidate: Neil P. Wu

Degree and Year: Master of Science, 1998

Thesis directed by: Professor Jose Torero  
Department of Fire Protection Engineering

A modified ASTM E1321 (LIFT) apparatus is used to experimentally study piloted ignition and flame spread of a slick of oil on a water sublayer. The objective of this work is to provide a tool that will serve to assess a fuels ease to ignite under conditions that are representative of oil spills. An existing one-dimensional heat transfer model is used correlate the experimental results. Crude oils were tested in their natural state and at different levels of weathering. The methodology for accelerated laboratory weathering is validated. Piloted ignition is inhibited by premature boiling of the water sublayer and weathering significantly increases the ignition delay time. Critical heat flux for ignition could be obtained to characterize the fuel propensity to ignite in the presence of a strong pilot. The minimum heat flux that will permit ignition before boiling also needs to be considered. Flash point data for crude oils in their natural state and various levels of weathering complements the ignition parameter and validates the methodology. Extraction of the thermal properties of the fuel ( $k\rho C$  and  $\phi$ ) is made which can be used to rank the material. Although the critical heat flux increases as with level of evaporation, thermal properties remain invariant. To characterize the entire in-situ combustion, mass burning properties must be considered.

## ACKNOWLEDGEMENTS

Funding for this work was provided by the National Institute of Standards and Technology (NIST). The author would like to express thanks to Mr. Jay McElroy for his multiple suggestions and help in the development of the experimental apparatus. The technical comments, encouragement, and support of Dr. Marino di Marzo are greatly appreciated. Flash point data is provided by Stephen Olenick and Tyler Mosman. Most importantly, the support, knowledge, and motivation supplied by Dr. Jose Torero were invaluable.

## LIST OF SYMBOLS

$a$	= thermal properties, $s^{-1/2}$
$c$	= rate coefficient for flame spread
$F(t)$	= specimen thermal response function
$h$	= heat transfer coefficient, $kW/m^2-K$
$k\rho C$	= thermal inertia, $(kW/m^2-K)^2-s$
$\phi$	= flame heating parameter, $(kW)^2/m^3$
$\dot{q}_{o,B}''$	= critical heat flux to attain boiling, $kW/m^2$
$\dot{q}_{o,ig}''$	= critical heat flux for ignition, $kW/m^2$
$\dot{q}_e''$	= external heat flux, $kW/m^2$
$t$	= time, s
$t_{ig}$	= ignition delay time, s
$t^*$	= characteristic equilibrium time, s
$T_{ig}$	= ignition temperature, $^{\circ}C$
$T_{fl}$	= flash point temperature, $^{\circ}C$
$T_s$	= surface temperature, $^{\circ}C$
$V_f$	= flame spread velocity, m/s
$x$	= longitudinal position along centerline of specimen, m
$\alpha$	= thermal diffusivity, $m^2/s$
$\delta_f$	= flame heating distance, m
$\epsilon$	= surface emissivity
$\sigma$	= Stefan-Boltzman constant, $kW/m^2-K$

**BLANK PAGE**

## **CHAPTER 1 INTRODUCTION**

Burning of an oil spill is of interest as a result of offshore exploration, production, and transportation of petroleum [1]. Sensitive oceanic environments require immediate response to remove a hazardous oil slick. In-situ (Latin for “in place”) combustion is an effective response tool for the removal of an oil slick to reduce negative environmental impacts. Cleanup by combustion is more attractive than other spill mitigation methods. This approach requires less labor than other removal techniques, such as using mechanical recovery or chemical dispersants. Furthermore, the efficiency of in-situ burning, 85 – 99%, is greater than mechanical recovery or dispersant efficiency, 33 – 67% and 50 – 70%, respectively [2]. A review of oil spill combustion studies shows that oil removal by in situ combustion has been reported to be greater than 99% based on large-scale oil spill burn experiments [3]. In certain situations, in-situ burning is the only feasible response method. For example, the magnitude of an oil spill may overwhelm the containment and storage equipment, or remoteness of the oil spill may make accessibility difficult. Primarily, in-situ burning is employed to rapidly remove a large volume of oil from the surface of water to reduce subsequent environmental effects.

### **1.1 Background**

Although in-situ burning is relatively simple, effectiveness is limited by various physical factors, such as oil slick thickness, degree of weathering, amount of emulsification, and environmental conditions. Generally, quicker response by in-situ burning results in a higher efficiency. Thickness of the slick affects the burning of an oil slick. For instance, an oil slick continues to burn until it reaches a minimum

thickness range between 0.8mm to 3mm [4]. When the oil slick goes below this level, heat loss to the water underneath is sufficient to quench the fire. Since an oil slick tends to disperse and spread with time, more effective burning is achieved by quicker response.

Most accidental and deliberate burns of spilled oil at sea suffer from the effects of wind and waves. Spreading and evaporation can alter the characteristics of an oil slick. Volatiles tend to evaporate rapidly with time (weathering) and mixing tend to form oil/water emulsions making the oil difficult to ignite. Consequently, alteration of the physical or chemical properties of the oil can require additional energy for ignition. Several studies reported have attempted to characterize weathering and emulsions typical of oil-spill scenarios [5].

Weathering, or aging, is defined as the reduction of volatile components in oil through exposure to air. As a result of the loss of the lighter, more volatile combustibles, increased weathering results in more difficult ignition and slower combustion. Consequently, weathered oil requires more energy to evolve volatiles to ignite and subsequently, sustain burning. To ignite weathered oil, a primer, such as diesel fuel or fresh oil, may be necessary to vaporize the heavier remaining components. Weathering is dependent on environmental parameters such as wave height and period, water temperature, and wind conditions.

Emulsification is the process of mixing water into oil. At sea, constant wave action leads to emulsification of an oil slick with water. Burning is sustained by the release of combustible volatiles, thus, emulsions with higher water content require more energy to burn. However, priming an emulsion with fresh crude oil may provide

sufficient energy to initiate and sustain the combustion of an emulsified slick.

Generally, effectiveness of in-situ burning is affected by the amount of water present in an oil slick, which is a function of the emulsification time period.

Another criterion in determining the desirability of in-situ burning is the environmental and human health concerns. For instance, in-situ burning produces a heavy smoke plume that many might consider a serious hazard. According to Evans [6], only 10 through 15 percent of the mass of crude oil burned is converted to particulate that is carried in the plume. Environmental damage to precious sea life and shorelines is minimal in comparison other response methods which may take months or years. Besides being faster method, in-situ burning minimizes the number of people at risk. Manual cleanup exposes multiple cleanup crew to hazards of the oil spill, while in-situ burning requires only a minimal size crew.

On the other hand, in-situ burning may adversely impact on marine wildlife. For instance, the burning of oil conducts heat to the water, thus elevating the water temperature, including the water surface. Many marine organisms reside in this sensitive interface between oil and water. In addition, after burning off the lighter volatiles of the oil slick, a denser solid residue remains. This residue may sink and affect underwater habitats. These environmental effects must be weighed against the advantages of in-situ burning.

Though vast studies exist on the operational implications (applicability, cost, environmental damage, human health concerns ) of in-situ burning, actual burning characteristics, such as ignition and flame spread data, is limited. Thus, further experimentation is necessary to analyze the limitations of in-situ burning and to

characterize the potential of different fuels, or oil spill scenarios, to be treated by means of this response method.

In-situ burning of an oil spill is accomplished through three distinct stages of combustion; (1) ignition, (2) flame spread, and (3) self-sustained burning (or more commonly mass burning). An external source of energy will ignite the liquid fuel and, under ideal conditions, will be followed by the spread of flame parallel to the surface of the fuel. Once the flame spread process is self-sustained, mass burning will follow. Many studies have shown that ignition is not always followed by spread [7] therefore, is not sufficient to guarantee efficient removal of the oil slick. The need to understand the three stages necessary for the efficient removal of crude oil have resulted in the choice to use a modified version L.I.F.T. (ASTM-E-1321) [8] apparatus to characterize the burning process.

Information available on burning of a thin fuel layer floating on a water sub-layer is quite limited. Walavalkar and Kulkarni [3] compiled an extensive review of studies involving ignition, flame spread, and mass burning of crude oils. However, this review focuses primarily on the burning efficiency of crude oil emulsions, in which success is measured solely by the fraction of the spilled oil that is burned away. The authors further indicate there is a lack of fundamental studies to understand the basic mechanisms of crude oil combustion. Modeling of the all three stages of combustion process must be included in the prediction of the applicability of in situ burning.

Under certain conditions, the water sublayer starts to boil, penetrates the fuel layer, and ejects water droplets to the surroundings. This phenomenon is caused by thermal penetration of the heat wave reaching the fuel-water interface and is termed

“thin layer boilover.” Thin layer boil-over [1, 9, 10] has been found generally to enhance burning rate although Koseki et al. [1] noted that boiling at the fuel-water interface can limit flame spread. The effect of minimum fuel layer thickness necessary for sustained combustion has been studied extensively [9, 10]. Several models have been developed to describe the heat losses from a pool fire to the supporting water layer [11] and to attempt description of in-depth absorption of radiation by the fuel layer [12]. Flame spread across the liquid fuel surface has also been emphasized and excellent review papers have been published by Glassman [13] and Ross [14]. Glassman, summarizes the extensive literature on ignition, however, it is clear that little attention has been drawn to characterize the ignition process of liquid fuels on a water sub-layer.

Crude oils are generally complex in composition with multiple hydrocarbon components. Although ignition behavior of individual petroleum fractions has been studied using flash and fire points under quiescent conditions [13, 15, 16], complete multi-component crude oils has not been addresses either in the virgin or weathered states. The influence of weathering and the formation of oil/water emulsions on the flash and fire points have yet to be studied. Flash or fire point tests do not incorporate the effects that high heat insult has on the nature of the fuel, i.e. emulsions break down when subject to a high heat flux, thus are of reduced application for an oil spill scenario. Furthermore, heat transfer towards the water sub-layer is entirely dependent on the fuel properties and can preclude ignition, therefore needs to be incorporated when characterizing the ignition and flame spread processes. To the knowledge of the author, the only study that addresses the effect of weathering and formation of emulsions on ignition under conditions pertinent to the oil-spill scenario is Putorti et al. [17]. This

study was conducted in a cone calorimeter and quantified the necessary heat flux for ignition of various liquid fuels. In this work, emphasis was placed on the ignition delay time of weathered and emulsified samples.

Material flammability of liquid and solid fuels has been researched extensively. Nationally recognized testing standards containing strict testing protocols are currently available to facilitate material fuel properties. For solids, two ASTM standards are generally used to define thermal properties of materials under a radiative insult; ASTM E1321, *Standard Test Method for Determining Material Ignition and Flame Spread Properties* [8], and ASTM E1354, *Standard Test Method for Heat and Visible Smoke Release Rates for Materials and Products Using an Oxygen Consumption Calorimeter* [18].

#### 1.1.1 ASTM E1321 - LIFT Apparatus

The Lateral Ignition and Flame Spread Test, or LIFT standard has been developed to quantify material properties of combustible solids in a small-scale test. Material properties related to piloted ignition of a vertically orientated sample under a constant and uniform heat flux and to lateral flame spread on a vertical surface due to an external radiant flux, are obtained through this testing standard. The LIFT has the advantage that it allows for ignition and flame spread to be studied together which provides a more realistic scenario than other test methods. The background behind this test method is supported by a well-documented theoretical foundation. Therefore, it provides an adequate framework for the study of complex fuels.

The procedure for the test requires two independent tests; an ignition and a flame spread test. For both tests the fuel sample is placed in front of a radiant panel

(483 mm x 280 mm) forming an angle of  $15^\circ$  with the fuel surface with a minimal distance between fuel and panel of 125 mm. The radiant panel provides a heat flux distribution to the sample for approximately the nearest 1550 mm. Beyond this point, the radiant heat flux decays as the distance between the panel and the sample increases. Characteristic heat flux distributions can be found in references [19, 20, 21, 8]. The ignition specimen (155 mm x 155 mm) is placed in the region of nearly uniform heat flux and the full sample (155 mm x 806 mm) is used to study the effect of external radiation on lateral flame spread.

Using the extensive theoretical background, results from the ignition portion of the LIFT standard provide a minimum surface flux and temperature necessary for ignition ( $\dot{q}_{o,ig}''$  and  $T_{ig}$ ). The material properties of the fuel can be extracted from this information. From the lateral flame spread test, the minimum flux necessary for sustained flame propagation ( $\dot{q}_{o,s}''$ ), the minimum temperature required for flame spread ( $T_{s,min}$ ), an effective material thermal inertia ( $k\rho C$ ), and a flame-heating parameter ( $\phi$ ) which is dependent on test conditions, such as the opposed flow gas velocity, the ambient oxidizer concentration, and the properties of the fuel [21]. Together, these specific properties can be used to predict and explain material ignition and flame spread behavior.

### 1.1.2 ASTM E1354 – Cone Calorimeter

The Cone Calorimeter standard also provides a means for measuring the response of materials exposed to controlled levels of radiant with an external ignition source. Based on oxygen consumption, this test method is extremely versatile. The Cone can be used to determine ease of ignition based, heat release rates, mass loss rate,

effective heat of combustion, and visible smoke development of materials and products. The radiant element is configured as a truncated cone producing a uniform heat flux ranging from 0 to 100kW/m<sup>2</sup> on the sample surface. An external spark igniter is used as a piloted ignition source. The ASTM standard should be referenced for a detailed description of the hardware and protocol.

Although the Cone can be used in both the vertical and horizontal configurations, only the latter will be analyzed for experiments conducted with liquid fuels. As seen in the LIFT standard, ignitability is determined by a measurement of the time from initial exposure to the time sustained combustion, or ignition delay time. Similar theory is used for this test to provide  $k\rho c$ ,  $\dot{q}_{o,ig}''$ , and  $T_{ig}$ . Comparison of data obtained using this standard is compared to that of the modified LIFT in the following chapter.

## 1.2 Objective

Although the overall objective of this study is to characterize the entire burning process, the task is formidable. In the present work, emphasis will be given to piloted ignition and flame spread. This choice does not provide optimal conditions for the study of each individual element but it is justified in the general context of this problem. This study will use two different crude oils, as representative of those commonly extracted and transported, and SAE 30W oil as a reference of a known characterized fuel. Crude oils will be studied in their natural state and subject to different levels of weathering. The material properties of the fuels will be extracted using a modified LIFT apparatus in conjunction with existing theoretical correlations and used to characterize the piloted ignition and flame spread of crude oils on a water sublayer. The

formation of emulsions and its effect on ignition will be a subject of future study but goes beyond the objectives of the present work.

**BLANK PAGE**

## CHAPTER 2 DESCRIPTION OF HARDWARE

### 2.1 The LIFT Apparatus

Piloted ignition and opposed flame spread are measured using the LIFT apparatus shown in figure 2.1. Both the radiant heat source and sample are placed in the vertical orientation. The radiant panel and specimen holder form a  $15^\circ$  angle. Radiative exposures are produced via a natural gas-fired porous refractory tiles mounted on the front of a stainless steel plenum chamber to provide a flat radiating surface of approximately 280 by 483 mm. An air-acetylene diffusion flame is supplied for pilot ignition and flame spread. The ignition sample measures 155 by 162 mm and receives an approximate uniform heat exposure over the entire surface. To allow for an adequate testing configuration, the flame spread sample is elongated with a decreasing radiant flux with distance from the panel.

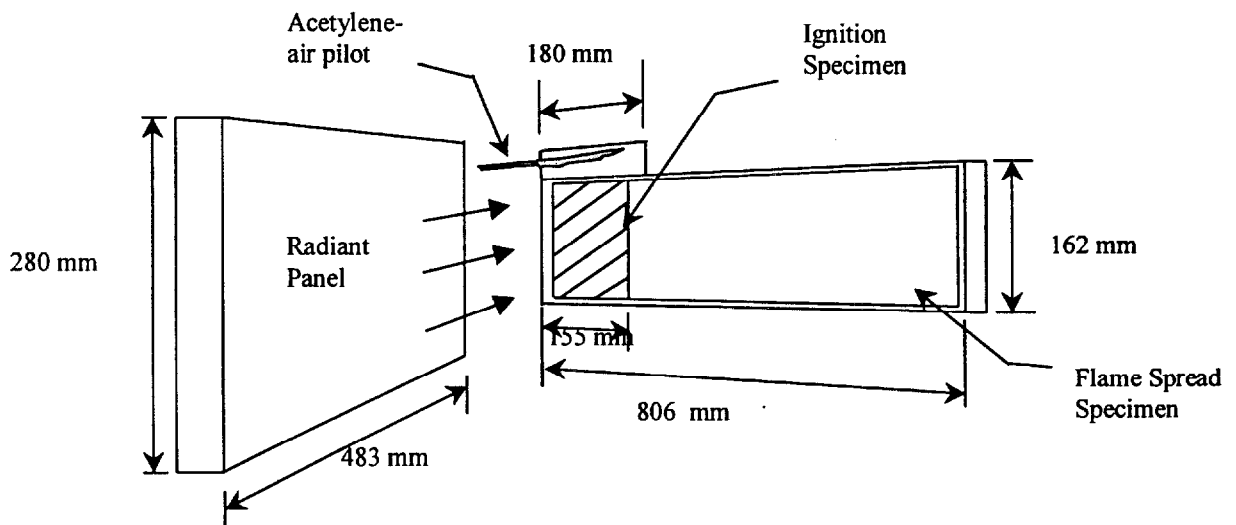


Figure 2.1. Schematic of the original LIFT apparatus.

The basis of the theoretical model behind this LIFT method can be described as piloted ignition and flame spread as a result of inert heating of a thermally thick homogeneous solid to an ignition temperature. The flame configuration applies to a flame spreading into an opposed ambient flow, which closely simulates the flame spread occurring in in-situ burning.

The experimental configuration used as starting point for the design of these experiments is the ASTM standard for the determination of material ignition and flame spread properties.

Details on the LIFT hardware, testing protocol and theoretical underpinnings have been extensively documented by Quintiere and co-workers [19, 20, 21] and will not be detailed here. A summary of the theory and basic assumptions is presented in chapter 3.

## **2.2 Modification of the L.I.F.T. Apparatus**

The ASTM E1321 experimental apparatus previously described has been used to study the ignition and flame spread characteristics of liquid fuels on a supporting bed of water. The L.I.F.T. hardware had to be significantly modified for this purpose. Figure 2.2 shows a schematic of the modified hardware. Since both the panel and sample-holder apparatus are rotated 90° to the horizontal configuration, the modified hardware is commonly referred as H.I.F.T. (Horizontal Ignition and Flame Spread Test). Previously, this geometrical configuration has been used to study materials from which the vertical configuration was not convenient [22].

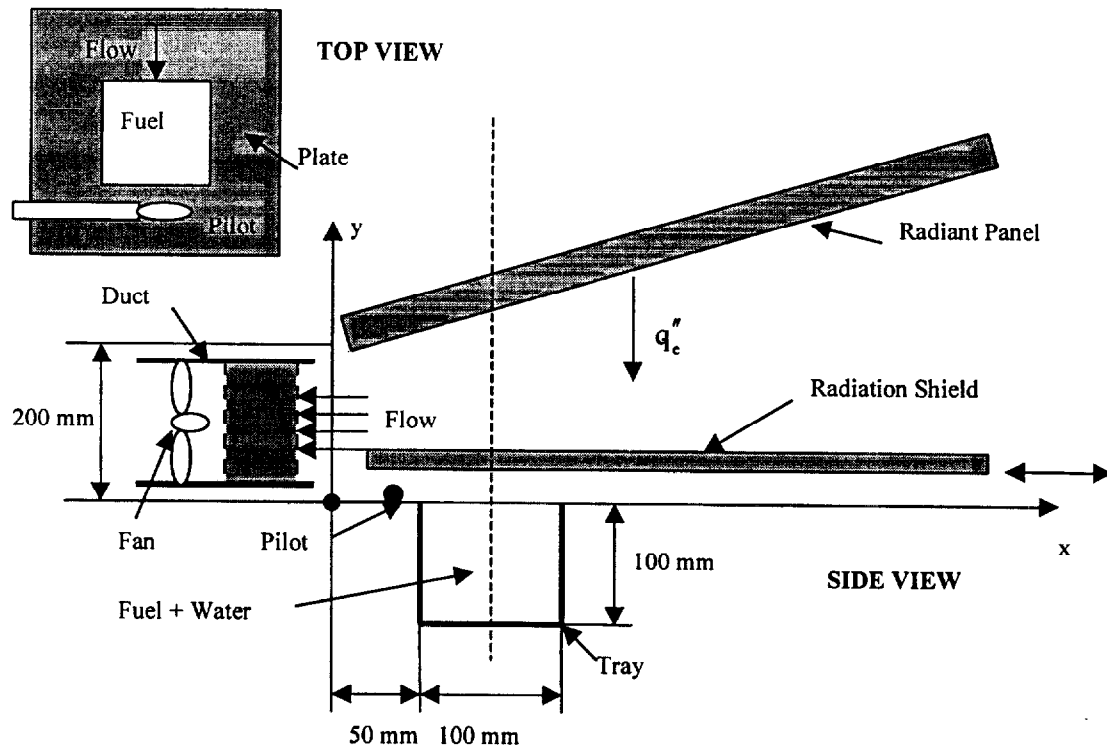


Figure 2.2. Schematic of the modified LIFT apparatus in the horizontal configuration.

The configuration is similar to the LIFT apparatus. However, the experimental HIFT apparatus contains six major modifications from the LIFT apparatus. The modified elements are the following: (1) an induced flow; (2) a radiation shield; (3) sample holders; (4) a pilot flame; (5) a data acquisition system; and (6) the radiant panel. Additionally, revised procedures are required for use of the modified apparatus.

### 2.2.1. Forced Flow

An electric powered fan 4 inches in diameter is used to induce a draft to establish a well-defined fuel boundary layer. The flow-generating device is placed 3.5 inches from the leading edge of the sample. Additionally, a metal duct is used to develop a parallel flow to the fuel surface. The duct shown in figure 2.2 has a 200mm

square cross section which contains an 80mm thick bed of packed steel wool located at the end nearest to the sample. The steel wool serves homogenize the induced flow creating a constant laminar flow for at least the 100 mm region over the ignition tray surface.

### 2.2.2. Protective Radiation Shield

A calcium silicate board of 10mm thickness is used as a radiation shield to prevent premature heating of the sample. The shield is positioned above the sample and extends beyond the length of the entire flame spread tray (500mm). A roller-based system is used to facilitate movement of the radiation shield. Rollers are attached to the frame of the shielding device for rapid removal and replacement.

### 2.2.3. Sample Holding Devices

All sample holders are constructed from bare 1.2mm thick stainless steel. The ignition and flame spread specimen holders are reduced in size compared to the original LIFT equipment to 100 mm square and 100 by 500mm, respectively. Figure 2.3(a) shows the dimensions of the ignition tray used for experimentation. Not pictured is the lip-ignition tray, which differs only with a 5mm interior lip at the top edge of the tray. Additionally, a 250by 250mm aluminum plate (1.2mm thickness) is placed around the ignition sample to simulate a floor around the liquid pool. A hole measuring to the exact dimensions of the ignition tray is removed from the center of the plate. A thermocouple tree is placed on the side of the tray (figure 2.3(a)) with the thermocouple tips positioned in the axis of symmetry of the tray. Further details on the thermocouple locations are given in the following section. No correction for radiation will be performed for the measurements.

Figure 2.3(b) shows a schematic of the experimental tray used in the flame spread tests. Ten thermocouple identical to those used in the ignition tests are placed down the center plane of the flame spread tray. Heights are adjusted to position the thermocouples at the surface of the liquid fuel. Considerations for fuel expansion are taken, but the inherent limitation of this technique is the accurate positioning of the thermocouple tip. Both flame spread and ignition trays are transported to the testing position by a precision metal roller and track system.

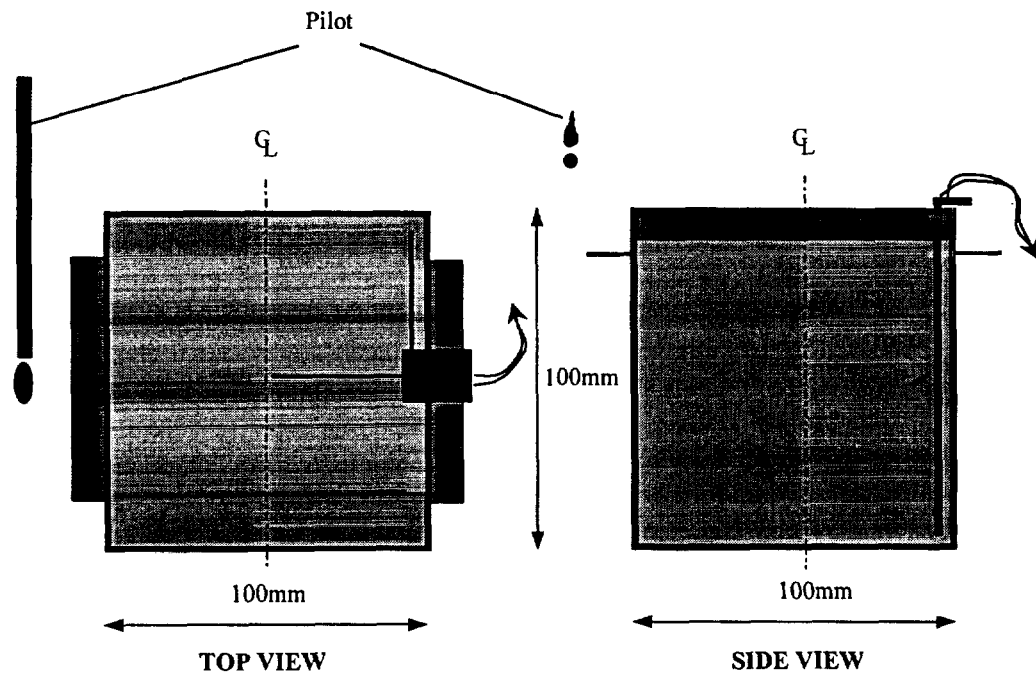


Figure 2.3(a). Schematic of experimental ignition tray.

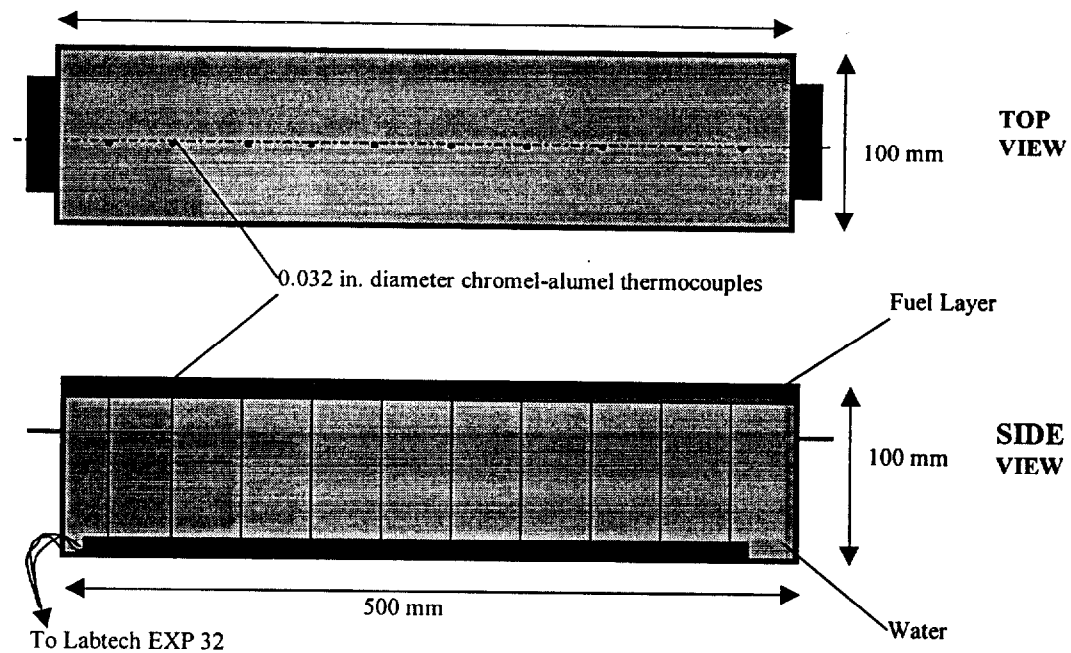


Figure 2.3(b). Schematic of experimental flame spread tray.

#### 2.2.4. Pilot Flame

A propane diffusion flame is provided to ensure piloted ignition of the sample. A small propane diffusion flame (20 mm in height) established on a 4 mm stainless-steel nozzle was used as an ignition pilot. Pilot location and height is fully adjustable. Flame height is adjusted by regulating the propane gas flow. As illustrated in figure 2.3(a), the pilot flame was positioned 10mm above the fuel surface in the centerline 10mm downstream of the trailing edge of the ignition tray. Size and location of the pilot were a subject of a systematic study, and the final positioning was chosen to maximize repeatability of the results.

#### 2.2.5. Data Acquisition System

The data acquisition system software is a PC/Windows-based program by Labtech (Release 9). Measurement devices are Omega Type K stainless steel sheathed thermocouples with a diameter of 0.8mm. The thermocouples are attached to an Omega

EXP-32 external input board. The system allows for 32 input channels with a scan frequency of 1Hz. Furthermore, the system can be initiated either manually or automatically using the data acquisition software.

#### 2.2.6. Radiative Panel

The radiant panel and sample orientation are rotated 90° to the horizontal axis. Other than orientation, the radiant panel design and operation is unaltered from the ASTM standard. Although distance of the radiant panel is lengthened to increase sensitivity of the radiant exposure, inclination of the panel remains at 15°. Initially, the panel was calibrated according to the ASTM E1321 standard protocol. As described in detail by the standard, the gas-fired radiant panel should emit a uniform heat flux over the length of the ignition sample. Calibration of incident heat flux results is shown in figure 2.4. Over the length of the ignition sample holder, the incident heat flux is  $\pm 6\%$ . Similar to the LIFT apparatus, the modified experimental apparatus produces an identical heat flux distribution with distance from the radiant panel.

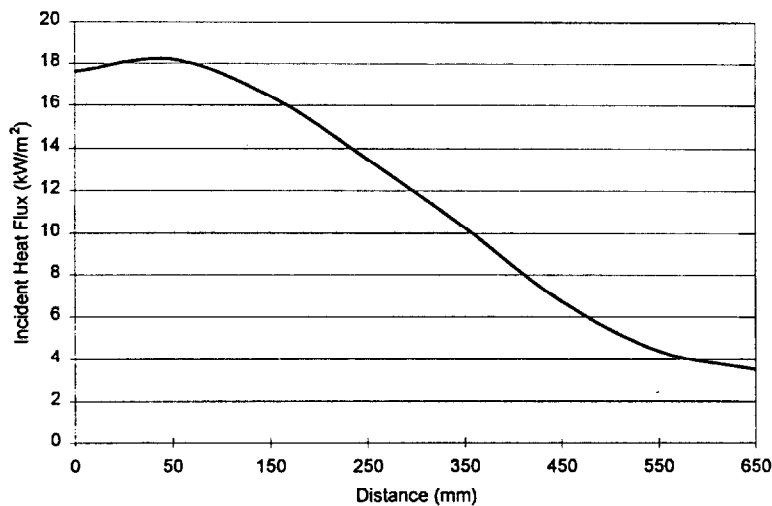


Figure 2.4. Plot of incident heat flux distribution of the experimental apparatus.

### 2.2.7. Protocol

Although similar to the LIFT apparatus, tests conducted with the HIFT require additional procedures resulting from the modifications to the hardware. The additional procedures are the following:

- (1) Ignite radiant panel and obtain desired heat flux.
- (2) Position radiation shield above sample.
- (3) Ignite propane pilot flame.
- (4) Place sample in breach of testing apparatus.
- (5) Initiate data acquisition system.
- (6) Transport sample to test position.
- (7) Remove radiation shield.
- (8) Extinguish sample after completion of test.
- (9) Replace radiation shield above sample.

### 2.3 Preliminary Tests

Although the ASTM E1321 apparatus is well characterized, modification into the HIFT apparatus generates some testing complexities. To study these small-scale testing phenomena, a series of tests were conducted using SAE 30-Weight oil. Selection of the SAE 30W oil is not arbitrary; the increased flash point temperature (254°C) allows for longer observation times during testing. Topics addressed during these are (1) the effect of the container geometry, (2) the effect of a flush floor surrounding the ignition sample, (3) the effect of an induced draft, and (4) the effect of pilot position on ignition delay time.

### 2.3.1 The Effect of Temperature Gradients Between the Fuel and the Container

It has been previously observed that the container has significant effects on the formation of recirculation currents inside the liquid. Temperature gradients in the fuel surface induce thermo-capillary motion combined with natural convection causing recirculation currents [14, 24]. These recirculation currents enhance heat transfer inside the liquid resulting in a more homogeneous temperature distribution and in longer ignition delay times. To validate this theory, ten thermocouples were placed in the liquid bed at the axis of symmetry of the tray to verify the effects of heat transfer from the tray towards the fuel. The thermocouples were spaced to provide a finer grid close to the surface and to cover the entire depth of the tray. This configuration enabled measurement of the approximate surface temperature of the liquid fuel. Figure 2.5 shows a schematic of the thermocouple placement for the ignition tests.

Heat from the radiant panel increases the temperature of not only the fuel, but also of the container. The inclusion of a 5mm lip increased the solid surface receiving radiation from the panel. In this case, temperatures of the upper part of the tray were observed to be significantly higher than those observed for the no-lip tray. In contrast the fuel surface temperature was found to be consistently higher for the no-lip tray, while the temperatures recorded by the thermocouples deeper in the fluid were higher for the lip tray. This is shown in figure 2.6 where the surface thermocouple temperatures for the no-lip tray are greater than 40% over the lip tray. Figure 2.7 illustrates the effect of homogenous heating for the lip trays. The temperature differentials for thermocouples at the surface and 3mm below the fuel surface are

compared for both tray configurations. As stated previously, the temperatures recorded for the thermocouple submerged in the fluid in the lip tray displayed a substantial increase in temperature. For the tray with a lip, the temperature at the surface is almost identical to the 3mm below. Instead, with the no-lip tray, a strong temperature gradient is observed near the liquid surface.

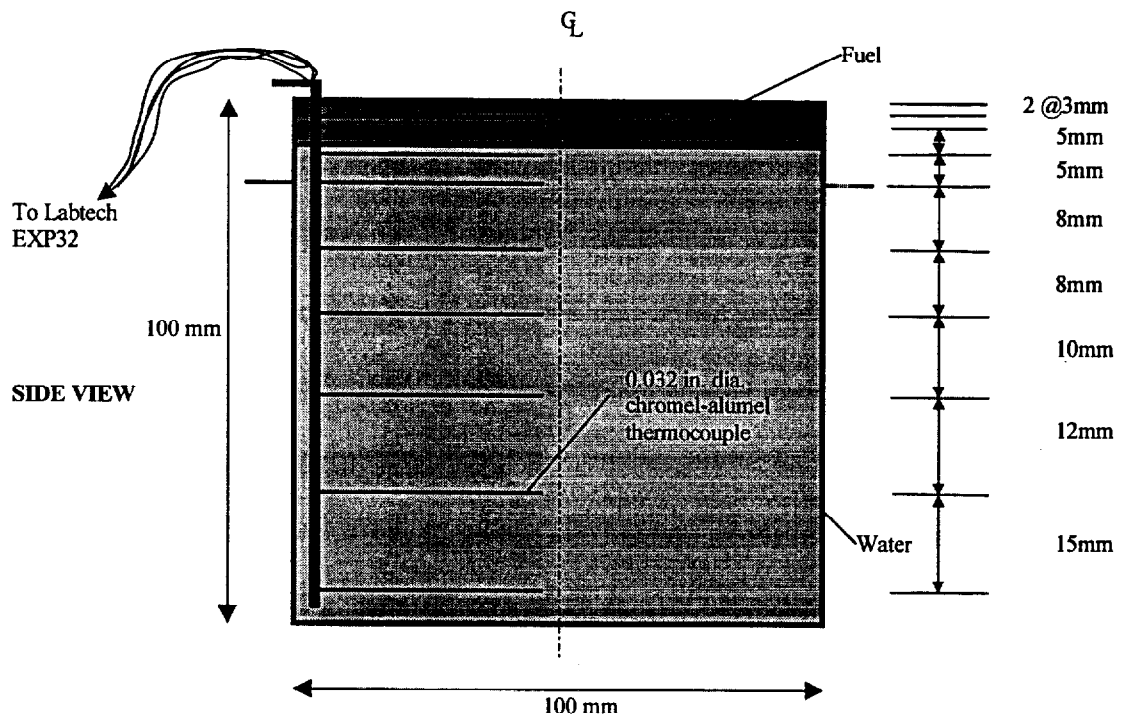


Figure 2.5. Schematic of the thermocouple configuration for the ignition tests.

It was observed that the temperature gradients created close to the lip resulted in buoyantly-induced motion that redistributed the heat in the liquid. As a consequence, the temperature gradient at the liquid surface is small. When using the tray with no lip, these temperatures are minimized, and thus, the liquid behaves more like a semi-infinite solid. The result is a steep temperature gradient close to the fuel surface. The former case is characterized by slow heating of a large amount of fuel, while the latter by fast heating of a thin liquid layer.

To explore the nature of the recirculation currents, a fine metallic powder was used to coat the surface of the fuel with both trays. Observations of the flow in the lip tray indicated increasing eddy activity of the fuel layer as the temperature difference between the container and the fuel increased. These flow patterns were found to be restricted to approximately 10 mm from the tray in the absence of an interior lip. Motion of the powder was observed to be almost negligible in a circle approximately 80 mm in diameter.

Ignition was observed to occur when the surface temperature had attained 254°C. Recirculation inside the liquid bed resulted in a 30% increase in the ignition delay time when the tray with a lip was used. For identical fuel layer thickness and external heat flux, boiling occurred faster in the tray with an interior lip. This is also seen in figure 2.7 for the thermocouple temperature of no-lip versus lip tray configuration. Similar small-scale testing phenomenon of liquid fuels is noted in references [14, 23, 24, 25]. In these experiments, it was determined that the sample container geometry had a significant effect on the liquid-phase flows due to temperature gradients.

This issue is worth an independent study but escapes the objectives of the present work. By selecting the no-lip configuration, effect of heat transfer from the tray was considered minimized.

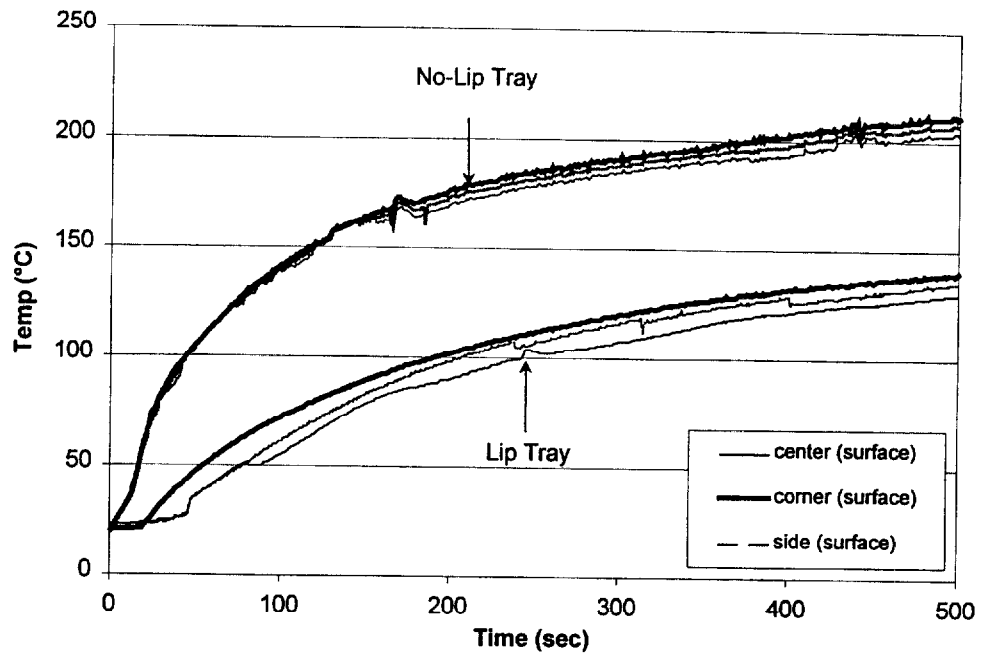


Figure 2.6. Comparison of no-lip tray and lip tray surface temperature profiles for SAE 30W oil for various locations in the fuel sample.

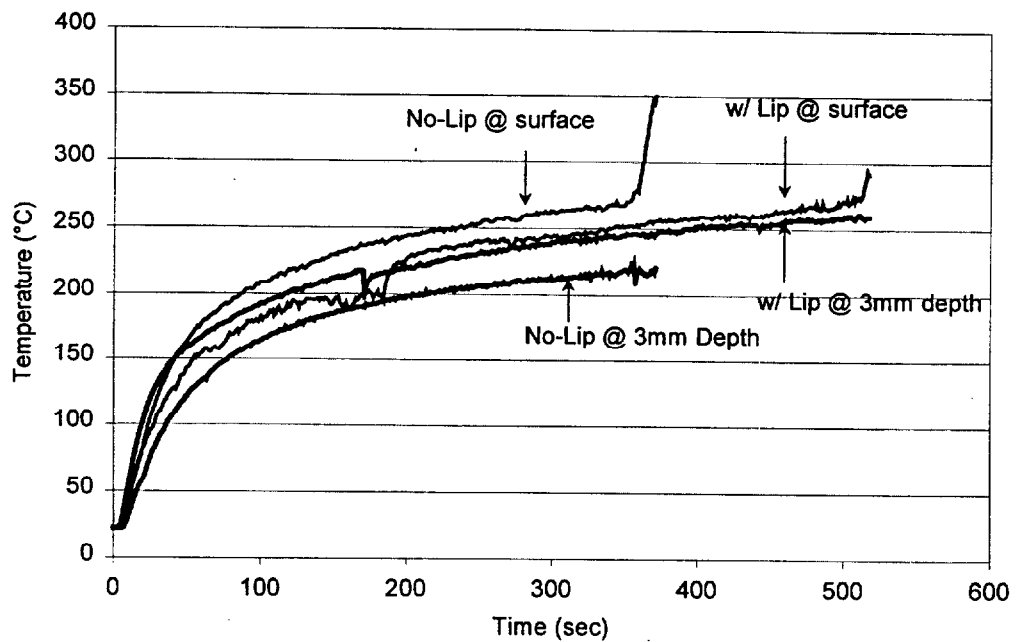


Figure 2.7. Comparison of no-lip tray and lip tray temperatures for thermocouples at the fuel surface and 3mm below the surface.

### 2.3.2 Flow Structures Above the Fuel Surface

To study the flow characteristics over the fuel sample, a 0.5W red diode laser (SDL-820) was used to create a light sheet for visualization of the smoke emerging from the fuel surface. The images have been processed using an EPIX video card. A threshold value was established below which all pixels were assigned a 0 value, to obtain a more clear image of the flow structure, as evidenced by the smoke. Figures 2.8, 2.9, and 2.10 show a set of three typical images.

In the absence of a flush floor surrounding the fuel tray, clear eddies could be observed at the edges of the tray (Figure 2.8). It was observed that these eddies could grow and cover the entire surface of the fuel tray. When a floor surrounded the fuel tray (as shown in figure 2.2) the eddies disappeared and a random upward flow of gases was observed (Figure 2.9). As a consequence of the decreased mixing of fuel and air at the fuel surface, the ignition delay time increased by approximately 20% over the no-floor case. By introducing a 0.1 m/s flow parallel to the surface a boundary layer is formed and the all eddies were eliminated (Figure 2.10). Although the ignition delay time remained dependent on the magnitude of the flow, this configuration allowed for greatest repeatability. The configuration with a surrounding flush floor and induced flow resulted in the most reproducible results.

### 2.3.3 Pilot Size and Location

Premature ignition by a pilot flame is addressed in several references [14, 23, 24, 26, 27]. Obviously, ignition delay time will decrease when influenced by an additional energy source. Special attention must be given to not only the location, but the size of the ignition source. Using the HIFT apparatus, pilot contribution is also

minimized by introduction of the draft. A small propane diffusion flame (20 mm in height) established on a 4 mm stainless-steel nozzle was used as an ignition pilot. Ignition tests were conducted and results indicated ignition delay times did not change beyond the 10 mm height and distance. Therefore, the pilot flame was placed 10 mm above the fuel surface in the centerline 10 mm downstream of the trailing edge of the ignition tray. It was concluded that heat contributed from a 12 mm pilot flame at a distance of 10 mm from the surface of the fuel is considered negligible. Since the pilot contribution is negligible,  $t_p$  is expected to remain unchanged when the pilot is moved. Conversely,  $t_i$  and  $t_m$  are expected to increase with distance and height from the fuel surface.



Figure 2.8. Smoke visualization of the ignition tray with no flush floor.

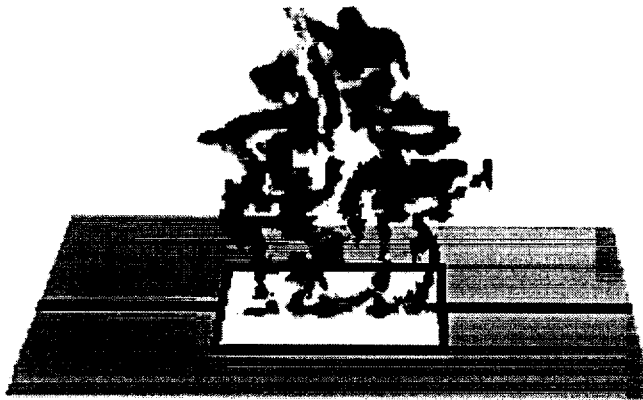


Figure 2.9. Smoke visualization for ignition tray with a flush floor surrounding the sample.



Figure 2.10. Smoke visualization for ignition tray with flush floor and induced flow.

#### 2.3.4 Ignition Delay Time

A set of characteristic values is presented in Table 1 to show typical ignition delay times for fixed heat flux ( $14 \text{ kW/m}^2$ ) and fuel bed characteristics (SAE 30, 10 mm fuel layer thickness). All values presented are averages of no less than 5 tests. It can be noted that the ignition delay time is a strong function of all the parameters shown in Table I. As illustrated previously, the ignition process has shown extreme dependence on ignition source location. Therefore, the pilot location, type of ignition tray, and surrounding floor geometry were chosen based on repeatability of results. It was concluded that a stable laminar flow is necessary, both to eliminate the need to keep the

pilot flame over the fuel surface and to create a robust flow structure that can be considered independent of the environment. The use of the floor and parallel flow was justified on the basis of producing a homogeneous flow structure and avoiding any recirculation zones, possibly present at the leading edge close to the fuel surface. Representative values of the ignition delay time are presented in the table below to provide an order of magnitude to the effects of the above described parameters on the ignition delay time.

Table I. SAE 30 Weight oil ignition tests as 14 kW/m<sup>2</sup>.

Pilot Location	Time (sec)			
	No-Lip Tray (with no floor)	Lip Tray (with no floor)	No-Lip Tray (with floor)	Lip Tray (with floor)
0 mm	342	777	1075	1470
50 mm	455	820	415	727
100 mm	510	830		

## 2.4 Weathering

### 2.4.1 Introduction

Evaporation is the dominant weathering process that affects the crude oils in the marine environment. Depending on the conditions, the physical, chemical, and toxicological properties of a crude oil can be altered significantly by evaporation. The changes induced by evaporation will have a determinant effect on in-situ burning, since they will affect ignition [17] and most probable, flame spread and mass burning.

Therefore, characterization of the weathering process is of importance to the application of the overall testing methodology. Few references are available that provide sound results relating accelerated laboratory evaporation of crude oils to actual field conditions. However, the scope of this research is quantification of the evaporation by mass loss, which is sufficient for characterization of the crude oil combustion.

Hydrocarbons constitute the most important fraction in any crude oil. Although the proportions of each fraction varies significantly, (e.g. from 30-40% to 100% in gas condensates), they account for up to 70% in all petroleum on the average [28]. The light boiling fractions of standard crude oil can contain up to 150 different hydrocarbons. The complexity of petroleum hydrocarbon makes identification of individual elements difficult. However, in the early 1960's an elaborate analytical method was developed called gas chromatography-mass spectrometry. This allowed classification of fractions individual groups according to molecular structure: (1) Alkenes ( $C_5$ - $C_{40}$ ); (2) Napthenes or Cycloalkenes; and (3) Aromatic Hydrocarbons (Arenes).

The least complicated are the Alkenes, which are divided into three fractions. Fraction I is of primary interest since the  $C_5$ - $C_{11}$  hydrocarbons are distilled from the crude oil at a temperature range of 30-200 °C, which corresponds to most of the range of interest. McAuliffe [29] characterizes evaporation as a function of time to liberate the  $C_9$  and lower hydrocarbons. Similarly, the Bartlesville Project Office (BPO) Crude Oil Analysis Data Base User's Guide specifies the  $C_8$  fraction (light gasoline) to be distilled at temperatures of 100°C [30]. The selection of this criteria is not arbitrary as the lighter fractions were not only the most likely to evaporate, but also the most biologically hazardous. This is the referencing standard to compare accelerated laboratory weathering to field conditions. Therefore, an analysis of only simple unsaturated hydrocarbons ( $<C_{11}$ ) is made between individual petroleum fractions and weathered Cook inlet and ANS crude oils. Complicated components such as saturated

cyclic hydrocarbons (naphthenes) and aromatic hydrocarbons have been omitted because of the complex nature of these fractions.

As mentioned previously, data correlating accelerated laboratory evaporation to weathering in a marine environment is relatively limited. One particular computational model, EUROSPILL, was developed to provide information of a chemical release of hydrocarbons from a slick of oil to the atmosphere and water [31]. Data extracted from several laboratory experiments were used as inputs for the spill algorithm. For tests conducted using pure styrene and divinylbenzene on open water with winds of 10 knots and 0.9 meter high waves, the model accurately predicted the rate of evaporation. In a similar effort, Reijnhart and Rose [32] investigated the effects of temperature, mixing, wind, and slick thickness on the rate of evaporation. Batch evaporation experiments with Ekofisk, Brent, Kuwait, and Burgan crude oils correlated very well with their evaporation model. Although simulating controlled field conditions was difficult, predicted evaporation by their model was in good agreement with full-scale sea spills.

Finally, Ostazeski and coworkers [33] provide a detailed study of the weathering properties and the predicted behavior at sea of a No. 6 fuel oil. Because of the similarities to crude oil, No. 6 fuel oil was artificially weathered in a laboratory and used as inputs to the IKU Oil weathering model. Although large-scale experiments were not conducted to validate this predictive evaporation model, a mass loss of 10-20% by weight is predicted after 5 days with a sea surface temperature of 20°C. A similar evaporation trend is expected from both Cook Inlet and ANS crude oils

## 2.5.2 Description of the Laboratory Weathering Station

Weathering is simulated in the laboratory using an Arrow Engineering, Inc. Model 493SG rotary evaporator. Figure 2.11 shows a schematic of the laboratory evaporating apparatus. Using this method of evaporation, time, temperature, volume and mixing velocity can be controlled to produce exposures that will result in a mass loss of comparable magnitude to those observed in the first days of an oil-spill. Temperature of the sample is controlled by using a thermostatically controlled water bath, and mixing velocity is regulated by the controlling the input air pressure of the pneumatic rotary evaporator. Weathering is measured on a mass loss basis using an Acculab Model V-1200 digital scale with an accuracy of  $\pm 0.05\text{g}$ .

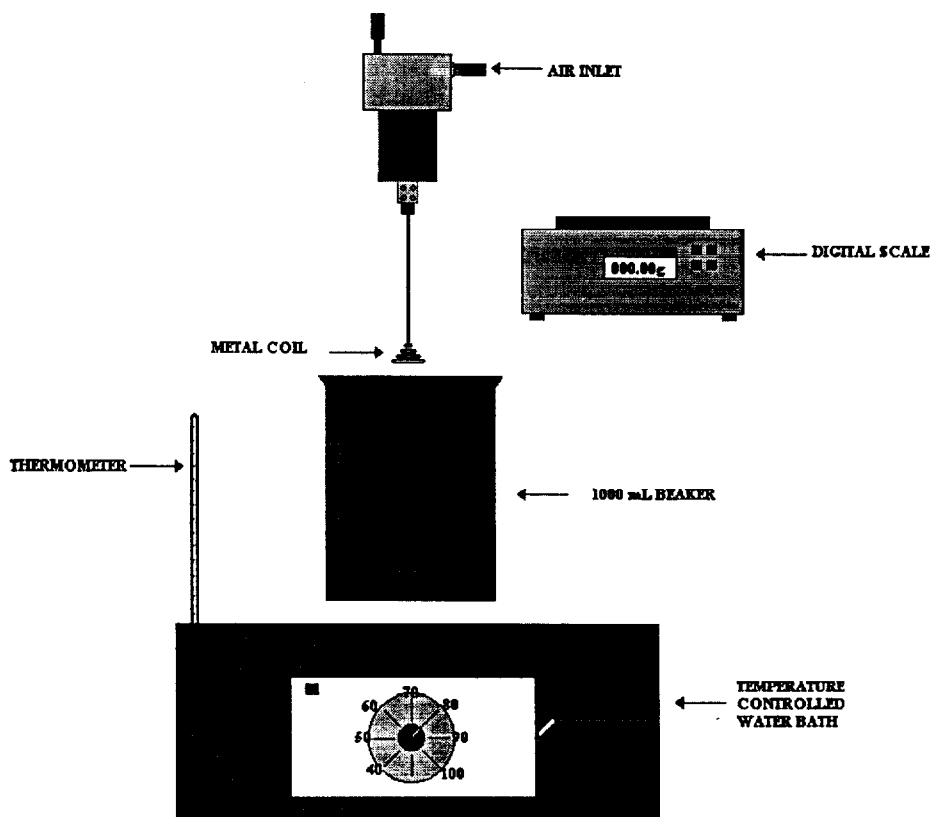


Figure 2.11. Schematic of the temperature controlled rotary evaporation equipment.

Weathering a crude oil sample involves a simple protocol using the equipment described. First, the evaporation goal is specified and a water bath temperature is selected. A fresh crude oil sample is poured from the container into a graduated glass beaker for volume measurement. Visual observation of the volume is approximate and may be a possible source of error. The weight of the metal vessel used in the weathering apparatus is determined electronically and documented. Next, the fresh crude oil sample is carefully poured into the metal testing beaker. All weathering procedures are conducted inside a chemical hood to prevent contamination of hazardous volatiles to the environment. Immediately, the crude oil sample with the metal container are weighed using the electronic scale and documented. Next, the metal beaker is placed into the warm-water bath. Then, the rotary evaporator is inserted into the metal vessel containing the crude oil. After adjusting the height of the metal coil inside the container, the rotation speed is adjusted by varying the input pressure of air into the pneumatic motor. Finally, the beaker is removed periodically for measurements of the crude oil and metal beaker, which are taken and recorded until the evaporation goal is accomplished. Transport of the testing vessel to the electronic scale results in slight mass loss due to human operational effects, which may also be sources of experimental error.

### 2.5.3 Experimental Results

The following section illustrates the effect of varying the volume, mixing and temperature conditions. Results obtained in this study are in good agreement with all known sources of laboratory crude oil evaporation.

### *2.5.3.1 The Effect of the Initial Volume and Mixing*

It has been observed during oil-spills that evaporation starts at the surface of the fuel and penetrates with time, thus fuel layer thickness has a significant effect on the weathering process. In a laboratory scale it is necessary to obtain homogeneously evaporated oil, therefore mixing is introduced to guaranty this homogeneity. The initial volume of the fuel sample influences the effectiveness of mixing, therefore, these parameters were varied systematically and the total mass loss recorded. Experiments were conducted with Cook Inlet and ANS crude oils for a variety of conditions, but for brevity only representative cases will be presented to explain the trends.

The initial volume of the sample was increased keeping all other parameters invariant while the mass loss was recorded. The results are presented in figure 2.12 and 2.14. These figures show that an increase in the volume of fuel reduces the evaporation rate. Thus a smaller percentage of fuels evaporate for a specific time period. When the mass loss is plotted as a function of the initial volume, for different times (Figure 2.13 and 2.15) it can be noticed that the dependency is linear for both ANS and Cook Inlet crude oils.

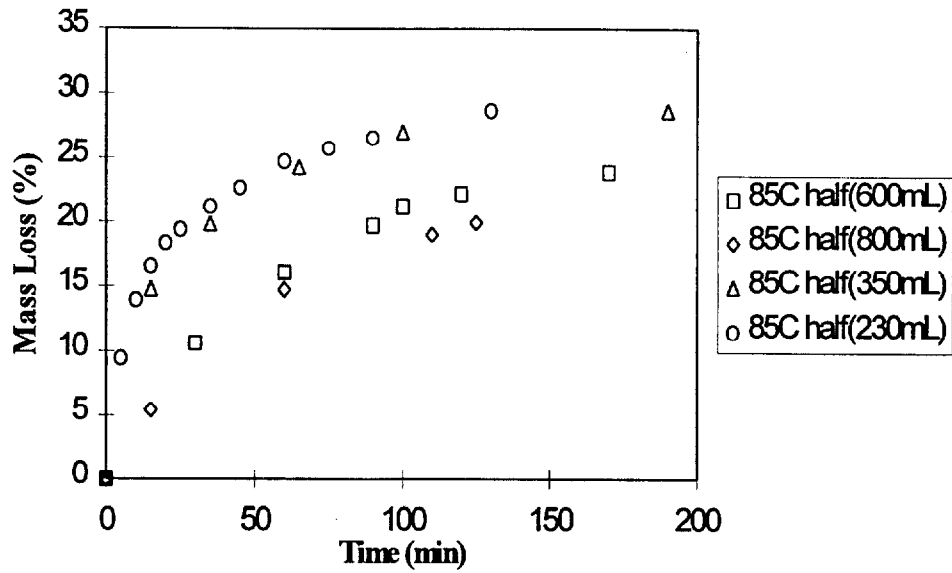


Figure 2.12. Cook Inlet crude evaporation as a function of time for various initial volumes.

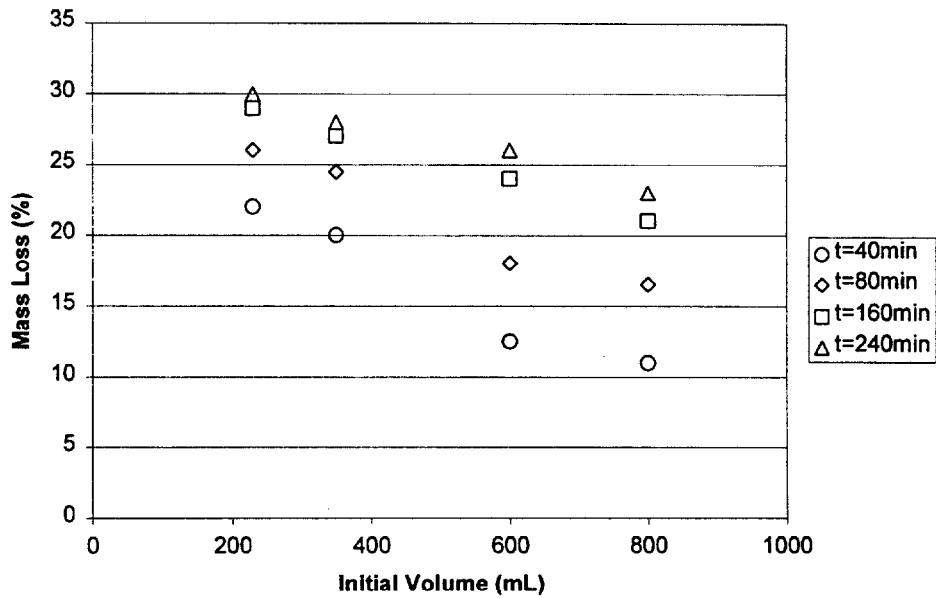


Figure 2.13. Cook inlet crude evaporation as function of the initial volume for specific times.

Similar trends are noticed for the evaporation of ANS crude oil as a function of initial volume. Figure 2.14 shows the evaporation rate as a function of volume for ANS

crude oil. It can be seen that the linear dependency of the mass loss with the initial volume (figure 2.15), observed for Cook Inlet oil, is also present in this case.

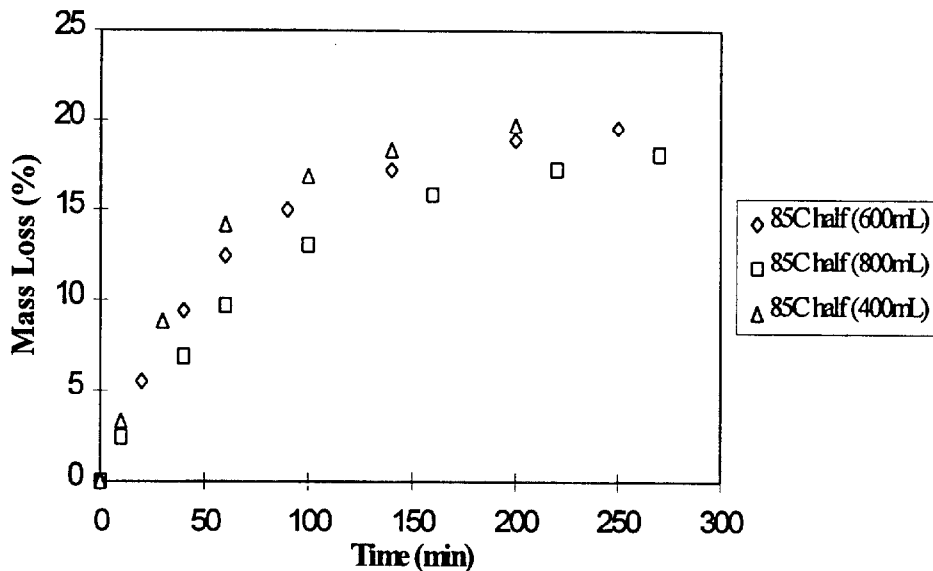


Figure 2.14. ANS crude evaporation as a function of the time for various initial volumes.

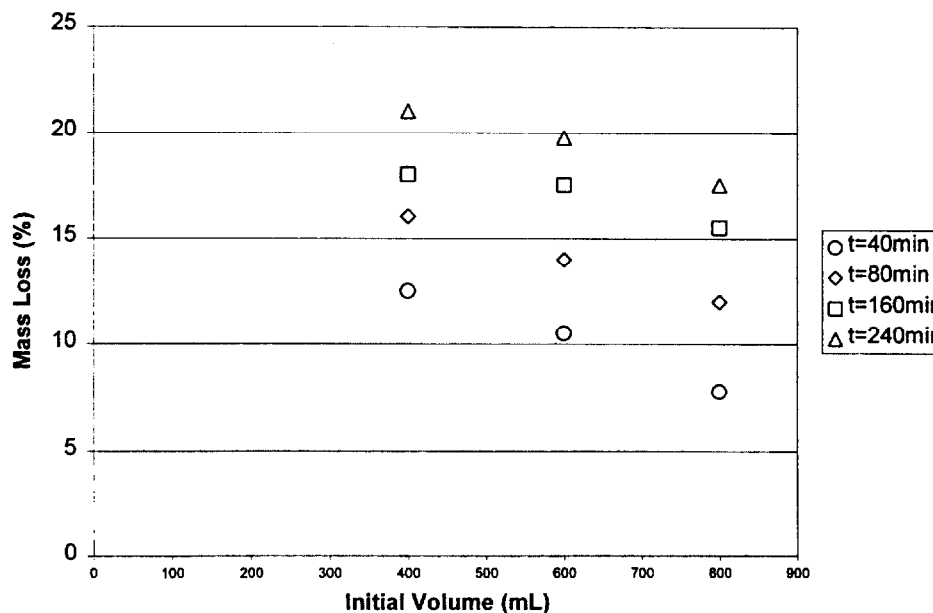


Figure 2.15. ANS crude evaporation as a function of the initial volume for specific times.

A similar trend can be observed when a rotary evaporator was introduced to enhance mixing. When mixing is introduced evaporation occurred faster (Figures 2.16 and 2.17), independent of the speed of the rotor. Enhancement of the evaporation rate due to mixing occurred for a very low rotor speed, and it was impossible to determine the speed at which the transition between the slow and fast evaporation rate occurred. This limitation was imposed by the discrete number of speeds of the rotary evaporator used for the present study. As mentioned before, larger volume results in a slower evaporation rate. Figure 2.16 shows data for two different volumes and various rotator velocities for Cook Inlet crude oil.

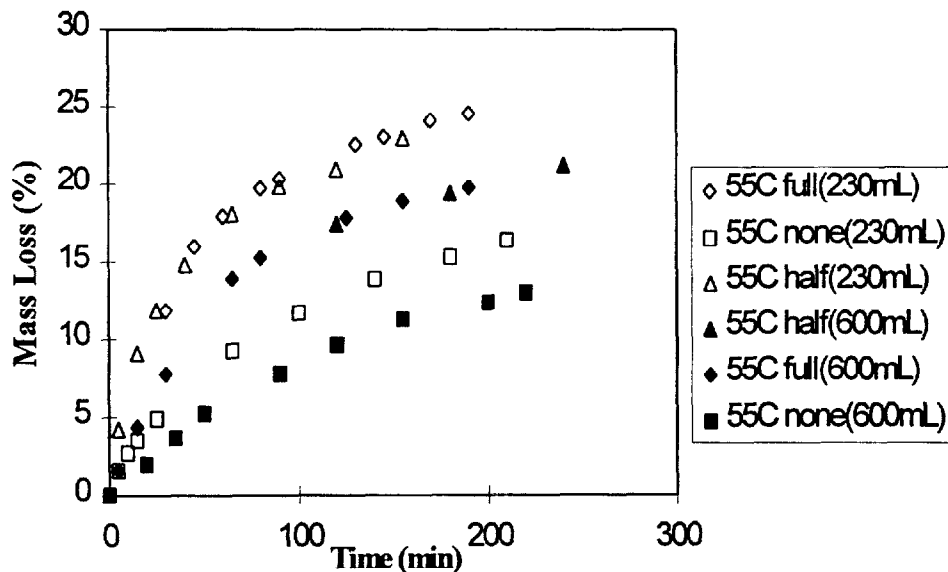


Figure 2.16. Cook inlet crude evaporation as a function of time for various rotator velocities.

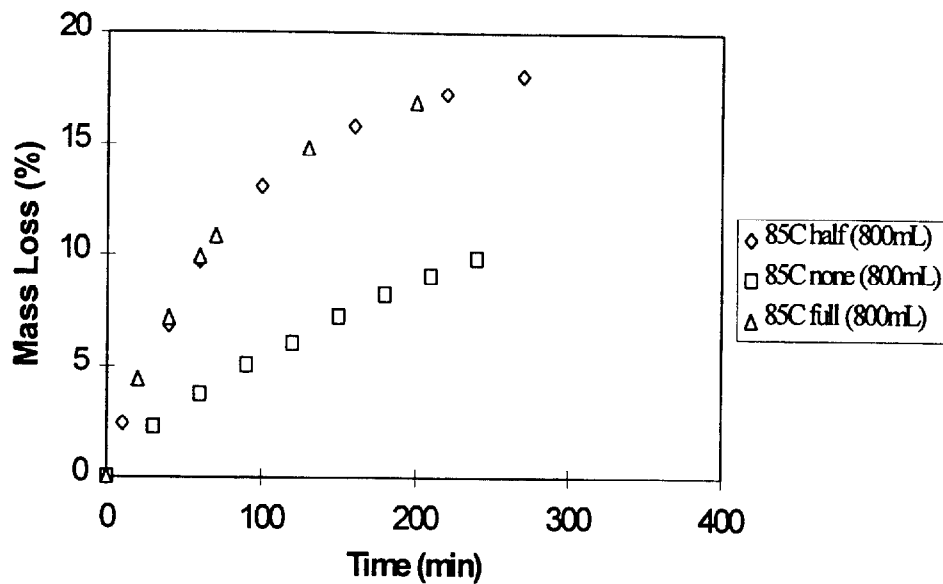


Figure 2.17. ANS crude evaporation as a function of time for various rotator velocities.

### 2.5.3.2 The Effect of Temperature

To study the effects of temperature on the rate evaporation, all other parameters were held constant and mass loss was recorded. To ensure the temperature of the crude oil remained constant through the test duration, the automated thermostatic control specified previously was used. Results are located in figures 2.18. and 2.20. These plots show that an increase in temperature results in an increased evaporation rate.

Therefore, a larger percentage of fuels evaporate for a specified time period.

Furthermore, figures 2.19. and 2.21 illustrate that these change mass loss is linear with change in temperature for the two crude oils.

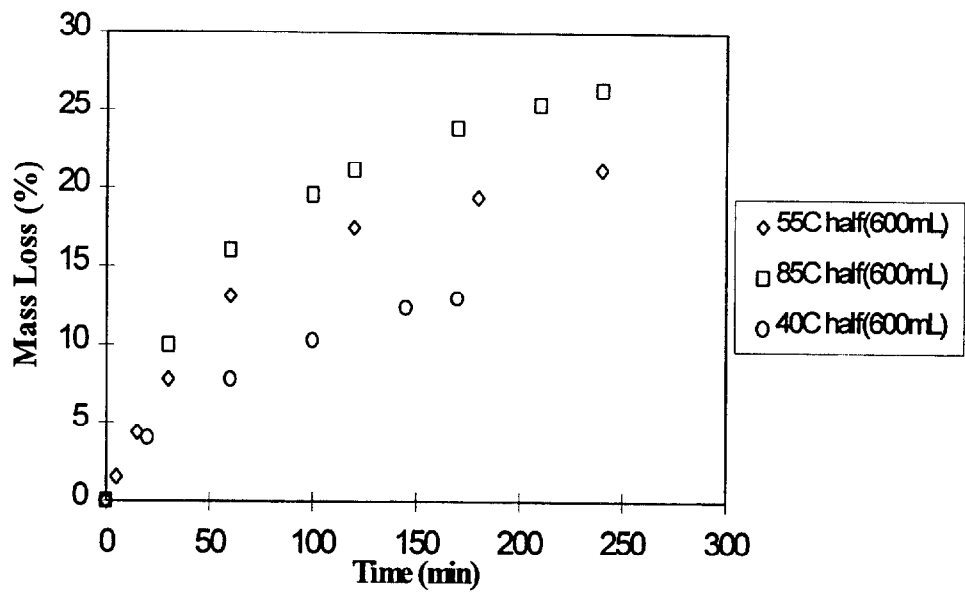


Figure 2.18. Cook Inlet crude evaporation as a function of time for various temperatures.

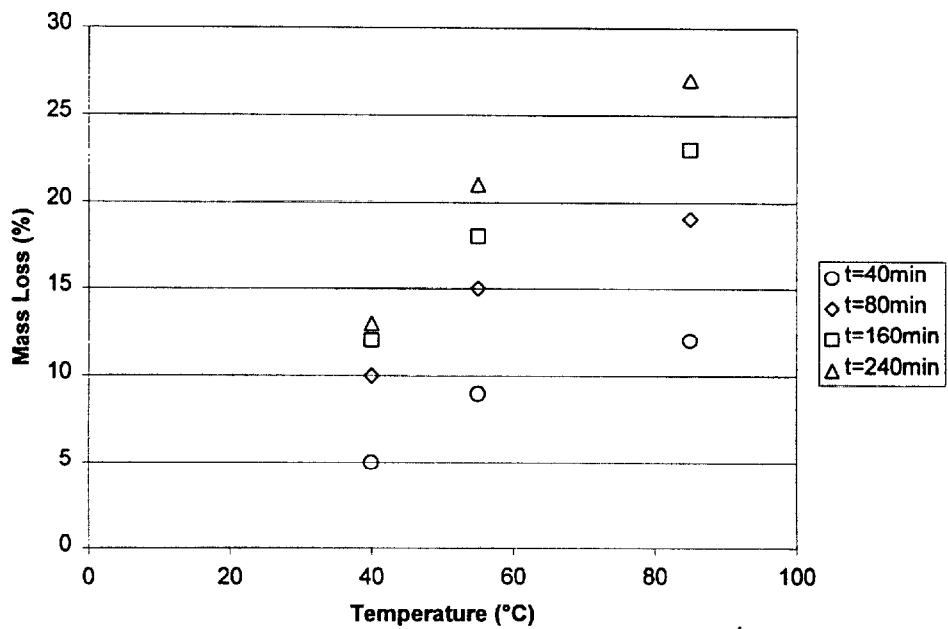


Figure 2.19. Cook Inlet crude evaporation as a function of temperature for various times.

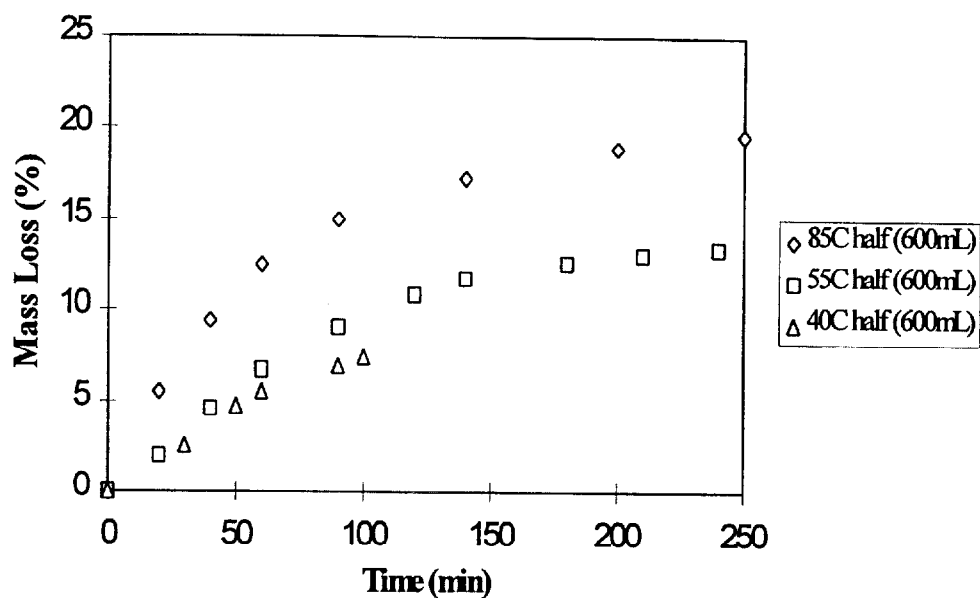


Figure 2.20. ANS crude evaporation as a function of time for various temperatures.

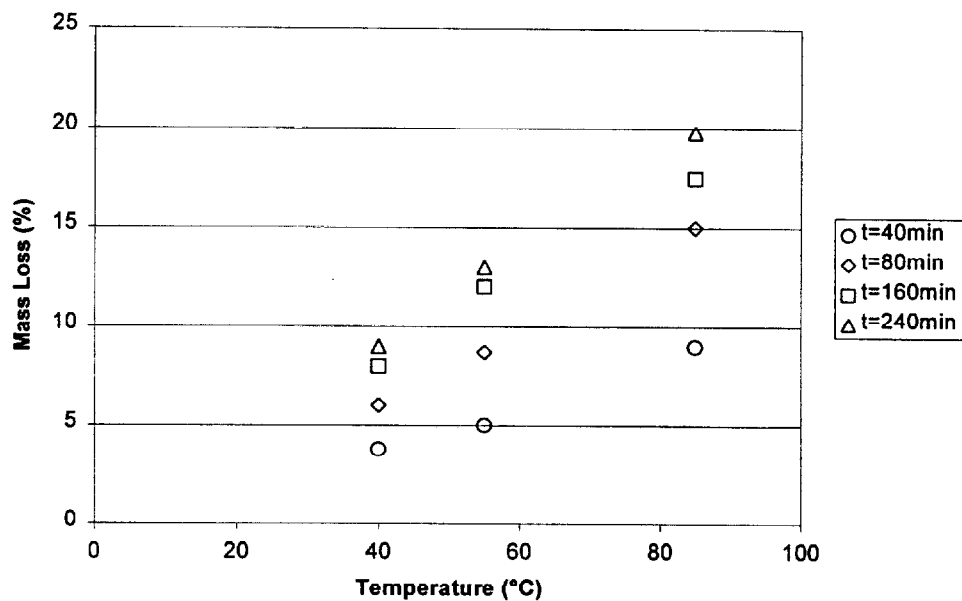


Figure 2.21. ANS crude evaporation as a function of temperature for various times.

Fingas [34] reports that the evaporation of crude oils, based on absolute weight, has a logarithmic relation with time. Examples of equations to predict evaporation are provided in Table II. Eventually, mass loss asymptotically reaches a limit of

evaporation as a function of the time. This relationship is experimentally confirmed from the previous figures for the evaporation of Cook Inlet and ANS crude oils. The empirical values presented by Fingas [34] show a dependency of the parameter with temperature as

$$\%Ev. = (x + y \cdot T) \ln(t) \quad (2.1)$$

Therefore, the percent mass loss is expected to change in a linearly with temperature, where x and y are empirical constants obtained experimentally. Expression such as those presented in Table II are only empirical correlations, thus, are presented only as background to the present study. Validation of the logarithmic dependency goes beyond the scope of this work.

Table II. Equations for predicting evaporation of crude oils [34].

Oil Type	Equation
Arabian Light	$\%Ev = (2.52+0.037T)\ln(t)$
Cook Inlet-Swanson River	$\%Ev = (3.58+0.045T)\ln(t)$
North Slope-Middle Pipeline	$\%Ev = (2.64+0.045T)\ln(t)$
Prudoe Bay	$\%Ev = (1.4+0.04T)\ln(t)$
Santa Clara	$\%Ev = (1.65+0.045T)\ln(t)$

Bobra [5] takes a similar approach for experiments conducted with ANS and other common crudes, but also varies the initial fuel volume. Similarly, his results show a logarithmic relation of mass loss over time using a rotary evaporator and identical decrease in evaporation with an increase in volume. This logarithmic trend is physically representative of the additional effort required to volatize the heavier remaining crude fractions. However, in the study conducted by Bobra, the evaporation time was extended to an order of magnitude of a week, which resulted in mass losses of 30-40% for ANS. Due to safety precautions, evaporation tests in this research were limited to 8 hours producing approximately 20% weight loss of ANS crude.

## 2.6 Summary

Selection of the weathering method (temperature, rotator velocity, and initial volume) is based upon three criteria: (1)time; (2) accuracy; (3) and repeatability. Therefore, from the data presented above, it is justified that a minimum initial volume of 600mL, the “half” rotator velocity setting, and a temperature of 85°C are used. The “half” setting is selected since the “full” setting resulted in slight mass loss due to splashing and subsequent experimental error. These settings allow for accurate, repeatable tests that minimize the time to reach the desired mass loss goal. The percent mass loss will be used as a reference parameter for the level of weathering. No attempt to correlate this value with actual oil spill scenarios will be presented.

**BLANK PAGE**

## CHAPTER 3 THEORETICAL BACKGROUND

### 3.1 Introduction

To analyze a fuel layer floated on water, the fuel and water layers are assumed as one thermally thick bed with properties corresponding to a unknown combination of both liquids. Furthermore, the bed is assumed a semi-infinite slab. Thus, all convective and thermo-capillary motion in the bed is neglected. This assumption is not necessarily correct [14], especially for a small scale where the possibility of temperature gradients between the tray and the liquids is significant, but will be accepted as a possible source of error. The liquid bed is considered initially at a constant ambient temperature,  $T_i$ . Throughout the heating process the fuel layer is assumed inert with negligible pyrolysis before ignition. The solution to the one-dimensional transient heating of a semi-infinite slab is given by Carslaw and Jaeger [35] as

$$\begin{aligned} T_{ig} - T_i = & \frac{\dot{q}_f''}{h_T} \frac{2}{\sqrt{\pi}} \sqrt{\frac{a\delta_f}{V_f}} \left( 1 - \frac{\sqrt{\pi}}{2} \sqrt{\frac{a\delta_f}{V_f}} \right) + \frac{\sqrt{a}}{h_T \sqrt{\pi}} \int_0^t \frac{\dot{q}_c''(x_f, s)}{\sqrt{t-s}} ds \\ & - \frac{a}{h_T} \int_0^t \dot{q}_c''(x_f, s) \exp(a(t-s)) \operatorname{erfc}(\sqrt{a(t-s)}) ds \end{aligned} \quad (3.1)$$

where

$$V_f = \frac{dx_f}{dt}$$

Equation (3.1) is then an integro-differential equation for the flame front position  $x_f$ . The left-hand side represents the temperature rise required to sustain flame spread and the right-hand side represents the sum of the temperature increases due to

the flame heat transfer,  $\dot{q}_f''$ , and the heating imposed by the flux field,  $\dot{q}_e''(x, t)$ . The thermal properties are expressed by the “a” parameter and is defines as

$$a = \alpha(h/k)^2 \quad (3.2)$$

where “ $\alpha$ ” is the thermal diffusivity and “k” the thermal conductivity. It needs to be noted that “k” and “ $\alpha$ ” are not the fuel or water properties but an equivalent set of properties that includes the contribution of both liquids.

Making the imposed flux field independent of time will result in significant simplification of equation (3.1) and of the experimental procedure, therefore,  $\dot{q}_e''$  will be considered only a function of x and thus, equation (3.1) can be written as:

$$h_T(T_{ig} - T_i) - \dot{q}_e''(x_f)[1 - \exp(at)\text{erfc}(\sqrt{at})] = \frac{2}{\sqrt{\pi}} \dot{q}_f'' \sqrt{\frac{a\delta_f}{V_f}} \left( 1 - \frac{\sqrt{\pi}}{2} \sqrt{\frac{a\delta_f}{V_f}} \right) \quad (3.3)$$

Additional assumptions and the derivations pertaining to the present study are given by Quintiere [15].

Heat losses at the surface result in a minimum external heat flux necessary,  $\dot{q}_{o,p}''$ , to obtain attain a pyrolysis temperature,  $T_p$ , required for ignition to occur. For  $\dot{q}_e'' < \dot{q}_{o,p}''$  the surface will attain thermal equilibrium at  $T_{EQ} < T_p$ . A linearized heat transfer coefficient,  $h_T$ , is used to describe heat transfer at the surface. The heat transfer coefficient,  $h_T$ , represents the summation of the convective heat losses and the fraction of the external heat flux not absorbed by the surface and can be described as

$$h_T = h_r + h_c \quad (3.4)$$

Both heat loss terms can be expressed by  $h_T (T - T_i)$  as a result of a linear approximation to convective and radiative heat losses. Values for “ $h_T$ ” have been

shown to vary with orientation and environmental effects. Examples of typical values found in the literature are:  $8.0 \text{ Wm}^2\text{K}^{-1}$  for natural turbulent convection and a vertical sample [19],  $13.5 \text{ Wm}^2\text{K}^{-1}$  for a horizontal orientation [36], and up to  $15.0 \text{ Wm}^2\text{K}^{-1}$  [37] for experiments with a vertical orientation and rough surface such as with wood. Further exploration of the total heat transfer coefficient will be presented in later sections.

### 3.2 Ignition

The mechanisms leading to gas phase ignition under these circumstances are complicated and difficult to predict. In a phenomenological way the process is as follows: after attaining  $T_p$ , the vapor (pyrolysate) leaves the surface, is diffused and convected outwards, mixes with the ambient oxidizer, and creates a flammable mixture near the solid surface. This period will be referred here as the mixing time,  $t_m$ . The flow and geometrical characteristics determine the mixing time.

If the mixture temperature is increased, either by heat transfer from the hot ambient gas, a pilot or any other mechanism, the combustion reaction between the fuel vapor and the oxidizer gas may become strong enough to overcome the heat losses to the solid and ambient. Thus becoming self-sustained and at which point flaming ignition will occur. This period corresponds to the induction time,  $t_i$ , and is derived from a complex combination of fuel properties and flow characteristics.

Extending the analysis proposed by Fernandez-Pello [38], the ignition time ( $t_{ig}$ ) will be given by

$$t_{ig} = t_p + t_m + t_i \quad (3.5)$$

Under ideal conditions, introducing a pilot reduces the induction time making it negligible when compared to the pyrolysis and mixing times. Furthermore, mixing has been commonly considered as a fast process compared to heating of the fuel, therefore, the fuel and oxidizer mixture becomes flammable almost immediately after solid pyrolysis starts. Pyrolysis temperatures and times are, thus, commonly referred as ignition temperature and ignition time [15, 21] and equation (3.5) simplifies to

$$t_{ig} = t_p \quad (3.6)$$

and  $T_{ig}$  can be defined as  $T_p$ . Although such a definition is not physically correct [39] it can be very useful in some practical applications since provides a reference parameter that could serve to characterize the ignitability of a solid material.

For most practical situations, the flow over the fuel surface will control the mixing of fuel and oxidizer as well as the transport of this mixture towards the pilot ( $t_m$ ), therefore, can have a significant effect on  $t_{ig}$  and on the validity of equation (3.6). The relative effect of the flow on  $t_{ig}$  will decrease as the characteristic velocity of the system increases (characteristic time for mixing and transport decrease) and as  $\dot{q}_e''$  decreases ( $t_p$  increases). This will be satisfied best as the external heat flux approaches the critical heat flux for pyrolysis ( $\dot{q}_e'' \approx \dot{q}_{0,p}''$ ) and  $t_p \rightarrow \infty$ . This is important because it implies that the error incurred in the experimental determination of  $t_{ig}$ , (due to the unknown nature of the flow) will decrease as  $\dot{q}_e''$  approaches  $\dot{q}_{0,p}''$ . Therefore,  $\dot{q}_{0,p}''$  is a property of the fuel that can be extrapolated, independent of the flow. Instead, equation (3.6) could be extrapolated only if the experimental conditions at which the ignition delay time is obtained satisfy the assumption that  $t_m \approx t_i \ll t_p$ .

The flow field is a determinant factor in the magnitude of  $t_m$ , for the present experiments it was chosen such that the condition  $t_m \approx t_i \ll t_p$  was satisfied, therefore  $t_{ig} \approx t_p$  and  $T_{ig} \approx T_p$ .

### 3.2.1 The Time to Pyrolysis ( $t_p$ )

Since there is no flame before ignition,  $\dot{q}_f'' = 0$  and equation (3.3) can be simplified. The following solution is derived for the attainment of the pyrolysis temperature as a function of time

$$h_T(T_p - T_i) = \dot{q}_c'' [1 - \exp(-at_p) \operatorname{erfc}(at_p)] \quad (3.7)$$

where  $t_p$  is the time necessary to attain  $T_p$  at the surface.

If  $\dot{q}_c'' = \dot{q}_{o,p}''$ ,  $T_p$  is expected to be reached when  $t \rightarrow \infty$  and the critical heat flux that would lead to pyrolysis can be derived from equation (1) and is given by

$$\dot{q}_{o,p}'' = h_T(T_p - T_i) \quad (3.8)$$

For  $\dot{q}_c'' \gg \dot{q}_{o,p}''$  it can be assumed that  $[1 - \exp(-at_p) \operatorname{erfc}(\sqrt{at_p})] \approx \frac{2}{\sqrt{\pi}} (at_p)^{1/2}$  which leads to the approximate expression valid for short times ( $t_p$ )

$$t_p = \frac{\pi}{4a} \left( \frac{\dot{q}_{o,p}''}{\dot{q}_c''} \right)^2 \quad (3.9)$$

Equation (3.9) is of great practical importance since shows that a plot of  $t_p^{-1/2}$  as a function of the corresponding  $\dot{q}_c''$  will be linear for  $t_p \ll 1/a$ . From the slope of this line the value of "a" can be determined. For long ignition delay times,  $t_p \gg 1/a$ , is expressed with the simplified equation

$$t_p^{-1/2} = \frac{\sqrt{\pi \cdot k \rho c}}{h_T} \left[ 1 - \frac{h_T (T_p - T_i)}{\alpha \dot{q}_c''} \right] \quad (3.10)$$

where  $\alpha = \varepsilon$ . Results from this expression are highly dependent on the selection of the heat transfer coefficient.

### 3.3 Flame Spread

$$h_T (T_{ig} - T_i) - \dot{q}_c''(x_f) [1 - \exp(at) \operatorname{erfc}(\sqrt{at})] = \frac{2}{\sqrt{\pi}} \dot{q}_f'' \sqrt{\frac{a \delta_f}{V_f}} \left( 1 - \frac{\sqrt{\pi}}{2} \sqrt{\frac{a \delta_f}{V_f}} \right) \quad (3.11)$$

Once ignition has been achieved, the flame spreads through the surface at a rate determine by a combination of the fuel and flow properties. The flame spread rate,  $V_f$ , can be determined from equation (3.11). It has been previously shown that  $a \delta_f / V_f \rightarrow 0$ , therefore equation (3.11) can be simplified to

$$V_f = \frac{\frac{\pi}{4a \delta_f (\dot{q}_f'')^2}}{\left[ h_T (T_p - T_i) - \dot{q}_c''(x_f) [1 - \exp(at) \operatorname{erfc}(\sqrt{at})] \right]^2} \quad (3.12)$$

It is a standard procedure for flame spread tests using the LIFT apparatus to preheat the sample until the surface attains thermal equilibrium this leads to a definition of a characteristic time ( $t^*$ ) beyond which no further changes in the fuel surface temperature occur. Under these conditions equation (3.12) can be written as

$$V_f = \frac{\frac{\pi}{4a \delta_f (\dot{q}_f'')^2}}{\left[ \dot{q}_{0,p}'' - \dot{q}_c''(x_f) \right]^2} \quad (3.13)$$

In the particular case of crude oils thermal equilibrium can not be attained since, the fuel will be modified throughout the pre-heating process. Flame spread has to be studied under transient heating conditions.

Assuming that  $t \ll 1/a$  equation (3.12) can be modified by means of a first order Taylor series expansion leading to

$$V_f = \frac{\pi}{4a\delta_f(\dot{q}_f'')^2} \left[ \dot{q}_{0,P}'' - \dot{q}_c''(x_f)(2\sqrt{\frac{at}{\pi}}) \right]^2 \quad (3.14)$$

As mentioned before, “a” is constant and can be obtained from the slope of the ignition plots. Equation (3.14) can be found in the literature [21] expressed as

$$V_f^{-1/2} = C(\dot{q}_{0,P}'' - \dot{q}_c''(x_f).F(t)) \quad (3.15)$$

where

$$C = 2\dot{q}_f''\sqrt{a\delta_f/\pi} \quad (3.16)$$

and is referred as the rate coefficient, and

$$F(t) = \left[ 1 - \exp(-at)\operatorname{erfc}(\sqrt{at}) \right] \approx 2\sqrt{at/\pi} \quad (3.17)$$

Plotting the results as  $V_f^{-1/2}$  versus  $\dot{q}_c''F(t)$  allows for determination of C (slope) and  $\dot{q}_{0,P}''$  (intercept) separate from the ignition data.

The time to attain thermal equilibrium is controlled by the fuel and water bed properties which are incorporated in the value of the parameter “a”. It is therefore important to notice that the fuel layer thickness will have a significant effect on the value of F(t) and this will translate to the flame spread velocity. Figure 3.1 serves to illustrate this phenomenon. The flame spread velocity tends to vary significantly for various fuel layer thickness. The fuel has not attained thermal equilibrium, therefore

the spread velocity is not a direct function of the external heat flux but is influenced by the value of  $F(t)$ .

Flame spread over a liquid has been shown to be a complex phenomena that can not be fully, in contrast with solid fuels, described by means of equation (3.1).

Glassman and Dryer [13], Sirignano [24], and more recently Ross [14], have shown that flow structures formed ahead of the flame front due to capillary motion and buoyancy affect significantly the flame spread rate. Infra red thermography has been used by Inamura et al. [40] to show the enhanced heat transfer due to convective motion in the fuel bed. This observations preclude the use of  $F(t)$  to predict the flame spread velocity, since the temperature distribution will not only be a function of the external heat flux but also of convective motion. To attempt correlation of the data characteristic temperatures of the fuel surface were determined by means of thermocouples and used to correlate the data. It is important to note that these temperatures are subject to a significant error due, mainly, to misplacement of the thermocouple. This error will result in data scatter but, for the purpose of characterizing flame spread in an oil-spill scenario, can be considered of adequate accuracy, since uncertainty in other parameters, such as fuel properties, motion of the water bed, etc. will introduce comparable errors.

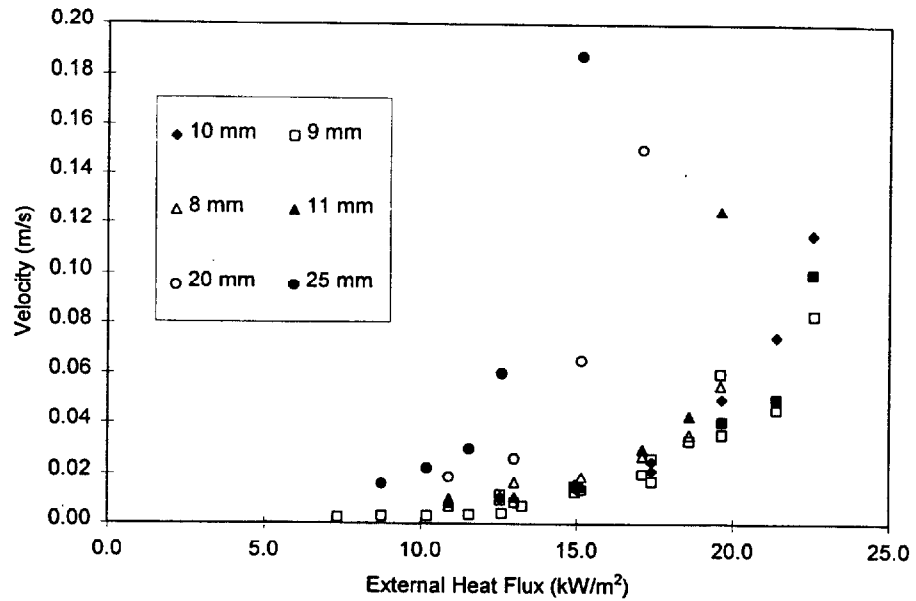


Figure 3.1. Flame spread velocity of SAE 30W oil for various fuel layer thicknesses.

An alternate model, proposed by DeRis [41] that uses equivalent assumptions can be used to correlate the flame spread rate with the fuel surface temperature. For opposed flow flame spread over thermally thick fuels the following expression is proposed by DeRis [41]

$$V_f = \frac{\phi}{k\rho c(T_{ig} - T_s)^2} \quad (3.18)$$

where the flame spread parameter is given as

$$\phi = V_a (k\rho c)_g (T_f - T_{ig})^2 f(D) \quad (3.19)$$

In the same way as equation (3.15) can be used to characterize the flame spread velocity by means of the parameters  $C$  and  $\dot{q}_{0,p}''$ , from equation (3.18) the parameters  $(k\rho c)$  and  $\phi$  can be extracted and serve to describe the flame spread process. The first is the product of the solid fuel's conductivity, density, and specific heat ( $k\rho c$ ), which is defined as the thermal inertia of the fuel. The parameter  $\phi$  incorporates the flame

temperature,  $T_f$ , the properties of the flow,  $V_a$  (air flow velocity) and  $(k\rho C)_g$ , and  $f(D)$  which is a function of the Damkohler number. A good approximation to  $T_{ig}$  is the flash point temperature of the liquid fuel and the surface temperature is obtained, as mentioned before, by means of thermocouples.

Although the individual parameters incorporated in  $\phi$  and  $(k\rho C)$  are difficult to evaluate, the global “fire properties” give a good measure of the energy provided by the flame ( $\phi$ ) and the energy necessary to bring the fuel to its ignition temperature ( $k\rho C$ ). Thus, provide a good description of the flame spread characteristics of the fuel/water composite.

### 3.3.1 The Non-Spread Limit

Understanding of the conditions that will lead to non-spread of a flame over a fuel bed are of great importance to the present work. The process leading to non-spreading and subsequent extinction of the diffusion flame is the result of a complex combination of the flow field characteristics and fuel properties with a finite chemical reaction. Among the heat losses are those to the geometrical boundaries, flame radiation to the environment, and surface radiation [22].

The solution to equation 3.3 has a lower limit,  $V_f = \pi a \delta_f$ , that, under the condition of thermal equilibrium, yields a minimum external heat flux,  $\dot{q}_{0,s}''$ , necessary for the flame to spread [19]. Therefore, the following expression is an energy balance to describe the minimum heat flux for sustained flame spread.

$$\dot{q}_{0,s}'' \equiv \dot{q}_c'' = h(T_{ig} - T_i) - \frac{\dot{q}_f''}{\pi} \quad (3.20)$$

Although this approximation agrees qualitatively with results for solid fuels [19], it is noted that this model is insufficient to truly predict an extinction limit because of its dependence on kinetics and three-dimensional heat conduction. Yet, equation (3.20) is useful when the extinction limit can be approximated and serve as a qualitative parameter to rank materials.

### 3.4 The Total Heat Transfer Coefficient ( $h_T$ )

The above equations attempt to describe the problem of ignition and flame spread by means only of a energy balance between the heat provided by the flame and external sources and the heat losses. Correct calculation of the total heat transfer coefficient will be of great importance when determining the magnitude of the flame spread velocity as well as the characteristics of the ignition process.

The energy balance at the surface of the fuel is given by

$$\dot{q}'' = \alpha \dot{q}_c'' - \varepsilon \sigma (T_s^4 - T_i^4) - h_c (T_s - T_i) \quad (3.21)$$

where  $h_c$  is the convective heat transfer coefficient,  $\alpha$  the absorptivity,  $\varepsilon$  the emissivity,  $\sigma$  the Stefan-Boltzmann constant ( $\sigma = 5.67 \times 10^{-8} \text{ W/m}^2\text{-K}^4$ ). Typical assumptions are to use  $\varepsilon = \alpha = 1$  and a linear approximation for radiation that yields the following expression

$$\varepsilon \sigma (T_s^4 - T_i^4) = h_r (T_s - T_i) \quad (3.22)$$

By means of this assumption the energy balance at the surface can be simplified to

$$\dot{q}'' = \dot{q}_c'' - h_T (T_s - T_i) \quad (3.23)$$

Where  $h_T = h_c + h_r$ . The values of  $h_c$  and  $h_r$  deserve further attention since they will affect the ignition and spread process.

### 3.4.1 The Convective Heat Transfer Coefficient ( $h_c$ )

The fuel sample is placed vertically in the LIFT apparatus, therefore a natural boundary layer is formed close to the combustible surface. The nature of this boundary layer will determine the magnitude of the convective heat transfer coefficient.

Correlations for the average Nusselt number for a heated vertical wall can be found in any heat transfer book [42] and an alternative calculation of  $h_c$  can also be found in the reference [20].

The forced flow induced by the fan will determine, in the case of the HIFT, the convective heat transfer coefficient, thus, characterization of this flow is necessary.

Figure 3.2 shows the velocity of the induced draft on the modified experimental apparatus. Measurements were made at ambient temperatures using a vane anemometer along the center axis of the sample tray. An approximate value for the flow velocity is 0.1 m/s at the initial sample position.

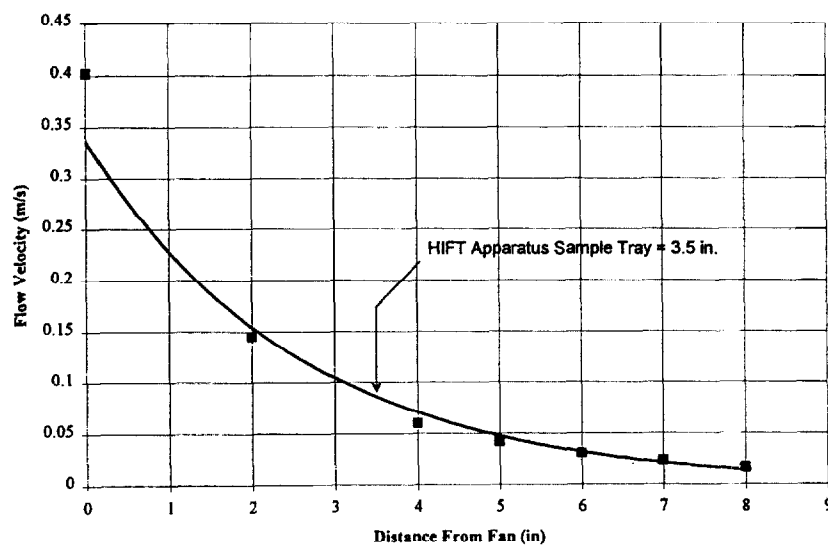


Figure 3.2. Induced flow velocity of the modified LIFT apparatus as a function of distance.

Convection on the HIFT apparatus is best described as parallel flow over a flat plate. Under steady, forced-flow conditions over a horizontal flat surface, the average convective heat transfer coefficient,  $h_c$  is solely a function of the Reynolds number, and temperature differentials will only affect  $h_c$  through the material constants. Therefore, the average convective heat transfer coefficient is best obtained with the following correlations:

$$\overline{Nu} = 0.664 Re^{1/2} Pr^{1/3} \quad (3.24)$$

For the temperature range for liquid fuels studied,  $h_c$  is found to be  $12.5 \text{ W/m}^2\text{K}$  using the relation

$$\overline{h}_c = \frac{\overline{Nu}_L k_{air}}{L} \quad (3.25)$$

As a means of comparison, figure 3.3 shows the dependency of the heat transfer coefficient with temperature, for a vertical wall (the LIFT apparatus) and for a forced flow boundary layer (HIFT apparatus). Although the velocities of the two are comparable in magnitude ( $\approx 0.1 \text{ m/s}$ ) in the case of the LIFT  $h_c$  is a function of the temperature difference between the flow and the fuel surface. Also presented in figure 3.3 is the total heat transfer coefficient as obtained experimentally by Quintiere [20]. It can be noted that the difference between the convective and total heat transfer coefficients is significant. The radiative component of the total heat transfer coefficient is, therefore, of comparable magnitude to the convective heat losses.

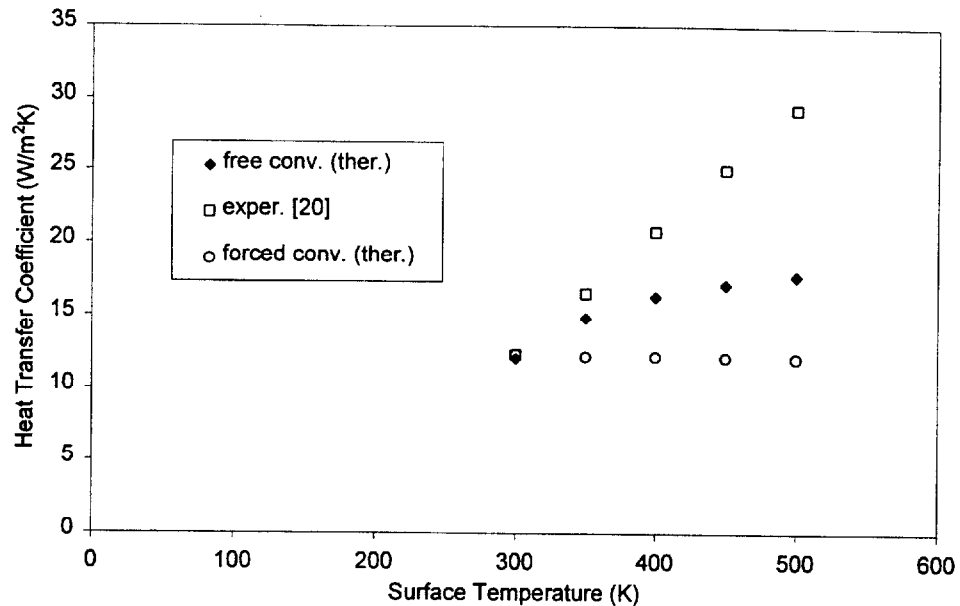


Figure 3.3. Calculation of the convective heat transfer coefficient.

### 3.4.2 The Radiative Heat Transfer Coefficient ( $h_r$ )

Although the linearized radiative heat transfer coefficient is a useful approximation, it is clear that its dependency on temperature will have an effect on the ignition and spread characteristics, specially for low incident heat fluxes (close to  $\dot{q}_{0,p}''$ ) and near the non-propagation heat flux ( $\dot{q}_{0,s}''$ ). Calculation of  $h_r$  was conducted for different emissivities and is presented in figure 3.4. The thermal emissivity is unknown so data is presented for a range of common values ( $0.6 < \epsilon < 0.9$ ). Figure 3.4 illustrates the dependence of temperature for the radiative heat transfer coefficient. For the fuels of interest, in general, surface temperatures remain below 100°C during testing so, using an emissivity of 0.8, a reasonable value for  $h_r$  can be obtained. For this work,  $h_r$  will be taken as approximately 7.5 W/m<sup>2</sup>-K and this value will be used as representative for all fuels tested.

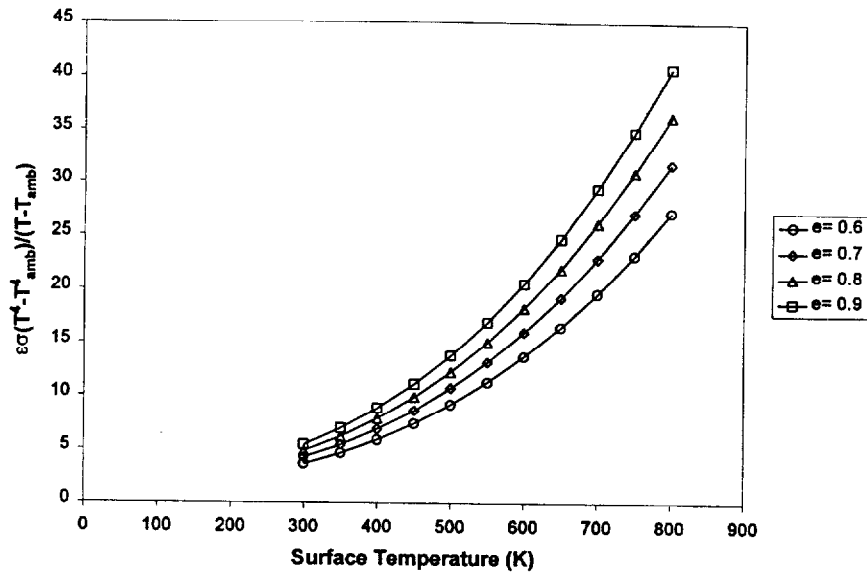


Figure 3.4. Approximation of the radiative heat transfer coefficient as a function of emissivity.

### 3.5 Summary

The above theory represents the basis of an experimental procedure to give a quantitative assessment of the flammability of a fuel through its “fire properties.”

Materials can be ranked based on three different principles: (1) ease of piloted ignition; (2) susceptibility to flame spread; and (3) extinction characteristics.

Ease of ignition is described by the critical heat flux for ignition ( $\dot{q}_{o,ig}''$ ) and by the combined property ( $k\rho C$ ). To obtain ( $k\rho C$ ) it is necessary to know the pyrolysis temperature,  $T_p$ , which will be considered to be the flash point temperature. The flame spread process is characterized by the parameter  $\phi$ , by the critical heat flux for non-propagation ( $\dot{q}_{o,s}''$ ) and, again, by ( $k\rho C$ ).

**BLANK PAGE**

## **CHAPTER 4 IGNITION**

### **4.1 Methodology**

Fuel properties vary significantly when subject to a strong heat insult, therefore, they need to be evaluated under “fire conditions.” These properties are generally referred as “fire properties” [19]. Although there is little available information relevant to the burning of a liquid fuel supported by water, extensive data exists for piloted ignition of solid fuels using a radiant heat source. The concept of minimum heat flux for ignition has been commonly applied to solid fuels. Using heat transfer fundamentals, ignition behavior can be predicted or measured using small, bench- scale experiments. In a similar fashion, ignition behavior of liquid fuels can be studied. Evaluation of the “fire properties” allows ranking of fuels in various states; natural, weathered, and emulsified. The scale dependency will always be a matter of controversy, thus, large scale tests remain a necessity for validation. Yet, the number of tests needed to determine feasibility, protocols, and procedures for in-situ burning will be greatly reduced.

### **4.2 Procedure**

Care is taken to assure fuel and water samples are at room temperature of  $22^{\circ}\text{C} \pm 2^{\circ}\text{C}$ . After pouring the liquid fuel on the water subsurface, time is allowed for gaseous and liquid currents to subside. A radiation shield (calcium silicate board) is placed in front of the panel before the sample is introduced to its test position (Figure 2.2). Once the sample has been placed, the radiation shield is removed and time recording starts. The pilot is a 20 mm long propane diffusion flame placed 20 mm downstream of the fuel trailing edge in the plane of symmetry, 5 mm above the fuel surface (Figure 2.2).

#### 4.2.1 Ignition Delay Time and Critical Heat Flux for Ignition ( $\dot{q}_{0,ig}''$ )

To calibrate the apparatus, SAE 30 Weight oil was first used for the ignition tests. This fuel was used for comparison to previously reported results on ignition delay time [17]. Also, the high flash point (approximately 250°C) results in an extended ignition delay time providing a longer period to observe the different processes affecting ignition. Radiation absorption is also lower with SAE 30 oil favoring boiling of the water sublayer. Although the viscosity of SAE 30 oil is generally higher than that of crude oils, it is very sensitive to temperature (approximately  $1 \times 10^{-2}$  at 0°C and  $1 \times 10^{-5}$  at 100°C) reaching comparable values after only a small temperature increase.

The results from these experiments are presented in figure 4.1 together with data obtained for the same fuel by Putorti et al. [17]. Following equation (3.9), the ignition delay time is presented as  $t^{-1/2}$ . It can be observed that, although the ignition delay time significantly differs from the values found by Putorti et al. all data converges to a unique critical heat flux for ignition. Since these experiments were conducted using different ignition procedures and under different environmental conditions,  $t_m$  is expected to be different, thus, affecting ignition delay time. On the contrary,  $t_p$  should not be affected if the convective losses are similar in magnitude. As the external heat flux approaches  $\dot{q}_{0,ig}''$ ,  $t_m$  becomes neglectable compared to  $t_p$  and all data converges to a unique point ( $\dot{q}_{0,ig}'' \approx 5 \text{ kW} / \text{m}^2$ ), as observed in figure 4.1. This linear dependency corresponds well with the data reported in the literature for solid fuels [19, 37] and serves to validate the above mentioned assumptions. It has to be noted that the linear dependency will break down close to the critical heat flux for ignition, since the Taylor series expansion used to obtain equation (3.9) is only valid for  $t < t_c$  ( $t_c$  is of the order of

$10^3$  sec). As the external heat flux approaches the critical heat flux for ignition  $t \geq t_c$ , equation (3.10) has to be used. The value of  $\dot{q}_{0,ig}''$  obtained from extrapolation carries the error inherent to the approximation used to obtain equation (3.10) but, for the present fuels, was found to be smaller than 10%. Furthermore, the exact magnitude  $\dot{q}_{0,ig}''$  is of little meaning to the present methodology, the value of  $\dot{q}_{0,ig}''$  relies on the comparative nature of this parameter not on its exact value.

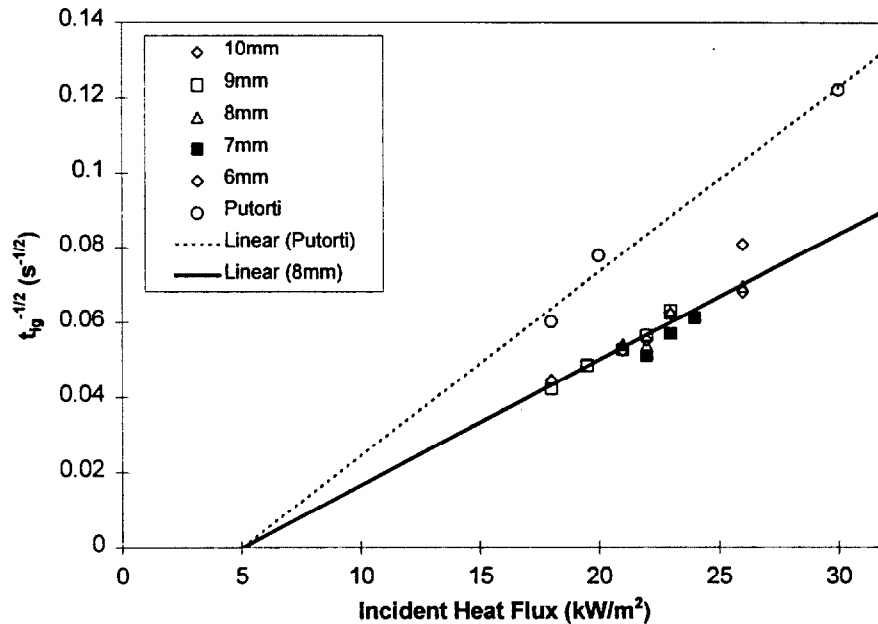


Figure 4.1. Ignition delay times for SAE 30W oil using the HIFT apparatus and Cone Calorimeter.

#### 4.2.2. Critical Heat Flux for Boiling ( $\dot{q}_{0,B}''$ )

For the particular case of an oil slick on a water sublayer, the water underneath the fuel might attain boiling before ignition occurs. It was observed that once boiling started ignition of the fuel was precluded. Heating of the bed can be treated as a semi-infinite solid and temperature distributions can be predicted quite accurately [11]. The

analytical prediction of a characteristic time to boiling goes beyond the scope of this work. But, the determination of a minimum heat flux that will lead to boiling ( $\dot{q}''_{0,B}$ ) before ignition can occur is of great practical importance therefore needs to be included as a complement to the critical heat flux for ignition.

As the external heat flux decreases the temperature gradient at the surface decreases and thermal penetration increases before the surface attains  $T_p$ . If the thermal wave can increase the water temperature at the fuel/water interface to the boiling point before the surface reaches  $T_p$ , boiling will prevent ignition from occurring. The minimum heat flux that will allow the surface temperature to reach  $T_p$  before boiling is given by  $\dot{q}''_{0,B}$  and presented in figure 4.2. Under the assumption that convective heat losses are negligible,  $\dot{q}''_{0,B}$  can be considered independent of the environmental conditions and only a property of the fuel and the fuel layer thickness. Figure 4.2 shows the progression of  $\dot{q}''_{0,B}$  as a function of the fuel layer thickness. As the fuel layer decreases in thickness, the heat wave will reach the water faster allowing for a shorter available time for the surface to reach  $T_p$  and consequently requiring a higher temperature gradient at the surface (higher  $\dot{q}''_{0,B}$ ).

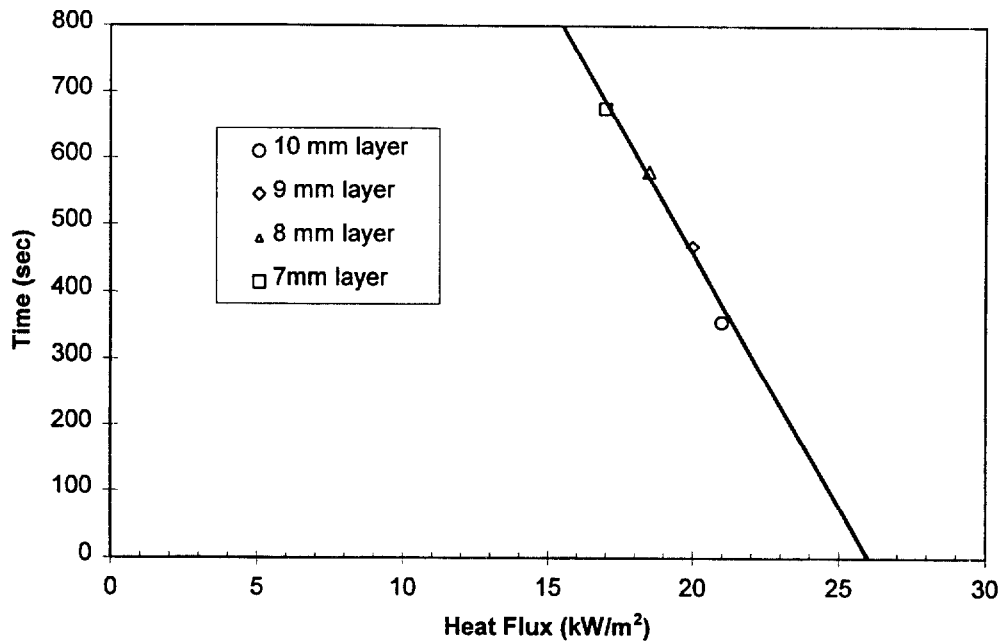


Figure 4.2. Critical heat flux to boil for SAE 30W oil using the HIFT apparatus.

#### 4.3 Crude Oils and the Effect of Weathering

To further demonstrate the validity of this experimental methodology a series of tests were conducted with crude oils. A series of tests were conducted with two crude oils. Figure 4.3 shows these results and others obtained for ANS crude oil by Putorti et al. [17]. The data presented for is an average of at least five experiments conducted under identical conditions. It was observed that ANS crude oil in its natural state ignited at ambient temperature, therefore no external heat flux was necessary. Flash points for this type of fuel have been reported as low as  $-10^{\circ}\text{C}$  [43] showing agreement with the above observations.

When weathered, the ignition delay time decreases as the heat flux increases, and a linear dependency between the external heat flux and  $t_{ig}^{-1/2}$  is obtained. The intercept with the horizontal axis will provide the critical heat flux for ignition.

Therefore, negative values imply that the fuel will ignite at ambient temperature.

Figure 4.3 shows that the critical heat flux for ignition will increase with weathering.

When a line fit is made through the data corresponding to a specific mass loss, it can be observed that these slopes remain invariant with the weathering level. The amount of evaporation does not significantly change the thermal properties of the crude oils. The critical heat flux corresponding to the data reported by Putorti et al. [17] fits well with the data collected in the present work. As previously mentioned, the experimental conditions account for the difference in slope.

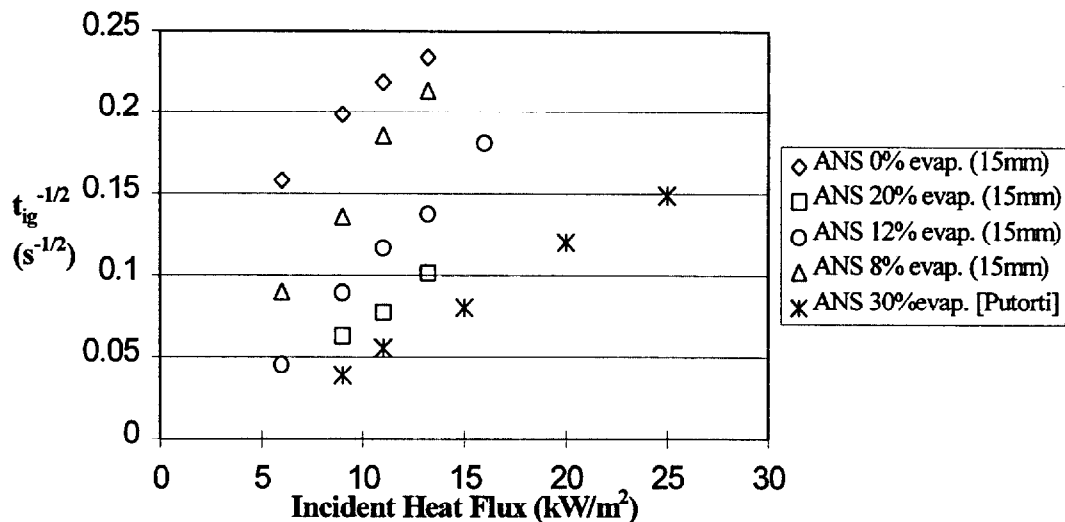


Figure 4.4. ANS crude oil ignition delay time for various levels of evaporation.

Tests were also conducted for different levels of evaporation and fuel layer thickness. Figure 4.5 corresponds to an example of the complete set of data for Cook Inlet crude oil. It is important to observe that for a fuel layer thicker than 8mm, the results are independent of fuel layer thickness. Thus, systematic determination of the critical heat flux for ignition should be done using layers thicker than 8mm. In contrast, it will be necessary to determine  $q''_{o,B}$  for all fuel layers.

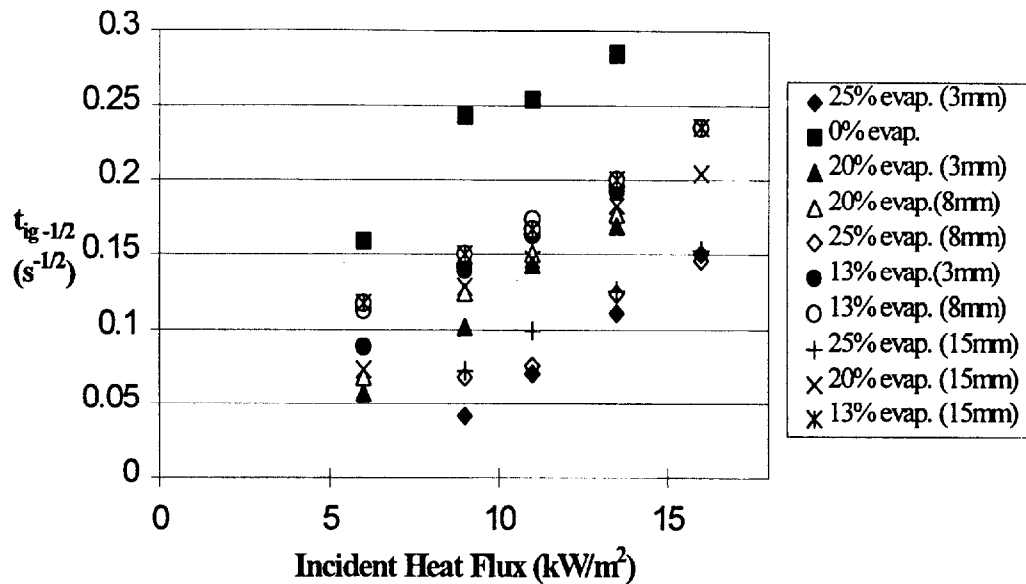


Figure 4.5. Cook Inlet ignition delay time for various levels of evaporation.

As demonstrated by equation (3.9), the slope of the line fit to the data presented in figures 4.4 and 4.5 provide the thermal property, “a”, of the fuel. These figures show that the slope remains invariant with the mass loss due to weathering. This is of importance since it proves that although the ignition event is controlled by the most volatile fractions of the crude oil (thus affected by weathering), the heating process and the properties that characterize it are determined by the heavier fractions, which remain invariant with weathering. In opposition, figure 4.5 shows that the water sublayer has a significant influence on both the global thermal properties as well as the critical heat flux for ignition.

The critical heat flux for ignition ( $\dot{q}_{o,ig}''$ ) as obtained from figures 4.4 and 4.5, is presented in figure 4.6. Results are presented for Cook Inlet and ANS crude oils for different fuel layer thickness. Figure 4.6 shows a discrepancy between the critical heat flux for ignition for 3 mm as opposed to almost identical values obtained for 8 and 15

mm layers. Thus, it can be verified that the fuel layer thickness affects the critical heat flux for ignition up to a thickness of 8mm. Thicker layers result in almost identical curves. The effect of fuel layer thickness was mostly manifested on the curves being truncated by boiling before attaining  $\dot{q}_{o,ig}''$ . The increasing value of  $\dot{q}_{o,ig}''$  with mass loss shows that the weathering makes ignition more difficult. The increasing slope of the curve points towards the possibility of an asymptotic value at which the crude oil will not ignite. Based on values of  $\dot{q}_{o,ig}''$ , ANS crude oil was observed to be more prompt to ignition than Cook Inlet crude oil. Cook Inlet ignited without an external heat flux for a mass loss rate smaller than 10%, and ANS crude oil for a mass loss smaller than 7%.

The results presented are representative of all other cases studied.

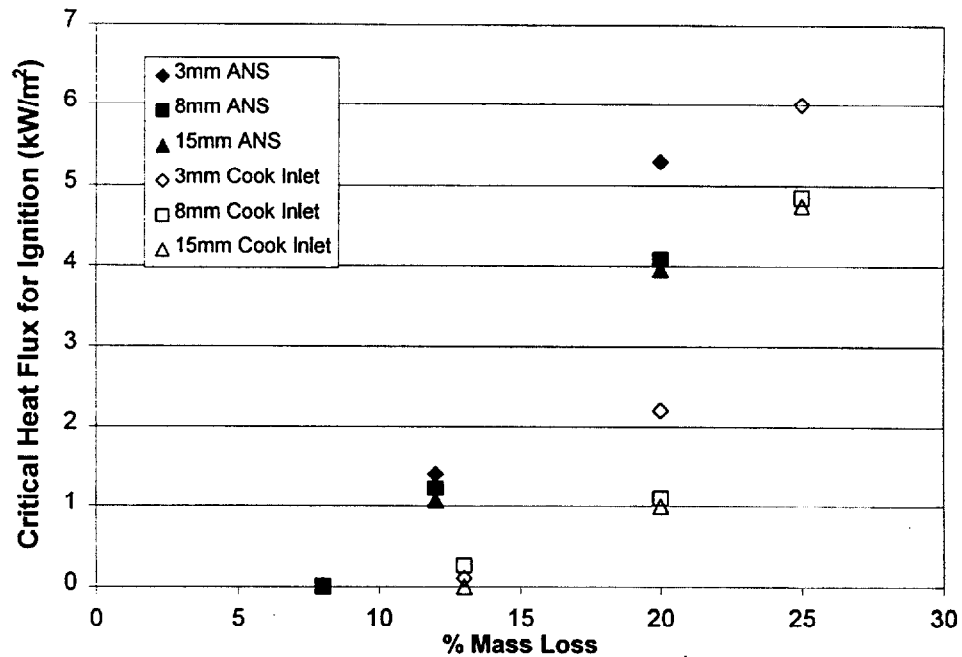


Figure 4.6.  $\dot{q}_{o,ig}''$  for ANS and Cook Inlet crude oils at various fuel layer thickness.

#### 4.4 Closed Cup Flash Point

The ASTM D56 Tag Closed Cup flash point tester is used to characterize the thermal properties under a controlled environment. The standard should be referenced for details of the apparatus. Flash point is defined as the lowest temperature corrected to as pressure of 760 mm Hg at which application of a test flame causes the vapors of a portion of the sample to ignite under specified conditions. The flash point measures the tendency of a fuel to form a combustible mixture with air under a controlled laboratory condition. It is only one of a number of properties that must be considered in assessing the overall thermal characteristics of a liquid fuel.

For the test for flash point, a liquid fuel is placed in the cup of the tester. With, the lid closed, the sample is heated up at a slow constant rate. A small flame of specified size is directed into the cup at regular intervals. The lowest temperature at which application of the flame ignites the vapors above the sample specifies the flash point. The flash point gives an indication of the pyrolysis temperature of the fuel. However, testing to the flash point does not describe the thermal properties of the fuel. Therefore, the flash point temperature is of importance to characterizing crude oils, but not sufficient to describe the ignition process.

Flash point test results for the crude oils as a function of the mass loss due to weathering are presented in figure 4.7. Each point in the figure represents the average of 10 tests conducted in accordance with ASTM D56 standard. As seen from the figure, flash points extracted using the ASTM D56 closed cup tester have a linear dependence on the level of evaporation for both crude oils. More importantly, the flash points for ANS crude oils are significantly higher than the Cook Inlet crude. Note that data is

only presented for flash points above ambient ( $>20^{\circ}\text{C}$ ), since no ignition tests have been conducted for temperatures lower than ambient. A mass loss greater than 20% has been shown to require weeks of weathering under natural conditions [33]. Therefore, 20% will be used as an upper limit to the mass loss.

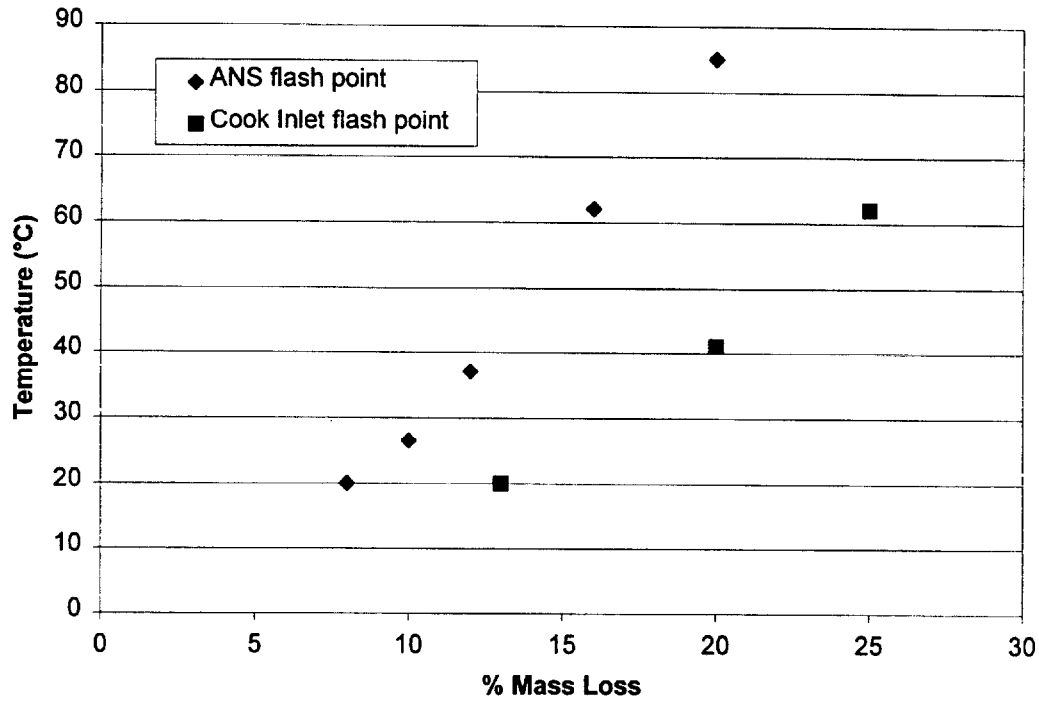


Figure 4.7. ASTM D56 closed cup flash point tests for ANS and Cook Inlet crude oils.

A comparison of the flash point and the critical heat flux for ignition obtained by the HIFT apparatus ignition tests is presented in figure 4.8. The data points correspond to different levels of weathering. It is noticed that the flash point temperature has a linear dependence with the critical heat flux for ignition, as predicted by equation (3.8). The line fit for ANS and Cook Inlet crude oils converge to an ambient temperature ( $20^{\circ}\text{C}$ ) for  $\dot{q}_{o,ig}'' = 0$ . This observation is of great practical importance since it shows the flash point temperature can be used as a characteristic ignition temperature. More

importantly, by use of the previous expression, the global heat transfer coefficient can be evaluated since  $h$  corresponds to the slope of the line fit.

From theory, equations (3.21) and (3.22) can be combined and expressed as

$$\varepsilon\sigma(T^4 - T_\infty^4) + h_c(T - T_\infty) \approx h_T(T - T_\infty) \quad (4.1)$$

As shown by equation (4.1), the global heat transfer coefficient consists of both a radiative and convective component. Since the convective component is a function of the orientation and flow conditions and independent of the fuel, the slope of the flash point data presented in figure 4.8 provides an indirect measure of the emissivity of the fuel. Moreover, if the global heat transfer coefficient ( $h_T$ ) is known, and the thermal property “ $a$ ” is extracted from the ignition delay time, the product of the thermal conductivity, density, and specific heat capacity ( $k\rho C$ ) can be obtained using the expression

$$(k\rho C) = \frac{h_T^2}{a} \quad (4.2)$$

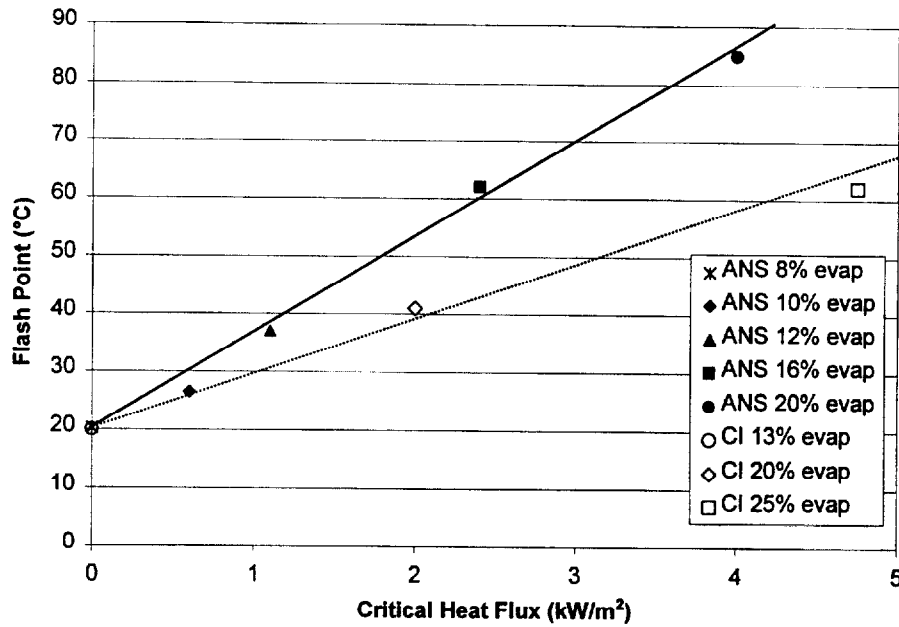


Figure 4.8. Flash points of ANS and Cook Inlet crude oils at various levels of weathering.

#### 4.5 Summary

To study piloted ignition of a slick of oil on water sublayer, a modified LIFT apparatus is used. As for solids, ignition delay times and critical heat flux for ignition of a liquid fuel supported by water can be extracted using this testing methodology. Closed cup flash points are presented to complement the piloted ignition tests. The propensity of a crude oil to ignite can be characterized by three parameters:

- (1) The critical heat flux for ignition ( $\dot{q}_{o,ig}'' \approx \dot{q}_{o,p}''$ ), it is independent of the environmental and experimental conditions. Thus, it provides a measure of the minimum heat insult necessary to guarantee attainment of a pyrolysis temperature, and therefore, production of sufficient gaseous fuel for ignition. The critical heat flux for ignition is obtained by extrapolation to  $t_{ig} \rightarrow \infty$  of the ignition delay time data.

- (2) The critical heat flux for boiling ( $\dot{q}''_{o,B}$ ), which provides a measure of the minimum heat flux necessary to attain ignition before boiling of the sublayer occurs.
- (3) The thermal “fire properties” of the fuel (kpC) can be extracted from flash point temperature in combination with the critical heat flux and provides a measure of the heating process. It is a function of the fuel and is independent of the experimental and environmental conditions.

The experimental methodology and its theoretical underpinnings were validated with experiments using SAE 30W oil and ANS and Cook Inlet crude oils in their natural state as well as different levels of weathering. The results show consistency and correlate well with other data presented in the literature.

**BLANK PAGE**

## **CHAPTER 5 FLAME SPREAD**

### **5.1 Methodology**

As in the ignition tests, the modified ASTM E1321 apparatus is also used for flame spread testing of the liquid fuels. Three types of fuels are used for flame spread tests. Again, SAE 30 weight oil is used for calibration because of its pure characteristics and known properties. Multi-component fuels that contain numerous fractions, such as crude oils are also of interest. Therefore, flame spread tests include ANS and Cook Inlet crude oils at various levels of weathering. All flame spread tests are conducted using the unlined aluminum tray illustrated in figure 2.3(b). Fuel surface temperature measurements are obtained using thermocouples placed in the center axis of the flame spread tray. Flame speed and surface temperature are recorded for each test. Various fuel layer thicknesses are obtained by adjusting the gross volume of supporting water and the corresponding amount of fuel.

### **5.2 Background**

Flame spread over liquid fuels is a complex phenomenon that involves the understanding of natural convection inside the fuel layer as well as the chemical and thermal aspects leading to ignition in the gas phase. The multiple applications where flame spread over liquid pools is of relevance have made this issue the subject of numerous studies. A brief review of the relevant issues that need consideration in the particular context of this work will be presented. The treatment that the flame spread process will be given in this section might seem too general for such a complex subject, but the objective of this work is to provide global criteria that will serve to describe the propensity of a fuel to sustain flame spread. Thus, average spread rates will be

considered instead of tracking the pulsating flame front, and the controlling heat transfer mechanisms in the liquid phase will not be explored independently but globalized in the parameter  $\phi$ .

### 5.2.1 Qualitative Observation and Physical Description of the Spreading Flame

Observation of the spreading flame reveals a similarity in all fuels. After ignition, a fully developed flame is preceded by a pulsating blue flame very close to the surface. The blue precursor flame is considered premixed fuel and air. Ignition of the fuel will occur when the lower flammable limit for combustion is exceeded. Initially, the temperature of the fuel ahead of the well-developed flame is below the flash point, and there is insufficient fuel vapor to produce a combustible mixture above the liquid surface. However, as the developed flame approaches, heat is transferred to the liquid ahead until the flash point temperature is attained. At this temperature, there is sufficient fuel vapor to exceed the lean flammability limit and a premixed flame occurs consuming the mixture. Because the rate of vaporization is inadequate to sustain the flame, the premixed flame is extinguished. This process of flashing forward and backward is repeated until the necessary amount of heat is transferred forward to elevate the fuel temperature to its fire point. At the fire point, the rate of vaporization is sufficient for self-sustained combustion, and the flame is now developed at this point.

Transfer of heat ahead is the dominant factor for the rate of flame spread. References have indicated various modes of heat transport to the region ahead of the flame front [13, 14, 24]. However, observation of flame propagation, verifies that the concept of flash point temperature is critical in determining the controlling mechanism

in flame spread. The physical processes accompanying flame spread over a liquid fuel are illustrated in figure 5.1.

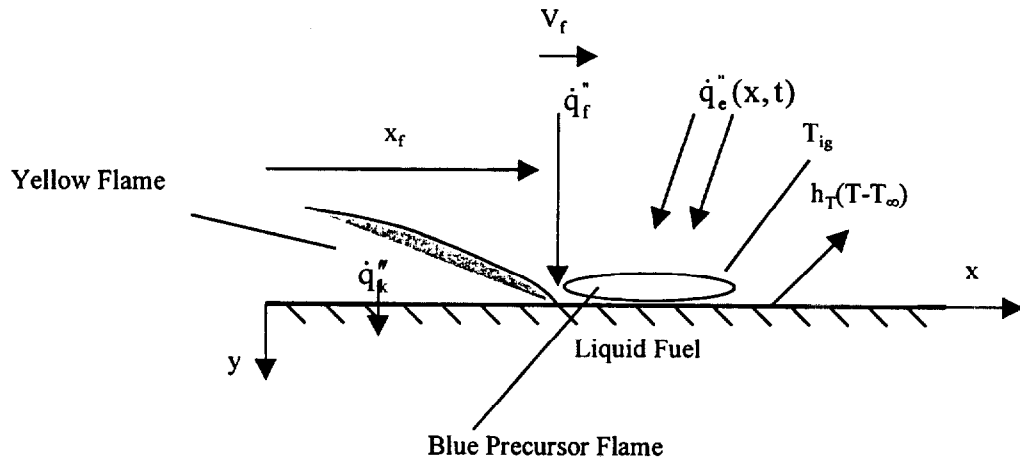


Figure 5.1. Schematic representation of the physical processes accompanying the flame spread.

Heat is transferred from the flame, precursor flame, and fuel to the atmosphere. The radiant panel imposes an external flux on the fuel as a function of distance. For this work, the movement of the established yellow flame will be used to track the flame propagation front. Also, heat is transferred from the flame to the fuel surface and to the bulk of the fuel or water layer. Although the precursor flame is the real leading edge, its size, pulsating frequency and existence is governed by experimental conditions such as the temperature of the fuel/water bed, therefore introduces uncertainty in the calculation of the spread rate.

### 5.2.2 Subsurface flows preceding flame spread

Determination of the controlling mechanism for flame spread is dependent upon the relation to the flash point of the liquid fuel. Depending on the temperature of the

liquid fuel, flame spread over the surface may be controlled by events in the liquid or gaseous phase. When the initial temperature of the liquid is at or above the flash point, adequate fuel is vaporized to create a combustible gas-phase mixture. After ignition, a flame will propagate at the characteristic gaseous flame spread velocity similar to that of a premixed laminar flame. In this case, gas phase heat transfer mechanisms are the controlling factors. Determination of the contribution of gas-phase heat transfer has been attempted by Hirano and coworkers by studying flame spread over a methanol layer floating on a water sub-layer [45]. Results from this study reemphasize that gas phase heat transfer is the controlling factor of flame spread for liquid fuels just below flash point temperature.

When the initial temperature of the liquid is significantly below the flash point, additional energy must be transferred ahead of the flame to elevate the surface temperature to the flash point value. Consequently, a temperature differential is formed resulting in a variation in surface tension and fuel density. If radiation heat transfer to and from the leading edge is neglected then convection in the liquid phase is left as the rate-controlling mechanism. Previous studies by Inamura and coworkers have found that radiation back to the fuel surface is significant only for established liquid pools fires supported on water [44]. For the transient process of flame spread, the effect of radiation is small when compared to the liquid phase convection. Therefore neglecting radiation is well justified.

Surface temperature variations due to the spreading of flame cause a deviation in surface tension. Well upstream of the flame front, temperature decreases and surface tension increases. Consequently, this variation in surface tension results in a stress that

pulls surface liquid away from the advancing flame region. Hot liquid is displaced forward in the direction of propagation leading to convective heat transfer ahead. This phenomenon is well documented in experiments studying flame spread of liquid fuels supported by water [13, 14, 24, 25, 45]. These experiments have shown that surface tension gradients due to temperature differences have an important effect on the flame spread velocity.

Liquid convection contributes significantly to the flame spread velocity of a liquid fuel. Sirignano and Schiller [46] reference several studies demonstrating the liquid surface velocity below the flame leading edge is of the same order of magnitude as the observed flame velocity. Since flame spread velocity is heavily dependent on the liquid-phase convection, the properties of the fuel, such as viscosity, are determinant in the calculation of the spread rate. The combined effect of natural convection and surface tension served to explain the pulsation of the flame propagation front. Although the subsurface flow ahead of the flame remains to be quantified, the overall heat transfer effect is included into the flame spread model proposed by Sirignano and Schiller.

Although none of these detailed mechanisms can be addressed by the present experiments, the value of the combined thermal inertia ( $k\rho C$ ) and the parameter  $\Phi$  serve as a global measure of the combined effect of natural convection, conduction and surface tension.

### **5.3 Procedures**

Flame spread tests were conducted for SAE 30W oil, ANS and Cook Inlet crude oils, in their natural state and weathered. The protocol followed for the flame spread

tests will be explained as follows. It needs to be noted that fuel exposure to the radiant panel had to be kept to a minimum since the pre-heating process resulted in changes in the composition of the fuel. Extreme care was taken to control initial conditions, which are needed for reproducible flame spread data. External air currents are standardized by adjusting the flow of the overhead hood. Temperatures of the water sublayer and fuel are carefully monitored prior to each test and maintained at the ambient room temperature of  $22^{\circ}\text{C} \pm 2^{\circ}\text{C}$ . Fuel and water are added to the flame spread tray and time is allowed for currents in the air and liquid to subside before exposure to external radiation.

In all tests, there is a 1mm free board height, the space above the fuel surface to the rim of the flame spread tray. Under external heating, the liquids are not expected to immediately ignite and thus, require additional capacity for expansion during testing. Studies have shown [25] that a freeboard height of this magnitude is negligible in flame spread testing of liquid fuels.

The flame spread tray is carefully moved to the proper testing position and the sample is ignited. After determination of the critical heat fluxes for ignition ( $\dot{q}_{o,ig}''$ ) and boiling ( $\dot{q}_{o,B}''$ ), an external radiant flux is selected to avoid the boiling of the water sublayer prior to ignition. The sample is, therefore, heated at  $\dot{q}_{o,ig}'' + 5 \text{ kW/m}^2$  until piloted ignition occurs at the end nearest to the radiant panel. Flame spread measurements are recorded using a high resolution 8mm video camera operating at 30 frames per second. After the flame has spread to the end of the tray and the necessary measurements have been taken, the flame is extinguished by covering the tray with a smother board.

#### 5.4 Experimental Observations

Several authors have visually characterized flame spread over liquid fuels [13, 14, 24, 25, 45] . These authors present a typical sequence of events characteristic of flame spread on most liquids, with the exception of certain alcohols [45]. In general, a blue flash or flame indicates ignition of the fuel, and will occur when the lean flammable limit has been attained. This flame propagates at with a velocity of a premixed flame. After ignition, a luminous yellow flame is established which is characteristic of self-sustained combustion. For flame spread in the sub-flash temperature regime, a small pulsating blue flame proceeds the established flame region. A transition region of intermittent dark yellow flames advances between the blue pulsating flame and bright yellow flame. For this work the leading edge of the stable self-sustained yellow flame region is referred to as the flame front.

A sequence of frames is presented as figure 5.2 for a flame spread test of 20% evaporated ANS crude oil with a layer thickness of 8mm. Features of flame spread on a liquid fuel from the previously mentioned research can be found within the film sequence. Ignition begins with a small blue flash or flame followed by a bright yellow flame. Then, the bright yellow self-sustained flame propagates preceded by a bright blue pulsating region. The creeping velocity of the bright yellow flame region is designated as the flame propagation front. Figure 5.2 shows that flame spread over a crude oil on a water layer exhibits similar characteristics of propagation as liquid fuels described in the literature [13, 14].

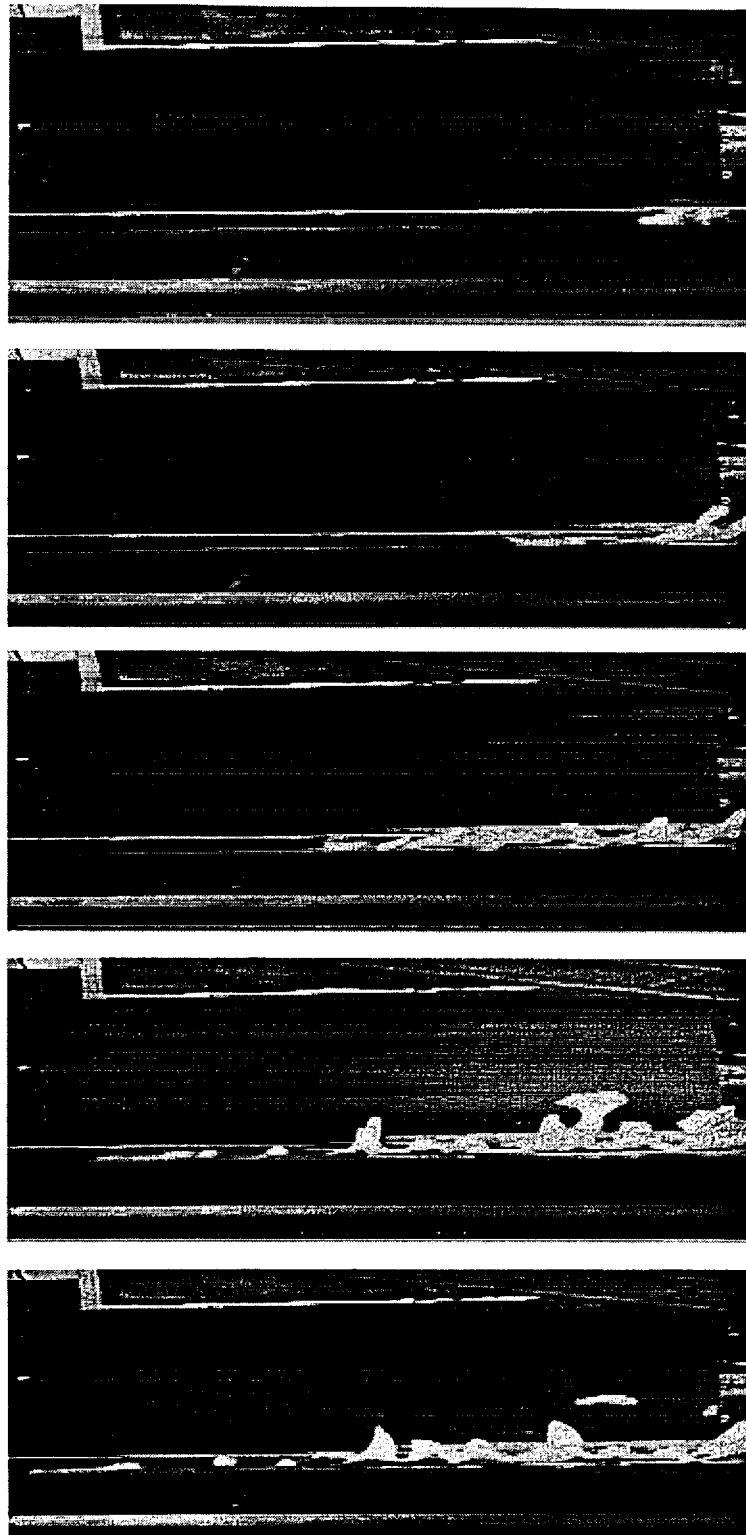


Figure 5.2. Flame spread image sequence for 20% evaporated ANS crude oil.

#### **5.4 Measurement of flame spread**

Numerous techniques are available for measuring the rate of progress of the flame across the surface of the fuel. Some simple methods give a mean velocity of spread while other more complex, time-consuming methods produce instantaneous spreading velocities at a particular position. In this work, three techniques are employed to accurately measure flame spread. Of primary concern is the determination of the position of the flame front. In all tests, the flame front is taken as the leading edge of the yellow luminous flame (either transitional or fully developed). Methods for flame spread measurements are listed below.

##### *Method 1- Stopwatch timing between two fixed points*

The first method used has the advantage of being the simplest, but it is also the most arbitrary. Specific increments of 25cm are marked along the flame spread tray and the flame progress is timed with a stopwatch. Results from this method produce only mean velocity measurements that are dependent on experimentalists' eyesight to determine the position on the leading edge of the flame. This human intervention factor is a major disadvantage of this method.

##### *Method 2- Cinematography of flame position and time*

A Sony 8mm video camera is used to simultaneously record the time and position of the flame front on the fuel surface. Similar to the first method, graduated markings are used along the length of the tray. Advantages over the first method also

include the ability to review and distinguish exact flame front position. This allows for instantaneous velocities in exchange for the tedious delays in analyzing film.

#### *Method 3- Surface thermocouple measurements*

Ten 0.8mm diameter thermocouples are placed along the center axis of the tray length at 5 cm intervals according to figure 2.3(b). Using the Labtech data acquisition software, the flame speed can be tracked via surface thermocouple temperature readings. At the same time, surface temperature of the fuel can be obtained at the instant prior to flame propagation at each reference point. However, the distance between thermocouple locations regulates the resolution of the mean flame velocity. This method has an advantage over the previous two since results from this method do not rely on visual interpretation of the flame front.

In most flame spread trials, a combination of all three of the above techniques is utilized. Redundancy allows for visual calculation to be backed numerical confirmation of the propagation front.

### **5.5 Characteristic Temperature Histories**

Temperature measurements are taken at the surface of the Cook Inlet and ANS crude oils and presented in figures 5.3 and 5.4. The profiles are characteristic of the flame spread phenomenon. Initially, the surface is preheated by the radiation from the external source. Consequently, thermocouples positioned nearest to the radiant panel reflect a higher temperature. When the temperature of the fuel surface approaches the flash point and the pilot ignition source is supplied, the gaseous mixture ignites. The

sudden peak in recorded temperatures indicates this event. As a result of convective (gas and liquid phase) and radiative heating, the flame propagates down the sample. Heat transfer from the flame and the external radiant source elevates the thermocouple temperatures downstream. Flame propagation at the thermocouple positions corresponds to the sudden peaks in the following temperature histories.

Both figures presented show uneven preheating before peak that represents the flame arriving the thermocouple. As can also be observed the temperature histories have not reached steady state conditions. Once the pilot initiates the flame, a sudden increase in temperature is evidenced by the thermocouples closest to the ignition point. Preheating at these locations had attained the flash point temperature, thus, a gas phase flame propagates through this zone. The latter thermocouples will show a less sudden increase in temperature. This zone is where actual flame spread occurs. Immediately after the sudden temperature increase a decrease in slope is observed. A second sudden temperature raise follows the slope change. This non-uniformity of the heating process has been attributed to the bulk motion of the fuel ahead of the flame front. Determination of the actual ignition temperature is quite complicated under these circumstances and significant scatter of the data is expected but should not preclude the determination of the global parameters that describe the spread process.

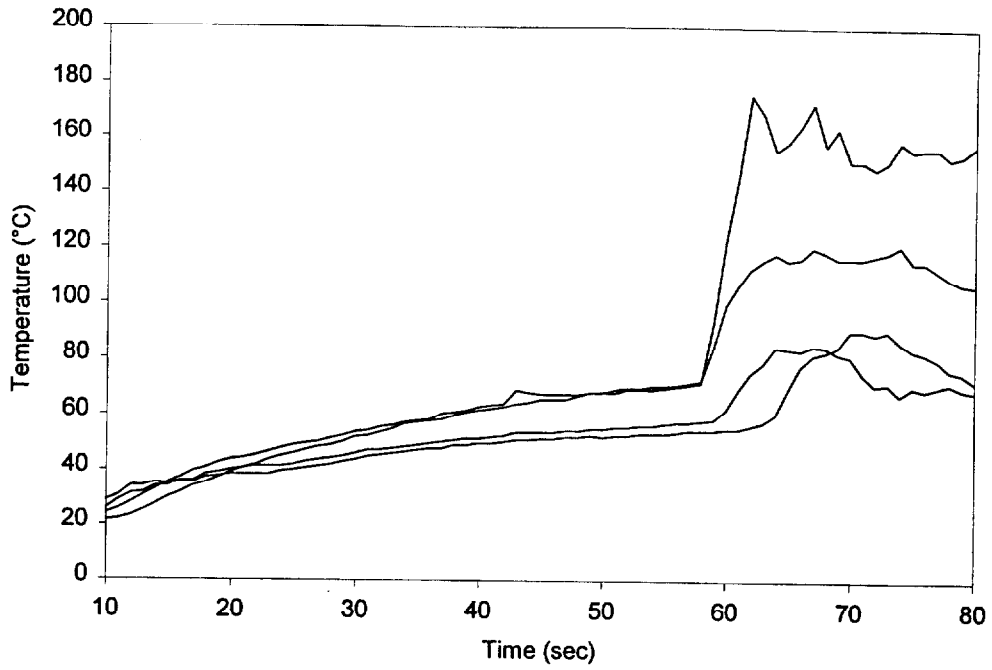


Figure 5.3. Surface thermocouple temperature for aflame spread test of 25% evaporated Cook Inlet crude (8mm fuel layer thickness).

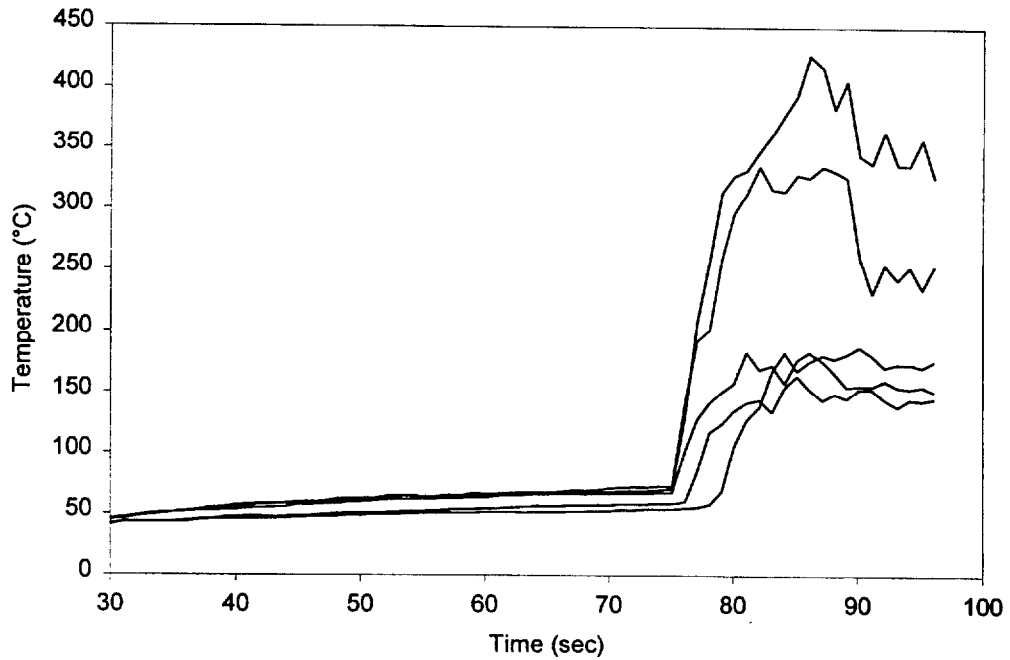


Figure 5.4. Surface thermocouple temperatures for flame a spread test of 12% evaporated ANS crude (8mm fuel layer thickness).

## 5.6 Flame Spread Test Results

### 5.6.1 Flame Spread over SAE 30W Oil

To validate the flame spread methodology, tests were conducted with SAE 30 Weight oil. Results for SAE 30 Weight oil were previously presented in Chapter 3 as figure 3.1. For the various thickness fuel layers, flame velocity data points are plotted as a function of the incident flux to the surface. It is realized that the fuel layer thickness influences the flame spread velocity. For thinner layers, thermal equilibrium is delayed due to the water bed that acts a heat sink, consequently requiring additional energy to compensate for heat losses. Therefore, flame spread of thin fuel layers of SAE 30 W oil is considered to be in the transient state since the thinner fuel layers are influenced by the supporting water layer. Application of equation (3.15) is possible to extract the fuel properties. However, the fuel layer thickness affects the value of  $\phi$  and alters the flame velocity. Fuel properties representative of the oil have to be obtained by conducting experiments with a fuel layer thicker than the minimum value ( $> 8$  mm) as determined from figure 3.1. Experiments with thinner layers will give an estimate of the global properties of the combined fuel and water layers. This information is of great importance since it allows to quantify the effect of the water bed on the spread characteristics.

### 5.6.2 Crude Oils and the Effect of Weathering

Results for flame spread tests using ANS crude oil at various levels of evaporation are shown in figure 5.5. Flame spread data, presented as  $V_f^{-1/2}$ , is plotted according to equation (3.18) as function of the surface temperature ( $T_s$ ). Thus, the slope of the line gives a constant which is a function of the flame spread parameter ( $\phi$ ) and

thermal properties ( $k\rho C$ ) of the fuel. Since, the thermal properties are extracted from the ignition tests, the " $\phi$ " parameter can be calculated. The definition of the flame spread parameter is given by equation (3.19), and describes the energy provided by the flame.

From the previous ignition tests, it was determined that an 8mm fuel layer thickness was required to avoid influence of the supporting water layer. For mass loss less than 20%, it is shown that the flame spread velocity is independent of the fuel layer thickness. This is illustrated by the convergence of 3 and 8mm data points to the least-squared line fit for the respective levels of evaporation. However, for the 20% evaporated ANS crude, there is 25% difference in temperature indicating an influence of heat losses to the supporting water sublayer.

Previously in Chapter 4, it has been shown that the weathering process does not alter the thermal properties ( $k\rho C$ ) of the fuel for ignition. In figure 5.5, the least-squared fit lines for various levels of weathering are parallel indicating an equivalent  $\phi$  value regardless of weathering. As seen in the ignition tests, the thermal properties of the crude oil are governed by the heavier fractions. Therefore, as the crude oil loses the lighter volatiles, the heat transfer is dominated by the remaining heavier fractions of the crude oil.

Test were also conducted on Cook Inlet crude oil at various evaporation states and fuel layer thickness. Similar conclusions are drawn from test conducted with Cook Inlet crude oil at various fuel layer thickness and levels of weathering. The slope of the least-squared fit line remains constant regardless of state of evaporation. Results for these tests are found in figure 5.6. Unlike the 20% evaporated ANS crude oil, flame

spread velocities for the evaporated Cook Inlet samples remained invariant with layer thickness. It is also noticed that the flame spread temperatures required for flame spread are generally lower than those for ANS. This serves to validate the ignition and flash point criteria.

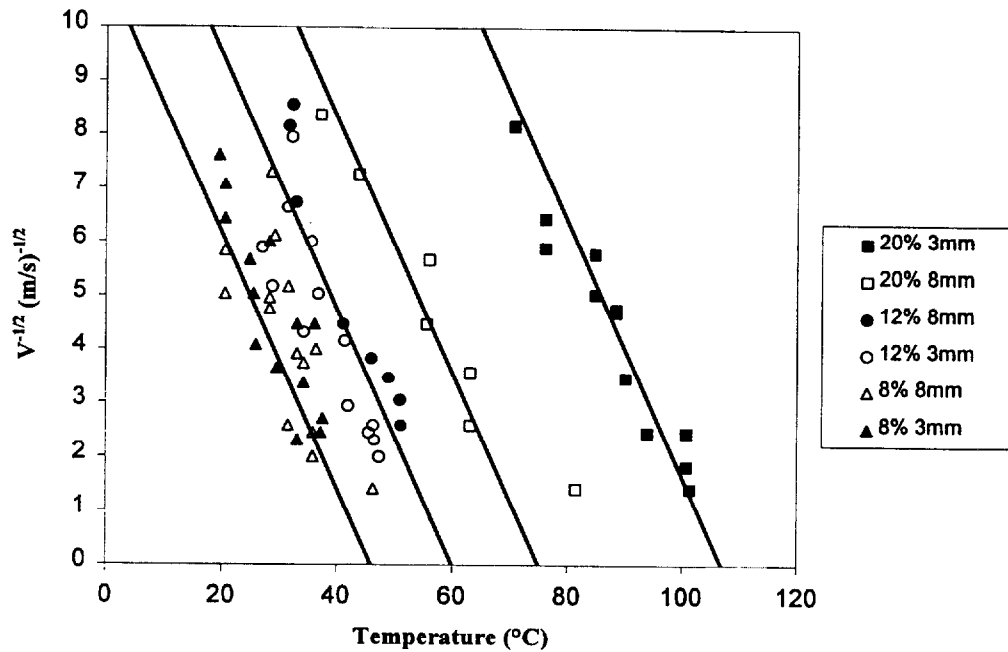


Figure 5.5. Flame spread velocity in terms of the fuel surface temperature for ANS crude oil.

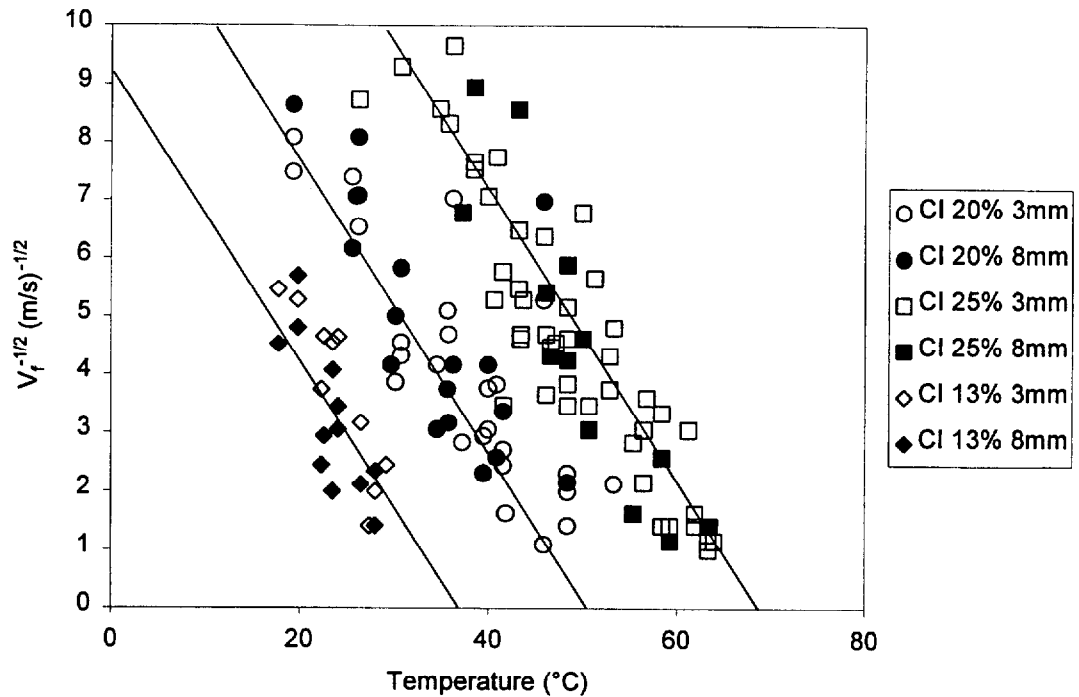


Figure 5.6. Flame spread velocity in terms of fuel surface temperature for Cook Inlet crude oil.

### 5.7 Summary

To flame spread of a slick of oil on water sublayer, the HIFT apparatus is used. As for solids, flame spread parameter and the thermal properties of a liquid fuel supported by water can be extracted using this testing methodology. For fuels that do not permit attainment of thermal equilibrium ( $t^*$ ) before flame spread, flame spread can be theoretically correlated to the fuel surface temperature. The propensity of a crude oil to propagate a flame can be characterized by two parameters:

- (1) The thermal inertia of the fuel ( $k\rho C$ ) or “fire properties” can be extracted from flash point temperature in combination with the critical heat flux and provides a measure of the heating process. It is a function of the fuel and is independent of the experimental and environmental conditions.

(2) The flame spread parameter ( $\phi$ ), which describes the energy of the flame, can be extracted with knowledge of the thermal properties. Like the thermal properties, the flame spread parameter is a function of the fuel and is independent of the experimental and environmental conditions.

The experimental methodology and its theoretical underpinnings were validated with experiments using SAE 30W oil and ANS and Cook Inlet crude oils in their natural state as well as different levels of weathering. The results show consistency previous ignition and flash point data presented in Chapter 4. The slope generated from the flame spread plot remains invariant with the level of evaporation. Although a shift in temperature occurs due to increasing flash point with level of weathering, the difference between flash point and surface temperature regardless of evaporation level should be equivalent for the same velocity. This could not be verified due to uncertainties in the thermocouple measurements.

**BLANK PAGE**

## CHAPTER 6 CONCLUSIONS

Removal of an oil slick by combustion can serve as an effective spill mitigation tool. In-situ burning of crude oil floating on water is accomplished through three distinct regimes of the burning process: ignition, flame spread and mass burning. The protocol used to achieve in-situ burning has been generally determined by means of costly large-scale tests. This work examined a methodology to assess the burning of crude oils on a water sub-layer by means of a bench scale procedure. A modified ASTM E1321 (LIFT) together with flash point measurements is used to extract fuel properties in conjunction with existing theoretical correlations. The methodology to assess the burning characteristics of a liquid fuel on a water sublayer has been presented and verified. SAE 30 Weight oil as well as ANS and Cook Inlet crude oils in various levels of evaporation have been used to provide validation. Although this methodology provides relevant information on the burning characteristics of crude oils on a water bed is not meant as a substitute to large scale tests. Instead it is meant as a complement that will lead to reduction of the number of large scale tests required to establish a protocol for in-situ burning of oil spills.

For ignition; the critical heat flux for ignition as identified in ASTM E1321 was found to be the parameter that better describes the capability of a fuel to ignite. For experimental conditions similar to those of the present experiments, the critical heat flux for ignition was found to be independent of the geometry and flow conditions and a parameter that could be extrapolated to attempt a relative evaluation of ignition at more realistic length scales. The minimum heat flux for ignition needs to be accompanied by a minimum heat flux that will lead to boiling of the supporting water layer. The critical

heat flux for boiling, when greater, than the critical heat flux for ignition, will take the place of the minimum external heat flux that is needed to achieve ignition. The values obtained for the critical heat flux for ignition and boiling are not necessarily correct due to the strong theoretical and experimental simplifications incurred during the present work. Therefore they should not be taken as absolute values but as a means of assessing the relative susceptibility of a fuel to ignite.

The ASTM D56 Tag Closed Cup flash point tester is used to characterize the lowest temperature at which application of the flame ignites the vapors above the sample specifies the flash point. The flash point gives an indication of the pyrolysis temperature of the fuel under a controlled environment, but does not give any information on the thermal properties. Therefore, is not sufficient to characterize ignition, but can be used to complement the ignition criteria. It was demonstrated that the flash point temperature can be used as a characteristic ignition temperature allowing for the determination of the total convective heat transfer coefficient ( $h_T$ ) from a plot of the critical heat flux for ignition as a function of the flash point temperature. This information permits the determination of the parameter ( $k\rho C$ ), fuel property that can be used to characterize ignition and flame spread.

For flame spread; the minimum external heat flux that will sustain propagation together with the parameter  $\phi$  (function of the fuel properties) will serve to describe the flame spread characteristics. Although the liquid convection mechanisms can not be addressed by the present experiments, the value of the combined thermal inertia ( $k\rho C$ ) and the parameter  $\phi$  serve as a global measure of the combined effect of natural convection, conduction and surface tension.

Using the appropriate theoretical correlations, a summation of results for SAE 30 Weight, ANS crude, and Cook Inlet crude oils are presented in Table III.

Table III. Parameters for characterization of piloted ignition and flame spread.

Fuel	$\dot{q}_{o,ig}''$ (kW/m <sup>2</sup> )	T <sub>fp</sub> (°C)	kρC (W/m <sup>2</sup> -K) <sup>2</sup> -s	φ (kW <sup>2</sup> /m <sup>3</sup> )
SAE 30 W	5.0	250	1.15 x 10 <sup>4</sup>	1.36
ANS 0% evap.	0	<3	4.6 x 10 <sup>3</sup>	4.0
ANS 8% evap.	0	20	4.6 x 10 <sup>3</sup>	4.0
ANS 12% evap.	1.3	37	4.6 x 10 <sup>3</sup>	4.0
ANS 20% evap.	4.0	85	4.6 x 10 <sup>3</sup>	4.0
Cook Inlet 0% evap.	0	<0	3.7 x 10 <sup>3</sup>	2.72
Cook Inlet 13% evap.	0.3	20	3.7 x 10 <sup>3</sup>	2.72
Cook Inlet 20% evap.	1.0	41	3.7 x 10 <sup>3</sup>	2.72
Cook Inlet 25% evap.	4.8	62	3.7 x 10 <sup>3</sup>	2.72

The values of  $\dot{q}_{0,B}''$  are not presented in this table since they depend on the fuel layer thickness. As shown on Table III the values of (kρC) and φ are not a function of weathering, only the critical heat flux for ignition is influenced by evaporation of the light volatiles.

Although the overall objective of this study is to characterize the entire in-situ combustion process, only work relating piloted ignition and flame spread is presented. Mass burning is an integral regime of the combustion process that can be used to describe the efficiency of in-situ combustion as a clean up tool. To assess the feasibility of in-situ burning as a spill mitigation tool, the mass burning process must be included.

## REFERENCES

1. Koseki, H., Kokkala, M., and Mulholland, G.W., *Fire Safety Science-Proceedings of the Third International Symposium*, pp865-875, 1991.
2. Tebau, P., "Operational Implications of In Situ Burning", *Proceedings of the In Situ Burning Oil Spill Conference*, Orlando, Florida, pp57-62, 1994.
3. Walavalkar, A.Y, Kulkarni, A.K., "A Comprehensive Review of Oil Spill Combustion Studies", *Proceedings from the 19<sup>th</sup> AMOP Technical Seminar, Calgary, Alberta, Canada*, pp1081-1104, July 1996.
4. Kennedy, D., Barnea N., and Shigenaka, G., "Environmental and Human Health Concerns Related to In situ Burning", *Proceedings of the In Situ Burning Oil Spill Conference*, Orlando, Florida, pp47-56, 1994.
5. Bobra, M., "A Study of the Evaporation of Petroleum Oils," Publication EE-135, Environmental Canada, Ottawa, Ontario, K1A OH3, 1992.
6. Evans, D., "Smoke Production and Plume Behavior", *Proceedings of the In Situ Burning Oil Spill Conference*, Orlando, Florida, pp29-38, 1994.
7. Kasiwagi, T., Mell, W.E., McGrattan, K.B. and Baum, H.R., *Fourth International Micro-gravity Combustion Workshop*, NASA Lewis Research Center, pp411-416, 1997.
8. Annual Book of ASTM Standards, *ASTM E-1321 Standard Test Method for Material Ignition and Flammability*, Vol. 04.07, pp1055-1077, 1994.
9. Garo, J.P., Vantelon, J.P., and Fernandez-Pello, A.C., *Twenty-fifth Symposium (International) on Combustion*, The Combustion Institute, Pittsburgh, PA, pp1481-1488, 1994.
10. Arai, M., Saito, K., and Altenkirch, R.A., *Combustion Science and Technology*, 71, pp25-40 1990.
11. Brzustowski, T.A., and Twardus, E.M., *Nineteenth Symposium (International) on Combustion*, The Combustion Institute, Pittsburgh, PA, pp847-854, 1982.
12. Twardus, E.M. and Brzustowski, T.A., *Archivum Combustionis*, Polish Academy of Sciences, 1, 1-2, pp49-60, 1981.
13. Glassman, I., and Dryer, F., "Flame Spread Across Liquid Fuels," *Fire Safety Journal*, 3, pp123-138, 1980.
14. Ross, H., *Progress in Energy and Combustion Science*, 20, pp17-63, 1994.
15. *SFPE Handbook*, 2<sup>nd</sup> Edition, Society of Fire Protection Engineers, Quincy, MA, pp2.161-2.170, 1994.
16. Hillstrom, W., *Eastern States Section: Combustion Institute Fall Technical Meeting*, The Combustion Institute, 1975.
17. Putorti, A., Evans, D., and Tennyson, E., "Ignition of Weathered and Emulsified Oils," *Proceedings from the Seventeenth Arctic and Marine Oil Spill Program Technical Seminar*, pp657-667, 1994.
18. *ASTM E-1354 Standard Test Method for Heat and Visible Smoke Release Rates for Materials and Products Using an Oxygen Consumption Calorimeter*, ASTM Fire Test Standards, 3<sup>rd</sup> Edition, pp803-817, 1990.
19. Quintiere, J., "A Simplified Theory for Generalizing Results from a Radiant Panel Rate of Flame Spread Apparatus," *Fire and Materials*, 5, 2, pp52-60, 1981.

20. Quintiere, J., Harkleroad, M., and Walton, D., "Measurement of Material Flame Spread Properties," *Combustion Science and Technology*, 32, pp67-89, 1983.
21. Quintiere, J., and Harklroad, M., "New Concepts for Measuring Flame Spread Properties," U.S. Department of Commerce, NBSIR 84-2943, 1984.
22. Motevalli, V., Chen, Y., Gallagher, G., Sheppard, D., "Measurements of Horizontal Flame Spread on Charring and Non-Charring Material Using the LIFT Apparatus," *Fire and Materials*, Interscience Communications Unlimited, pp23-32, 1992.
23. Drysdale, D., An Introduction to Fire Dynamics, John Wiley and Sons, 1985.
24. Sirignano, W. and Glassman, I., "Flame Spreading Above Liquid Fuels: Surface-Tension-Driven Flows," *Combustion Science and Technology*, 1, pp307-312, 1970.
25. Mackinven, R., Hansel, J.G., and Glassman, I., "Influence of Laboratory Parameters on Flame Spread Across Liquid Fuels," *Combustion Science and Technology*, 1, pp293-306, 1970.
26. Simms, D., *Combustion and Flame*, 11, p377, 1967.
27. Dryer, F.L., and Newman, J.S., "Flame Spread Over Liquid Fuels: The Mechanism of Flame Pulsation," *Proceedings of the Western States Section: The Combustion Institute*, La Jolla, CA, 1976.
28. Petrov, A.A., Petroleum Hydrocarbons. Springer-Verlag, 1987.
29. McAuliffe, C.D., "The Weathering of Volatile Hydrocarbons from Crude Oil Slicks on Water," *Proceedings Form the 1989 Oil Spill Conference*, San Antonio, Texas, pp357-363, 1989.
30. Sellers, C., Fox, B., Pautz, J., "Bartlesville Project Office Crude Oil Analysis Data Base User's Guide", Department of Energy, DOE/BC-96/3/SP, p4, March 1996.
31. Rusin, J., Lunel, T., and Davies, L., "Validation of the EUROSPILL Chemical Spill Model", *Proceedings of the 19<sup>th</sup> AMOP Technical Seminar*, Alberta, Canada, 1996, pp.1437-1485.
32. Reijnart, R. and Rose, R., "Evaporation of Crude Oil at Sea", *Water Research*, v16, 1982, pp1319-1325.
33. Ostazeski, S.A., Daling, P.S., Macomber, S.C., Fredricksson, D.W., Durell, G.S., Uhler, A.D., Jones, M., and Bitting, K., "Weathering Properties and the Prediction Behavior at Sea of a Lapio Oil (weathered No. 6 Fuel Oil)", *Proceedings of the 19<sup>th</sup> AMOP Technical Seminar*, Alberta, Canada, 1996, pp137-162.
34. Fingas, M., "The Evaporation of Oil Spills: Variation with Temperature and Correlation with Distillation Data, *Proceedings of the 19<sup>th</sup> AMOP Technical Seminar*, Alberta, Canada, pp29-135, 1996.
35. Carslaw, H.S. and Jaeger, J.C., *Conduction of Heat in Solids*, 2<sup>nd</sup> Edition, Oxford University Press, Oxford, pp70-76, 1963.
36. Janssens, M., *Fire Safety Science-Proceedings of the Third International Symposium*, pp167-176, 1991.
37. Mikkola, E. and Wichman, I., *Fire and Materials* 14, 1989.
38. Fernandez-Pello, A.C., "Combustion Fundamentals on Fire: The Solid Phase," *Academic Press*, pp31-100, 1995.
39. Alveres, N. and Martin, S.B., *Thirteenth Symposium (International) on Combustion*, The Combustion Institute, pp905-914, 1971.
40. Ito, A., Saito, K., Cremers, C.J., *Fire Safety Science-Proceedings of the Fourth International Symposium*, pp445-456.

41. DeRis, J., "Spread of a Laminar Diffusion Flame," *Twelfth International Symposium on Combustion*, The Combustion Institute, pp241-252, 1969.
42. Incropera, F.P., and DeWitt, D.P., Fundamentals of Heat and Mass Transfer, John Wiley and Sons, 4<sup>th</sup> Ed., 1996.
43. Per Sveum, C.G., Buist, I., Aunaas, T., and Godal, L., "In-Situ Burning of Water In-Oil Emulsions", Sintef Applied Chemistry Report, STF21 A94053, p8, June 1996.
44. Inamura, T., Saito, K., and Tagavi, K.A., "A Study of Liquid Pool Fires Supported on Water. Part II: The Effect of In-depth Radiation Absorption," *Combustion Science and Technology*, Vol. 86, pp105-119., 1992.
45. Hirano, T., Suzuki, T., Mashiko, I., and Tanabe, N., "Gas Movement in Front of Flames Propagating Across Methanol," *Combustion Science and Technology*, Vol. 22, pp83-91, 1980.
46. Sirignano, W.A. and Schiller, D.N., "Mechanisms of Flame Spread Across Condensed-Phase Fuels", Physical and Chemical Aspects of Combustion: A Tribute to Irvin Glassman, Gordon Breach Science Publishers, pp354-407, 1997.

NIST-114 (REV. 11-94) ADMAN 4.09	U.S. DEPARTMENT OF COMMERCE NATIONAL INSTITUTE OF STANDARDS AND TECHNOLOGY		(ERB USE ONLY)	
			ERB CONTROL NUMBER	DIVISION
	<b>MANUSCRIPT REVIEW AND APPROVAL</b>		PUBLICATION REPORT NUMBER NIST-GCR-98-750	CATEGORY CODE
INSTRUCTIONS: ATTACH ORIGINAL OF THIS FORM TO ONE (1) COPY OF MANUSCRIPT AND SEND TO THE SECRETARY, APPROPRIATE EDITORIAL REVIEW BOARD.			PUBLICATION DATE June 1998	NUMBER PRINTED PAGES

TITLE AND SUBTITLE (CITE IN FULL)  
 Enhanced Burning of Difficult to Ignite/Burn Fuels Including Heavy Oils

CONTRACT OR GRANT NUMBER 60NANB6D0073	TYPE OF REPORT AND/OR PERIOD COVERED Final Report April 1998
--	---

AUTHOR(S) (LAST NAME, FIRST INITIAL, SECOND INITIAL)  Wu, N. and Torero, J. L.	PERFORMING ORGANIZATION (CHECK (X) ONE BLOCK) <input checked="" type="checkbox"/> NIST/GAITHERSBURG <input type="checkbox"/> NIST/BOULDER <input type="checkbox"/> JILA/BOULDER
--	--

LABORATORY AND DIVISION NAMES (FIRST NIST AUTHOR ONLY)

SPONSORING ORGANIZATION NAME AND COMPLETE ADDRESS (STREET, CITY, STATE, ZIP)  
 U.S. Department of Commerce  
 National Institute of Standards and Technology  
 Gaithersburg, MD 20899

PROPOSED FOR NIST PUBLICATION

<input type="checkbox"/> JOURNAL OF RESEARCH (NIST JRES)	<input type="checkbox"/> MONOGRAPH (NIST MN)	<input type="checkbox"/> LETTER CIRCULAR
<input type="checkbox"/> J. PHYS. & CHEM. REF. DATA (JPCRD)	<input type="checkbox"/> NATL. STD. REF. DATA SERIES (NIST NSRDS)	<input type="checkbox"/> BUILDING SCIENCE SERIES
<input type="checkbox"/> HANDBOOK (NIST HB)	<input type="checkbox"/> FEDERAL INF. PROCESS. STDS. (NIST FIPS)	<input type="checkbox"/> PRODUCT STANDARDS
<input type="checkbox"/> SPECIAL PUBLICATION (NIST SP)	<input type="checkbox"/> LIST OF PUBLICATIONS (NIST LP)	<input checked="" type="checkbox"/> OTHER NIST-GCR
<input type="checkbox"/> TECHNICAL NOTE (NIST TN)	<input type="checkbox"/> NIST INTERAGENCY/INTERNAL REPORT (NISTIR)	

PROPOSED FOR NON-NIST PUBLICATION (CITE FULLY)	<input type="checkbox"/> U.S. <input type="checkbox"/> FOREIGN	PUBLISHING MEDIUM <input checked="" type="checkbox"/> PAPER <input type="checkbox"/> CD-ROM <input type="checkbox"/> DISKETTE (SPECIFY) _____ <input type="checkbox"/> OTHER (SPECIFY) _____
--	--	---

SUPPLEMENTARY NOTES

ABSTRACT (A 2000-CHARACTER OR LESS FACTUAL SUMMARY OF MOST SIGNIFICANT INFORMATION. IF DOCUMENT INCLUDES A SIGNIFICANT BIBLIOGRAPHY OR LITERATURE SURVEY, CITE IT HERE. SPELL OUT ACRONYMS ON FIRST REFERENCE.) (CONTINUE ON SEPARATE PAGE, IF NECESSARY.)

An experimental technique has been developed to systematically study the ignition, flame spread and mass burning characteristics of liquid fuels spilled on a water bed. The final objective of this work is to provide a tool that will serve to assess a fuels ease to ignite, to spread and to sustain a flame, thus helping to better define the combustion parameters that affect in-situ burning of oil spills. A systematic study of the different parameters that affect ignition, flame spread and mass burning has been conducted in an attempt to develop a bench scale procedure to evaluate the burning efficiency of liquid fuels in conditions typical of oil spill scenarios. To study ignition and flame spread, the Lateral Ignition and Flame Spread (LIFT) standard test method (ASTM E-1321) has been modified to allow the use of liquid fuels and a water bed. Characteristic parameters such as the critical heat flux for ignition, ignition delay time and flame spread velocity as a function of the external heat flux have been obtained. A series of "fire properties" corresponding to the fuel can be extrapolated from these tests and used to assess the tendency of a fuel to ignite and to sustain flame spread.

KEY WORDS (MAXIMUM OF 9, 28 CHARACTERS AND SPACES EACH; SEPARATE WITH SEMICOLONS; ALPHABETIC ORDER; CAPITALIZE ONLY PROPER NAMES)

crude oils; flame spread; heat flux; ignition; in situ combustion; lateral ignition; liquid fuels; oil spills; weather effects

AVAILABILITY <input checked="" type="checkbox"/> UNLIMITED <input type="checkbox"/> FOR OFFICIAL DISTRIBUTION - DO NOT RELEASE TO NTIS <input type="checkbox"/> ORDER FROM SUPERINTENDENT OF DOCUMENTS, U.S. GPO, WASHINGTON, DC 20402 <input checked="" type="checkbox"/> ORDER FROM NTIS, SPRINGFIELD, VA 22161	NOTE TO AUTHOR(S): IF YOU DO NOT WISH THIS MANUSCRIPT ANNOUNCED BEFORE PUBLICATION, PLEASE CHECK HERE.
--	--